

Air Force Institute of Technology

AFIT Scholar

Theses and Dissertations

Student Graduate Works

3-2006

Development of Autonomous Unmanned Aerial Vehicle Platform: Modeling, Simulating, and Flight Testing

Nidal M. Jodeh

Follow this and additional works at: <https://scholar.afit.edu/etd>



Part of the [Systems Engineering and Multidisciplinary Design Optimization Commons](#)

Recommended Citation

Jodeh, Nidal M., "Development of Autonomous Unmanned Aerial Vehicle Platform: Modeling, Simulating, and Flight Testing" (2006). *Theses and Dissertations*. 3563.

<https://scholar.afit.edu/etd/3563>

This Thesis is brought to you for free and open access by the Student Graduate Works at AFIT Scholar. It has been accepted for inclusion in Theses and Dissertations by an authorized administrator of AFIT Scholar. For more information, please contact richard.mansfield@afit.edu.



**DEVELOPMENT OF AUTONOMOUS UNMANNED AERIAL
VEHICLE RESEARCH PLATFORM: MODELING, SIMULATING,
AND FLIGHT TESTING**

THESIS

Nidal M. Jodeh, Captain, USAF

AFIT/GAE/ENY/06-M18

**DEPARTMENT OF THE AIR FORCE
AIR UNIVERSITY**

AIR FORCE INSTITUTE OF TECHNOLOGY

Wright-Patterson Air Force Base, Ohio

APPROVED FOR PUBLIC RELEASE; DISTRIBUTION UNLIMITED

The views expressed in this thesis are those of the author and do not reflect the official policy or position of the United States Air Force, Department of Defense, or the U.S. Government.

AFIT/GAE/ENY/06-M18

**DEVELOPMENT OF AUTONOMOUS UNMANNED AERIAL VEHICLE
RESEARCH PLATFORM: MODELING, SIMULATING, AND FLIGHT
TESTING**

THESIS

Presented to the Faculty

Department of Aeronautics and Astronautics

Graduate School of Engineering and Management

Air Force Institute of Technology

Air University

Air Education and Training Command

In Partial Fulfillment of the Requirements for the
Degree of Master of Science in Aeronautical Engineering

Nidal M. Jodeh, BS, MAS

Captain, USAF

March 2006

APPROVED FOR PUBLIC RELEASE; DISTRIBUTION UNLIMITED

**DEVELOPMENT OF AUTONOMOUS UNMANNED AERIAL VEHICLE
RESEARCH PLATFORM: MODELING, SIMULATING, AND FLIGHT
TESTING**

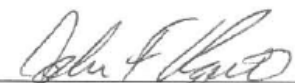
Nidal M. Jodeh, BS, MAS
Captain, USAF

Approved:



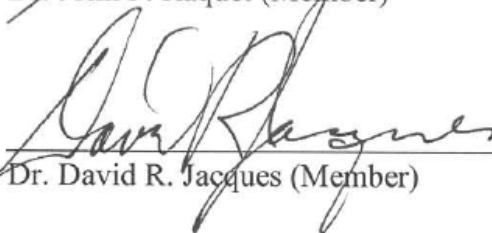
Paul A. Blue, Major, USAF (Chairman)

16 Mar 06
Date



Dr. John F. Raquet (Member)

16 MAR 06
Date



Dr. David R. Jacques (Member)

16 MAR 06
Date

Abstract

The Advanced Navigation Technology (ANT) Center at the Air Force Institute of Technology (AFIT) conducts extensive research in advanced guidance, navigation, and control to exploit the full potential of autonomous Unmanned Aerial Vehicles (UAV). The research in this thesis describes a UAV research platform developed to support the ANT Center's goals. This platform is now the bedrock for UAV simulation and local flight test at AFIT. The research has three major components. The first component includes development of a physical, inertial, and aerodynamic model representing an existing aircraft. A systematic analysis of the airframe leads to a complete geometric, inertial, and aerodynamic representation. The airframe analysis includes the use of USAF Digital Datcom, an aerodynamic modeling software tool. Second is the development and implementation of a non-linear, six degree of freedom simulation, employing the developed model. Constructed in Matlab/SIMULINK, the simulation enables control design and pre-flight analysis throughout the entire flight envelope. Detailed post-flight analysis is also performed in Matlab/SIMULINK. Additionally, a Hardware in the Loop benchmark simulation is constructed for initial flight test planning as well as test team training. The third and final component of the research includes the development of an experimental flight test program with both open loop and autonomous flights. Open-loop flights characterize the aircraft dynamics for comparison with the Matlab simulation results. Autonomous flights tune the autopilot controller through waypoint tracking in preparation for future advanced navigation research and provide data for Hardware in the Loop simulation validation. This report, along with other significant legacy documentation and procedures, builds the foundation on which AFIT and ANT Center UAV simulations and flight tests are based.

Acknowledgments

I would like to express my deepest gratitude to my faculty advisor, Major Paul Blue, for his guidance and insight. His monumental commitment to the success of this project truly inspired me. I would like to thank Dr John Racquet for making the experimental thesis possible by allowing us to use the lab's aircraft and equipment. I must also acknowledge other people whose work was critical to the success of this project. First to Athan Waldron, as my right hand he worked tirelessly to ensure the aircraft were properly prepared for flight. His meticulous understanding of the autopilot system and documentation saved countless hours of work. Randy Plate, who also worked on preparing the aircraft, jump started our work during the summer of 2005. John McNees, our radio control aircraft expert and pilot, guided our aircraft through the flight test phase with ease. His in-depth knowledge allowed us to make timely and proper modifications, as well as expertly pilot the aircraft. The project could not have been done without these men. Second Lieutenant Brett Pagel brought prior autopilot experience and shaved weeks off our autonomous flight learning curve. Don Smith, the lab's expert technician in everything mechanical and electrical. Don was the "go-to" guy when all else failed. Bill Blake, from the Air Force Research Lab, provided timely much needed expertise in aircraft modeling and simulation. To my peers, whose contributions and help over the last year was immeasurable. To my wife and children, and their unlimited patience and support. You are the bedrock of my life. Finally to God, without whom nothing is possible

Nidal M. Jodeh

Table of Contents

	Page
Abstract.....	iv
Acknowledgments.....	v
Table of Contents.....	vi
List of Figures.....	x
List of Tables.....	xiv
I. Introduction.....	1
1.1 – Background.....	1
1.2 - Problem Statement.....	4
1.3 - Research Objectives.....	4
1.4 – Significance of Research.....	5
1.5 – Methodology.....	6
1.6 – Preview.....	8
II. Background.....	9
2.1 - Overview.....	9
2.2 – Aircraft.....	9
2.2.1 – Airframe.....	9
2.2.2 – Engine and Propeller.....	11
2.3 – Avionics.....	11
2.3.1 – Radio Control System.....	12
2.3.2 – Piccolo II Autopilot.....	12
2.3.3 – Fail Safe Control Relay.....	16
2.4 – Flight Testing.....	18

	Page
2.4.1 – Overview of Flight Test.....	18
2.4.2 – Flight Dynamics	21
2.4.3 – Flight Test Range	25
2.4.4 – Ground Equipment	27
2.4.5 - Criteria for Flight Test of UAVs at WPAFB	28
2.4.6 – Autopilot Tuning – Transformation from R/C to Autonomous UAV.....	30
2.4.7 – Data Collection and Handling	34
2.5 – Chapter Conclusion	36
III. Development of UAV Physical, Inertial, and Aerodynamic Simulation Model	38
3.1 – Chapter Overview.....	38
3.2 – Physical Measurements and Mass Properties.....	38
3.3 – Inertia Measurements and Calculations.....	46
3.4 – Center of Gravity Determination.....	53
3.5 – Airfoil Analysis	54
3.6 – Engine and Propeller Model.....	63
3.7 – US Air Force Stability and Control Datcom	64
3.7.1 – Datcom Inputs	65
3.7.2 – Datcom Outputs – Stability Derivatives.....	71
3.8 – Hardware in the Loop (HITL) Aircraft Model Inputs	72
3.9 – Modeling Errors.....	73
3.10 – Chapter Conclusions.....	73

	Page
IV. Development of UAV Simulation	75
4.1 – Chapter Overview.....	75
4.2 – Matlab/SIMULINK Simulation.....	75
4.2.1 – Forces and Moments Build Up.....	76
4.2.2 – Equations of Motion.....	81
4.2.3 – SIMULINK.....	85
4.3 – Hardware in the Loop Simulation	92
4.4 – Chapter Conclusions.....	93
V. Flight Test of UAV Platform	94
5.1 – Chapter Overview.....	94
5.2 – Open Loop Flight Tests	94
5.2.1 – Flight Procedures and Configurations.....	94
5.2.2 – Maneuvers	95
5.3 – Autopilot Flight Tests.....	95
5.3.1 – Procedures	96
5.3.2 – Waypoint Tracking.....	96
5.4 – Testing Issues	98
5.4.1 – Non-Flight Test Issues.....	98
5.4.2 – In-Flight Test Issues	99
5.4.3 – Autonomous Flight Test Issues	100
5.5 – Chapter Conclusions.....	101
VI. Results and Analysis.....	102

	Page
6.1 – Chapter Overview.....	102
6.2 – Open Loop Flight Test Results.....	102
6.2.1 – Flight Test and Matlab/SIMULINK Simulation Results.....	102
6.3 – Autonomous Test Flights	108
6.3.1 – Waypoint Hardware in the Loop Simulation Results.....	108
6.3.2 – Waypoint Flight Test Results	111
6.4 – Chapter Conclusions.....	115
VII. Conclusions and Recommendations.....	116
7.1 – Conclusions	116
7.2 – Recommendations	118
Appendix A: Open Loop Flight Test Results	120
Appendix B: Autonomous Waypoint Flight Test Results	126
Appendix C: Hardware in the Loop Aircraft Model Inputs.....	131
Appendix D: Hardware In the Loop Actuator Model Inputs.....	140
Appendix E: Hardware In the Loop Sensor Model Inputs	141
Appendix F: Digital Datcom Input File	144
Appendix G: Digital Datcom Output File.....	145
Appendix H: Matlab M-Files: Force, Moment, and Equations of Motion	172
Bibliography	182
Vita	185

List of Figures

	Page
Figure 1. Rascal 110's Out for Preflight Checks.....	11
Figure 2. Piccolo II Block Diagram (Vaglienti et al. 2005:6)	13
Figure 3. Piccolo II Airborne Avionics Package (Vaglienti et al., 2005:9).....	14
Figure 4. Ground Station and Pilot Control Box (laptop not pictured)	15
Figure 5. Fail Safe Control Relay (Marker, 2005).....	17
Figure 6. Ground and Airborne Avionics Flow Diagram.....	18
Figure 7. Open and Closed Loop Control Systems.....	21
Figure 8. Phugoid and Short Period Motion	23
Figure 9. Flight Test Range (Dashed Line) at WPAFB Area B	27
Figure 10. Ground Equipment and Test Team during Flight Tests	28
Figure 11. Screen Shot of Operator Interface with Gains Page Opened.	34
Figure 12. SIG Rascal Wing Planform View.....	39
Figure 13. Rascal Cross Sectional Area Definitions.....	45
Figure 14. Schematic of Typical Inertia Swing Test Setup	48
Figure 15. a) Inertia Test Set Up, b) Reverse View, and c) Wire Harness Apparatus.....	48
Figure 16. Rascal UAV Center of Gravity Location	54
Figure 17. Rascal Airfoil vs. Eppler 193 Airfoil	58
Figure 18. Rascal Airfoil vs. Eppler 205 Airfoil	58
Figure 19. Lift Curve Slopes of E193 and E205.....	59
Figure 20. Rascal 110 Representation; Input to Digital Datcom	68

	Page
Figure 21. Rascal 110 for Comparison (Courtesy of Tower Hobbies).....	68
Figure 22. Rascal 110 Representation; Input to Digital Datcom Top View.....	69
Figure 23. Rascal 110 for Comparison; Top View.....	69
Figure 24. Rascal 110 Representation; Input to Digital Datcom Front View.....	70
Figure 25. Rascal 110 for Comparison; Front View.....	70
Figure 26. Rascal 110 Representation; Input to Digital Datcom Side View	71
Figure 27. Aircraft Moments; Axis and Direction Definitions.....	77
Figure 28. Wing Forces and Moments.....	79
Figure 29. Wing and Tail Forces and Moments	80
Figure 30. SIMULINK UAV Simulation	87
Figure 31. Control Surface Inputs to SIMULINK; Level Flight at 64.8 ft/sec.....	88
Figure 32. Altitude Output Response of SIMULINK to Elevator Doublet Command	89
Figure 33. SIMULINK Output; Aircraft States 8-12.....	90
Figure 34. SIMULINK Output; Aircraft States 1-7.....	91
Figure 35. Typical Hardware in the Loop Simulation Set Up	92
Figure 36. Autopilot Waypoints and Planned Pattern	97
Figure 37. Short Period Response to Elevator Doublet – Flight Test #2 v Matlab Sim.	103
Figure 38. Comparison of Flight Test #3 to Matlab Sim; Elevator Input.....	104
Figure 39. Comparison of Flight Test #1 to Matlab Sim; Elevator Input.....	105
Figure 40. Comparison of HITL Run #6 to Matlab Sim; Elevator Input	106
Figure 41. Comparison of HITL Run #7 to Matlab Sim; Elevator Input	107

	Page
Figure 42. Waypoint HITL Simulation Results - Actual Track.....	109
Figure 43. Waypoint HITL Simulation Results - Larger Track.....	110
Figure 44. HITL Simulation Output; Airspeed and Altitude.....	111
Figure 45. Autopilot Waypoint Flight Test #3.....	112
Figure 46. Autopilot Waypoint Flight Test #3 – Altitude	113
Figure 47. Autopilot Waypoint Flight Test #4 – Altitude	114
Figure 48. Autopilot Waypoint Orbits; Airspeed and Altitude.....	115
Figure 49. Short Period Flight Test Results.....	120
Figure 50. Short Period Flight Test #1.....	120
Figure 51. Short Period Flight Test #2.....	121
Figure 52. Short Period Flight Test #3.....	121
Figure 53. Short Period Flight Test #4.....	122
Figure 54. Phugoid Flight Test – Combined.....	122
Figure 55. Phugoid Flight Test #1	123
Figure 56. Phugoid Flight Test #2	123
Figure 57. Phugoid Flight Test #3	124
Figure 58. Phugoid Flight Test #4	124
Figure 59. Phugoid Flight Test #5	125
Figure 60. Phugoid Flight Test #6	125
Figure 61. HITL Autopilot Simulation #1, TAS: 88 ft/sec, Alt: 1083 ft, Conv: 100	126
Figure 62. HITL Autopilot Simulation #2, TAS: 88 ft/sec, Alt: 1083 ft, Conv: 50	126

	Page
Figure 63. HITL Autopilot Simulation #3, TAS: 67 ft/sec, Alt: 1083 ft, Conv: 50	127
Figure 64. HITL Autopilot Simulation #4, TAS: 61 ft/sec, Alt: 1083 ft, Conv: 100	127
Figure 65. HITL Autopilot Simulation #1, TAS: 88 ft/sec, Alt: 1083 ft	128
Figure 66. HITL Autopilot Simulation #2, TAS: 88 ft/sec, Alt: 1083 ft, Conv: 50	128
Figure 67. HITL Autopilot Simulation #3, TAS: 67 ft/sec, Alt: 1083 ft, Conv: 50	129
Figure 68. HITL Autopilot Simulation #4, TAS: 61 ft/sec, Alt: 1083 ft, Conv: 100	129
Figure 69. HITL Autopilot Simulation Altitude and Airspeed Comparisons.....	130

List of Tables

	Page
Table 1. Example of Selected Criteria for Flight Tests	29
Table 2. Example Available Telemetry from Piccolo II Autopilot Logs	36
Table 3. Rascal Physical Dimensions	41
Table 4. Component Weights	41
Table 5. Planform Taper Ratios and Tip Chord Lengths.....	42
Table 6. Rascal Incidence, Dihedral, Twist, and Sweep.....	44
Table 7. Cross Sectional Area Dimension Definitions	44
Table 8. Rascal Cross Sectional Dimensions.....	46
Table 9 Inertia Test – Displacement in XY Plane	49
Table 10 Inertia Test – Displacement in XZ Plane.....	50
Table 11 Inertia Test – Displacement in YZ Plane.....	50
Table 12. Damped and Undamped Frequencies of Oscillation	53
Table 13. Damped and Undamped Moments and Products of Inertia.....	53
Table 14. E193 Airfoil Data at $Re = 204,200$	61
Table 15. Engine Model Look up Table	63
Table 16. Estimated 16x8 Propeller Performance Data at 5000 RPM's.....	64
Table 17. Inputs to Digital Datcom; A Brief List	66
Table 18. Component Lift, Drag, and Moment Coefficients.....	71
Table 19. Rascal Stability Derivatives at Trimmed Steady Level Flight	72
Table 20. Flight Test and Simulation Flight Parameters	76

	Page
Table 21. Flight Path Components Variable Definition	83
Table 22. Example Trim Conditions for Given Velocity and Altitude.....	85
Table 23. Equations of Motion Initial Conditions for given Velocity	86
Table 24. Autopilot Waypoints Latitude, Longitude, and Altitude	97

DEVELOPMENT OF AUTONOMOUS UNMANNED AERIAL VEHICLE RESEARCH PLATFORM: MODELING, SIMULATING, AND FLIGHT TESTING

I. Introduction

1.1 – Background

The Department of Defense's (DoD) drive towards using autonomous Unmanned Aerial Vehicles (UAVs) of all sizes, and the visions of using them for almost any task leads the way for a more lethal and efficient force. In addition to providing a better platform for the dull, dirty, and dangerous missions, autonomous UAVs provide the possibility of performing tasks and missions that are not currently possible. For example, autonomous UAVs and micro-UAVs (MAVs) enable autonomous search and destroy, persistent combat intelligence, surveillance, and reconnaissance (ISR), and over-the-hill and around-the-corner reconnaissance using field deployed MAVs, just to name a few.

This increased interest in UAVs by the DoD has resulted in a rapidly growing number of organizations, both military and civilian, conducting research to develop fully autonomous UAVs. Small UAVs are of particular interest to many researchers, as they are relatively inexpensive, yet offer the ability to address a multitude of autonomous flight research applications that once seemed out of reach.

The Air Force Institute of Technology's (AFIT) Advanced Navigation Technology (ANT) Center has ongoing research in all areas of guidance, navigation, and control. Previously, much of the research conducted at the ANT Center was demonstrated

in simulation with an occasional flight demonstration at the USAF Test Pilot School at Edwards AFB, but there was no in-house flight test capability. However, the work presented in this thesis expanded the ANT Center's in-house research capabilities by developing autonomous UAV research platforms including a control design simulation, a hardware in the loop (HITL) simulation, and an autonomous UAV flight test platform and flight test program. Some of the current research being conducted at AFIT using the research platforms developed in this thesis include autonomous formation flight, collision avoidance, autonomous sensors platform, and advanced non-GPS navigation.

In general, modeling, simulating, and flight-testing of full scale aircraft is well documented. However, literature becomes less available when it comes to small UAVs. Few relevant articles discussing the detailed modeling, stability, and simulation development of small UAVs were found. The most notable researchers include Uy-Loi Ly and Shin-Ichiro Higashino of the Universities of Washington, Seattle, and Kyushu, Japan respectively. In 2003, Ly and Higashino conducted research similar to this thesis, but used full-scale aircraft wind tunnel data to build an aerodynamic model. In 2004, Ellis T. King, at the Massachusetts Institute of Technology, utilized a hardware-in-the-loop simulation and a small UAV model to demonstrate distributed coordination and control of a multi-UAV test bed. In 2001, Eric N. Johnson and Sebastien Fontaine at the School of Aerospace Engineering, at the Georgia Institute of Technology, experimented with simulation to compliment low-cost UAVs. All the aforementioned researchers conducted excellent work, but do not address the needs of this research; specifically, they

do not address the problem of developing high-fidelity simulation models for small UAVs.

Furthermore, a literature review reveals there are no specific standards for small autonomous UAV handling qualities. Current standards for handling qualities apply to only piloted aircraft. Without the pilot in the loop, the envelope for handling qualities surely expands, becoming less restrictive, especially for autonomous UAVs. Although handling qualities is not a direct goal of this paper, this research directly contributes to handling qualities determination. Researchers such as Foster (2005:3) also found a lack of relevant articles on the subject of UAV stability and handling qualities. Foster also stated there were “no direct relevant articles discussing dynamic stability and handling qualities for small UAVs.”

The research community does not clearly define the term *small* UAV. Foster and Bowman (2005:1) define a *small* UAV as one with a wingspan approximately 1.64 to 4.92 feet for purposes of their research. Capt Higgs (USAF) (2005:5) references a Micro Air Vehicle (MAV) with a two foot wingspan. Frew, et al, (2004:1) also characterizes a small UAV as one with a nine foot wingspan. The 2002 Unmanned Aerial Vehicles Roadmap, from the Office of the Secretary of Defense, states that small UAVs are those having a Reynolds number less than 1 million (Roadmap, 2002:62). The aircraft chosen for this research meets the Roadmap criteria for Reynolds number, shown later. For purposes of this research, UAVs with wingspans of 10 or fewer feet are considered *small*. For the remainder of the research presented in this thesis, the term *small* UAV is implied.

1.2 - Problem Statement

The ultimate goal of this research is to provide AFIT and the ANT Center with a well-documented and fully capable UAV research platform, including an autonomous UAV, a control design simulation, and a hardware in the loop simulation. The research platform will support a multitude of advanced guidance, navigation, and control research objectives. The problem statement has four parts. Part one, deliver a well documented, integrated and fully capable unmanned aerial vehicle system. Part two, accurately model the UAV's physical, inertial, and aerodynamic characteristics for simulation. Part three, develop a six-degree of freedom simulation in Matlab/SIMULINK incorporating the developed UAV model. In addition, in part three, set up a commercial autopilot Hardware in the Loop simulation for testing and training. Finally, part four, demonstrate both the open loop and autonomous flight-testing capability of the UAV system. Part four also includes developing flight-test procedures and maneuvers to fully characterize the airframe and autopilot. Furthermore, the flight test results obtained in part four should be used to validate the simulation results in part three.

1.3 - Research Objectives

- Develop a UAV test vehicle by integrating a commercial autopilot controller with a SIG Rascal 110 R/C aircraft, including calibration and ground testing of the complete system.
- Develop a physical, inertial, and aerodynamic model of the Rascal 110 for use in simulations. The use of classical airframe analysis as well as more modern techniques will be incorporated to improve the model's fidelity.

- Create a Matlab/SIMULINK simulation of the aircraft using the models developed. This simulation seeks to represent the aircraft's open loop flight characteristics for future control law design.
- Incorporate the Rascal 110 model into a Hardware in the Loop (HITL) simulation provided by the autopilot manufacturer. This simulation seeks to represent the aircraft's closed loop flight characteristics for use in test team training and bench testing flight tests.
- Demonstrate the performance of the UAV through flight tests and collect open and closed loop flight data that can be used to validate the simulations.

1.4 – Significance of Research

The significance of this research is the fact that it provides the AF Institute of Technology a foundation for future flight test capability. Prior to this research, no medium existed at AFIT for autonomous UAV flight test, and now a fully capable UAV and a well developed flight-test program is in place.

Providing future students a validated flight test program required overcoming significant hurdles. Rather than spending time building and evaluating the equipment, researchers can begin to collect valuable research data instead. The administrative approval to flight test autonomous UAVs at Wright Patterson Air Force Base (WPAFB) is now a complete and well-documented procedure. The well-understood autopilot controller and HITL simulation allow future students to spend more time on research than system set up and learning. The Rascal 110 is meticulously modeled with significant

documentation. Any user of this aircraft will save months of time that would have otherwise been spent measuring and analyzing the airframe.

While the Rascal 110 is widely used as a research platform, no aerodynamic data existed. Therefore, the aerodynamic model and simulation developed in this research will contribute to the UAV research community as a whole. Furthermore, future researchers will be able to apply the methods presented to develop aerodynamic models and simulations for any small UAV.

A complete six-degree of freedom, nonlinear differential equation simulation designed in Matlab/SIMULINK is now available. Control law design can move forward using the Matlab/SIMULINK design as the core for future research.

1.5 – Methodology

Methodology differed for each objective. The construction, integration, and set up of the autopilot and aircraft system extensively relied upon manuals from each respective manufacturer. Furthermore, the advice of local R/C experts and users of the same autopilot system was sought throughout the entire research program, especially early on. Physical, inertial, and aerodynamic modeling of the aircraft used well-established methods. Physical measurements of the aircraft were performed in the ANT Center lab. Inertia measurements followed the procedures established by NASA (formerly NACA) in the 1930's. Inertia was calculated by hanging the actual aircraft and timing prescribed oscillations. Aerodynamic stability and control coefficients were derived mainly from the use of the USAF Digital Datcom software. In addition to the software, classical techniques given in (Roskam, 1982:Ch 4), (Etkin and Reid, 1996:Ch

3), were used to aid in determining aerodynamic data. Then a Matlab/SIMULINK simulation was constructed by incorporating the model of the Rascal 110 into aircraft force and moment equations, which are required for the nonlinear, six-degree of freedom equations of motion.

The forces, moments, and equations of motion are called by the SIMULINK software, and simulated over a specified length of time. The resulting aircraft states are then plotted. The SIMULINK program is capable of accepting elevator, aileron, rudder, and throttle inputs. This allowed the user to input the identical control surface deflections that were input during actual flight test; the output was compared against flight test data to validate accuracy of the simulations. Flight-testing the UAV at AFIT required a minimum five-person test team. The guidelines for UAV flight at Wright Patterson were in-place, but still required extensive administrative approval procedures. Open loop flight test methods followed classical techniques for exciting longitudinal and lateral modes of the aircraft. These techniques were readily found in textbooks such as Kimberlin (2003). However, performing these techniques on UAVs was not discussed. Therefore, the full-scale aircraft test techniques are applied to the UAV. The methodology for autonomous flight-testing followed the procedures recommended by the autopilot manufacturer. These procedures included calibration in the lab, simulation, followed by a meticulous systematic method of activating the autopilot. The incremental procedure tuned gains for each of the autopilot's control loops. Telemetry available from the autopilot will be used for analysis of both the open loop and autonomous flights. The telemetry was manipulated in both Excel and Matlab/SIMULINK.

1.6 – Preview

Chapter II takes an in-depth look at the equipment used and provides some background on flight-testing. To build an accurate model, Chapter III methodically steps through complete collection and development of the physical, inertial, and aerodynamic characteristics of the aircraft. Chapter IV then covers the development of the Matlab/SIMULINK and Hardware in the loop simulations. Chapter V details the development of the open loop and autonomous flight tests procedures specific to flight test of the Rascal 110. Chapter VI compares results from the Matlab/SIMULINK simulation to the open loop flight tests and the HITL simulation. An additional comparison of the HITL simulation to the autonomous flights was also performed. Chapter VII includes the conclusions and recommendations.

II. Background

2.1 - Overview

Chapter II describes background information on equipment used and the basic flight test procedures. It also provides the reader necessary information in order to fully understand and appreciate the remaining chapters. First, the aircraft, engine, and propeller used for flight test are discussed. Details concerning the avionics are also included. Second, flight test of the Rascal 110 UAV is discussed. Details concerning open-loop and autonomous flight test, as well as the airspace, equipment, and procedures developed and used are included. The chapter concludes with a detailed overview of flight-testing, setup, procedures for autonomous flight, and telemetry collection and handling.

2.2 – Aircraft

2.2.1 – Airframe

The aircraft chosen as the research platform was the Rascal 110 R/C aircraft constructed by the SIG Manufacturing Company, Inc. It was chosen for its cavernous interior, stable flight characteristics, and use by other research institutions around the United States. The University of California-Berkeley's Center for Autonomous Intelligent Networks and Systems and Center for Collaborative Control of Unmanned Vehicles has utilized up to three of the Rascals in research of vision based road following using small autonomous aircraft (Ryan, et al, 2005:1). Dr. Eric Frew from the University of Colorado, and formerly from the University of California-Berkeley has also conducted

vision based navigation work with the SIG Rascals (Frew, et al, 2004:1). The Rascal 110 is a high wing, tail wheel configured aircraft, commonly referred to as a tail dragger. The manufacturer constructed the aircraft of plywood, balsa wood, aluminum, and fiberglass and covered it with polyester film. Additionally, with a few modifications, the aircraft was upgraded with a 50 oz fuel tank, pushing the flight time to nearly two hours.

According to the manufacturer, the Rascal uses an airfoil married from two Eppler airfoils. The top airfoil is an Eppler 193, while the bottom is an Eppler 205, joined at the chord lines. The manufacturer further stated the resultant section is 11.5% of the root chord and the aspect ratio is 6.875:1, although Aspect Ratio calculations resulted in a higher value, see Section 3.2. Stability, performance, weight, and balance data was not available from SIG and had to be determined during the course of this research. Chapter III includes detailed aircraft data.

The Rascal is an Almost Ready to Fly (ARF) R/C aircraft, meaning the manufacturer preassembled major aircraft components at the factory prior to shipping. Despite this feature, the aircraft required about 40 hours to assemble and configure for flight-testing. Figure 1 shows two of the AFIT Rascal 110's being prepared for flight.



Figure 1. Rascal 110's Out for Preflight Checks

2.2.2 – Engine and Propeller

The aircraft is powered by the FS-120S III four-cycle engine by O.S. Engines. Equipped with a diaphragm fuel pump, matching carburetor, and built in pressure regulator, it output 2.1 brake horsepower at 12,000 revolutions per minute (rpm) and displaces 1.218 cubic inches (20 cc) (Engine Manual, 2000:5). The engine was fitted with a 16 x 8 propeller from APC. Combined, the engine and propeller weighed was 32.5 ounces and was capable of pulling the SIG Rascal 110 over 60 knots on a calm day.

2.3 – Avionics

The avionics incorporated into the Rascal 110 for flight test has four main components, the basic R/C system and Servo Actuators, the Piccolo Autopilot System, and Fail Safe Control Relay.

2.3.1 – Radio Control System

The R/C system is a Futaba 9CAP/9CAF 8 Channel transmitter with a Futaba R149DP PCM 1024 receiver. High torque servos from Futaba actuated the control surfaces.

2.3.2 – Piccolo II Autopilot

The autopilot system, acquired commercially from Cloud Cap Technologies, includes the airborne avionics, Ground Station Interface, manual control box, hardware in the loop simulator, and software. The airborne component, the Piccolo II, is a fully autonomous autopilot system for small-unmanned aircraft. Built around a Motorola MPC555 microcontroller, which processes inputs through a Reduced Instruction Set Computer (RISC), the Piccolo II delivers 40 MHz PowerPC operation (Vaglienti, Hoag, and Niculescu, 2005:7). Piccolo II incorporates three gyros and two two-axis accelerometers for rate and acceleration measurements. To calculate true airspeed (TAS), absolute altitude, and outside air temperature, the Piccolo II collects air data through a dual ported 4kPa dynamic pressure sensor, an absolute ported barometric pressure sensor, and a board temperature sensor (Vaglienti et al. 2005:7). Winds aloft are calculated by comparing GPS Ground Speed and TAS when the aircraft turns. A Kalman filter estimates aircraft attitude and gyro bias, which uses the GPS-derived pseudo-attitude as the measurement correction (Vaglienti et al. 2005:7). Command and control, autopilot telemetry, payload data transfer functions, differential GPS corrections uplink, and pilot in the loop modes are data linked through a 1W 900MHz and 1W 2.4GHz radio modem at up to 40 Kbaud of throughput (Vaglienti et al. 2005:7). The GPS receiver

from u-Blox, the TIM-Low Power, is a 16 channel receiver with 8192 simultaneous time-frequency search bins and a 4Hz position update rate (u-Blox, 2005). The Piccolo II measures 2 inches wide by 2.5 inches high and 5.25 inches deep. Electromagnetically shielded carbon fiber encases the electronics. Figure 3 illustrates the entire block diagram layout of the avionics inside the Piccolo II and Figure 4 pictures the carbon case with faceplate and air and data ports.

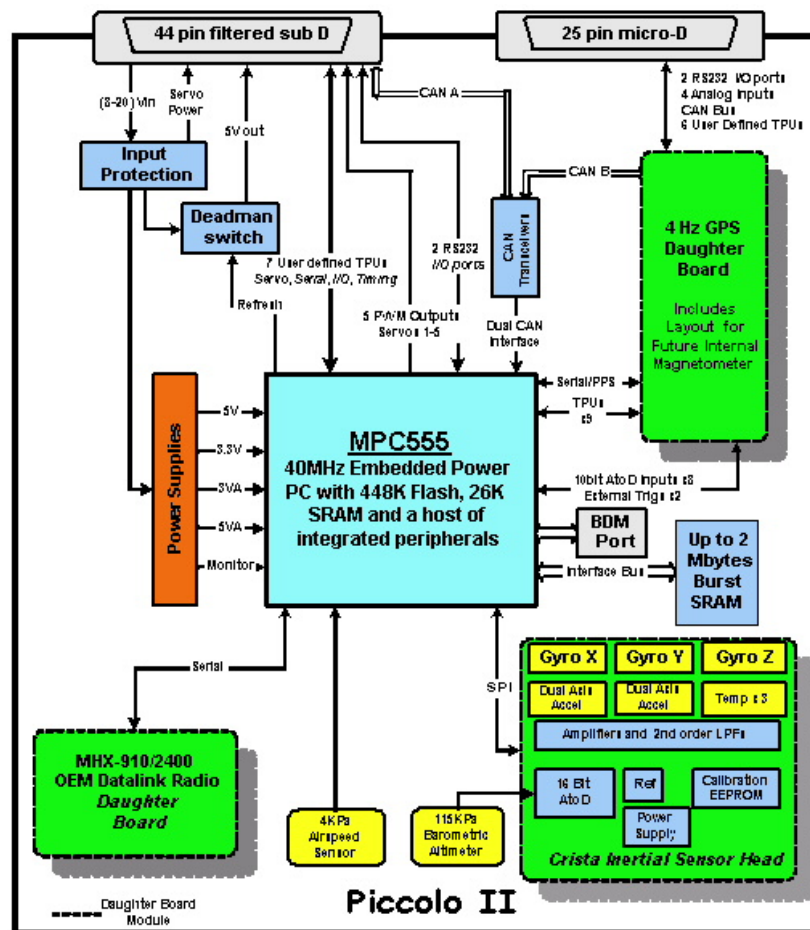


Figure 2. Piccolo II Block Diagram (Vaglienti et al. 2005:6)



Figure 3. Piccolo II Airborne Avionics Package (Vaglianti et al., 2005:9)

The ground-based equipment of the autopilot control system included a manual R/C control box, Ground Station Interface, UHF and GPS antenna, and a laptop. The manual R/C control box allows for a direct pilot in the loop interface with the aircraft, sending manual commands through the Ground Station to the Piccolo. The laptop Operator Interface software is the command station for the Piccolo during autopilot mode. The Operator Interface is the primary interface with the Piccolo both on the ground and in the air. The laptop interface monitors and controls telemetry, tracking, ground and airborne equipment status, commands, calibrations, gains settings, and a host of other parameters.

The laptop operator transmits commands to the Piccolo during flight for specified maneuvers or waypoints. Detailed information about the Operator Interface can be found

in the Piccolo System User's Guide Version 1.3.0 from Cloud Cap Technology, written by Vaglienti et al. (2005).

The Ground Station Interface acts as the communication link between the manual R/C control box, the Operator Interface Laptop, and the Piccolo. The ground UHF and GPS antennas also plug into the Ground Station Interface. The entire Ground Station Interface set is pictured in Figure 4.

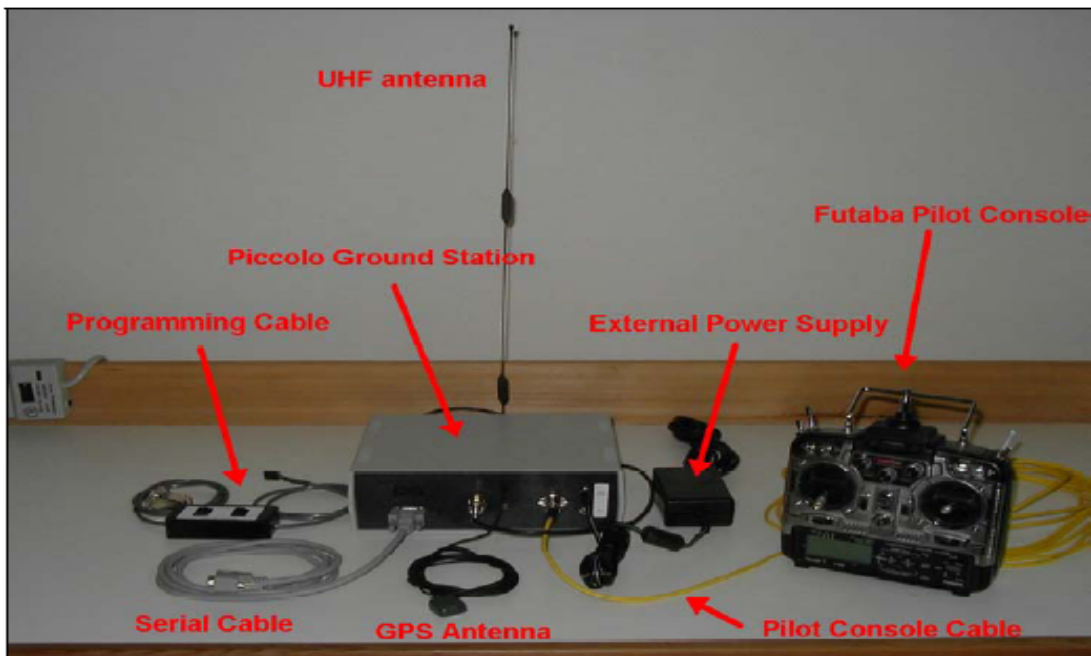


Figure 4. Ground Station and Pilot Control Box (laptop not pictured)

2.3.3 – Fail Safe Control Relay

The Air Force Research Labs Sensors Directorate (AFRL/SN) constructed the Fail Safe Control Relay. Its function allowed the R/C pilot to toggle control between the autopilot system and the R/C system, and to toggle automatically if control signals drop below predetermined levels. This added security ensures redundant control in the event of a total failure of either the R/C transmitter or autopilot system. For example, if under control of the R/C transmitter and the signal were lost to the R/C receiver, the relay would automatically switch to the autopilot controller, and vice versa. William J. Schmoll and Richard Marker of AFRL/SN designed the system and ExpressPCB manufactured the flight hardware. Operationally, the relay receives inputs from the R/C receiver and the autopilot; inputs A and B respectively (see Figure 5). Schmoll and Marker (2005) describe the system in detail;

The channel 8 output of receiver A goes to the monostable multivibrator 74C221 trigger. The 15k ohm resistor, the 5k ohm potentiometer, and the 0.2 uF capacitor form the external timing circuitry for the 74C221. The multivibrator is adjusted by the 5k ohm potentiometer for exactly 1.5 milliseconds. The channel 8 pulse also goes to the 74C175 flip-flop's "D" input. When the monostable pulse ends (goes low) the output of the 74C175 is latched in the state of the channel 8 pulse. If the channel 8 pulse is longer than 1.5 msec then the 74C175 output will be high and if shorter than 1.5 msec then it will be low. The output of the 74C175 goes to the select inputs (pin 1) of the 74C157 data selector chips. If "Select A/B" is low, receiver A (R/C) is selected and if high then receiver B (autopilot) is selected.

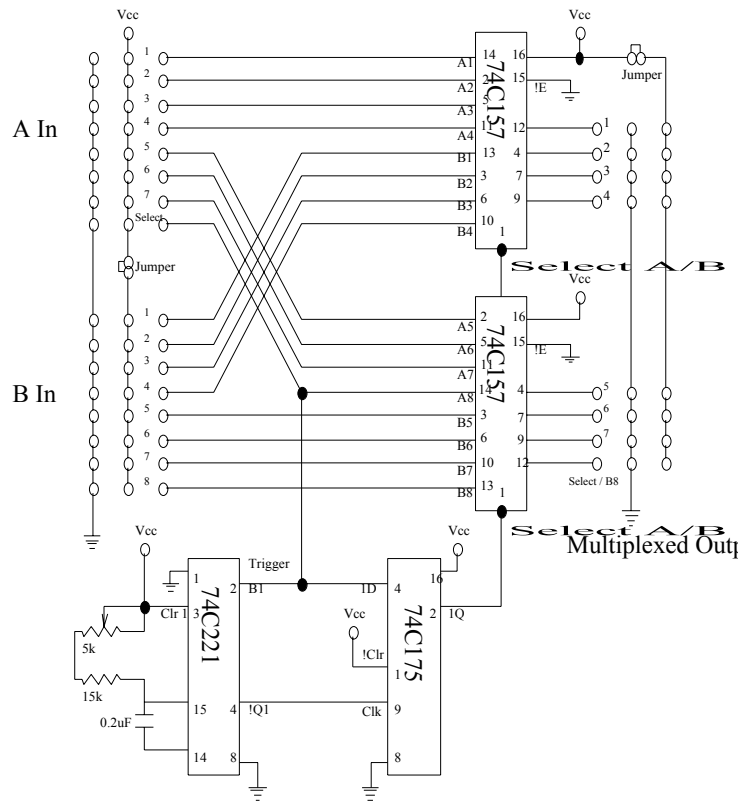


Figure 5. Fail Safe Control Relay (Marker, 2005)

The following block diagram depicts the entire air and ground avionics, signal, and power paths (see Figure 6).

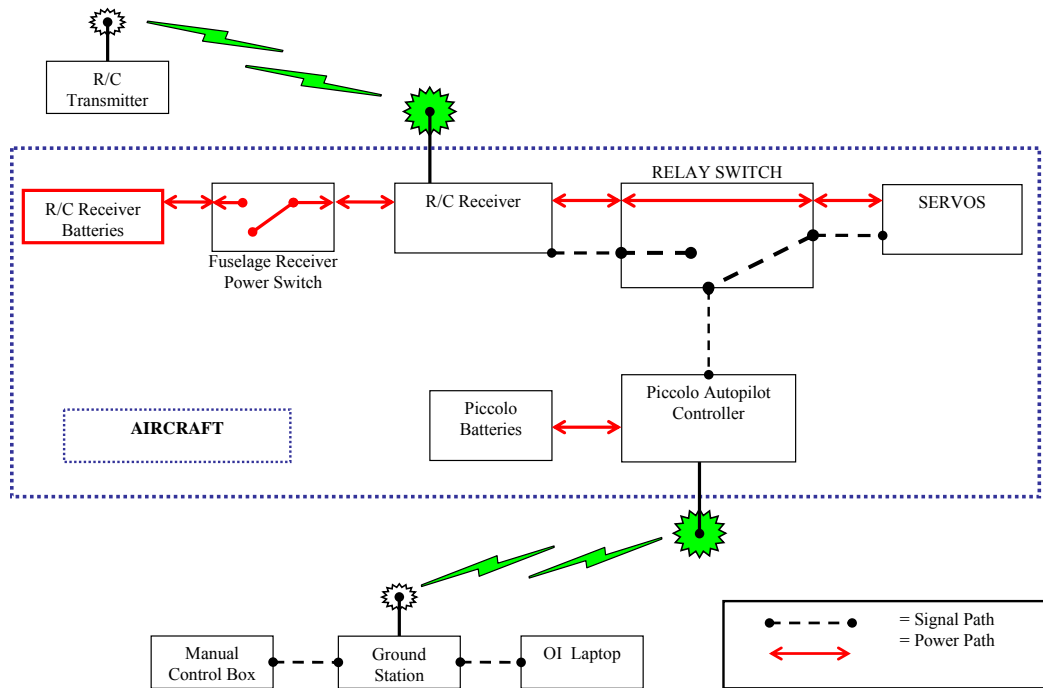


Figure 6. Ground and Airborne Avionics Flow Diagram

2.4 – Flight Testing

2.4.1 – Overview of Flight Test

The flight-testing of aircraft is a well-documented engineering procedure. However, every aircraft tested is unique and presents different challenges to engineers, pilots, and test team. The same can be said about UAVs. The criteria for UAVs can be dramatically different from manned aircraft.

Flight-testing a UAV such as the Rascal 110 proved to be a challenging task. The R/C pilot had over 20 years of radio controlled flight experience and thus hundreds of “first flights” of newly assembled aircraft. The commercially available Rascal 110 was a proven design, but it still required meticulous care during assembly and, of course, a maiden voyage. Airworthiness flights checked for controllability, stability, and overall performance. Engine break in time was also required per the manufacturer. A series of basic maneuvers; slow flight, coordinated turns, loops, rolls, touch and go’s, and landings were performed over three different flights, totaling about two hours of flight time. The aircraft configuration for open loop and autonomous flight tests included the aforementioned engine, propeller, fuel tank, and avionics package. The aircraft used a 20% nitromethane 2/4 Stroke fuel with 18% synthetic oil. This period of initial flights was also essential for pilot familiarity, actuator and control surface adjustments, and throttle settings. Having proven a stable and capable R/C aircraft, the vehicle was now ready to be equipped with avionics for telemetry gathering for basic airframe and autonomous flight-testing using common flight test procedures. The previously described autopilot controller, the Piccolo II, and the Fail Safe Control Relay were now installed on the aircraft. The transition from R/C aircraft to autonomous UAV begins here. Chapter V details the flight test procedures for both airframe and autopilot tests.

Autopilot controllers use feedback control loops to maintain desired aircraft states (e.g. velocity, altitude, etc). With the control loops turned off, the autopilot has no information about the aircraft’s current state. Thus, when the control surfaces receive

commands, the aircraft behaves in an open loop condition, meaning the response to the command is purely the aircraft's natural response.

Robert Nelson (1998:236) classifies control systems as either open loop or closed loop controllers. In an open loop system, the control input is independent of the system output or response. In closed loop systems, the system output influences the input command. Autopilot controllers are closed loop control systems. According to Nelson, 1998:236, closed loop systems, also known as feedback systems, are more accurate than open loop, because of feedback between system output and input. Calculating the difference between the output and input signals, an *error* is determined. If output matches the input, the error equals zero, and the current input is maintained. If the desired input and the resultant output differ, an error exists. The input is adjusted accordingly to reduce the error. Since open loop systems do not account for any error between the input and output, the natural system response can be observed, without the influence of feedback control. Nelson provides Figure 7 to illustrate the difference between the open loop control system and the closed loop control systems.

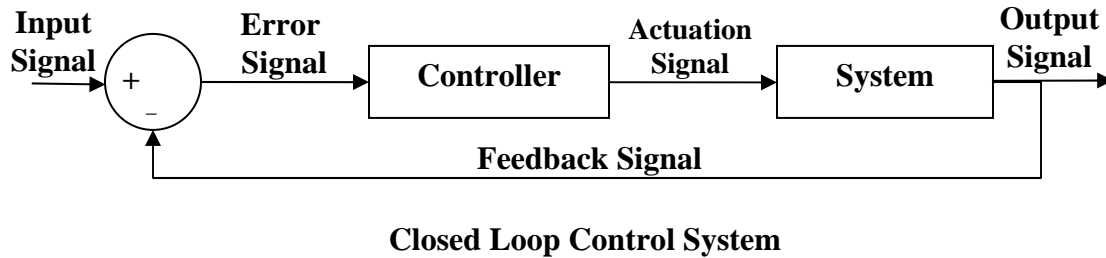
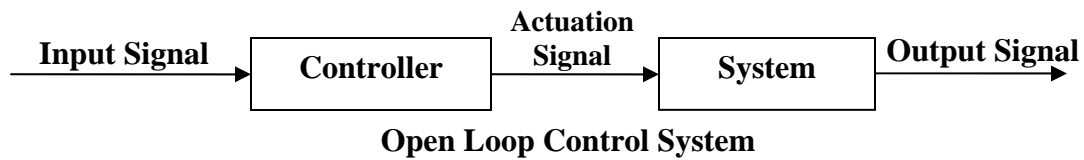


Figure 7. Open and Closed Loop Control Systems

Open loop flight test seeks to capture the natural system response to prescribed control inputs. Flight tests without feedback control can reveal the natural response of the aircraft at different airspeeds, altitudes, and configurations. Any significant flaws or undesired responses in the aircraft performance are visible. The aircraft is classified as a stable or unstable system depending on its open loop response. Feedback controllers can improve some undesirable aircraft characteristics.

2.4.2 – Flight Dynamics

Many excellent texts are available on the subject of aircraft stability, and a brief review will now follow. Open loop flight tests capture different aircraft information along different axes. Aircraft motion is categorized as longitudinal and lateral directional. First, the longitudinal degrees of freedom are translation along the x- and z-axis, and rotation (pitch) about the y-axis. Figure 27, in section 4.2.1, illustrates the axes

of an aircraft. All longitudinal motion occurs in the xz-plane of the aircraft. Stability along the longitudinal axis is both static and dynamic. John Hodgkinson (1999:21) defines longitudinal static stability as “the tendency of the airplane to return to pitch equilibrium following an angle of attack disturbance.” Static stability is the aircraft’s initial response to an input command. In the case of flight test, aircraft considered statically stable immediately tend to return to its steady level flight condition. When viewed over time, the aircraft is dynamically stable if it tends to return to steady level flight condition (Nelson, 1998:40).

Examining two oscillatory motions along the longitudinal axis, Dr. Ralph D. Kimberlin (2003:235) explains the first as the long period motion, or phugoid, a lightly damped oscillation of low frequency. The phugoid mode of oscillation is essentially a gradual exchange of potential and kinetic energy, in other words, a slow altitude and airspeed oscillation at near constant angle of attack (Kimberlin, 2003:238). Kimberlin also describes the second longitudinal motion, the short period, as a well-damped mode of oscillation of fairly high frequency. The aircraft’s elevator directly affects both the phugoid and short period modes of oscillation. Nelson (1998:148) illustrates the phugoid and short period motions in Figure 8.

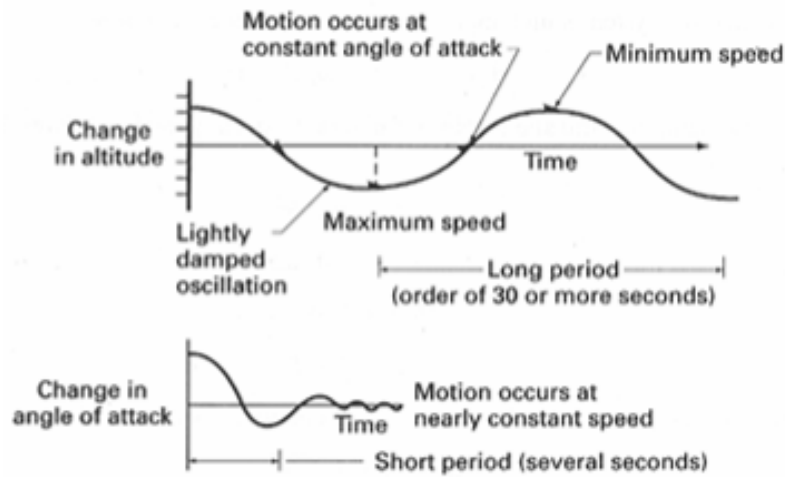


Figure 8. Phugoid and Short Period Motion

The next two paragraphs examine the aircraft's lateral-directional motion. The three degrees of freedom of the lateral-directional dynamics are roll about the x-axis, yaw about the z-axis, and side translation about the y-axis. Authors usually consider the longitudinal motion to be of primary concern, while placing slightly less emphasis on lateral motion (Hodgkinson, 1999:87). Due to time and weather constraints, examining both longitudinal and lateral-directional motion was impractical; and since the Rascal 110 UAV is not aerobatic by design, nor is it expected to do highly complex maneuvers in the future, the primary focus of this research was on the longitudinal-directional motion.

Hodgkinson (1999:89) states an aircraft is stable in lateral motion if an increment of sideslip angle results in a restoring moment and side force. The two control surfaces that typically affect the lateral motion include the ailerons and rudder. The lateral-directional dynamics consist of three primary motions, a relatively high frequency

oscillatory motion called dutch roll, a rapid mode known as the roll mode, and a more neutrally stable spiral mode.

To characterize the flying qualities of the aircraft, recommended maneuvers excite specific longitudinal and lateral-directional modes. Many authors describe very similar maneuvers to excite each mode of an aircraft. Kimberlin (2003:248) describes the suggested maneuvers clearly and concisely, and a brief explanation follows. To evaluate the phugoid mode, the aircraft is flown at a trimmed steady level flight condition. Then, using elevator control, the pilot displaces the airspeed by 17 – 25 feet per second. The recommended airspeed displacement is typically for full-scale conventional fixed wing aircraft and not necessarily for UAV's. Recall from Chapter I, little research on UAV flying qualities flight test was available. Once displaced, the elevator is returned to the trim position and the resulting oscillations recorded. The aircraft is allowed to oscillate with the elevator either fixed in the trim position or floating freely. Since it is not possible for the UAV's control surfaces to float freely, all UAV control surfaces are held fixed during the aircraft oscillations.

Three methods excite the short period mode according to Kimberlin (2003:250) the doublet input, pulse input, and 2-g pull up maneuver. Kimberlin states the doublet input is the best to evaluate the short period while suppressing the phugoid. The pilot first trims the aircraft in steady level flight prior to rapidly controlling the nose down, nose up, and then back to trim condition (Kimberlin, 2003:250). The elevator is then fixed in the trim position during the resultant oscillations. To find the best oscillatory response, Kimberlin recommends varying the amplitude and frequency of the doublet

input to the elevator. Different airspeeds and headings may also produce different responses. Typically for the phugoid and short period, the altitude and elevator deflections are recorded, although information about longitudinal dynamics is also available in angle of attack, pitch rate, and airspeed responses.

Again, Kimberlin (2003:322) recommends a doublet command to excite the dutch roll mode. Unlike the short period doublet command to elevator, the doublet command to the rudder excites the dutch roll mode. As in previous maneuvers, the aircraft starts in trimmed steady level flight, followed by moving the rudder left and right in phase with the natural motion of the aircraft. At the completion of the doublet input, the rudder is returned to the trimmed position and held fixed. Telemetry equipment must continuously record the sideslip, bank, and rudder deflection angles through out the maneuver.

Finally, Kimberlin (2003:322) explains methods to excite the spiral mode. Begin with trimmed steady level flight, holding the ailerons and elevator fixed, and banking the aircraft 5° with rudder. Return the rudder to the trimmed position and record bank angle versus time. Military specifications state the bank angle should double in 20 seconds for small disturbances in the lateral mode (Kimberlin, 2003:322).

2.4.3 – Flight Test Range

All flight-testing was completed at Wright Patterson Air Force Base (WPAFB), Area B, in Dayton, Ohio. This area proved to be an invaluable resource due to its proximity and familiarity to the test team. Once known as Wright Field, and full of aviation lore dating back to 1927, history marks this airfield as the center of military

aviation research and engineering. US Air Force Flight testing was originally taught and performed here, making it only appropriate to continue that legacy.

The airspace appropriated to the test team measured approximately one and one half mile in length by one-quarter mile in width and a ceiling of 400 feet above ground level. Field elevation is 785 feet above sea level at the center of the runway. Figure 9 shows WPAFB, Area B with the allotted airspace boundaries. The test range is a multi-use facility; AF Research Laboratory Sensors Directorate (AFRL/SN) performed scheduling and range clearance. Autonomous UAV flight-testing is certainly not a new phenomenon to this airfield. The AFRL/SN conducts regular flight tests of UAV's, including conventional fixed wing and rotary wing aircraft. Autonomous research flights include multiple aircraft as well. For example, the 2005 AFRL/SN Small UAV Persistent Visualization for Operational Response tests used the same airspace as the Rascal and AFIT test team (Wilson, 2005).



Figure 9. Flight Test Range (Dashed Line) at WPAFB Area B

2.4.4 – Ground Equipment

The ground equipment included a 20-foot trailer that acted as a base station for all flight tests. The Ground Station Interface operator worked on the Operator Interface laptop from the trailer. An external gasoline powered generator provided power to run the laptop, battery charging equipment, and Ground Station. Additional equipment mounted to trailer's roof included the windsock, GPS, and UHF antennas. Folding tables and chairs, and two Rascals fit nicely into the trailer when packed. Miscellaneous equipment included an R/C toolbox, headset based two-way radios, RF meter/scanner, cones, fire extinguisher, spill kit, first aid kit, video camera, battery testers, and a handheld GPS unit. Figure 10 shows the open end of the trailer with test team. The pilot, of Wyle Laboratories, (left) on a two-way radio headset with the test conductor (center,

with headset). The test team included Test Director, Safety Officer, Pilot, Ground Station Operator, Spotters and Observers.



Figure 10. Ground Equipment and Test Team during Flight Tests

2.4.5 - Criteria for Flight Test of UAVs at WPAFB

Certain flight test conditions and safety of flight criteria constrained flight-testing at WPAFB, Area B. The test team completed a thorough review of the equipment and flight test plans by an external process. A Configuration Control Board (CCB), Technical Review Board (TRB), and Safety Review Board (SRB) conducted by AFIT and AFRL personnel provided an external assessment of the planned procedures and flights. Controlled airspace, proximity to residential areas, and test team and equipment

safety necessitated a thorough program review. The CCB, TRB, and SRB, required the test team develop detailed procedures and criteria for conducting flight test.

Detailed pre-departure, fail safe, and preflight checklists ensured meeting all flight test criteria. Based on experience and suggestions from the AFRL/SN flight test team, Cloud Cap Technologies, resident flight-test engineers, and R/C pilots, the checklists encompassed nearly every facet of proper preparation for any flight test.

Checklist items included battery checks, airfield notification, radio frequency checks, weather minimums, fail safe checks in all possible modes, GPS satellite acquisition, gyro operation, control surface operation, and many more. Table 1 lists a few of the major criteria for flight.

Table 1. Example of Selected Criteria for Flight Tests

Winds Less than 40 mph
Temperature Greater than 40° F
Visibility Greater than 3 Miles
Cloud Ceiling Minimum 500 ft AGL
Airspace Ceiling Maximum 400 ft AGL
GPS Satellites 6 or more visible
Radio Frequency Interference Check
Safety Equipment and First Aid Kit
Pitch, Roll, and Yaw Rate Gyro Operations
Static and Dynamic Pressure Port Operation
WPAFB Control Tower Notification

2.4.6 – Autopilot Tuning – Transformation from R/C to Autonomous UAV

Prior to conducting autonomous flights, the autopilot system went through a series of tuning procedures necessary to ensure the autopilot was properly calibrated.

Calibration flights included establishing trimmed flight condition and gain tuning, a required procedure prescribed by the autopilot manufacturer (Initial Flight Test Cards, 2005). When establishing a trimmed flight condition, the aircraft, flown under manual control, was established in a steady level unaccelerated flight condition while the Operator Interface records the current control surface deflections and throttle setting. These steady level flight conditions occur when the lift of the vehicle equals the weight, drag equals thrust, and the roll, pitch, and yaw moments are zero. Wind conditions, airspeeds, and fuel payloads vary prior to some flights and necessitate a trim pass prior to activating the autopilot.

The gains of the autopilot control loops required fine tuning prior to allowing the autopilot to have full control. The Piccolo II employs ten control loops to manage the aircraft in full autopilot mode. The control loops are Dynamic Pressure, Altitude, Altitude 2, Roll, Pitch, Yaw, Turn, Turn Compensator, Line Tracker, and Adjust Speed. Each loop employs some combination of proportional, derivative, and integral control. According to Vaglianti et al. (2005:44), the Dynamic Pressure control loop varies the speed of the aircraft with elevator by pitching over to gain speed and pitching up to slow. It also damps the long period oscillations. Vaglianti et al. (2005:44) recommend not using the Yaw Rate to Aileron since the Roll to Aileron gains “do a better job of managing the turn rate of the vehicle.” The Altitude to Throttle loop sets and feeds back

the vertical rate command and the vertical rate error to throttle. Line Tracker directs the aircraft to a preset waypoint. Heading error is fed back to the turn rate command. The Roll to Aileron loop is the primary method of controlling the aircraft turn rate by feeding back bank angle error to the ailerons (Vaglienti et al., 2005:45). Similarly, the Pitch to Elevator control loop feeds back pitch angle errors to the elevator. The Yaw Rate to Rudder loop feeds back yaw rate to the rudder (Vaglienti et al., 2005:45). The Altitude to Elevator terms are not usually required, but Vaglienti et al. (2005:45) suggest using it if tight altitude control is required. Finally, the Turn Compensator employs the bank angle to both elevator and throttle. The bank to elevator keeps the nose up through a turn by moving the elevator to affect the change in load factor dictated by the bank angle (Vaglienti et al., 2005:45). They also suggest using equation 1 to determine this value. The Piccolo manufacturer performs all calculations in metric units, but for purposes of this paper, English units are used.

$$\text{Bank to Elevator term} = \frac{W}{S_w \frac{\delta CL}{\delta E}} \quad (1)$$

where,

$$\begin{aligned} W &= \text{Weight (lbf)} \\ S_w &= \text{Wing Area (ft}^2\text{)} \\ \delta CL/\delta E &= \text{Change in lift coefficient per change in elevator.} \end{aligned}$$

For the Rascal,

$$\begin{aligned} W &= 17 \text{ lbf} \\ S_w &= 10.56 \text{ ft}^2 \\ \delta CL/\delta E &= .0049 \\ \text{therefore, Bank to Elevator} &= 328. \end{aligned}$$

Bank to throttle, maintains the energy state of a vehicle through a turn. Vaglianti et al. (2005:45), say the term represents the needed change in throttle to balance the increased drag due to change in load factor. Again, Vaglianti et al., 2005:45 supply an equation (2) to calculate this term.

$$\text{Bank to Throttle term} = \frac{W}{\pi e AR \frac{\delta P}{\delta T}} \quad (2)$$

where,

$$\begin{aligned} W &= \text{Weight (lbf)} \\ e &= \text{Span Efficiency Factor (1 for elliptical wings)} \\ AR &= \text{Aspect Ratio} \\ \delta P / \delta T &= \text{Change in power (Watts) per throttle motion.} \end{aligned}$$

For the Rascal,

$$\begin{aligned} W &= 17 \text{ lbf} \\ e &= .7 \text{ (estimated)} \\ AR &= 7.95 \\ \delta P / \delta T &= 150 \\ \text{therefore, Bank to Throttle} &= 0.02. \end{aligned}$$

The procedure of setting each of these terms proved to be an in-depth process. The procedure will be summarized here, but for further details the reader is encouraged to reference Cloud Cap Technology's Initial Flight Test cards, April 20, 2005. The Initial Flight Test Cards allow the user to methodically determine and tune the autopilot control loop gains. Setting the best possible gains ensures tightest waypoint tracking, altitude

and airspeed holds, and smoothest transitions to and from climbs, descents, and turns. The Initial Flight Test Cards are seven distinct procedures to verifying performance of the 1) Data link, 2) Turn Rate Control, 3) Airspeed Control, 4) Pitch Damper, 5) Altitude Control, 6) Tracker Control, and 7) Yaw Damper Control. All the control loops are initially disabled. Performing the test cards sequentially enables and validates each loop. The first, Datalink validation, ensures proper operation and telemetry reporting of the GPS, airspeed, altitude, gyros, and attitude data. Test Card 2, Turn Rate Control Validation checks the performance of the aircraft in a turn. Test Card 3 validates airspeed control. Smooth airspeed transitions without oscillations indicate good gain settings. Test Card 4 validates the pitch oscillations damp out and the nose stays up. Test Card 5 validates altitude gain settings allow smooth throttle changes without oscillation. Climbs and descents should be smooth with little to no overshoot. In conjunction with turn rate control, Test Card 6 validates the waypoint tracking control. Finally, Test Card 7, Yaw Damper control works best for unusual wing-body-tail configured aircraft. The Yaw Damper control loop was disabled during flight on the Rascal and Test Card 7 was not performed. Figure 11 shows the gain settings page of the Operator Interface with the results of the Test Cards for the AFIT SIG Rascal configured aircraft.

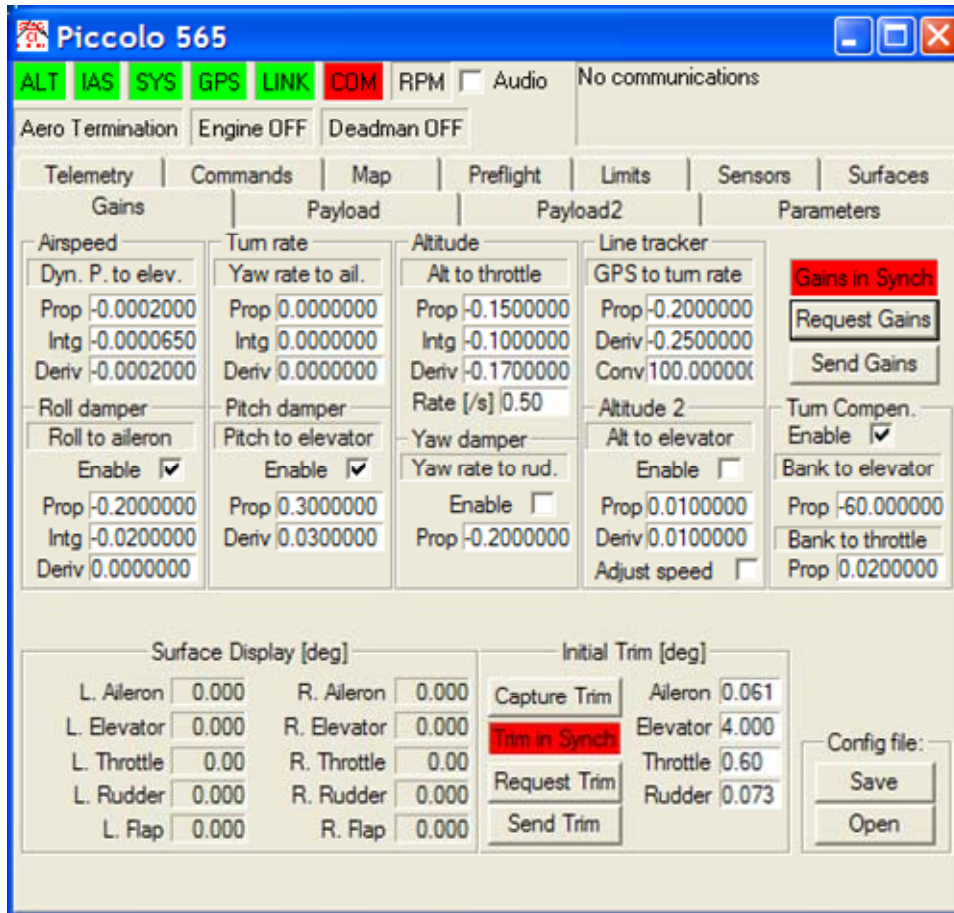


Figure 11. Screen Shot of Operator Interface with Gains Page Opened.

2.4.7 – Data Collection and Handling

Telemetry from the Piccolo II autopilot is stored on the Operator Interface Laptop in both ASCII and binary format. The analysis used in the research employed the ASCII format. The system measured and logged 70 parameters of data at either a 1 or 20 Hz rate. During the 20 Hz sampling, telemetry files can grow to over 20 Mb for a 30 minute flight. All flight tests were performed at the higher data-recording rate of 20 Hz. The raw

telemetry data was available for viewing and analysis only at the conclusion of a flight, and after the Ground Station and Operator Interface were turned off.

Opened in Microsoft Excel, the telemetry is displayed in column format with column headings for each measured parameter taken at specified time intervals. Once displayed, data cells that included any text, other than the column headers, were deleted. Deleting text facilitates a smooth transition into Matlab for further analysis. Not all 70 parameters, such as battery voltage or outside air temperature, are needed for a thorough analysis of the aircraft's performance, so cutting entire columns saved memory, made files smaller, and ultimately easier to manage. Entire rows were also shaved for instances when the aircraft was on the ground and the telemetry still being recorded. Otherwise, a complete telemetry log easily filled spreadsheet 60,000 rows by 70 columns, or 4,200,000 individual data cells. Once trimmed to a more manageable size of 37,000 rows by 50 columns or 1,850,000 data cells, it was sent to Matlab. The Excel spreadsheet of telemetry data was imported to Matlab as individual vectors that are automatically named after each column heading. Note: This can be done in the Matlab Workspace by selecting the "Load Data" button and choosing the Excel file. The larger files slowed Matlab, but eventually an Import Wizard appears. Select "Create vectors from column headings," and verify all column headings appear as vectors. Select finish, and now all the data is available for analysis. Save all the vectors collectively as one "*.mat" file. Table 2 provides a list of the more significant parameters available in the telemetry files.

Table 2. Example Available Telemetry from Piccolo II Autopilot Logs

1. System Time in milliseconds (From power up of Operator Interface and Ground Station)
2. Current Day, Month, Year, Hours, Minutes, and Seconds from GPS
3. Latitude and Longitude (rads)
4. GPS Height above Sea Level (m)
5. GPS Ground Speed and Pitot Static Airspeed (m/s)
6. Various Autopilot, Servo, and Battery Health Status parameters
7. Barometric Altitude above sea level (m)
8. Static and Dynamic Pressures (Pa)
9. Pitch, Roll, and Yaw Rates (rads/sec)
10. X, Y, and Z Axis Accelerations (m/s/s)
11. Pitch, Roll, and Yaw Angles (rads)
12. Throttle Position (1 = Full Throttle, 0 = Cut Off)
13. Elevator, Aileron, and Rudder Positions (rads)
14. Autopilot Command Status (On/Off)
15. Current Altitude, Turn, Waypoint, Airspeed, and Flap Setting Commands

2.5 – Chapter Conclusion

By presenting the available equipment and research infrastructure, the reader can fully understand the remaining chapters of this report. The aircraft, a SIG Rascal 110 R/C aircraft, outfitted with 1.218 cubic inch motor, a 16 x 8 propeller, larger fuel tank, and the Piccolo II autopilot, act as the flight test bed for the research. The avionics package, including the Piccolo II, incorporated a fail-safe relay and a commercial R/C

transmitter and receiver. The autopilot ground equipment collected the telemetry from the Piccolo during flight. Flight-testing was performed at Wright Patterson AFB, Area B. Post flight analysis of the telemetry was performed in Matlab and Excel. Matlab/SIMULINK was also used to build the aircraft simulation.

III. Development of UAV Physical, Inertial, and Aerodynamic Simulation Model

3.1 – Chapter Overview

An accurate representation of the Rascal 110 in the Matlab/SIMULINK and Hardware in the Loop (HILT) simulations required precise physical and aerodynamic data. Physical measurements, CG, inertia, throttle and control surface calibrations were performed manually in the lab. While the airfoil model, engine and propeller model, and stability and control derivatives were performed using analytical software. The following sections detail each of the measurements or calculations, methods and equations, software inputs, and results. In general this Chapter is also a guide for modeling any future small UAV.

3.2 – Physical Measurements and Mass Properties

The aircraft employs a high-wing semi elliptical planform. The term ‘semi-elliptical’ is used since the trailing edge and tips of the wing resembles that of an elliptical wing, but it has a straight leading edge. See Figure 12 for a top view of the aircraft.

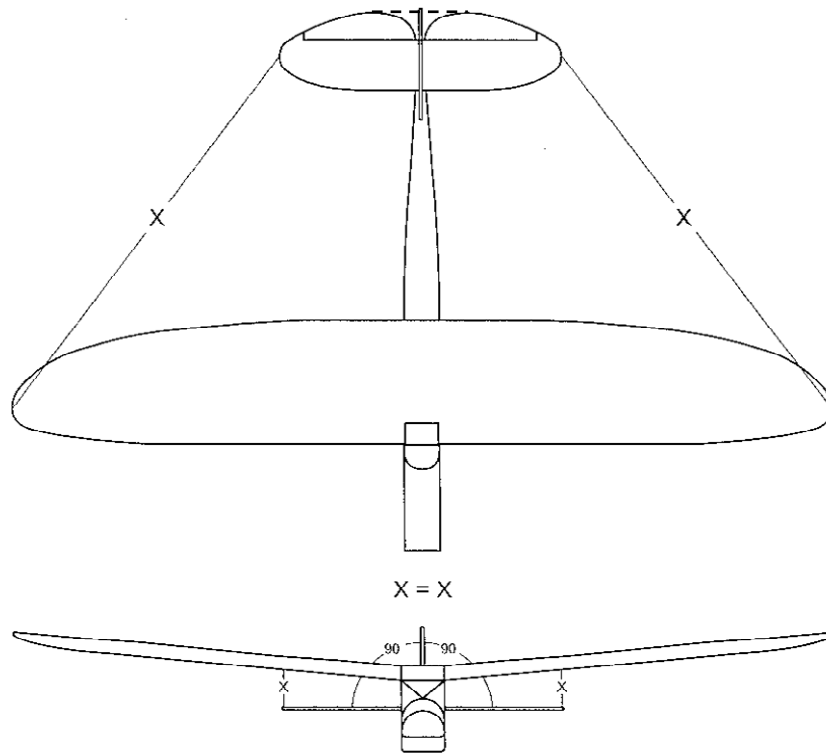


Figure 12. SIG Rascal Wing Planform View

The manufacturer provided some dimensions; wing span (b), wing area (S), and airfoil type. All the remaining dimensions were determined by physically measuring the aircraft.

The mass of the aircraft was determined by placing a digital scale under each of the three landing gear wheels. The aircraft was configured with the engine, propeller, empty fuel tank, five servos, R/C receiver, Piccolo II, Fail Safe Control Relay, and 14-AA Nickel Metal-Hydride (NiMH) batteries. The rear scale was placed on an 7-inch high box, which raised the tail to a level flight configuration. The center of gravity is rotated slightly forward with the tail raised as compared to being on the ground, and thus having the main gear carry more of the weight of the aircraft.

Root chord measurements for the vertical and horizontal tails included the respective control surfaces. Additionally, a theoretical elevator was used to determine the root chord of the horizontal tail. The theoretical elevator used the actual elevator without a notch cut out for the elevator deflection (see dotted line connecting trailing edges of elevator in Figure 12 above). Tables 3 and 4 list the major dimensions and mass properties of the Rascal 110 and its components.

Aspect Ratio (AR) was calculated using $AR = b^2/S$, the aspect ratio equation for a non-rectangular wing according to John Bertin (2002:162). Assuming a non-rectangular wing, the result is an $AR = 7.94$. Assuming the semi-elliptical planform of the Rascal is a rectangle, and using the calculation for a rectangular wing, $AR = b^2/c$, (Bertin, 2002:162), then $AR = 6.875$. The last calculation used span equal to 9.16 ft and the root chord length of 1.33 ft. However, using the average root chord of $c = 1.25$ ft, the latter equation results in an $AR = 7.33$. Bertin says typical aspect ratios vary between 35 for a sailplane and 2 for a supersonic fighter. Using the known span, area, and $AR = b^2/S$, the higher aspect ratio, $AR = 7.94$, was chosen to better represent the efficient nature of the elliptical wing. Appendix C, D, and H list and use the discussed dimensions.

Table 3. Rascal Physical Dimensions

NAME	SYMBOL	VALUE
Wing Reference Area	S_W	10.56 ft ²
Wing Span	b_W	9.16 ft
Aspect Ratio	AR	7.94 ft
Wing Root Chord	c_{RW}	1.33 ft
Horizontal Tail Area	S_H	1.99 ft ²
Horiz. Tail Span	b_H	3.04 ft
Horiz. Tail Root Chord	c_{RH}	0.833 ft
Vertical Tail Area	S_V	0.773 ft ²
Vert. Tail Span	b_V	0.937 ft
Vert. Tail Root Chord	c_{RV}	1.0833 ft
Aircraft Mass (Empty)	M	0.4895 Slugs

Table 4. Component Weights

Component	Weight (lbf)
Aircraft (Empty Tank, 5 Servos, Engine, Receiver)	14.19
Piccolo II with 10-AA NiMH Battery Pack	1.2
Fail Safe Control Relay	.1
4-AA NiMH Servo Battery Pack	.25
50 oz of Nitromethane fuel	3.0
Gross Take Off Weight	18.74

In 2004, researchers at the University of California-Berkeley made similar determinations concerning the mass of the vehicle. They measured an empty weight of 12.12 lbf, and did not account for avionics, batteries, or fuel. Furthermore, they measured a payload capacity of 9.92 lbf, for a total gross weight of 22.05 lbf (Frew, et al, 2004:7).

The wing, vertical tail, and horizontal tail planforms are analyzed next. The model input into the simulators, developed in the next chapter, use a theoretical rectangular wing, vertical and horizontal tail shape. More specifically, the aerodynamic math modeling software, discussed later, can treat a straight-tapered or non-straight

tapered wing, but not elliptical. The rectangular planform simplifies the modeling of the aircraft, due to its linear nature. Additionally, since the manufacture and use of elliptical planforms is nearly non-existent, literature on modeling such wings is also nearly non-existent. By using the earlier values for span, root chord, area, and equations 3 and 4, the chord length at the tip of the theoretical rectangular wing can be calculated. By first solving for the taper ratio (λ), the ratio of the tip to root chord, the tip chord can be determined. The horizontal stabilizer and elevator also shared a semi-elliptical planform, although slightly more distorted along the trailing edge to accommodate the rudder deflection. Calculation results are given in Table 5.

$$S = \frac{c_{RW}(1 + \lambda)}{2} b \quad (3)$$

$$\lambda = \frac{c_{RW}}{c_{TW}} \quad (4)$$

Table 5. Planform Taper Ratios and Tip Chord Lengths

Term Name	Symbol	Value
Wing Taper Ratio	λ_W	0.7295
Wing Theoretical Tip Chord	c_{TW}	0.9697 ft
Horiz. Tail Taper Ratio	λ_H	0.5708
Horiz. Tail Theoretical Tip Chord	c_{TH}	0.8336 ft
Vertical Tail Taper Ratio	λ_V	0.5708
Vert. Tail Theoretical Tip Chord	c_{TV}	0.6184 ft

Figures 22 and 23, later in this chapter, illustrate the difference between the actual semi-elliptical planforms and the calculated theoretical rectangular planforms used to model the aircraft.

Other key characteristics of the wing, vertical tail, and horizontal tail include dihedral (Γ), incidence angle (i), twist, leading edge sweep (Λ_{LE}), and quarter chord sweep ($\Lambda_{c/4}$). The wing dihedral was measured with the aircraft in the level flight configuration, as previously described. Dihedral is the angle between the spanwise inclination of the wing with respect to the horizontal (Nelson, 1998:79). Positive dihedral is defined as the wing tip being higher than the root section (Nelson, 1998:79). An inclinometer was placed centered and perpendicular to the chord direction and at one half the distance from the wing root chord to the wing tip. The fuselage was held rigid since the aircraft listed to one side with the weight of the inclinometer on the wing. The horizontal and vertical tail have no dihedral as shown in Figure 25. Wing incidence is the angle the root chord makes with the fuselage reference line. Positive incidence is defined as the leading edge above the trailing edge and with respect to the reference line. By observation, the aircraft has no twist associated with any surface. Both the wing and horizontal tail have no leading edge sweep. However, the vertical tail was determined to have a leading edge sweep of 25 degrees. The quarter chord was assumed not swept for purposes of modeling, and therefore the trailing edge is forward swept to accommodate the taper ratio and tip chord, see Figure 22. Table 6 shows the values for incidence, dihedral, sweep, and twist.

Table 6. Rascal Incidence, Dihedral, Twist, and Sweep

Term	Symbol	Wing (deg)	Horizontal Tail (deg)	Vertical Tail (deg)
Incidence	i	2 deg	2 deg	0 deg
Dihedral	Γ	2 deg	0 deg	0 deg
Twist	-	0 deg	0 deg	0 deg
Leading Edge Sweep	Λ_{LE}	0 deg	0 deg	25 deg
Quarter Chord Sweep	$\Lambda_{c/4}$	0 deg	0 deg	0 deg

The fuselage cross sectional areas were determined next. A reference plane defined from the center of the propeller to the end of the fuselage and parallel to the ground (with the aircraft in a level flight orientation) was established. The fuselage was then sliced at regular intervals, called Stations, and the cross sectional area was determined with respect to the distance from the front of the cowling (X) and the distance above (Z_U) and below (Z_L) the reference plane. Table 7 lists the meanings of each dimension while Figure 13 provides a visual representation. Table 8 lists the measured dimensions of the Rascal 110.

Table 7. Cross Sectional Area Dimension Definitions

Designation	Meaning
Station Number	Designation of Cross Section Location
X (ft)	Distance Back From Front of Engine Cowling
S (ft ²)	Cross Sectional Area of Station Number
Z_U (ft)	Coordinate Distance Above Reference Plane
Z_L (ft)	Coordinate Distance Below Reference Plane

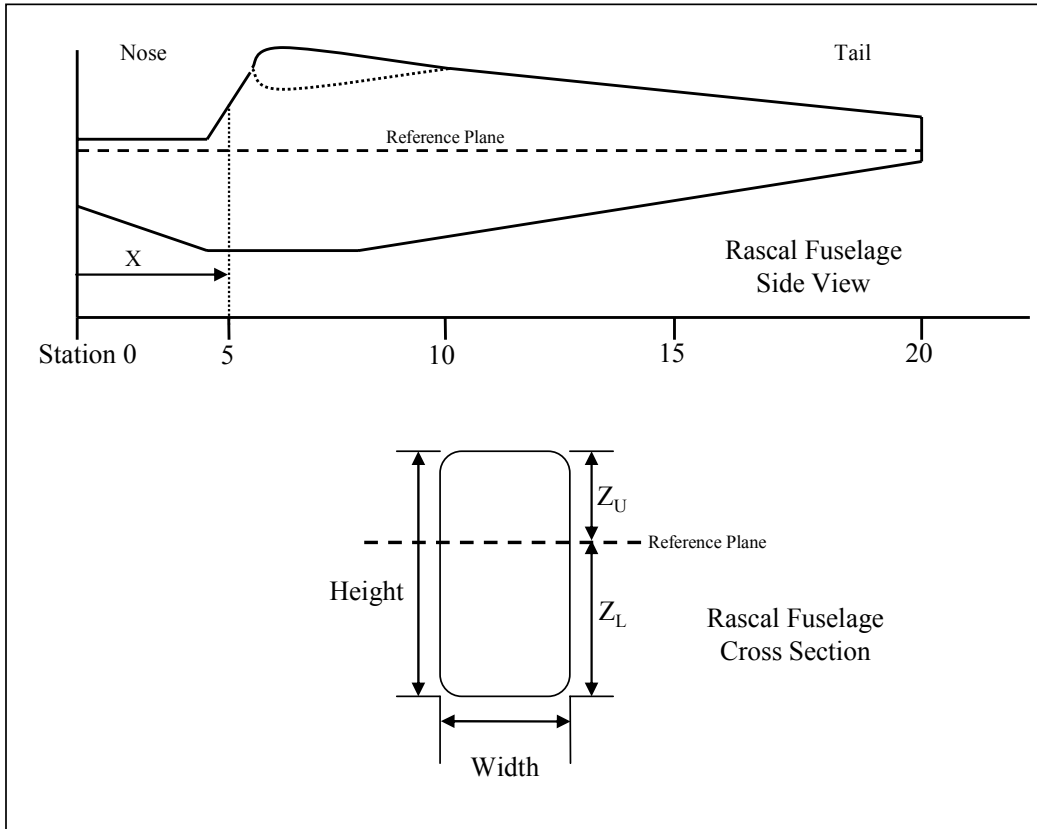


Figure 13. Rascal Cross Sectional Area Definitions

Table 8. Rascal Cross Sectional Dimensions

Station	X (ft)	S (ft²)	Z_U (ft)	Z_L (ft)
0	0.000	0.104	0.009	0.167
1	0.292	0.195	0.016	0.354
2	0.583	0.245	0.020	0.438
3	0.875	0.285	0.024	0.479
4	1.250	0.573	0.048	0.813
5	1.542	0.458	0.038	0.479
6	1.750	0.439	0.037	0.458
7	2.042	0.420	0.035	0.458
8	2.333	0.401	0.033	0.438
9	2.625	0.352	0.029	0.417
10	2.917	0.313	0.026	0.396
11	3.208	0.272	0.023	0.375
12	3.500	0.234	0.020	0.333
13	3.792	0.194	0.016	0.313
14	4.083	0.152	0.013	0.292
15	4.375	0.120	0.010	0.271
16	4.667	0.087	0.007	0.250
17	4.958	0.063	0.005	0.229
18	5.250	0.042	0.003	0.208
19	5.542	0.024	0.002	0.188

3.3 – Inertia Measurements and Calculations

Product of inertia values for the SIG Rascal were required for both the Matlab/SIMULINK and the hardware in the loop simulations. Two methods exist to determine inertia. The first method uses mathematical calculations based on physical measurements to predict inertia values. The second method also uses mathematical calculations based on both physical measurements and experimental data. Experimental data was obtained by physically hanging the aircraft and swinging it with constant oscillations. The latter method was chosen since it generated more accurate results using the actual flight test vehicle.

The aircraft hung from a single point in the ceiling. This allowed the CG to fall directly below the hanging point, much like a plumb bob. The aircraft was free to swing in the XY, XZ, and YZ planes. A swinging gear (i.e. a wire harness) was constructed to hang the aircraft. Figures 14 and 15 shows the Rascal in the vertical orientation; from here it was swung in the XY and XZ planes. A close up of the harness shows the construction and set up allowing the aircraft to hang directly below. Since the CG laid inline with the hanging wire, a laser-line was projected on to the body and aligned with the wire. The laser-line now passed through the CG. A secondary result of this procedure revealed the location of the CG along the Z-axis when the laser-line was projected down the side of the fuselage.

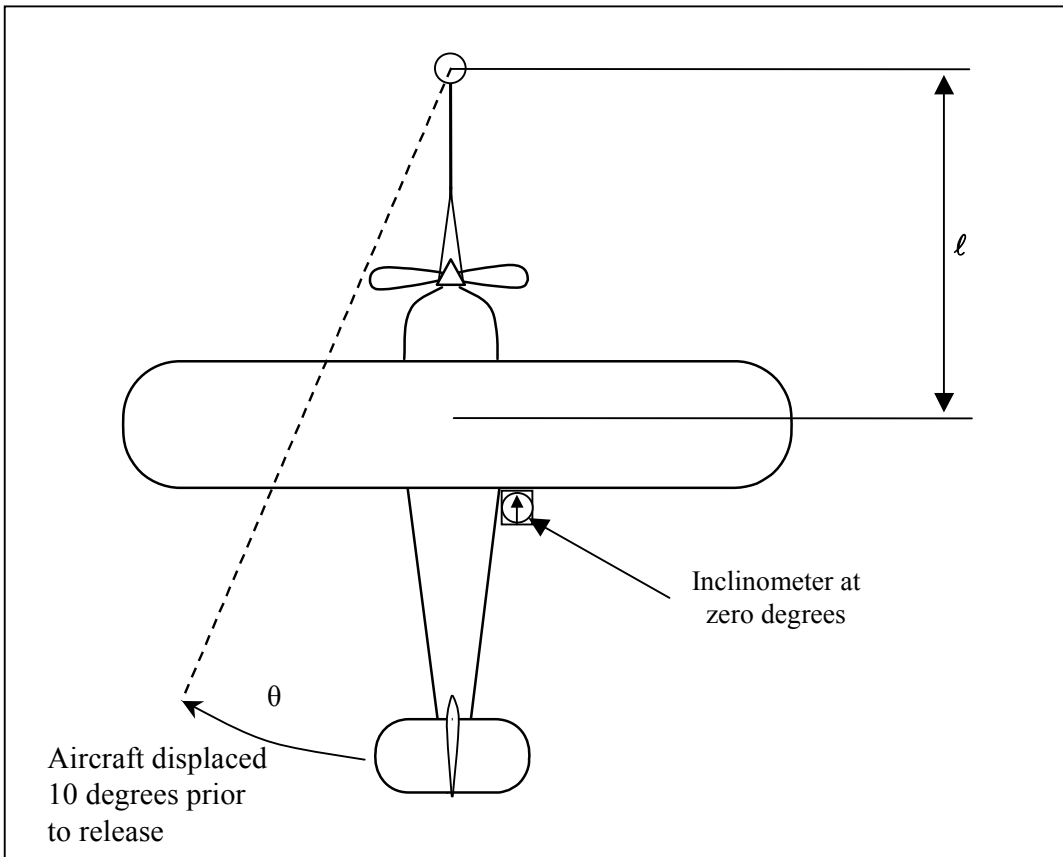


Figure 14. Schematic of Typical Inertia Swing Test Setup



Figure 15. a) Inertia Test Set Up, b) Reverse View, and c) Wire Harness Apparatus

Using an inclinometer placed in the corner where the wing trailing edge meets the fuselage, the aircraft was displaced 10 degrees from its resting position along the XY plane. It was then released and allowed to oscillate freely in the XY plane. Ten oscillations were counted and timed. These first ten cycles allowed the aircraft to settle into a natural and repetitive rhythm, minimizing effects of the first oscillation due to the initial release, but long enough to show significant damping. The aircraft was allowed to continue swinging until the oscillations completely dampened out; again total oscillations were counted and timed where the time final is T_f . The procedure was repeated three times in each plane. For the XZ plane, the aircraft was oriented parallel to the ground. In the XZ plane, the aircraft was only displaced 5 degrees as it provided a less aggressive arc, but sufficient results. Tables 9, 10, and 11 list the results of each swing.

Table 9 Inertia Test – Displacement in XY Plane

Test #	Displacement (deg)	Ref. Length l_{CG} (ft)	Time for 10 Oscillations (Sec)	Time to Damp Out T_f (min:sec)
1	10	2.67	22.567	2:25
2	10	2.67	22.69	2:30
3	10	2.67	22.33	2:30
Avg	10	2.67	22.52	2:28

Table 10 Inertia Test – Displacement in XZ Plane

Test #	Displacement (deg)	Ref. Length l_{CG} (ft)	Time for 10 Oscillations (Sec)	Time to Damp Out T_f (min:sec)
1	10	2.67	21.83	1:25
2	10	2.67	21.76	1:27
3	10	2.67	21.69	1:22
Avg	10	2.67	21.76	1:24

Table 11 Inertia Test – Displacement in YZ Plane

Test #	Displacement (deg)	Ref. Length l_{CG} (ft)	Time for 10 Oscillations (Sec)	Time to Damp Out T_f (min:sec)
1	5	3.125	23.24	No Data
2	5	3.125	23.08	No Data
3	5	3.125	23.37	No Data
Avg	5	3.125	23.23	No Data

The raw data from the inertia swing tests was placed through a series of equations to determine the inertia values. According to Miller (1930:5) the data reduction method for calculating product of inertia for a swinging aircraft requires mass of the vehicle and swinging apparatus, the length from the point of oscillation to the CG of the aircraft, and the time to swing through one oscillation. Miller based his procedures for calculating product of inertia on the equation of motion for a simple pendulum, about a fixed pivot point above the CG. The equations for a simple pendulum are manipulated to solve for product of inertia and applied here. Any good physics text, such as *The Fundamentals of Physics*, by Halliday and Resnick, 1988, discusses the motion of a simple pendulum but will not be addressed in this paper.

First, the average time per oscillation in each plane was computed,

$$\begin{aligned} T_{1X} &= 2.323 \text{ sec} \\ T_{1Y} &= 2.176 \text{ sec} \\ T_{1Z} &= 2.253 \text{ sec} \end{aligned}$$

The procedures suggested by Miller, calculate the damped natural frequency (ω_d) next by equation 5,

$$\omega_d = \frac{2\pi}{T_{1X}} \quad (5)$$

Since the oscillations were considered damped, the natural, undamped frequency is determined next. In order to extract the undamped frequency of oscillation, the real ($\mathcal{R}e$) and imaginary ($\mathcal{I}m$) portions of the damped oscillations must be calculated. The undamped natural frequency lies on the imaginary plane with real and imaginary components. The damped natural frequency, ω_d , is equal to $\mathcal{I}m$ portion of the undamped natural frequency and lies on the imaginary axis. The oscillations decay exponentially by,

$$e^{-\mathcal{R}e t} = e^{-t/\tau} \quad (6)$$

where,

$$\tau = 1/\mathcal{R}e, \text{ the time constant}$$

Noting that,

$$e^{-5} \approx 0$$

or where, $t = T_f = 5\tau$, the oscillation has essentially died out. Now, $T_f = 5\tau = 5/\mathcal{R}e$, or

$$\mathcal{R}e = 5/T_f \quad (7)$$

Based on the geometry of the imaginary plane and the location of the undamped natural frequency, ω_n can be determined (see equation 8).

$$\omega_n = \sqrt{\mathcal{R}e^2 + \mathcal{I}m^2} \quad (8)$$

Miller (1930:10) states, “the moment of inertia of the airplane about an axis through its center of gravity equals the moment of inertia of the entire pendulum about the axis of oscillation minus the moment of inertia of the swinging gear about the same axis minus the additional moment of inertia due to the displacement of the center of gravity of the airplane from the axis of oscillation.” Since the swinging gear has negligible mass compared to the aircraft, it was ignored. However if an apparatus used to hang the aircraft has a mass comparable to that of the aircraft, it must be considered in the calculations according to Miller. Using gravity (g) equal to 32.174 ft/sec² and the mass (M) of the vehicle equal to 0.489519 slugs, Equation (9) yields product of inertia for either the damped or undamped natural frequencies. The first term considers the entire swinging apparatus set up, including the aircraft and displaced CG. The second term, subtracted from the first, corrects for displaced CG (Miller, 1930:15).

$$I_{XX} = M\ell_{CG} \left(\frac{1}{\omega} \right)^2 g - M\ell_{CG}^2 \quad (9)$$

The resulting damped and undamped natural frequencies and respective product of inertias for each plane are collected in tables 12 and 13. Product of inertia in the I_{XZ} is considered zero since the aircraft is symmetric about that plane. The inertia values are calculated using the undamped frequency. The damped frequency and damped inertia values were also calculated for comparison (Tables 12 and 11, bold face). The values are clearly different, but the difference is not significant for the purposes of this research.

Table 12. Damped and Undamped Frequencies of Oscillation

Axis of Oscillation	Damped Frequency ω_d (sec)	Undamped Frequency ω_n (sec)
X	2.7048	2.7051
Y	2.8875	2.8881
Z	2.7889	2.7892

Table 13. Damped and Undamped Moments and Products of Inertia

Axis of Oscillation	Damped Inertia (slugs·ft ²)	Undamped Inertia (slugs·ft ²)
X	$I_{XX} = 1.9472$	$I_{XX} = 1.9456$
Y	$I_{YY} = 1.5525$	$I_{YY} = 1.5505$
Z	$I_{ZZ} = 1.9156$	$I_{ZZ} = 1.9147$
	$I_{XZ} = 0$	$I_{XZ} = 0$

3.4 – Center of Gravity Determination

The center of gravity was determined along all three axis. For the CG along the Y and X axis the aircraft was set upon three identical digital scales, one under each wheel. The tail wheel scale was raised seven inches in order to put the aircraft in a level flight configuration. An inclinometer was centered on wing root chord and aligned parallel with the X axis. The tail was raised until the inclinometer read zero. This method for

level flight was used as reference for all level flight lab measurements. The scales under the left and right main gear read 6.845 and 6.801 lbf respectively. The tail wheel scale reported 1.9841 lbf. A force and moment balance procedure indicated the center of gravity along the x-axis was 21 inches back from the front of the cowling. For ease of calculations, the CG along the y-axis was assumed to be at the center. These two positions were temporarily marked on the fuselage. When the aircraft was hung for the moment of inertia swing, a laser line was projected along the body to aid in finding the z-axis location of the CG. Section 3.3, paragraph 2, described how the z-axis was determined. Figure 16 shows where the CG of the Rascal was found.

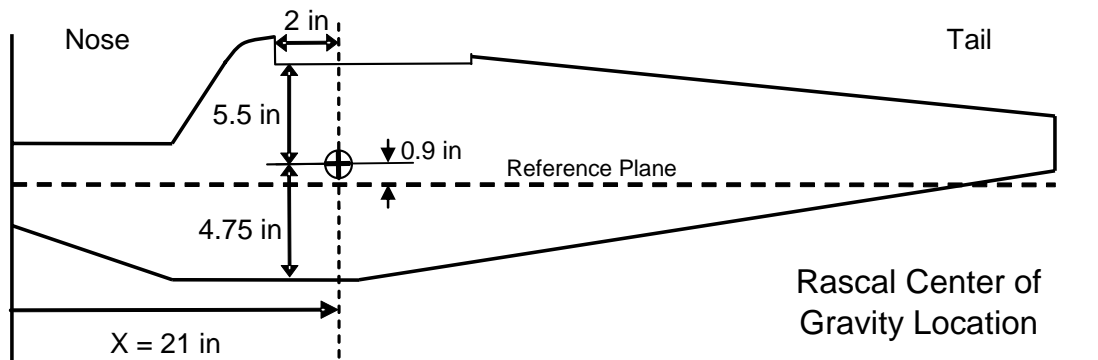


Figure 16. Rascal UAV Center of Gravity Location

3.5 – Airfoil Analysis

In order for both the HITL and Matlab simulation to accurately represent the Rascal 110, airfoil data was required. Since wind tunnel data existed on the two airfoils that comprise the Rascal’s airfoil, further wind tunnel analysis was not performed. Recall in Chapter 2, the Rascal’s wing employs an airfoil that is the sum of two airfoil designs

joined at the chord lines, an Eppler 193 (E193) upper half and an Eppler 205 (E205) lower half.

For accurate wing modeling, the HITL simulator specifically requires three values as a function of the wing angle of attack; the lift coefficient (Cl), drag coefficient (Cd) and coefficient of moment (Cm). The notation of Cl , Cd , and Cm use lower case letters to denote a two-dimensional infinite wing analysis. For an actual finite three-dimensional wing, the terms Cl , Cd , and Cm are modified with capital letters; for example C_L , C_D , and C_M . This notation is derived from the text, "Aerodynamics for Engineers," by John J. Bertin, 2002.

Data did not exist for the blended design, so the decision was made to choose either the E193 or E205 as the airfoil for the model. Which airfoil to choose was the challenge. Based on publicly available wind tunnel measurements, Cl , Cd , and Cm were obtained for both the E193 and E205 airfoils. The Nihon University Aeronautical Student Group (NASG) Airfoil Database was the primary source of airfoil data. The NASG database in turn credits the University of Illinois at Urbana-Champaign (UIUC) Airfoil Database and Massachusetts Institute of Technology's Subsonic Airfoil Development System for its findings. The NASG database was chosen for its ease of use, immediate access via the World Wide Web, and available information. The airfoil data provided in this paper was all derived from the NASG website, <http://www.nasg.com/afdb/index-e.phtml>, between the months of September 2005 to February 2006.

Airfoil data was provided as a function of Reynolds-number, the ratio of inertial to viscous forces (Bertin, 2002:34). In order to determine the correct Reynolds-number for the Rascal, an average flight speed, average wing chord, fluid density, and fluid viscosity were required. A flight speed of 67.51 feet per second (ft/sec) was selected. This flight speed was based on three flights of the Rascal with telemetry feedback. Based on pilot experience, 67.51 ft/sec, or 40 knots, proved to be the best airspeed for basic maneuvers and autopilot functions. The average wing chord was derived from measuring the chord length at regular intervals along the wing span. Fluid viscosity and density were looked up on a Standard Atmospheric Table at 1000 feet of altitude above sea level from Etkin and Reid, 1996:364. 1000 feet above sea level is the average flight altitude of the Rascal at the flight test range. Bertin suggests using equation 10, to calculate the Reynolds-number (Re).

$$Re = \frac{\rho V D}{\mu} \quad (10)$$

where:

$$\begin{aligned} \mu &= \text{Fluid viscosity} = 3.72 \times 10^{-7} \text{ slug/(ft}\cdot\text{sec)} \\ \rho &= \text{Fluid density} = 2.3081 \times 10^{-3} \text{ slug/ft}^3 \\ D &= \text{Characteristic distance (wing average chord)} = 1.25 \text{ ft} \\ V &= \text{Free-stream fluid velocity} = 67.51 \text{ ft/sec} \end{aligned}$$

which gives,

$$\text{Reynolds-number} = 523,588$$

NASG had data for lower Reynolds Numbers, so the highest two Reynolds-numbers available were chosen for the E193, $Re = 303,100$ and $Re = 204,200$, and for the

E205, Reynolds-number = 304,300. Unfortunately, the data for the E193 at the highest available Reynolds-number spanned a limited range of angle of attacks, and the second highest Reynolds-number offered a substantially wider range of experimental data.

Hiroshi Takeuchi registered the E193 data with NASG. Takeuchi states the E193 airfoil data was a wind tunnel measurement conducted at UIUC by M.S.Selig, J.F.Donovan, and D.B.Fraser. Takeuchi credits the Eppler Group as the Development Group for the E205 data.

Collecting information from the NASG website revealed that the E205 and E193 airfoils were similar in shape and properties. Figures 11 and 12 show the Rascal's blended airfoil compared to each of the Eppler airfoils. Notice the E193 has a slightly smaller trailing edge thickness below the chord line and behind the point of maximum thickness as compared to the Rascal airfoil. The E205 is thinner above the chord line and behind the point of maximum thickness. Since the manufacturer indicated the Rascal airfoil was blended, the results were expected, but the significance was not known.

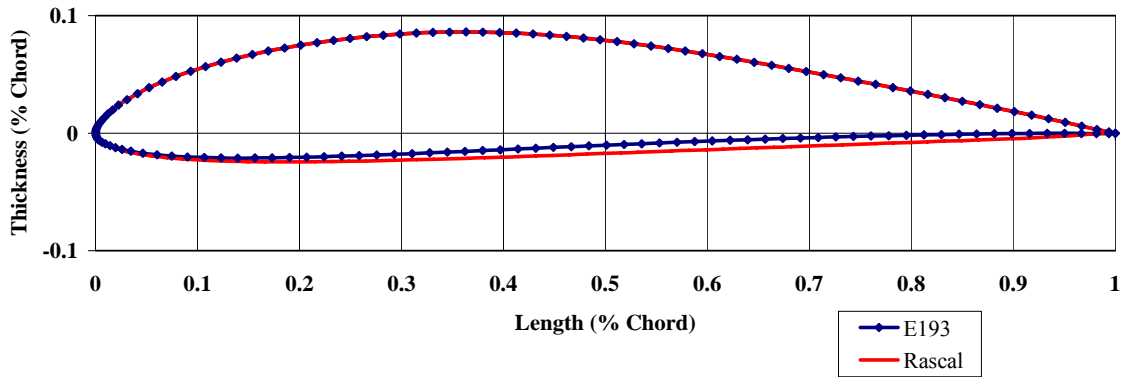


Figure 17. Rascal Airfoil vs. Eppler 193 Airfoil

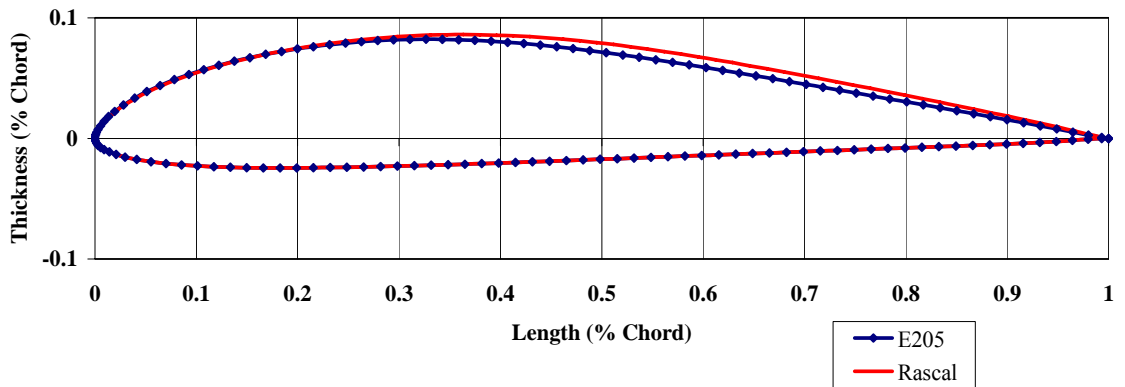


Figure 18. Rascal Airfoil vs. Eppler 205 Airfoil

Further investigation into the lift curves show the E205 has a slightly higher coefficient of lift per degree of angle of attack, α (see Figure 19). However, the rate of lift per degree of α , or the slope of the curves, is the same. Additionally, the E193 lift-curve slopes at the highest and second highest available Reynolds-numbers proved to be nearly identical for the range of measured data.

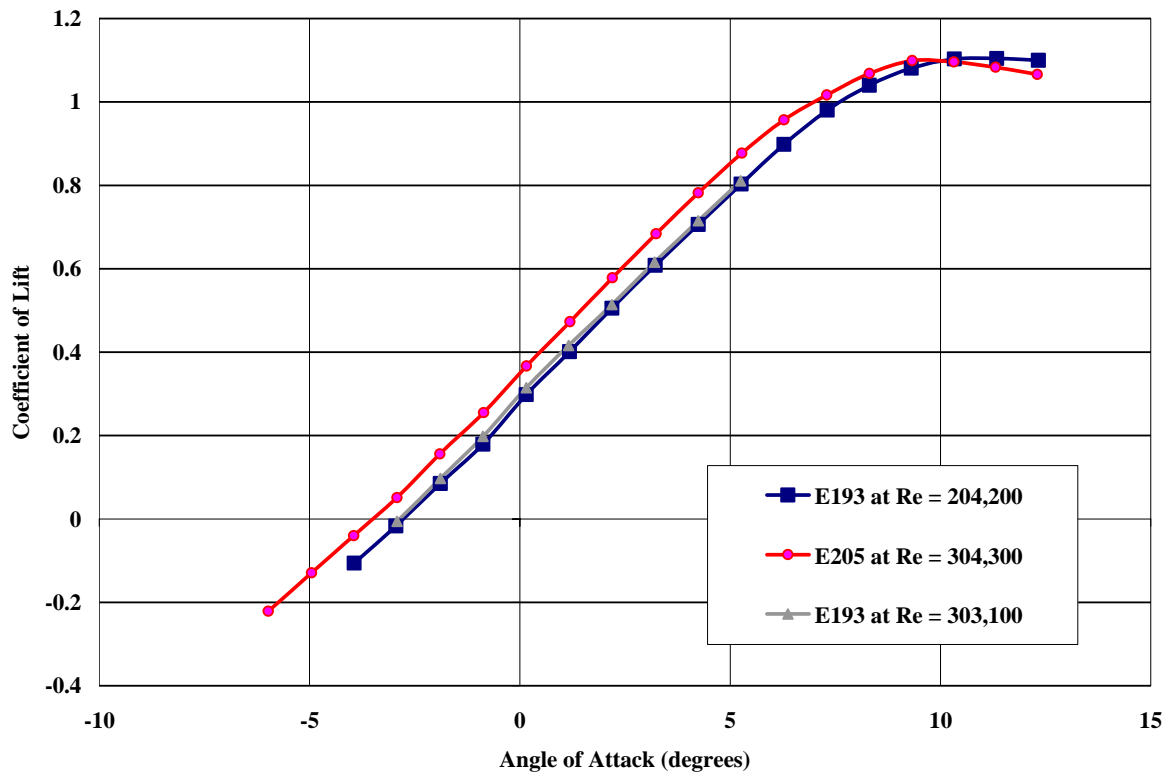


Figure 19. Lift Curve Slopes of E193 and E205

The E193 at a Reynolds-number of 204,200 was ultimately chosen as the airfoil for the HITL simulator. The E193 was chosen because it shared the same upper cambered surface as the Rascal airfoil. Based on the author’s opinion, the upper cambered surface is more significant than the lower and less cambered surface. Additionally, using the lower coefficient of lift curve of the E193, the simulator makes a slightly more conservative lift estimate. The difference in measured values at different Reynolds-numbers proves to have no significant effect at lower angles of attack, and thus the author felt comfortable proceeding with chosen airfoil data. The data for the E193 at the Reynolds-number of 204,200 is presented. The lift, drag, and moment characteristics

will not be identical to that of the actual airfoil. However, as earlier stated, the author believes this is a conservative estimate based on the lift curve slope of the E193 versus the E205, and thus an acceptable source of error.

The data for the coefficient of drag provided is assumed to be the drag coefficient when the lift is zero, also known as the parasite drag (Cd_o). Since total drag requires the wing aspect ratio and span efficiency factor, it is reasonable to assume the drag provided by the NASG database is not total drag. To find total drag, parasitic drag must be added to induced drag (Cd_i). Bertin (2002:190) describes the total wing drag, (Cd) as the parasite drag plus the induced drag, as shown in Equation (11). By Equation (12) the induced drag is a function of aspect ratio, lift coefficient, and span efficiency (Bertin, 2002:191). The span efficiency factor is 0.7 for a rectangular wing, and 1.0 for a true elliptical wing. Since the model represented in the simulation incorporates a rectangular wing, 0.7 was chosen as the span efficiency factor.

$$Cd = Cd_i + Cd_o \quad (11)$$

$$Cd_i = \frac{Cl^2}{\pi \cdot AR \cdot e} \quad (12)$$

where:

$$\begin{aligned} AR &= \text{Aspect Ratio} = 7.94 \\ Cl &= \text{Coefficient of Lift} = -0.106 - 1.1 \\ e &= \text{Span Efficiency Factor} = .7 \end{aligned}$$

Table 14. E193 Airfoil Data at Re = 204,200

<i>alpha</i>	<i>CL</i>	<i>Cdo</i>	<i>Cdi</i>	<i>CD</i>
-3.94	-0.106	0.0148	0.0006	0.0154
-2.95	-0.017	0.0129	2E-05	0.0129
-1.89	0.085	0.0123	0.0004	0.0127
-0.88	0.179	0.0106	0.0017	0.0123
0.15	0.298	0.01	0.0047	0.0147
1.18	0.401	0.0107	0.0086	0.0193
2.19	0.505	0.0112	0.0136	0.0248
3.22	0.608	0.0122	0.0197	0.0319
4.24	0.706	0.0127	0.0266	0.0393
5.26	0.803	0.0134	0.0344	0.0478
6.28	0.898	0.0133	0.043	0.0563
7.31	0.98	0.0147	0.0513	0.066
8.31	1.04	0.0177	0.0577	0.0754
9.31	1.081	0.0221	0.0624	0.0845
10.33	1.103	0.0282	0.0649	0.0931
11.34	1.104	0.0326	0.0651	0.0977
12.33	1.1	0.0382	0.0646	0.1028

The HITL simulator is capable of using the wind tunnel data for the E193. However, the Matlab simulator requires a wider range of data, specifically the stability derivatives. The US Air Force Stability and Control Digital Datcom software, to be discussed in section 3.8, outputs the required stability derivatives. Inputs to Digital Datcom include airfoil data, but unfortunately, the software only accepts airfoils with the National Advisory Committee for Aeronautics (NACA) designation. The remainder of this section details how an E193 airfoil is represented by a NACA equivalent airfoil, and thus satisfies the NACA requirement for Datcom.

William Blake of AFRL/VACA (Blake, 2006) recommended the following procedures. The remaining paragraphs of this section reflect his recommendations. The requirement is to produce an airfoil with a NACA designation to input into Digital

Datcom. A simple plot, like figures 17 and 18 depicting the E193 and E205 airfoils, satisfy the requirement.

Four digit NACA airfoil designations follow a standard identification convention. The first digit is the amount of camber as a percentage of hundredths of chord. The second digit is the position of maximum camber in tenths of percentage of chord. The third and fourth digits are the maximum thickness in hundredths of percentage of chord. For example, a NACA 2415 has a 2% maximum camber (0.02), located at 40% of the chord (0.4) with a maximum thickness of 15% chord.

The basic coordinate system is based on unit lengths of percent of chord, both in the x- and y-axis. The origin is located at the leading edge and $x = 1$, 100% chord length, is located at the trailing edge. Begin by assuming there is no built in incidence, meaning the leading and trailing edges of the airfoil being at the origin, $x = 0$, $y = 0$, and end at $x = 1$, $y = 0$. The airfoil thickness distribution is the difference between the upper y-coordinate and the lower y-coordinate at every x-coordinate,

$t(x) = y_{upper}(x) - y_{lower}(x)$. The mean camber line is found by adding the upper and lower y-coordinates and dividing the quantity by 2 at every x-coordinate, $z(x) = [y_{upper}(x) + y_{lower}(x)]/2$. From the NASG Airfoil Database, Takeuchi states the maximum camber to be 0.0354 percent of chord. The value of maximum camber, $z(x)$, was calculated of the E193 to be 0.037, or close to 0.04. The corresponding position of maximum camber was found at 35% of the chord length. Since this value must be in tenths, 0.3 or 0.4 chord must be used. A value of 0.3 chord was selected since it had a larger camber value than at 0.4 chord. Takeuchi also says maximum thickness is 0.1023.

Blake calculates maximum thickness, $t(x)$, approximately 0.1, corresponding to a 10% thickness section. Combining the maximum camber, 0.04, location of maximum camber, 0.3, and the maximum thickness, 0.1, the NACA equivalent airfoil is 4310. The NACA 4310 airfoil was used for all Digital Datcom inputs.

3.6 – Engine and Propeller Model

The engine model was a linear look up table used by the hardware in the loop simulation. Due to the lack of information available, the engine model is limited in detail. Only including the revolutions per minute and the power in watts, table 15 was generated from the engine manual.

Table 15. Engine Model Look up Table

RPM	Power (watts)
0	0
12000	1566

The propeller model consists of four variables. The coefficient of thrust (C_t), coefficient of power (C_p), and efficiency in percent are all functions of the Advance Ratio (J). The propeller model was developed using software provide by Jon Becker of Cloud Cap Technologies. In order to use this program, the geometric profile of the propeller must be known. There are three parameters needed to fully describe the propeller geometric profile. Chord length and pitch angle twist as a function of the propeller radius must be known and an airfoil data file similar to the wing data file is needed. The Rascal 110 was equipped with a 16x8 propeller from APC. Data on a 20x8 propeller was used as a starting point for building the propeller model; along with the Becker program, an

estimation of the 16x8 propeller was made. While the 20x8 propeller does not have the same diameter, it does have the same nominal pitch as our propeller.

Several assumptions were first made, 1) the chord length vs. radius curve is identical for both an APC 20x8 and APC 16x8 propeller, 2) the pitch angle vs. radius curve is identical for both, 3) the airfoil used for both is the same, and 4) the program generates accurate data. The resulting table lists the estimated 16x8 propeller performance data.

Table 16. Estimated 16x8 Propeller Performance Data at 5000 RPM's

<i>J</i>	<i>C_P</i>	<i>C_t</i>	%
0.000	0.023	0.073	0.000
0.010	0.023	0.072	0.031
0.020	0.024	0.071	0.061
0.030	0.024	0.071	0.090
0.040	0.024	0.070	0.118
0.050	0.024	0.070	0.146
0.060	0.024	0.069	0.173
0.070	0.024	0.068	0.199

3.7 – US Air Force Stability and Control Datcom

The Stability and Control Data Compendium, Datcom for short, provides a “systematic summary of methods for estimating basic stability and control derivatives.” (Ellison, Hoak, Carlson, and Malthan, 1965:1-1). The Datcom is over 1500 pages of detailed methodology to determine stability and control characteristics of a wide variety of aircraft and aircraft configurations. “For any given flight condition and configuration the complete set of derivatives can be determined without resort to outside information,” (Ellison, Hoak, et al, 1965:1-1). Primarily intended for preliminary use, ahead of test

data, it is designed to give an initial look at the stability performance of an aircraft design. However, it is not intended for use in lieu of wind tunnel or flight test data. In 1979, the Datcom was re-written in FORTRAN IV computer language. Re-named the USAF Stability and Control Digital Datcom, it became an efficient, user-oriented computer program (Williams, Murray, Mehlick, and Sellers, 1979:iv).

The Glenn L. Martin Company wrote the US Air Force Stability and Control Datcom, originally titled USAF Stability and Control Handbook, under contract in 1956. Later, under a Control Criteria Branch of the Flight Control Division of the AF Flight Dynamics Laboratory contract, it was revised again in 1965 by the Douglas Aircraft Company and re-titled the Stability and Control Datcom. The principle Air Force project engineers were J.W. Carlson and D.E. Hoak. The principle investigators for the Douglas Aircraft Company were D. E. Ellison and L.V. Malthan, and numerous principal collaborators. The computer program, the USAF Stability and Control Digital Datcom, was written under contract by the McDonnell Douglas Astronautics Company. The principle investigators for McDonnell Douglas were J.E. Williams, S.C. Murray, G.J. Mehlick, and T.B. Sellers. For the Air Force Flight Dynamics Laboratory, Flight Guidance and Control Division, the project engineers were J.E. Jenkins and B.F. Niehaus.

3.7.1 – Datcom Inputs

Inputs to Datcom include desired flight conditions, aircraft attitudes, physical geometry, and desired outputs. Datcom treats inputs that represent a traditional wing-body-tail configuration and any control or high lift devices (Williams, et al, 1979:5). Some non-standard geometries can be treated as well. Datcom inputs were assumed for a

straight-tapered or non-straight-tapered wing, which is why the theoretical rectangular wing was devised in an earlier section. For the longitudinal characteristics, the program assumes a mid-wing configuration. The Rascal uses a high-wing configuration, and this introduces a potential source of error. A brief list of input is found in table 18. The complete list of inputs and code format can be found in Appendix F.

Table 17. Inputs to Digital Datcom; A Brief List

Input	Symbol	Value	Comments
Mach	M	.061	Actual Flight Test Mach
Angle of Attack	A	-10 to 28 deg	Varied Range By 2 deg Increments
Altitude	Alt	1000 ft	Above Sea Level, Actual Flight Altitude
Weight	W	15.74 lbf	Measured, Empty Weight, Flight Configuration
Reference Area	S_{REF}	10.56 ft ²	Measured Wing Area
Reference Chord	\bar{c}_{REF}	1.25 ft	Measured Average Chord Length
Reference Span	b_{REF}	9.16 ft	Measured Wing Span
A/C x-axis CG	x_{CG}	2 ft	Measured Back From Front of Cowling
A/C z-axis CG	z_{CG}	0.08 ft	Measured up from Fuselage Reference Line
Wing and Tail Incidence	i_w, i_t	2 deg	Estimated, see section 3.2
Fuselage Cross Sectional Areas	S	Varies	Measured, see section 3.2
Fuselage Upper Coordinates	Z_U	Varies	Measured, see section 3.2
Fuselage Lower Coordinates	Z_L	Varies	Measured, see section 3.2

Figure 20 through 26 compare the aircraft represented by the Datcom inputs to the Rascal 110 manufacturer's drawing. Figures 20, 22, 24, and 26 were generated with Tech Plot using the Datcom inputs. Representing the Rascal's landing gear in Datcom was done by making the cross sectional area at the landing gear location slightly larger.

In turn, this represents a slightly larger fuselage that will hopefully model the aerodynamic effects of the landing gear. In addition, Datcom cannot treat a rectangular fuselage cross section; therefore, it is represented as a circular fuselage. Figure 22 shows the top view of the theoretical rectangular wing and tail planforms. Since the spans were input to Datcom, they match the actual aircraft exactly. The straight leading edge and tapered trailing edge are also visible. There is no accurate side view scale drawing of the Rascal available. Figure 23 and 25 show the rear and front view's respectively of the model and the Rascal. The highlight in this view is the dihedral of the wings. Figure 26 illustrates a side view of the model, showing the extended section of fuselage to represent the aerodynamic effects of the landing gear.

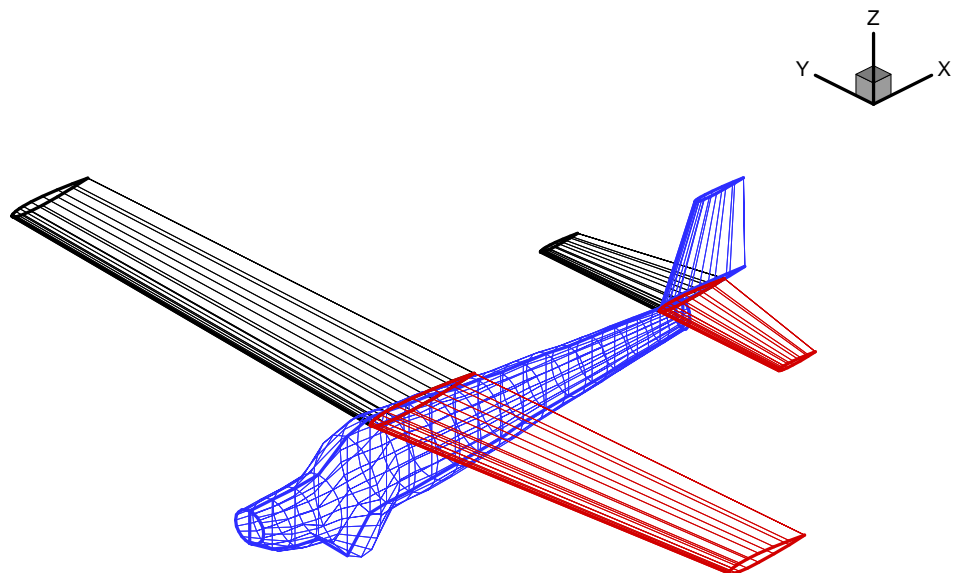


Figure 20. Rascal 110 Representation; Input to Digital Datcom



Figure 21. Rascal 110 for Comparison (Courtesy of Tower Hobbies)

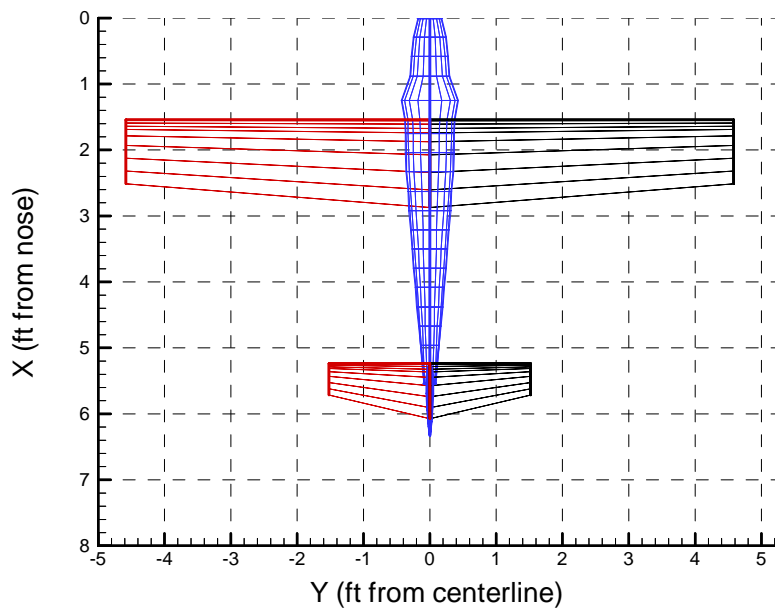


Figure 22. Rascal 110 Representation; Input to Digital Datcom Top View

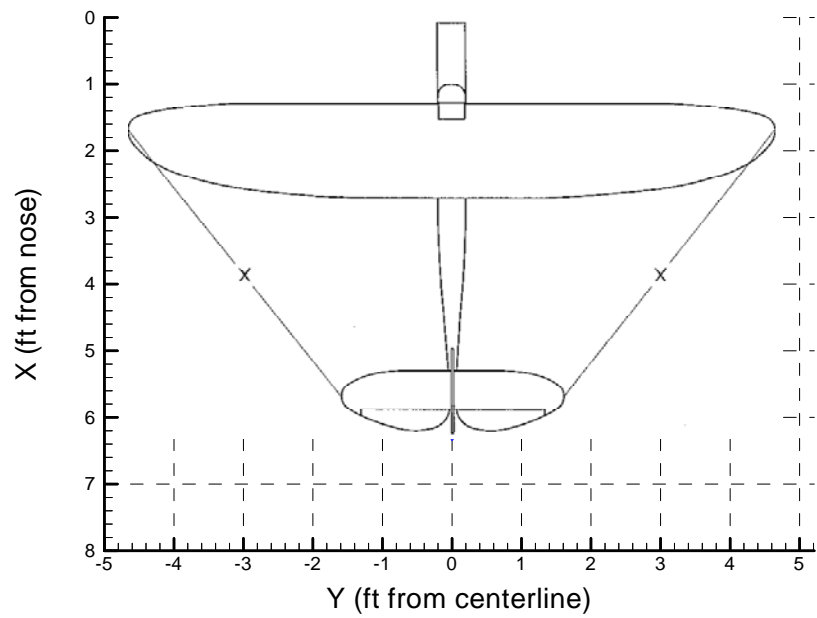


Figure 23. Rascal 110 for Comparison; Top View

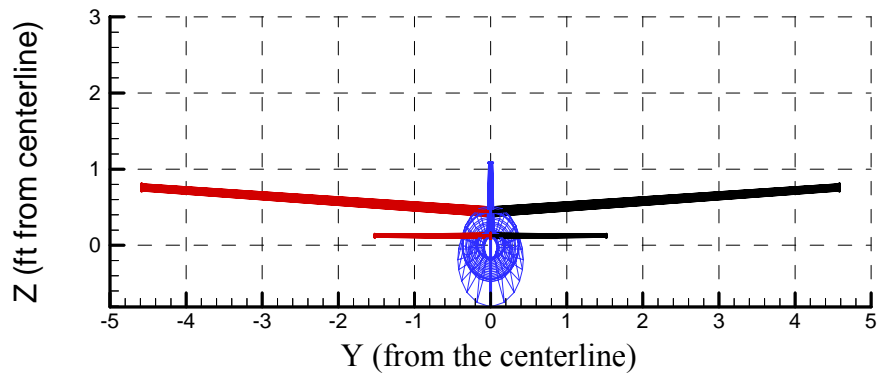


Figure 24. Rascal 110 Representation; Input to Digital Datcom Front View

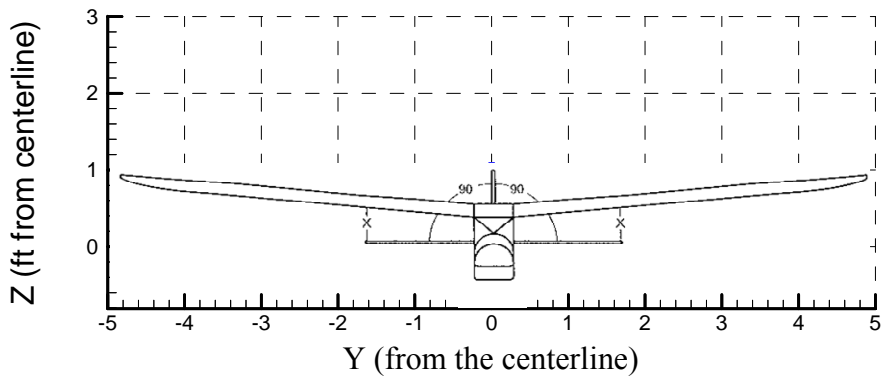


Figure 25. Rascal 110 for Comparison; Front View

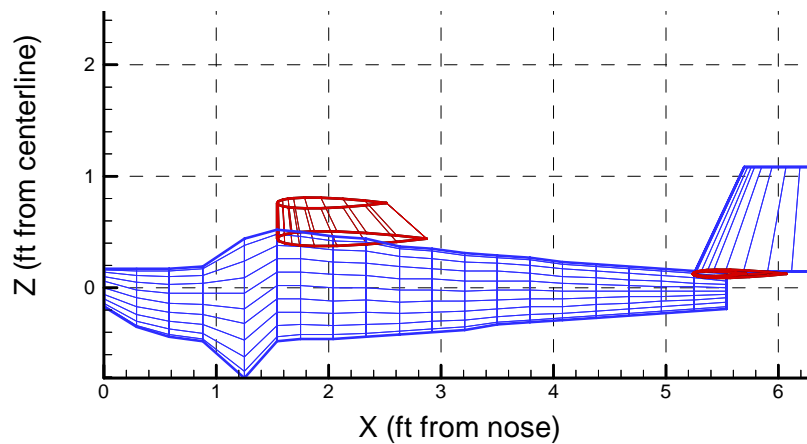


Figure 26. Rascal 110 Representation; Input to Digital Datcom Side View

3.7.2 – Datcom Outputs – Stability Derivatives

Datcom outputs a significant amount of useful data. Not all will be used or presented here. The major components of the coefficients of Lift, Drag, and Moment are listed in table 19. Stability Derivatives are listed in table 20. Appendix G presents the complete Datcom output.

Table 18. Component Lift, Drag, and Moment Coefficients

Coefficient	Symbol	Value	Datcom Output Line #
Wing Coefficient of Lift at 0° AoA	$C_{L_{0_w}}$.421	277
Wing Coefficient of Lift per AoA	$C_{L\alpha_w}$	4.59	276-277
Wing Minimum Coefficient of Drag	$C_{D_{min_w}}$	0.011	274 at AoA = -6°
Wing Moment Coefficient	C_{M_w}	-0.005	277 at AoA = 0°
Vert. Tail Coefficient of Lift per AoA	$C_{L\alpha_t}$	0.0969	190
Vert. Tail Minimum Coefficient of Drag	$C_{D_{min_t}}$	0.001	409 at AoA = -10°
Horiz. Tail Coefficient of Lift per AoA	$C_{L\alpha_h}$	0.76	346
Horiz. Tail Minimum Coefficient of Drag	$C_{D_{min_h}}$	0.002	345 at AoA = -2°
Fuselage Moment Coefficient per AoA	$C_{M\alpha_f}$	0.114	209 at AoA = 0°
Fuselage Coefficient of Drag	C_{D_f}	0.005	209 at AoA = 0°

Table 19. Rascal Stability Derivatives at Trimmed Steady Level Flight

Sea Level, Mach = 0.061			
Lateral	Value per degree	Longitudinal	Value per degree
$C_{y\beta}$	-0.0056	$C_{L\alpha}$	0.11
$C_{l\beta}$	-0.0018	$C_{m\alpha}$	-0.006
$C_{n\beta}$	0.00023	C_{mq}	-0.233
C_{lp}	0.013	$C_{m\delta_e}$	0.011
	C_{lr}	0.01	
	C_{nr}	-0.0006	
	$C_{l\delta_a}$	0.244	
	$C_{n\delta_a}$	-0.0128	

3.8 – Hardware in the Loop (HITL) Aircraft Model Inputs

Nearly all the inputs to the Datcom analysis model were also input to the HITL Model. The HITL model considered additional parameters not entered into Datcom. Originally developed by Cloud Cap Technologies, an outline and sample aircraft model were included with the Piccolo II autopilot. Rascal specific parameters for the wing, horizontal and vertical tail surfaces, fuselage, propeller, engine, weights, Inertia, and Airfoil were input. Additional information included the aircraft contact points, sensor, and actuator data. Contact points allow the Piccolo II to know coordinate locations of the physical aircraft, for example, the location of the wing tips, landing gear, and tail. Contact point data is used during autonomous landings. The default aircraft sensor and actuator data provided by Cloud Cap was used. The autopilot sensors were designed and incorporated by Cloud Cap into the Piccolo II system, and accompanying sensor data file

was left unchanged. The actuator data file was not changed since the test team felt that it represented a general servo-actuated radio control aircraft. The format and complete list of inputs to the HITL model are listed in Appendix C, D, and E.

3.9 – Modeling Errors

Since the exact aircraft was not modeled, errors are introduced as assumptions and conversions are made. By using the E193 airfoil for the HITL, a slightly more conservative estimate of the aerodynamic performance is introduced. When the E193 was converted to a NACA 4310 for Digital Datcom, some rounding was required to fit the E193 to the NACA system of designation. Calculations of the AR used the method for non-rectangular wings and resulted in a 12% increase compared to the method for a rectangular wing. The engine model in the HITL simulation was a linear assumption, although most engines have a non-linear power curve. The landing gear was not modeled directly, but rather incorporated into the fuselage for Digital Datcom, as shown in Figures 20 through 23.

3.10 – Chapter Conclusions

Chapter III accounted for nearly every possible measurable parameter of the Rascal. Although some estimates and assumptions were made, the author believes this model is an accurate representation. Undoubtedly, improvements can always be made to further improve the model, and future researchers should seek to minimize errors such as those listed in section 3.10 as well as incorporate flight test data. Furthermore, the

presented techniques provide a solid and well developed methodology to aircraft mathematical modeling.

IV. Development of UAV Simulation

4.1 – Chapter Overview

The development and use of two aircraft simulations is the focus of Chapter IV. The first simulation was developed in a Matlab/SIMULINK environment. The sections about the Matlab/SIMULINK simulation include the component build up of force, moment, and state equations. The second, a Hardware in the Loop (HITL) simulation, is provided by the autopilot manufacturer, Cloud Cap Technologies. An explanation about the set up and use of the HITL simulation is included.

4.2 – Matlab/SIMULINK Simulation

In Matlab, the aerodynamic math model developed in Chapter III was input, along with equations for the aircraft's forces and moments. These forces and moments were later used to find the trimmed, or steady level flight condition of the simulator at prescribed airspeed settings. The forces, moments, and the 12 initial steady level flight conditions became inputs to a SIMULINK simulation build up to evaluate the model over time. The SIMULINK program calls upon another set of files to calculate the 12 equations of motion of the aircraft. The output of the SIMULINK simulation is then evaluated in response to throttle, elevator, aileron, and rudder input commands

The Matlab simulation began by entering components of the model, listed in Tables 3 through 8, 13, 14, 15, 16, 17, and 19. The detailed list of the component values, symbols, usage, and comments in the Matlab code are listed in Appendix H. In addition to the inputs from Chapter III, the flight conditions of the simulation required

defining. Simulation airspeeds ranged from 64 – 90 feet per second to match the variation in airspeeds encountered during actual flight test. Actual and simulation flight parameters; density, gravity, airspeed, and altitude, are listed in Table 21.

Table 20. Flight Test and Simulation Flight Parameters

Term	Symbol	Value	Comment
Air Density	ρ	0.0023081 (slugs/ft ³)	at 1000 ft above sea level
Gravity	g	32.17 ft/sec ²	-
Aircraft Velocity	V	64.83 – 90.0 ft/sec	Range matches flight speeds
Altitudes	h	1100 ft MSL	Average flight altitudes

4.2.1 – Forces and Moments Build Up

The basic forces and moments that act upon an aircraft are listed below. The forces of Lift (L), Drag (D), and Sideforce (Y) act in the z, x, and y-axis respectively. The Roll (l), Pitch (m), and Yaw (n) moments, act about the x, y, and z-axis respectively. Bertin (2002:158) illustrates the moments and the axis about which they act, see Figure 27.

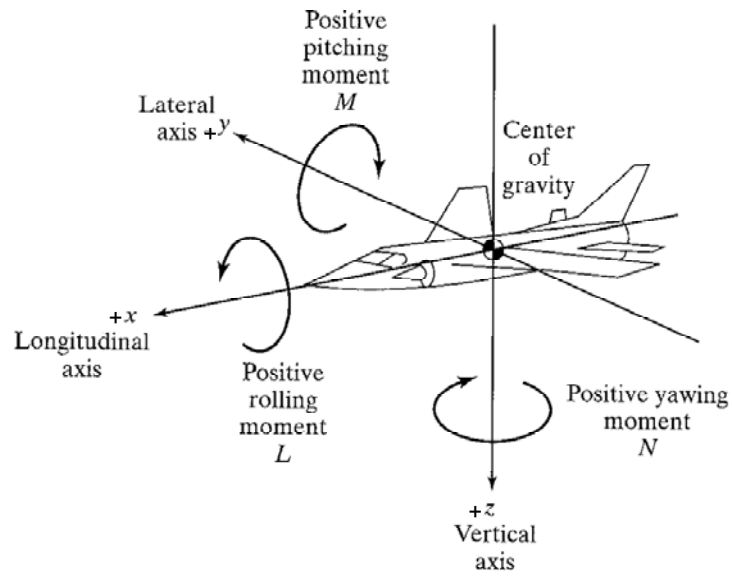


Figure 27. Aircraft Moments; Axis and Direction Definitions

Each of the general force and moment equations listed below can be found in nearly all aerodynamics and control texts. Some noted authors are listed in the next section. A paper released by the Honeywell Technology Center in 1996 captured the essential equations from those authors. Force and moment equations share the similar components of dynamic pressure (\bar{q}), wing reference area (S), wing span (b), and reference chord length (\bar{c}). However, the coefficient (C) build up is unique, and is discussed next.

$$\begin{aligned}
 L &= \bar{q} S C_L \\
 D &= \bar{q} S C_D \\
 Y &= \bar{q} S C_y \\
 l &= \bar{q} S b C_l \\
 m &= \bar{q} S \bar{c} C_m \\
 n &= \bar{q} S b C_n
 \end{aligned}
 \tag{13}$$

Where,

$$\bar{q} = 0.5\rho V^2$$

The coefficients that contribute to each of the forces and moments are determined at each surface upon which they act. All the aerodynamic coefficients acting upon the wing are collected in separate equations (14). The horizontal tail, fuselage, and vertical tail are also collected respectively. This notation and collection of terms is derived from Nelson (1998:35-95) and from Enns, 1994.

$$\begin{aligned}
 C_{L_w} &= C_{L_{ow}} + C_{L_{aw}} \alpha \\
 C_{D_w} &= C_{D_{min_w}} + K_w C_{L_w}^2 \\
 E &= 2 \left(C_{L_{aw}} + C_{L_{aw}} \left(\alpha - \dot{\alpha} \frac{(cg_t + cg_w)}{V} \right) \right) / (\pi A R_w) \\
 \alpha_t &= \alpha + i_t + T_e d_e + q \frac{cg_t}{V} - E \\
 C_{L_t} &= C_{L_{at}} \alpha_t \\
 C_{D_t} &= C_{D_{min_t}} + K_t C_{L_t}^2 \\
 C_{m_f} &= C_{m_{af}} \alpha \\
 C_{D_{vt}} &= C_{D_{min_{vt}}} \\
 C_{ip} &= -\frac{1}{12} C_{L_{aw}} \frac{(1+3\lambda)}{(1+\lambda)}
 \end{aligned} \tag{14}$$

The forces and moments are now re-written with respect to wing, tail, fuselage, and vertical tail. Equations (15).

$$\begin{aligned}
 L_w &= \bar{q} S C_{L_w} \\
 D_w &= \bar{q} S C_{D_w} \\
 M_w &= \bar{q} S c C_{m_w} \\
 L_t &= n_t \bar{q} S_t C_{L_t} \\
 D_t &= n_t \bar{q} S_t C_{D_t} \\
 D_f &= \bar{q} S c C_{m_f} \\
 M_f &= \bar{q} S c C_{m_f} \\
 D_{vt} &= n_t \bar{q} S_{vt} C_{D_{vt}}
 \end{aligned}
 \tag{15}$$

Nelson (1998:47), illustrates the component forces and moments in Figure 28.

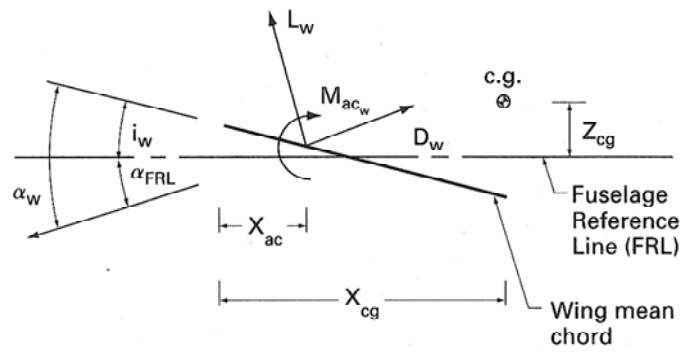


Figure 28. Wing Forces and Moments

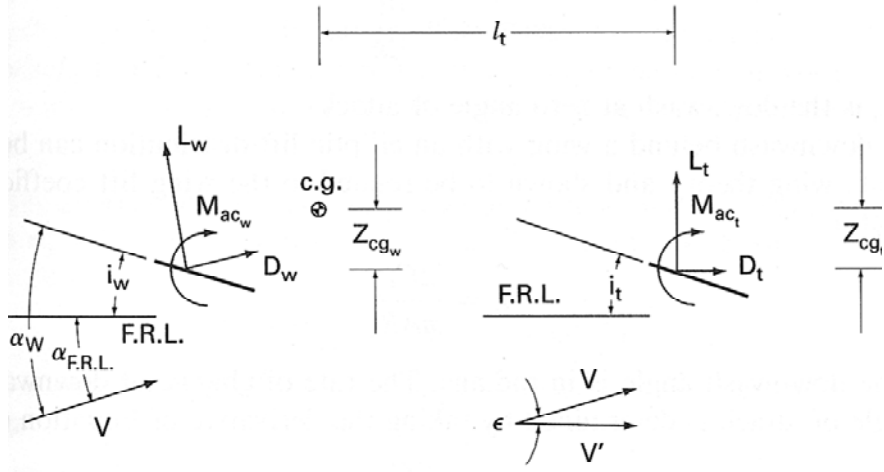


Figure 29. Wing and Tail Forces and Moments

The final force and moment equations (16) used for simulation are derived from Figure 29 and presented below.

$$\begin{aligned}
 L &= L_w + L_t \cos\left(E - \frac{qcg_t}{V}\right) - (D_t + D_{vt}) \sin\left(E - \frac{qcg_t}{V}\right) \\
 D &= D_w + (D_t + D_{vt}) \cos\left(E - \frac{qcg_t}{V}\right) + L_t \sin\left(E - \frac{qcg_t}{V}\right) + D_f \\
 Y &= n_{vt} q_b S_{vt} C_{L_{avt}} \left(-\beta + T_r d_{rt} + \frac{rcg_t}{V}\right) \\
 m &= L_w cg_w \cos(\alpha) + D_w cg_w \sin(\alpha) + M_w - L_t cg_t \cos\left(\alpha - E + \frac{qcg_t}{V}\right) \\
 &\quad - (D_t + D_{vt}) cg_t \sin\left(\alpha - E + \frac{qcg_t}{V}\right) + M_f \\
 n &= -q_b n_{vt} S_{vt} C_{L_{avt}} \left(-\beta + T_r d_{rt} + \frac{rcg_t}{V}\right) cg_{vt} + (-q_b S_b C_{nda} d_a) \\
 l &= \frac{q_b S b^2}{2V} \left(C_{lp} p + \frac{2V}{b} C_{lb} \beta + C_{lr} d_{rt} + \frac{C_{lda} d_a 2V}{b}\right)
 \end{aligned} \tag{16}$$

4.2.2 – Equations of Motion

Development of an accurate dynamic flight simulator began by defining its intended use. The future of the AFIT ANT Lab UAV program is open to a wide variety of research topics: navigation without the use of GPS, autonomous formation flight, and collision avoidance. Application of these missions to UAV's is also still in development. Therefore, the decision was made to develop a simulator capable of flying any future potential mission.

According to researchers from the University of Kansas, M. Sadraey and R. Colgren (2005:1) the best equations to use to completely and accurately model an aircraft's true motion are non-linear fully coupled ordinary differential equations. With these equations of motion, UAV response to any commanded inputs or wind disturbances is accurately modeled. Easier forms of the equations of motion include nonlinear semi-coupled, nonlinear decoupled, linear coupled, and linear decoupled. However with each successive simplification of the equations of motion come restrictions on aircraft performance. Such limitations include pitch angle, pitch rate, and bank angle. Sadraey, et. al (2005:14), says exceeding the linear range of performance invalidates the more simple equations of motion, and call upon the more complex nonlinear coupled equations. Sadraey, et. al (2005:14), examined each of the simplifications listed above, and concluded, "the most accurate dynamic model for a full envelope flight simulation is one based on the nonlinear fully coupled equations of motion," (Sadraey, et. al, 2005:14). Despite the robust nature of these nonlinear fully coupled equations of motion, they are also the most complex to handle. Due to the nature of these nonlinearities, Sadraey, et.

al (2005:14), contends that no closed form solution exists, and numerical methods must be used to solve for a steady state solution.

Implementation of the nonlinear, fully coupled, ordinary differential equations of motion was the goal of this portion of the research. The equations of motion are readily available from noted authors such as Etkin, Roskam, Blakelock, and McRuer. A paper released by the Honeywell Technology Center in 1996 captured the essential equations from the aforementioned authors, and presented here.

Aircraft move with six degrees of freedom along three axis. Motion caused by gravity, propulsion, and aerodynamic forces contribute to the forces and moments that act upon the body (Honeywell, 1996:60). To begin, Honeywell (1996:60) makes several major assumptions. First, the aircraft is rigid. Although aircraft are truly elastic in nature, modeling the flexibility of the UAV will not contribute significantly to the research at hand. Second, the earth is an inertial reference frame. Third, aircraft mass properties are constant throughout the simulation. Finally, the aircraft has a plane of symmetry. The first and third assumptions allow for the treatment of the aircraft as a point mass.

A system of twelve state variables, expressed in stability, or flight path components. As explained by Honeywell (1996:61), flight path components are defined by an inertial system with coordinates \hat{I} , as positive north; \hat{J} , as positive east; and \hat{K} , as positive down. Table 22 first defines each of the state variables. Although the forces and moments are relative to the atmosphere, the state variables are defined relative to the earth (Honeywell, 1996:64).

Table 21. Flight Path Components Variable Definition

Flight Path Components	
Variable	Symbol
Roll Rate (rad/sec)	P
Pitch Rate (rad/sec)	Q
Yaw Rate (rad/sec)	R
Velocity (ft/sec)	V
Sideslip Angle (rad)	β
Angle of Attack (rad)	α
Bank Angle (about velocity vector, in rads)	μ
Flight-Path Angle (rad)	γ
Heading Angle (rad)	χ
North Position (ft)	ξ
East Position (ft)	η
Altitude (ft)	h

V , χ , and γ represent the magnitude of the velocity vector, heading angle, and flight path angle respectively. P , Q , and R represent the components of angular velocity; roll, pitch, and yaw, respectively. The position of the aircraft relative to the earth in Cartesian coordinates is ξ , η , and h . Body attitude relative to the velocity vector are μ , β , and α (Honeywell, 1996:65). The 12 nonlinear, and fully coupled ordinary differential equations of motions used to simulate the six-degrees of freedom of the Rascal 110 assume that lift is perpendicular and drag is parallel to inertial velocity (Equations 17).

$$\begin{aligned}
I_{xx} \dot{p} - I_{xz} \dot{r} &= l + I_{yy} r q + I_{xz} p q - I_{zz} q r \\
I_{yy} \dot{q} &= m - I_{xz} p^2 + I_{zz} p r - I_{xx} r p + I_{xz} r^2 \\
-I_{xz} \dot{p} + I_{zz} \dot{r} &= n + I_{xx} p q - I_{xz} q r - I_{yy} p q \\
\dot{V} &= \frac{1}{m} (-D \cos \beta + Y \sin \beta + T \cos \beta \cos \alpha) - g \sin \gamma \tag{17}
\end{aligned}$$

$$\dot{\chi} = \frac{1}{mV \cos \gamma} [D \sin \beta \cos \mu + Y \cos \mu \cos \beta + L \sin \mu + T(\sin \mu \sin \alpha - \cos \mu \sin \beta \cos \alpha)]$$

$$\dot{\gamma} = \frac{1}{mV} [-D \sin \beta \sin \mu - Y \sin \mu \cos \beta + L \cos \mu + T(\cos \mu \sin \alpha + \sin \mu \sin \beta \cos \alpha)] - \frac{g \cos \gamma}{V}$$

$$\dot{\mu} = \frac{p \cos \alpha + r \sin \alpha}{\cos \beta} + \frac{1}{mV} \left[\begin{aligned} &D \sin \beta \cos \mu \tan \gamma + Y \tan \gamma \cos \mu \cos \beta + L(\tan \beta + \tan \gamma \sin \mu) \\ &+ T(\sin \alpha \tan \gamma \sin \mu + \sin \alpha \tan \beta - \cos \alpha \tan \gamma \cos \mu \sin \beta) \end{aligned} \right] - \frac{g \cos \gamma \cos \mu \tan \beta}{V}$$

$$\dot{\alpha} = q - \tan \beta (p \cos \alpha + r \sin \alpha) - \frac{1}{mV \cos \beta} (L + T \sin \alpha) + \frac{g \cos \gamma \cos \mu}{V \cos \beta}$$

$$\dot{\beta} = -r \cos \alpha + p \sin \alpha + \frac{1}{mV} (D \sin \beta + Y \cos \beta - T \sin \beta \cos \alpha) + \frac{g \cos \gamma \sin \mu}{V}$$

$$\dot{\xi} = V \cos \gamma \cos \chi$$

$$\dot{\eta} = V \cos \gamma \sin \chi$$

$$\dot{h} = V \sin \gamma$$

4.2.3 – SIMULINK

The SIMULINK model was designed to accept the exact same control surface inputs sent to the flight test vehicle, but then to use the math model to determine the response. For the first 100 seconds the SIMULINK simulation is running, only trim conditions are sent to the control surfaces. For example, Table 23 list the trim conditions at a true airspeed of 64.8 feet per second input to SIMULINK for the first 100 seconds. The output is verified by examining the altitude and pitch rates to observe that the sim is in steady level flight.

Table 22. Example Trim Conditions for Given Velocity and Altitude

At given Velocity	64.8280 ft/sec
At given Altitude	1119 ft MSL
Throttle Trim	1.29
Elevator Trim	- 0.1174 rads
Rudder Trim	0 rads
Aileron Trim	0 rads
AoA Trim	-0.0153 rads

The trim conditions are sent as inputs, labeled steady level flight/Trim Conditions on the SIMULINK diagram. At 100 seconds, a commanded deflection is sent to one of the control surfaces. The commanded deflection is taken from the telemetry data collected during flight test, ensuring the commands are identical. The trim and flight conditions make up the initial state vector used to begin solving the 12 non-linear differential equations of motion introduced above. The initial state vector with the trim conditions is listed in Table 24.

Table 23. Equations of Motion Initial Conditions for given Velocity

Equations of Motion Initial Conditions for Trimmed Flight at given Velocity and Altitude	
State	Trim Value
P	0 rads/sec
Q	0 rads/sec
R	0 rads/sec
V	64.8280 ft/sec
β	0 rads
α	-0.0153 rads
μ	0
γ	0
χ	0
ξ	0
η	0
h	1119 ft MSL

The SIMULINK diagram below, Figure 30, shows the complete simulation set up. The control inputs and trim conditions are input from the left and plotted on a scope for verification. Then the equations of motion are called. The output from the equations of motion are integrated prior to plotting.

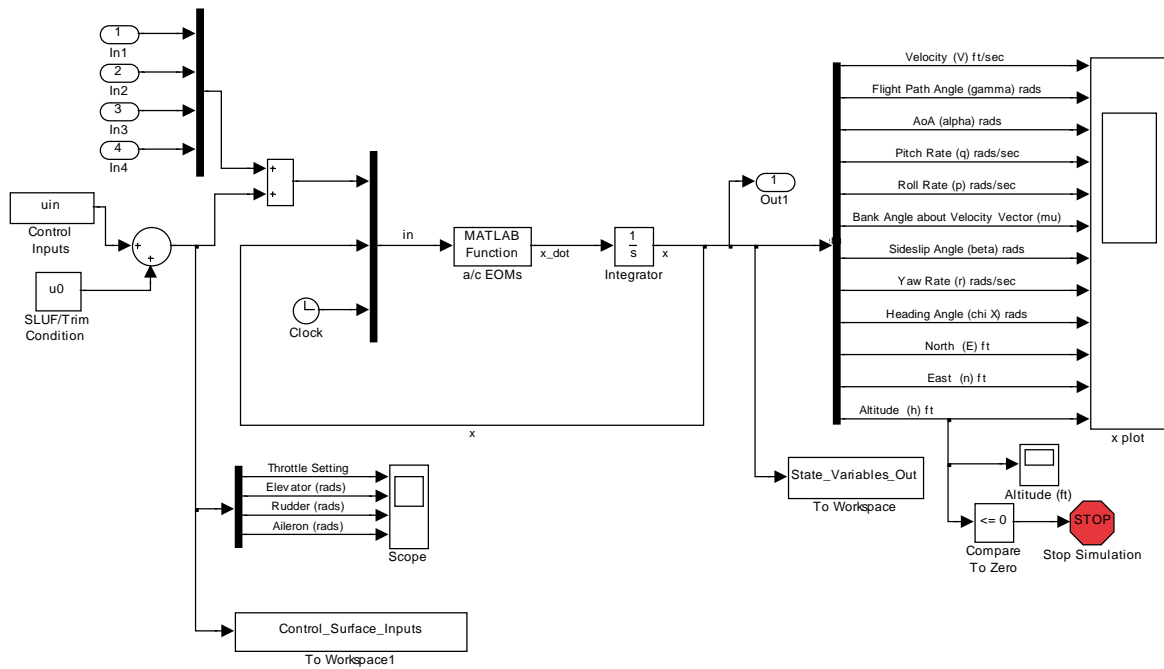


Figure 30. SIMULINK UAV Simulation

The SIMULINK input commands are presented next (Figure 31). Notice the throttle and elevator setting are held constant at the required setting for trimmed flight. The ailerons and rudder are held at zero since no lateral inputs are required for steady level flight. At 100 seconds, the input to the elevator is sent. The elevator returns to its trimmed setting and the aircraft is allowed to oscillate.

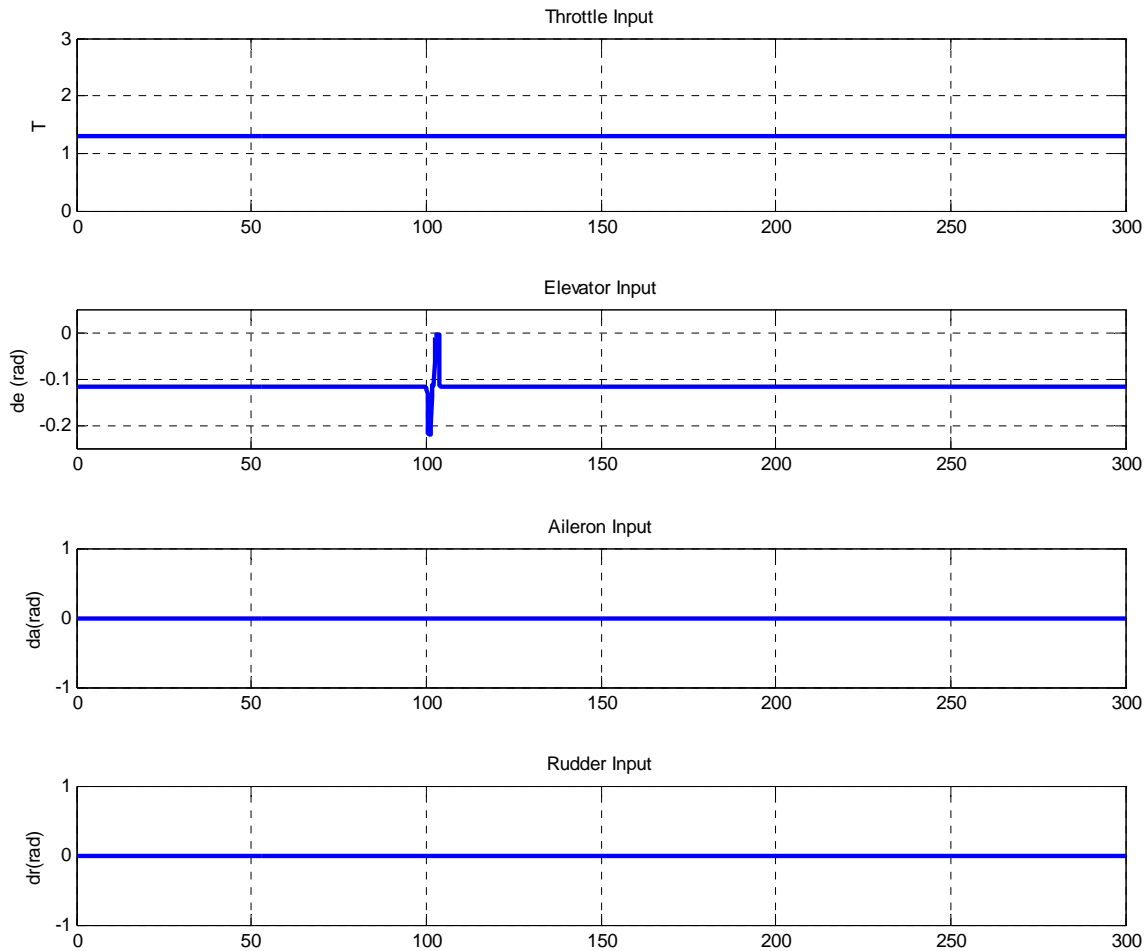


Figure 31. Control Surface Inputs to SIMULINK; Level Flight at 64.8 ft/sec

Figure 32 is the altitude as a result of the above inputs. The altitude response is usually of primary interest, as it is used for analysis of the aircraft's longitudinal response. Notice the aircraft is flying level prior to the elevator deflection.

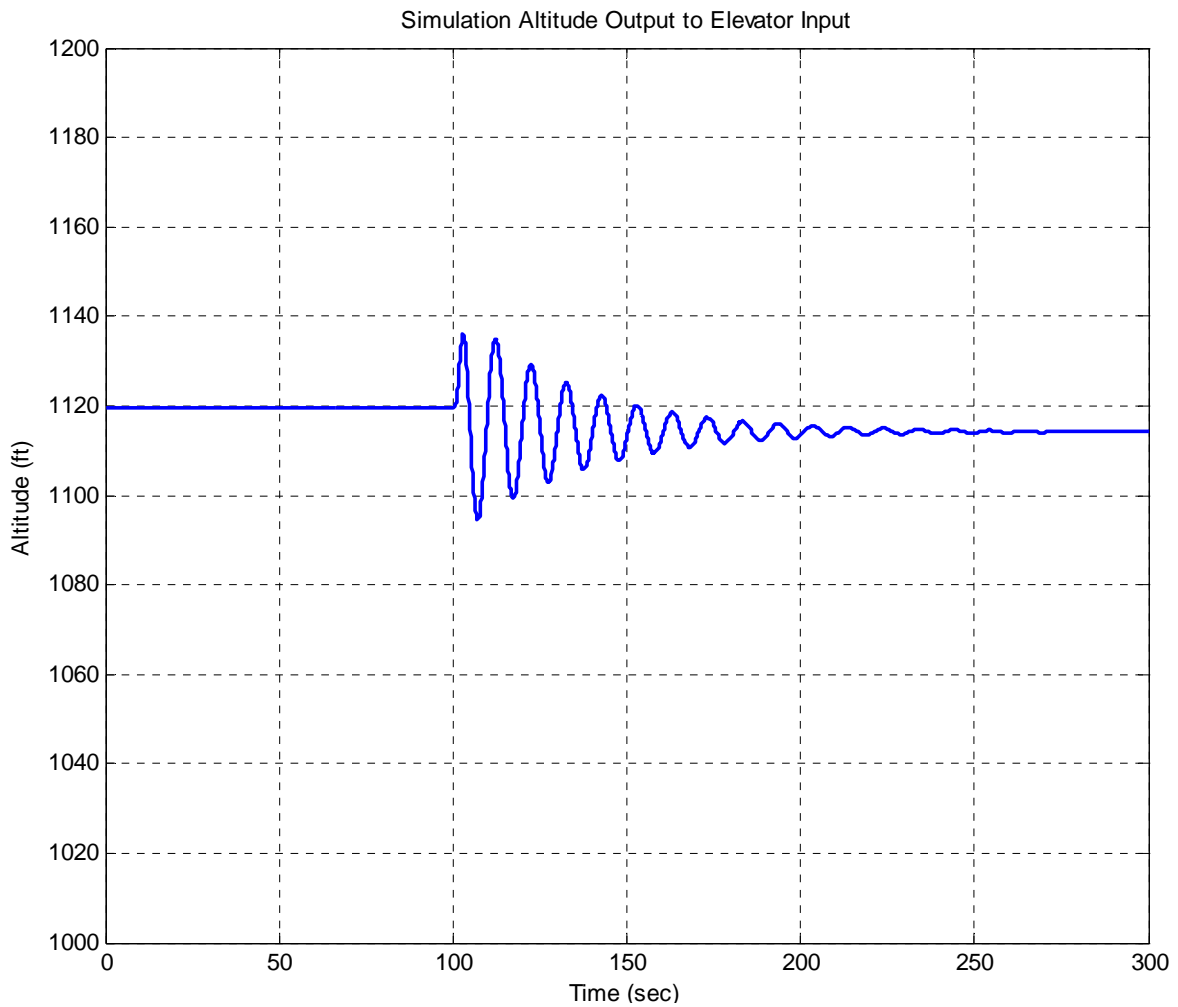


Figure 32. Altitude Output Response of SIMULINK to Elevator Doublet Command

Figures 33 and 34 shows all 12 states of the simulation for the duration of the 300 second run. Note the states are constant until the elevator input. The north position vector shows an increase in distance flown, but no deviation to the east, indicating a straight flight path in a northerly heading. Only pitch rate, angle of attack, velocity, flight path angle, and altitude change with respect to the elevator inputs. Roll rate, bank angle, sideslip, yaw rate, and heading angle all remain unchanged with respect to the elevator

inputs. All the results are expected for the input command, verifying the simulation is functioning properly.

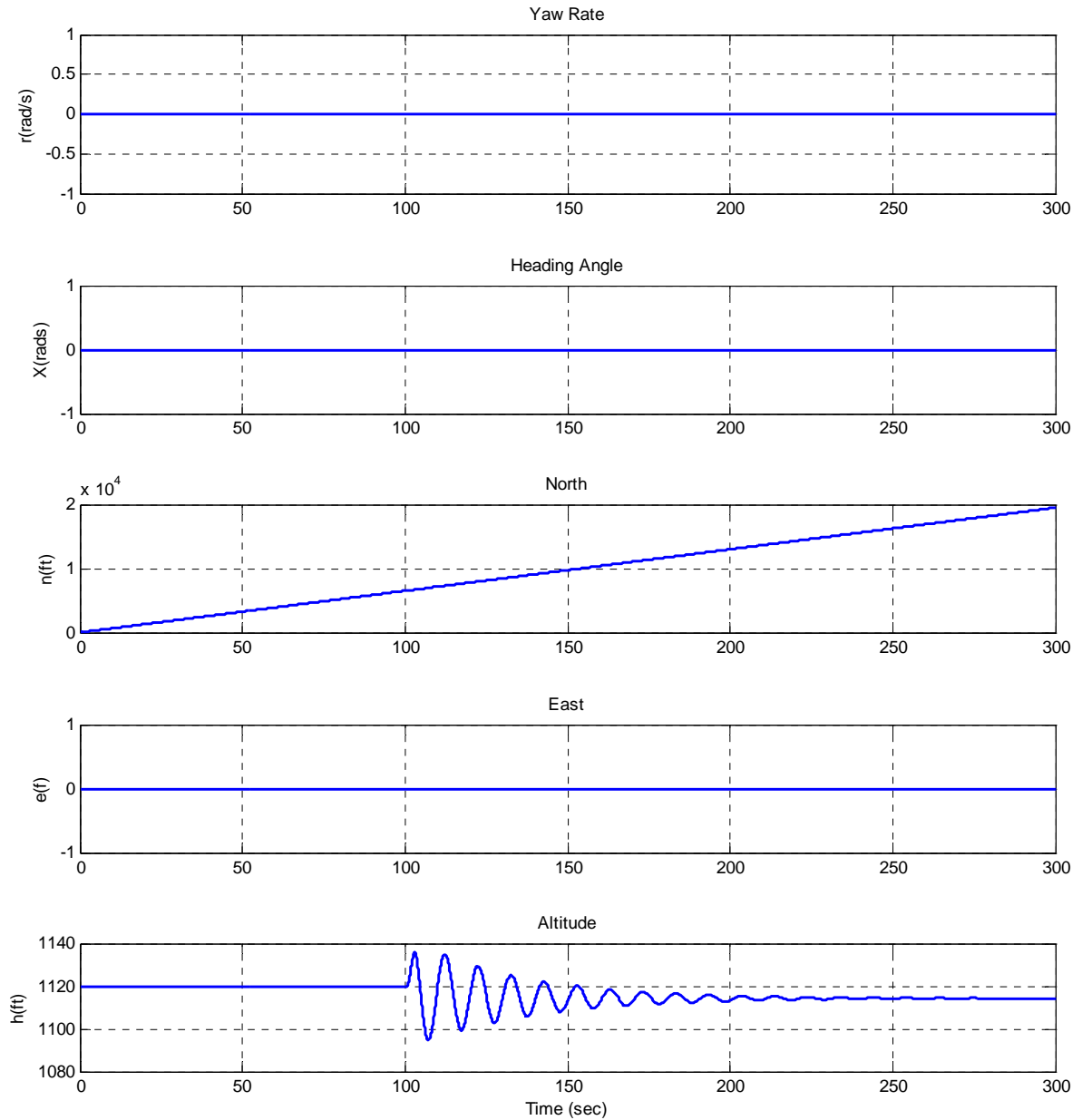


Figure 333. SIMULINK Output; Aircraft States 8-12

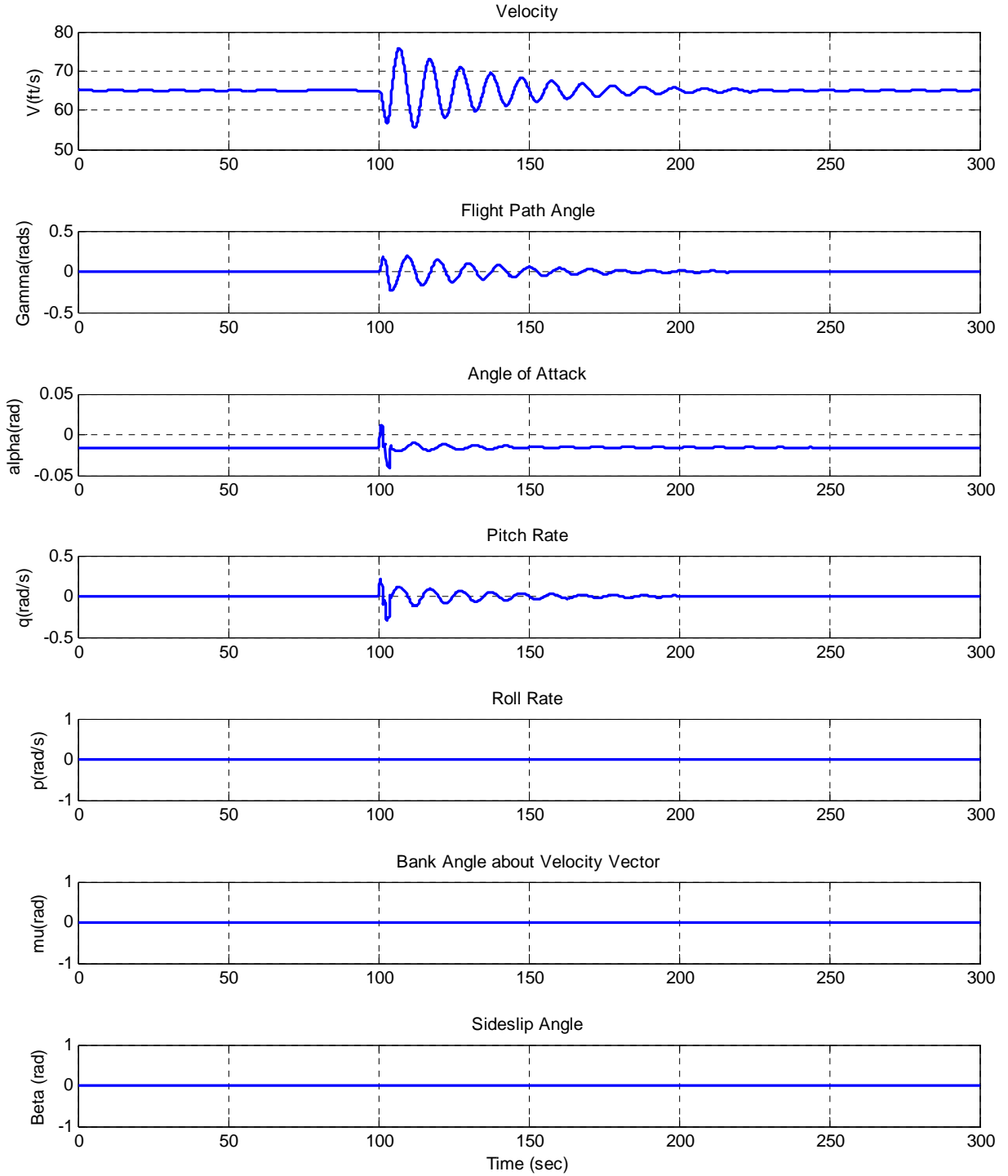


Figure 344. SIMULINK Output; Aircraft States 1-7

4.3 – Hardware in the Loop Simulation

The HITL simulation, provided by Cloud Cap Technologies, was used extensively for laboratory flight simulation and test team training. The HITL simulation used the same Operator Interface used during flight. The HITL environment is very nearly representative of the airspace and flight conditions of the Rascal although several differences exist. The wind conditions experienced in the test flights were not reproduced. No wind conditions were desired for simulation, and a majority of flight tests were conducted on calm days. Altitude and airspace restrictions were not observed during flight in the HITL simulation. The test team felt this would over constrain the simulation, and minimize its usefulness.

The HITL simulation uses the model constructed in Chapter III. The gain settings, waypoints, and all other parameters input to the Operator Interface were also identical to the settings input during actual flight. The main components included the Piccolo II, the Ground Station, Laptop with Operator Interface, and a simulator PC, Figure 34

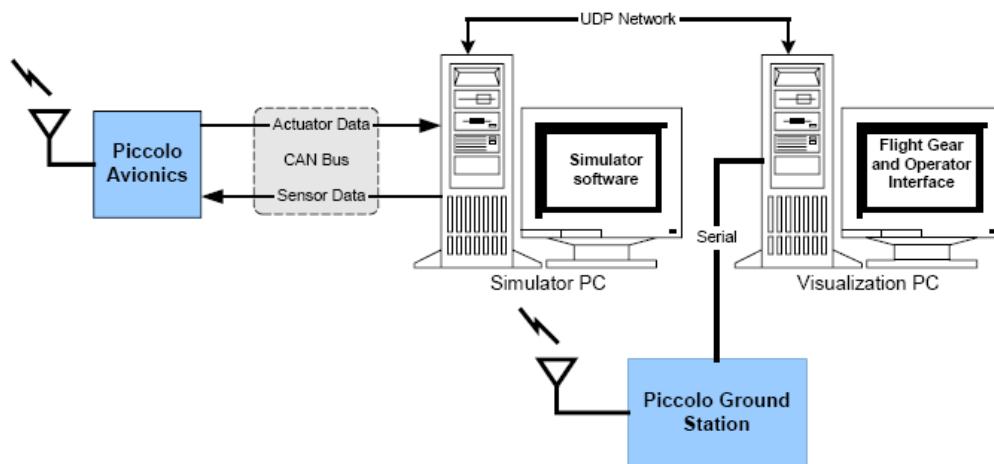


Figure 35. Typical Hardware in the Loop Simulation Set Up

4.4 – Chapter Conclusions

Chapter IV developed the force and moment equations necessary for the Matlab/SIMULINK simulation. Additionally, 12 non-linear equations of motion were used to simulate the dynamic response of the Rascal 110 to control surface inputs. The equation build up was done in Matlab and simulated in SIMULINK. The HITL simulator was also described.

V. Flight Test of UAV Platform

5.1 – Chapter Overview

Chapter V details the flight-testing introduced in Chapter II. The procedures and maneuvers flown for both open loop airframe and autonomous flight tests. Also discussed are flight-test issues encountered during the research.

5.2 – Open Loop Flight Tests

The challenge of implementing the procedures for open loop flight test required overcoming significant testing issues such as weather, equipment, scheduling, and ambiguities in aircraft attitudes. Development of a flight-test plan structured and maximized flight time. Each flight required the establishment of a constant communications link with the aircraft in order to collect telemetry at 20 Hz. Maneuvers were flown either into the wind or with the wind. Cross wind maneuvers were not flown.

5.2.1 – Flight Procedures and Configurations

The procedures for executing each maneuver were carefully scripted ahead of time. After take off, the pilot flew the aircraft to the end of the airspace and aligned it with the wind. The aircraft flew at airspeeds between 60 and 90 feet per second, as determined by the maneuver to be performed. Test altitudes were approximately 1100 feet. The pilot then established a trimmed and steady level flight condition. To study each maneuver in a post-flight analysis, the beginning time of each maneuver was logged. When the aircraft oscillations damped out after the maneuver, the time was again logged. To correspond with the telemetry log file, the Operator Interface clock was used.

5.2.2 – Maneuvers

The pilot performed the phugoid and short period maneuvers introduced in Chapter II. Only the elevator was used to perform these maneuvers, while the throttle, ailerons, and rudder were held in trim position. The phugoid maneuvers were started from trimmed flight when the pilot input a nose up command to bleed airspeed. Only the elevator was used. During several practice runs were performed to determine the correct pitch up angle to bleed about 15 feet per second of airspeed. Telemetry read outs from the Operator Interface determined the changes in airspeeds. Once the pitch up maneuver was performed, the pilot returned the elevator to the trimmed position and allowed the aircraft to oscillate until all the oscillations damped out.

The short period maneuver was performed in much the same way as the phugoid. Where the phugoid was just a nose up maneuver, the short period is a nose up, nose down, and back to trim procedure. Again, just the elevator was used and all maneuvers began from steady level flight.

5.3 – Autopilot Flight Tests

The Rascal flew under autopilot mode primarily for tuning and training of the ground crew. This phase of the research was a necessary step to ensure proper operation of the autonomous system, accurate telemetry, and delivery of a properly configured autonomous UAV for continued research. The autopilot system was given a set of predetermined waypoints and altitudes. The waypoints formed a track, or orbit inside the flight test range. Plots in this section illustrate the locations of the waypoints.

5.3.1 – Procedures

Flown under manual control, the Rascal UAV went to the planned orbit altitude. After reaching the proper altitude, the Rascal flew to the planned airspeed and Waypoint #1. The planned orbit was clockwise as viewed on the map in figures 9 and 35. The next section discusses waypoint specifics.

5.3.2 – Waypoint Tracking

The autopilot manufacturer recommends selecting waypoints in a large box type pattern for initial autopilot tuning. Airspace constraints also contributed to waypoint selection. A simple box pattern would have four waypoints, one at each corner. The test team chose to have seven waypoints instead. Figure 35 illustrates the waypoints and their connecting segments bounded by the flight test airspace. Starting waypoint #1 was added in the middle of the first segment to act as a starting point and to distinguish aircraft performance compared to the long straight segment, #4 to #5, without a center waypoint. Additional waypoints, #3 and #6, were added at the center of the end segments and extended slightly further than the corner waypoints. Based on initial autonomous flight tests, the test team believed this overhead pattern provided smooth turns in a race track pattern for the autopilot tuning. Without these waypoints the aircraft banked harder than desired in order to align to the next segment. It was also critical to ensure excess airspace was available for added maneuvering both under autopilot and manual control.

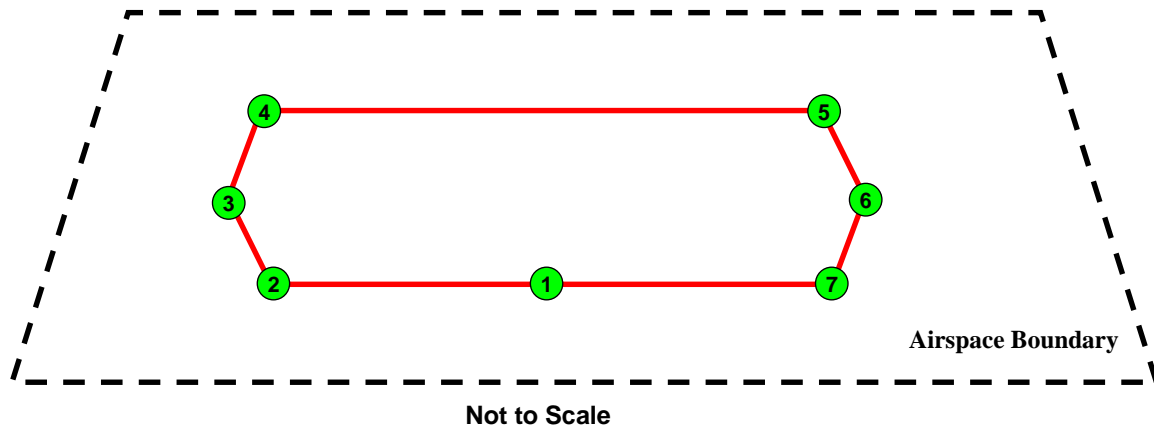


Figure 36. Autopilot Waypoints and Planned Pattern

The latitudes and longitudes corresponded to the WPAFB Area B map in Figure 9, section 2.6.2. They were determined by inserting the map into the Operator Interface with latitude and longitude reference information. Using the Operator Interface, waypoints were selected inside the flight test airspace boundary and the corresponding latitudes and longitudes were displayed. The desired altitude was originally 1100 feet above sea level, or roughly 315 feet above ground level. Recall the airspace ceiling was 400 feet above ground level. Despite inputting the desired altitude, the autopilot defaulted to 1085 instead, still an acceptable test altitude well within safety limits. Table 25 lists the waypoints north latitude, west longitude, and altitudes.

Table 24. Autopilot Waypoints Latitude, Longitude, and Altitude

Waypoint	North Latitude (deg)	West Longitude (deg)	Altitude (ft)
1	39.773427	-84.105419	1085
2	39.773600	-84.108343	1085
3	39.774877	-84.109116	1085
4	39.776215	-84.108017	1085
5	39.775921	-84.100934	1085
6	39.774413	-84.100123	1085
7	39.773234	-84.101051	1085

5.4 – Testing Issues

Significant issues hindering data collection during open loop and autonomous flight-testing. A host of non-flight test issues including scheduling, weather, personnel availability, equipment operation, test planning, pilot familiarity flights, and test team training all contributed to limited data collection. Issues arose during flight as well, including winds, airspace boundaries, maneuvering, and repeatability. Autonomous flight test issues involved real time gain settings and resultant performance.

5.4.1 – Non-Flight Test Issues

Scheduling and weather proved to be the largest contributors to flight test delays. The test range at WPAFB is a multi-use facility where other research is conducted on a regular basis. Unfortunately, the other research included experimental laser and radar tests and prevented access to the test range. Deconfliction of range time was handled by AFRL/SN, an agency external to AFIT. Weather also slowed the progression of flight-testing. High winds, rain, fog, and cold temperatures affected both the aircraft and the test team. A majority of flights were conducted between the months of September to November of 2005. During these months at Wright Patterson AFB, the weather is unpredictable and not suitable for regular flight-testing.

Autonomous flight-testing required the presence of the pilot, test conductor, Ground Station Interface operator, and safety observers. Coordinating availability of each test team member was not a significant hindrance, but did require at least two to three days of planning ahead of scheduled testing. Test team training and coordination during data collection also consumed valuable flight time. However, the coordination

was a mandatory if the test team desired any useful data. Equipment failures included a pinched GPS antenna wire, a safety of flight issue, low battery power, and loose servo connectors among other issues. Most equipment issues grounded the aircraft anywhere from a few minutes to several hours. Not all the aforementioned testing issues are significant when considered individually. Nevertheless, progress is noticeably slowed when two, three, or even four delays combine during a single flight test. All the test issues were successfully overcome, but nonetheless worth mentioning.

5.4.2 – In-Flight Test Issues

Once the non-flight test issues were overcome, in-flight issues were constantly challenging the test team. Since no procedures were found specifying the open loop flight test of a UAV like the Rascal, much of the procedures had to be adopted from full-scale aircraft flight-testing. Flight time was consumed to observe aircraft response to maneuvers in order to develop a reasonable flight test plan.

During open loop flight test, level flight was difficult to achieve on a consistent basis. Furthermore, level unaccelerated flight proved even more difficult to achieve regularly. The primary feedback method for aircraft performance is the pilot's opinion from his vantage point on the ground. Although telemetry was being transmitted and read aloud by the Ground Station Interface operator, he was not capable of trimming the aircraft in manual mode. The pilot is not in a position to read telemetry since he must keep his eyes on the aircraft at all times. Since all open loop flight is conducted while under manual control, the determination for level flight rested upon the opinion of the pilot with inputs from the test team based on observation and rapidly changing telemetry

read outs. Consequently, the necessity for steady level trimmed flight prior to performing any open loop test maneuver was achieved about 50% of the time. Data from maneuvers where trimmed flight was not achieved before hand is significantly less reliable. Untrimmed flight conditions introduce unwanted forces, moments, and rates on the vehicle. Conditions such as a slow climb or slight bank are difficult to model in simulation, especially when trying to isolate motion purely in one direction or axis.

Since steady level flight was partially subjective (the pilot's opinion) and partially objective (the aircraft telemetry), repeatability of maneuvers was difficult to achieve. Manual inputs from the pilot were not identical during every attempt. It is also important to note the pilot works very hard to establish a steady level trim condition and repeat every maneuver, all while working up against airspace boundaries. During analysis, airspace boundaries proved to be the most limiting factor of all the test issues. Flying at average test speeds of 70 feet per second, the aircraft was capable of spanning the length of the allotted airspace in just over a minute, severely limiting the test team. The Rascal is a large aircraft and requires substantially more airspace than initially allocated to operate effectively. While setting up the aircraft in a level flight condition to perform any maneuver, nearly a third of the length of the airspace was consumed, leaving only 2000-3000 feet of maneuvering space ahead of the vehicle. This distance proved to be too short, for example, to fully allow the phugoid and short period maneuvers to damp out.

5.4.3 – Autonomous Flight Test Issues

Despite being the most complex task, flying the Rascal under autopilot had relatively fewer issues. GPS Satellite visibility and signal acquisition is a requirement for

autonomous flight. During a few instances, satellites were not detected by Piccolo. After a detailed inspection of the hardware, the pinched GPS antenna wire was discovered and required replacement. The gain setting procedure, a critical task to smooth autonomous flight consumed nearly 75% of flight time under autopilot control. At the time of this paper, gain tuning is still ongoing with the current Rascal and Piccolo II configuration. Due to improper gains, the aircraft was experiencing altitude losses during maneuvers requiring banking more than 10 degrees. The altitude loss testing issue is discussed further in Chapter VI.

The test team overcame much of these flight related issues by repeating each maneuver nearly 20 times while performing real time optimization of gains, heading, inputs, and trim conditions. To make the data as robust as possible and adapt to the limitations, variation in headings, airspeeds, inputs, and trim conditions were incorporated into the test plan. Despite the constant in-flight and non-flight related test issues, the test team successfully collected over two hours of continuous flight test data during several days of testing.

5.5 – Chapter Conclusions

Chapter V discussed the flight-testing procedures and maneuvers flown over WPAFB. Open loop and autonomous flights were conducted, and detailed telemetry collected. Testing issues encountered through out the flight-testing portion of this research were also discussed. The results of the flight test phase are presented in Chapter VI.

VI. Results and Analysis

6.1 – Chapter Overview

Chapter VI will review the results of the open loop flight and autonomous waypoint flight tests comparisons are made between the actual flight tests, Hardware in the Loop Simulation, and Matlab/SIMULINK simulation.

6.2 – Open Loop Flight Test Results

Open loop flight test analysis examines the short period and phugoid modes of the aircraft in both simulation and flight. Section 6.2.1 presents the results of the actual flights and the Matlab/SIMULINK simulation. Section 6.2.2 presents the results of the HITL and Matlab/SIMULINK simulation.

6.2.1 – Flight Test and Matlab/SIMULINK Simulation Results

Many attempts to excite the short period and phugoid modes were made. As previously stated, due to airspace limitations, the aircraft was not allowed to continue oscillating until all the oscillations damped out. The Matlab/SIMULINK simulation was scaled to run for the same length of time the aircraft in flight. In Figure 37, the aircraft was trimmed at 64 feet per second when the elevator doublet command was input. The aircraft exhibited 30 feet higher altitude gains than the Matlab simulation during the initial oscillation. The period of oscillation was longer in flight as compared to the simulation's output. Notice the input commands to both simulators were identical. The altitude plot also reveals the aircraft was in a slight climb prior to the input, suggesting it was not in true steady level unaccelerated flight. This is confirmed by the True Airspeed (TAS) plot, which shows decreasing airspeed prior to the commanded input. The aircraft

also has a higher pitch rate than the Matlab/SIMULINK simulation. In general it seems the flight test data was not run long enough to compare significant damping effects over time.

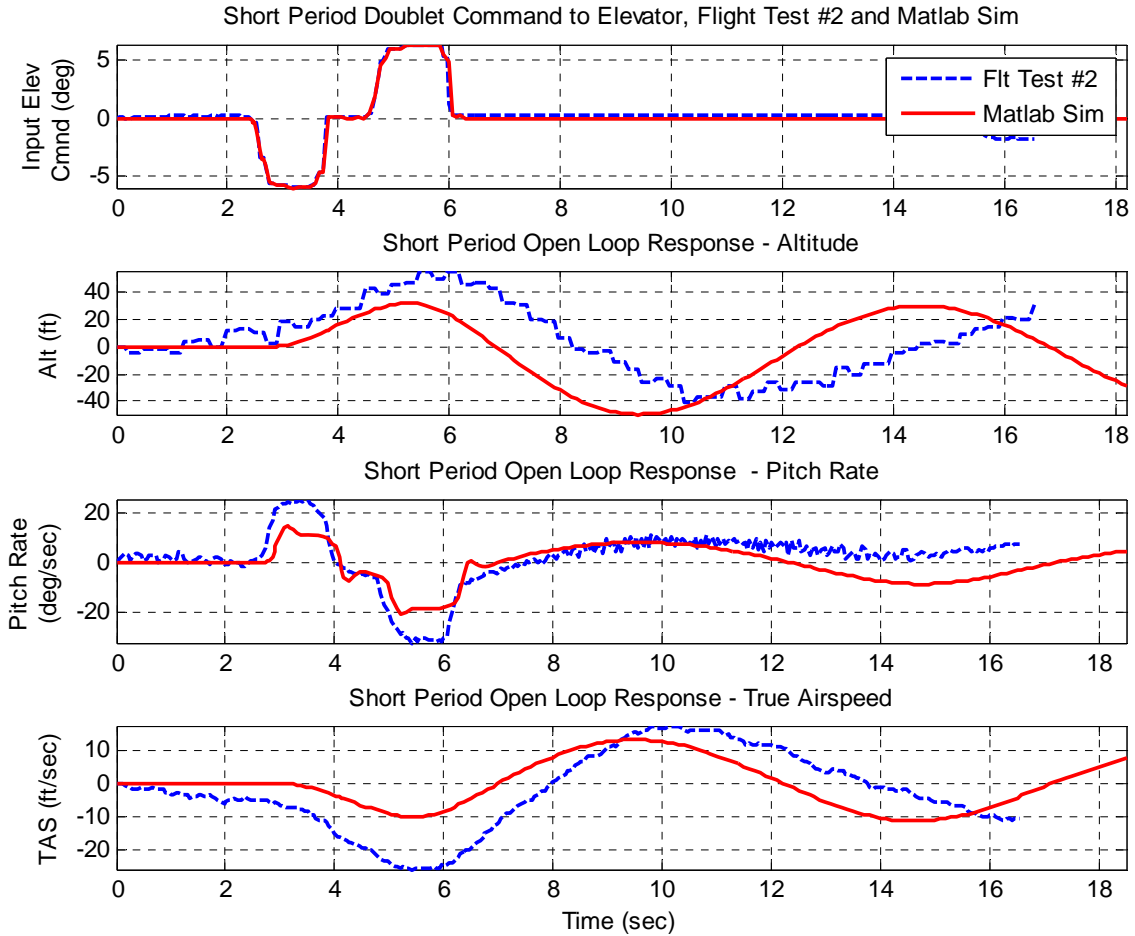


Figure 37. Short Period Response to Elevator Doublet – Flight Test #2 v Matlab Sim

The phugoid tests reveal a good initial response and similar oscillations over time. However, the aircraft seemed to perform the oscillations while climbing as exhibited by the final altitude of the aircraft, and compared to the simulation, which tends to center around the starting altitude. Although the amplitudes do not match, the periods of oscillations line up. The trimmed airspeed was approximately 88 feet per second.

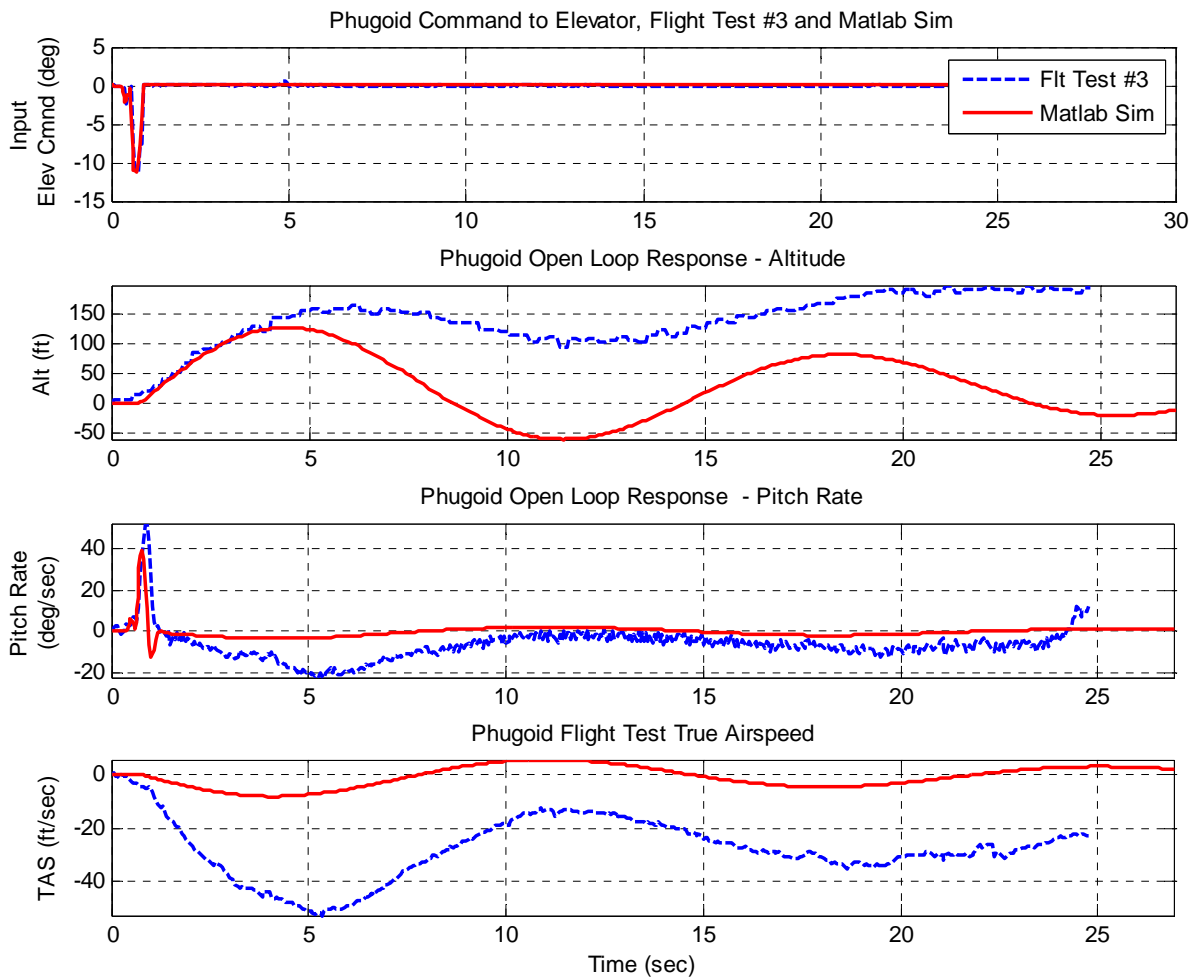


Figure 38. Comparison of Flight Test #3 to Matlab Sim; Elevator Input

The phugoid response to a smaller elevator input is depicted in Figure 38. The elevator input was only seven degrees as compared to the previous 11 degree deflection. Also, this deflection of the elevator was held for a longer period of time as compared to the previous rapid input. The output shows the periods lining up, but not the altitudes. The pitch rate is the first indication that the oscillations will differ. The initial pitch rate of the Matlab simulation did not reach the same magnitude of the aircraft during flight test.

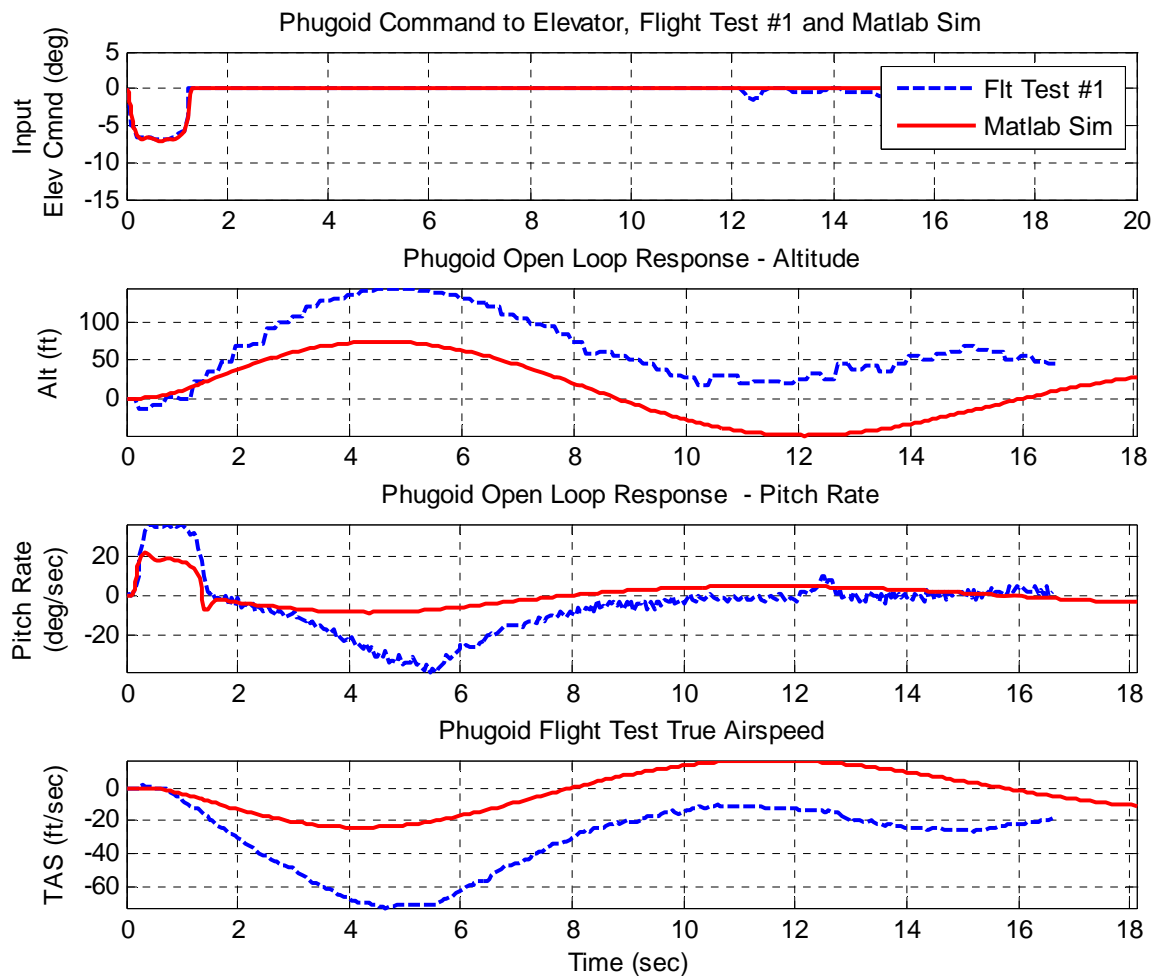


Figure 39. Comparison of Flight Test #1 to Matlab Sim; Elevator Input

The Hardware in the Loop simulation tended to match the Matlab simulation better than the flight test comparisons (Figure 39). The initial periods line up, but the oscillations quickly fall out of phase with each other. This indicates the pitch damping of the HITL simulation is slightly higher than the Matlab simulation. Overall, the response to the elevator input shows a promising result.

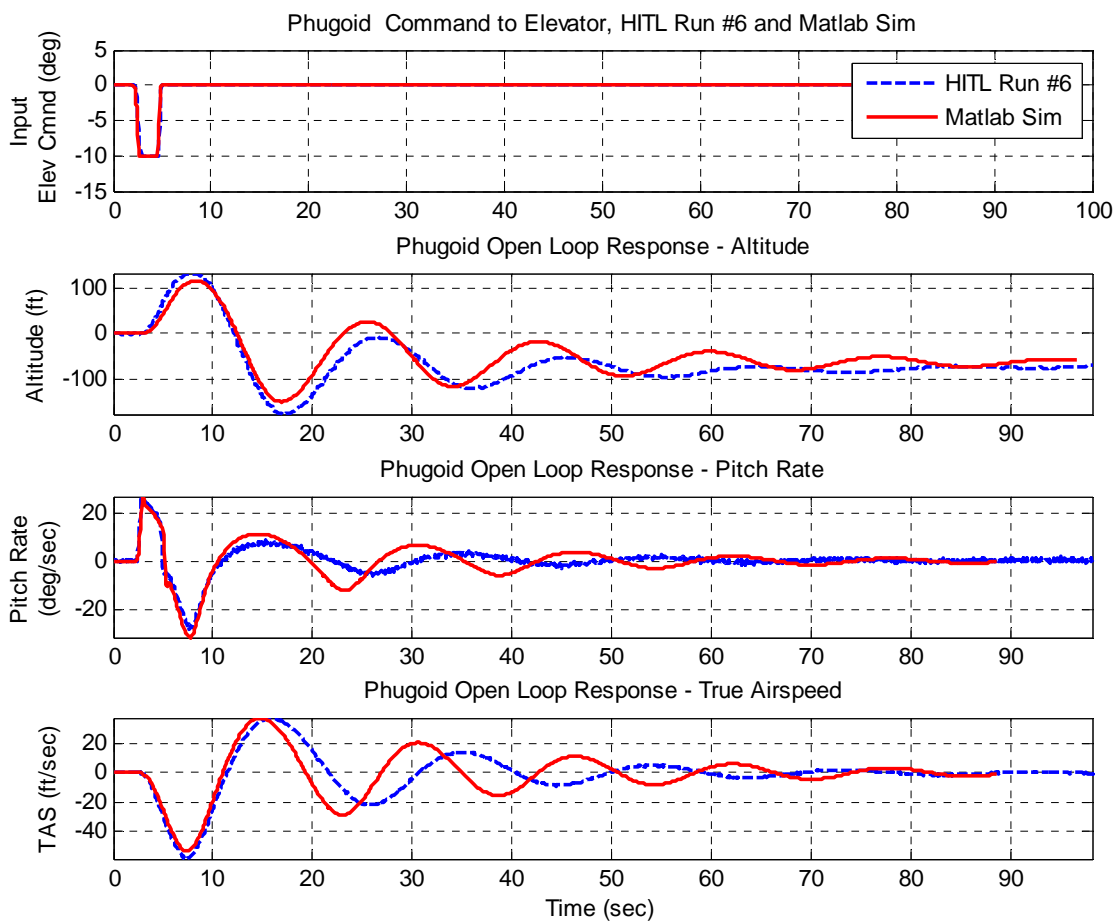


Figure 40. Comparison of HITL Run #6 to Matlab Sim; Elevator Input

Figure 40, represents the results of another HITL and Matlab comparison. The input here is much smaller than the previous comparison. The response is similar to the previous in terms of damping and oscillations. As expected, altitude was not as high, due to the smaller input. This output was expected and shown.

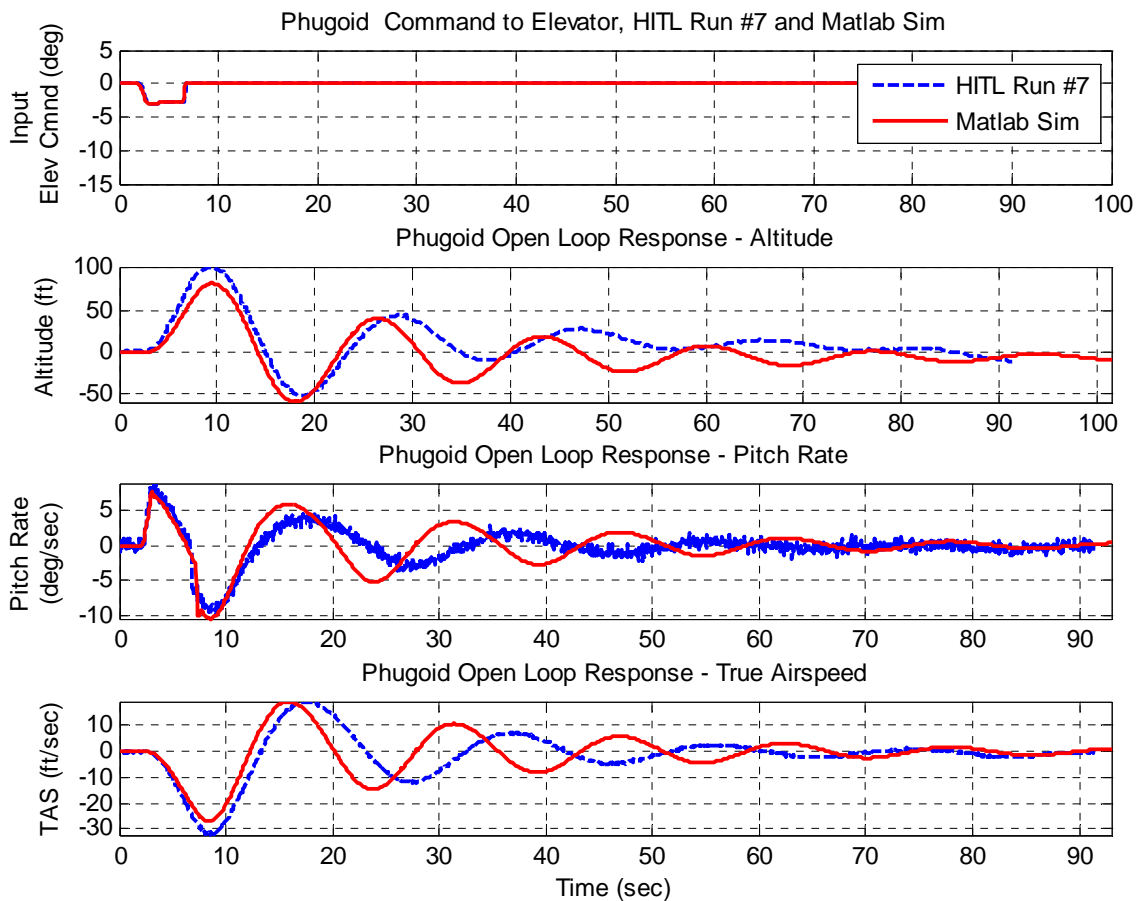


Figure 41. Comparison of HITL Run #7 to Matlab Sim; Elevator Input

6.3 – Autonomous Test Flights

Under autopilot control, the Rascal performed fairly well. This section reports the results of the HITL simulation and the Autonomous flights with the same configurations. The first section details the results of the HITL simulation with some added improvements. The second section illustrates the Autonomous flights performed by the Rascal 110 over WPAFB. Real time gain tuning was performed and reported

6.3.1 – Waypoint Hardware in the Loop Simulation Results

The HITL performed many iteration of the same waypoint orbit. Two of the better simulation are reported in this section. Appendix B contains all the HITL simulation results. The first set of waypoint orbits are performed at 88 feet per second, 1083 feet in altitude, and the waypoints presented in Chapter V. These conditions were also flown by the Rascal 110 and discussed in the next section. In Figure 41, the HITL simulation seemed to make the north east and south west waypoints, but clearly missed the north west and south east corners. During this simulation, the HITL failed to adequately converge to the desired waypoint paths.

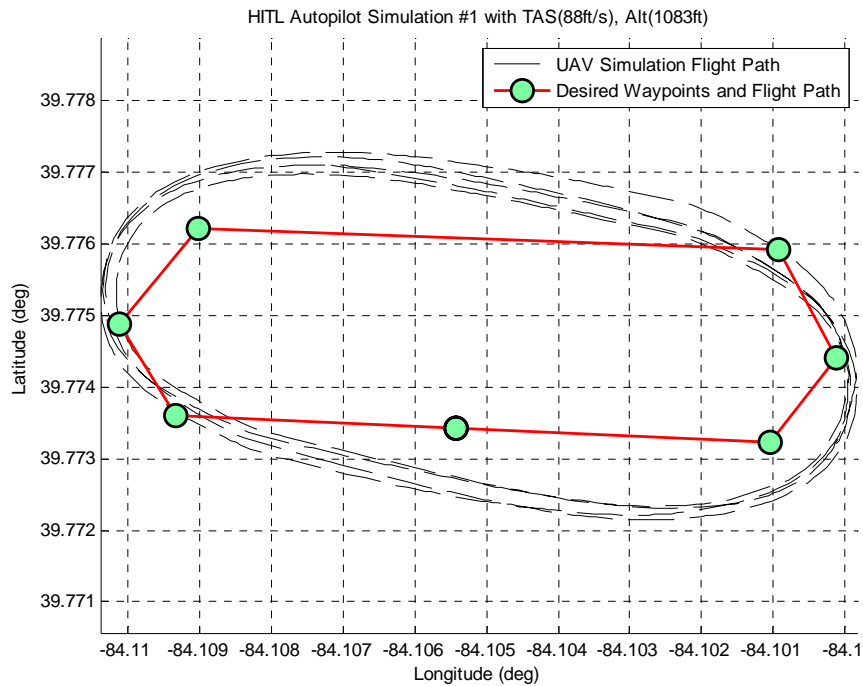


Figure 42. Waypoint HITL Simulation Results - Actual Track

The test team then re-accomplished the above HITL simulation with some changes. First the track was widened. The test team believes the original track was too narrow for large Rascal 110 to negotiate well enough. Also, the airspeed was reduced from 88 feet per second to 61 feet per second. This gave the aircraft a better chance of making necessary corrections to reach each waypoint. Finally, the convergence gain was adjusted using the manufacturer’s steps for improving convergence, commanding the autopilot to reach the waypoint track faster. The combinations of these changes were plotted in Figure 42.

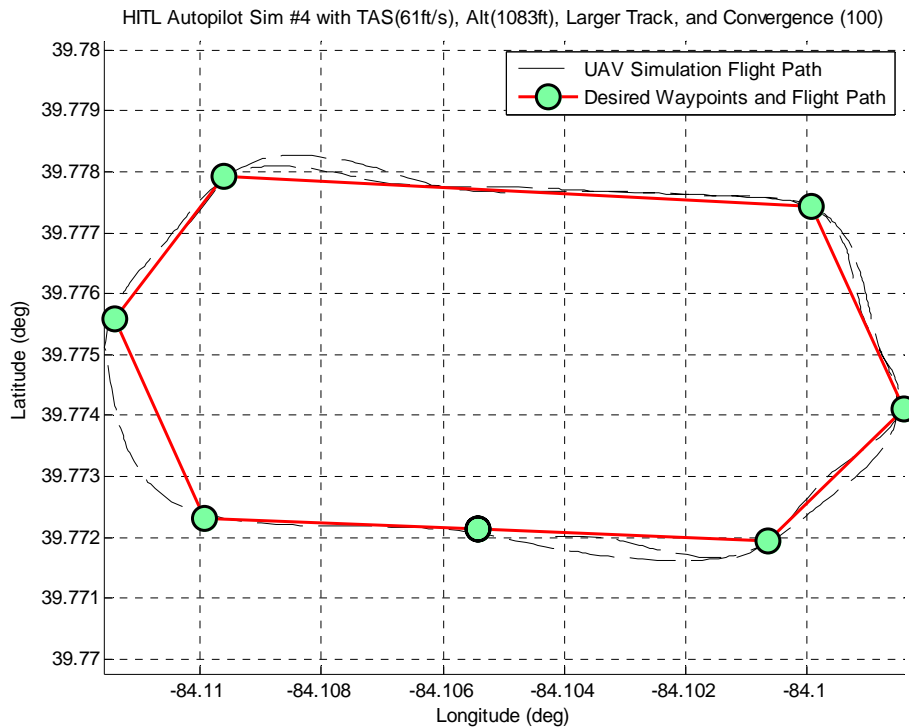


Figure 43. Waypoint HITL Simulation Results - Larger Track

The altitudes and airspeeds of the HITL simulation were also plotted versus time. The goal of this plot is to illustrate the performance of holding altitude and airspeed in the HITL simulation. Figure 43, shows the variation in altitudes and airspeeds between four HITL simulation runs. Simulations #1 and #2, flown at 90 feet per second, while simulations #3 and #4 started at 68 feet per second. At the 130 second mark, simulation #4 was commanded to 61 feet per second and is not shown. Altitude performance was also constant throughout the HITL Simulations. Clearly, a regular loss in altitude occurred at the same time, around 150 seconds. The HITL corrected back to the proper altitude. Simulation #3, shows signs of losing altitude again, indicated a possible repeating occurrence. Since no winds were introduced, the results suggest that either the altitude hold gains need to be improved or the waypoint orbit configuration is too tightly

constrained, causing the aircraft to bank harder to reach the next waypoint, and subsequently, lose altitude.

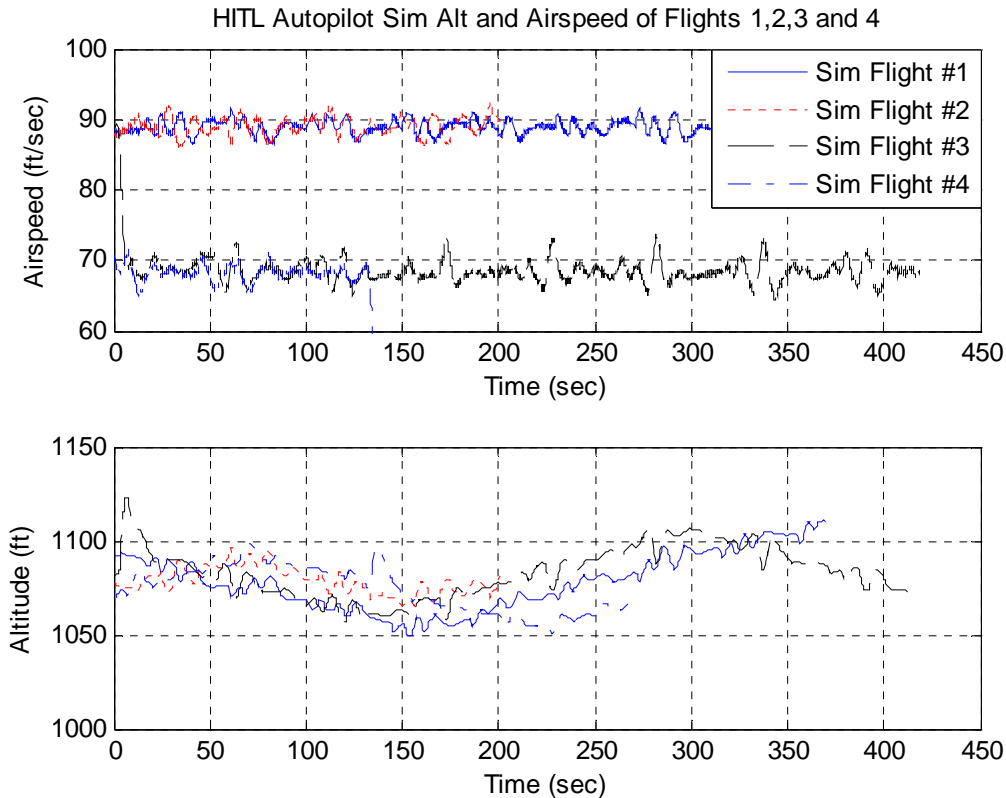


Figure 44. HITL Simulation Output; Airspeed and Altitude

6.3.2 – Waypoint Flight Test Results

Flying under the same conditions as flown during HITL simulation, the autopilot was tested in flight. Using the same gains, altitude, and airspeed settings from HITL simulation #1, as well as the same narrow waypoint orbit, the Rascal 110 was flown over Area B at WPAFB. Using the narrow waypoints, and an airspeed of 88 feet per second, the Rascal 110 flew a tighter pattern than the HITL, under the same conditions. The overhead views shows the Rascal 110 over shooting the waypoints and desired path during some portions of the orbits, while clearly flying over the waypoints during other

portions. Although a calm day, wind speeds did increase from time to time, possibly affecting the performance. The test team believes this race track is too narrow for the large Rascal 110 to negotiate at 88 feet per second. Waypoint flight test #4 is also shown in Figure 44.

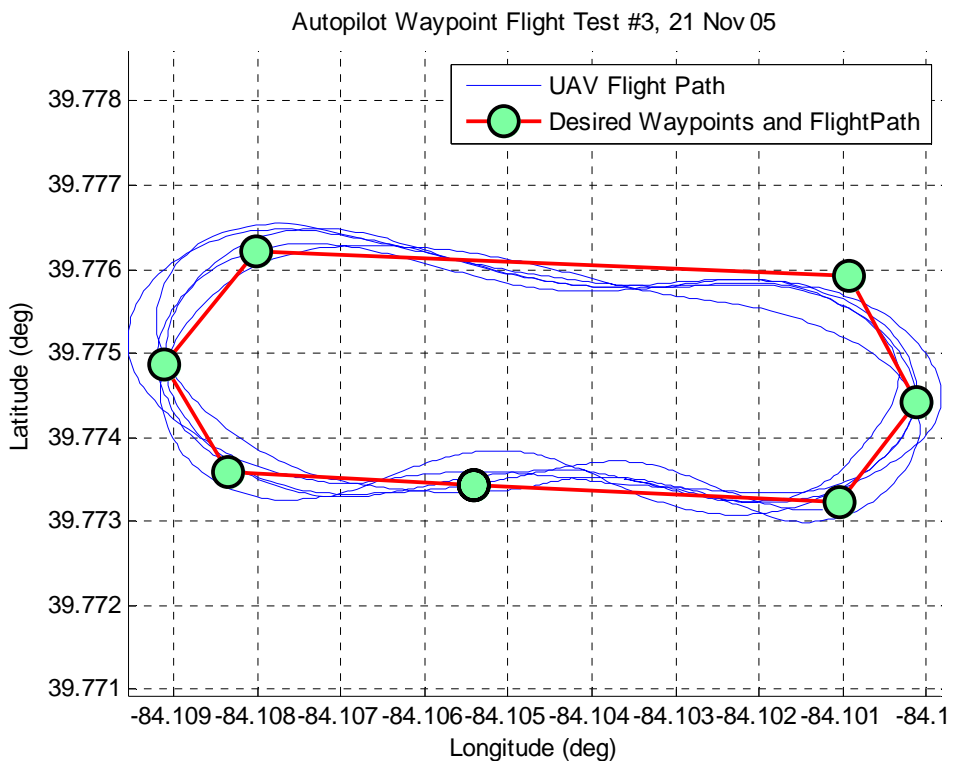


Figure 45. Autopilot Waypoint Flight Test #3

The altitudes and airspeeds of the autopilot waypoint flight tests are examined next. The first two figures are three-dimensional plots of the autopilot waypoints flights depicted in Figure 45. The next three perspectives illustrate the altitude changes as the autopilot transitioned from one waypoint to the next. During flight, the aircraft was observed losing significant altitude on the short end of the waypoint orbit. In waypoint flight test #3, the telemetry reveals over 200 feet of altitude was lost from the desired

altitude of 1083 feet, or over 20%. Waypoint flight test #4 showed an improvement by losing only 150 feet in altitude. The improvement was due to in flight gain tuning. Following the manufacturers procedures for gain tuning, the altitude shows immediate improvement. Clearly, continuing along this path would further improve the autopilot's performance. Although the test team wanted to continue flying in order to improve the autopilot gains, poor weather and hardware failures prevented further flights prior to the publication of this report.

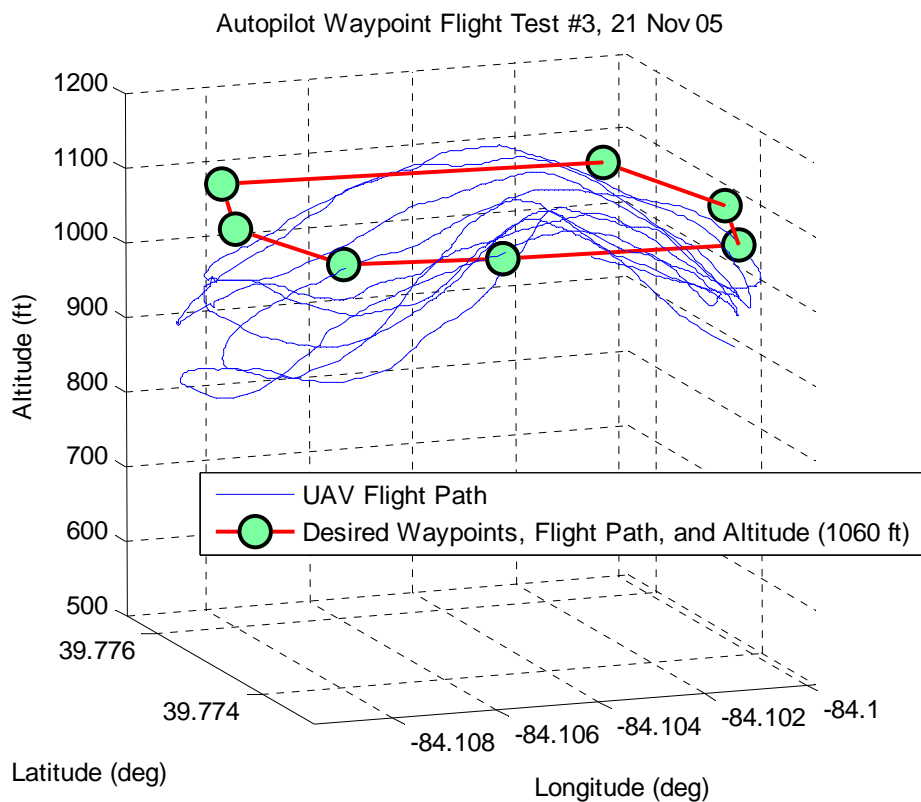


Figure 46. Autopilot Waypoint Flight Test #3 – Altitude

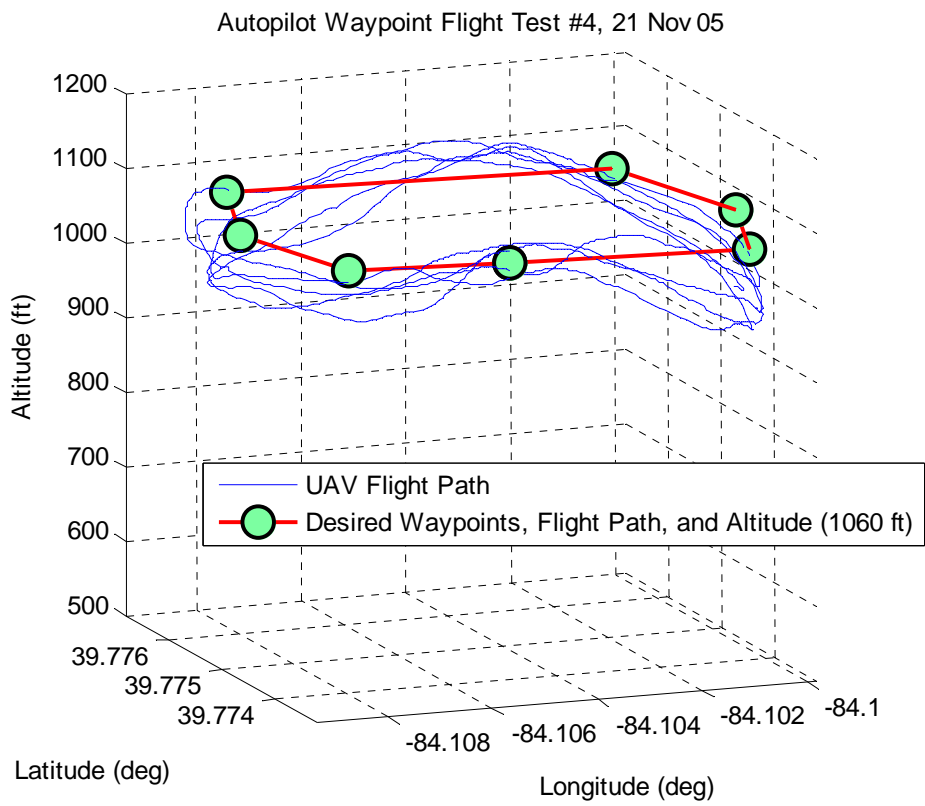


Figure 47. Autopilot Waypoint Flight Test #4 – Altitude

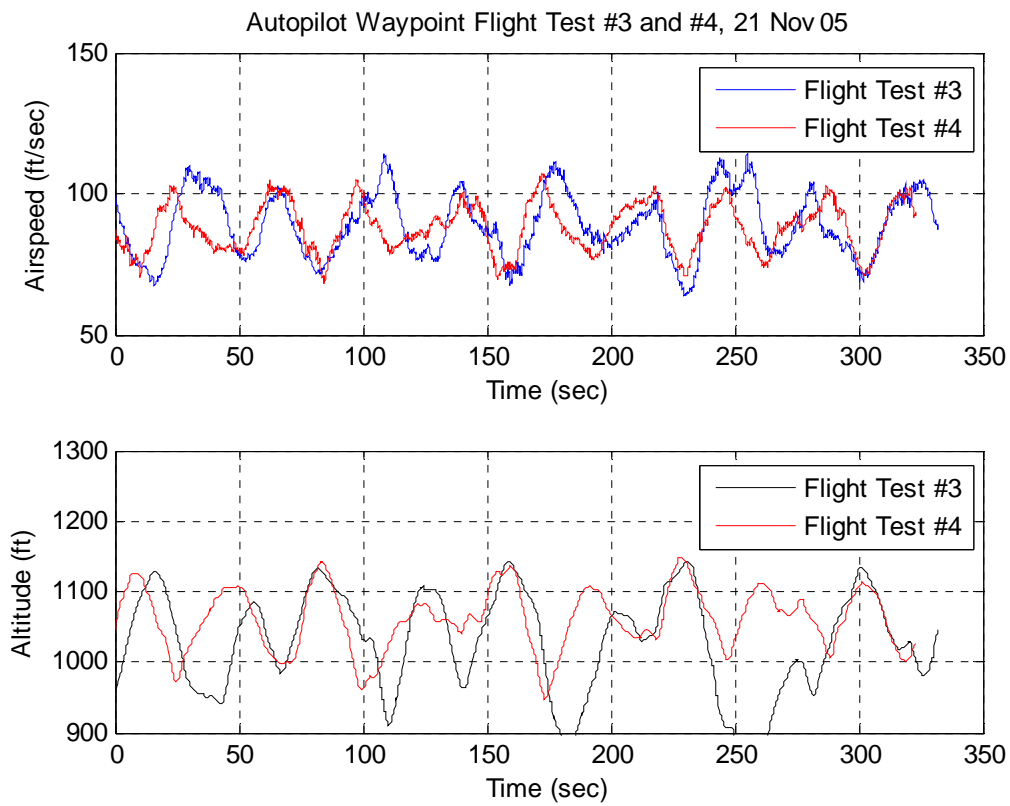


Figure 48. Autopilot Waypoint Orbits; Airspeed and Altitude

6.4 – Chapter Conclusions

Overall, the simulations and flight tests were successful. Open loop flight test data was collected and the autopilot system was demonstrated and analyzed. Open loop telemetry revealed differences in pitch damping between the simulations and the aircraft. The flight tests of the autopilot showed better performance than the HITL, getting to every waypoint, but altitude and airspeed performance was not as tight as the HITL. But in general, the simulations, based on a theoretical approach, performed well and the results were overall positive.

VII. Conclusions and Recommendations

7.1 – Conclusions

The research has accomplished several key objectives:

1. Construction, integration, calibration, and full documentation of the Piccolo II autopilot system with the SIG Rascal 110 UAV.
2. Developed a straightforward procedure for generating aerodynamic models for small UAVs. This procedure was then used to develop a Rascal 110 UAV physical, inertial, and aerodynamic model.
3. Incorporated the Rascal 110 aerodynamic model into two simulation programs. The first simulation, the Hardware In the Loop, proved an invaluable tool prior to flight-testing the autopilot and is now a prerequisite to all initial concept flights. The second, an open loop Matlab/SIMULINK six degree of freedom simulation for open loop flight test and detailed post flight analysis.
4. Complete development, from cradle to grave, of a localized flight test program for small UAV's at the Air Force Institute of Technology and the Advanced Navigation Technology Center. Documentation detailing approval procedures, locations, testing issues, checklists, and in flight maneuvers are readily available at the ANT Center.
5. Using the developed flight test program, open loop and autonomous flight data was collected using the Rascal 110 UAV and Piccolo II autopilot system. Open loop flight test revealed the dynamic flying qualities of the aircraft. This data validated the simulation model, and highlighted areas for improvement, such as increasing the pitch damping of the simulation. The autonomous flights also proved to be a success. HITL

simulations were compared against the flight test data. The Rascal 110 performed better in a narrow waypoint orbit than the HITL, but traded significant losses in altitude. Real time improvements of the gains demonstrate the rapid ability to minimize the altitude losses.

Flight test results were positive overall. Performing the open loop maneuvers demonstrated the aircraft was capable of some degree of longitudinal testing. The gain settings procedures proved to be one of the more challenging tasks. Autopilot gains tuning in the Hardware in the Loop simulation are only a starting point, and to date, any error observed in simulation is magnified in flight. This is a process of fly, analyze in Matlab, Hardware in the Loop simulate, and fly again. Despite completing three of these cycles, time and weather constraints did not allow for further tuning. The most significant error was maintaining altitude during banked turns. Additionally, both Hardware in the Loop and Matlab/SIMULINK simulations tended to have less damped oscillations as compared to the flight test results.

Research of this nature is always limited by time. As an outdoor experimental thesis, weather and equipment further constrain added progress. Continued flight-testing is encouraged to improve autopilot performance. At the conclusion of several more tuning flights, the aircraft will be fully prepared to perform advanced navigation research flights. Detailed recommendations are listed in next section.

7.2 – Recommendations

The following recommendations incorporate improvements to the model, simulation, and flight test program. Additionally, recommendations for future research are suggested.

- Improvements to the Aerodynamic Model – A wind tunnel analysis of the Rascal 110 UAV would greatly enhance the aerodynamic model input to the simulators. Experimentally determining the stability coefficients is a natural next step from the Digital Datcom analysis. Additionally, this would give validation to the Digital Datcom outputs. Chapter 8 of the Digital Datcom provides techniques to validate the inertia calculations performed experimentally. Additionally, a dynamometer bench test of the engine to map power, torque, and RPM's would improve the model's performance during simulation. The engine bench test should be accomplished with the propeller and spinner mounted on the engine.
- Simulation Enhancements – The Matlab simulation should be tied to a flight visualization software package such as AVDS or Flight Gear. It should also be set up to run in real time with inputs from a joystick or R/C transmitter. An operator could use this set up as a verification tool of the aircraft's performance compared to actual flight.
- Use optimization to tune the simulation model (i.e. estimated aerodynamic and mass properties) so that it better matches the flight test results, and therefore providing a better prediction of future flights.
- Flight Test Recommendations – The flight test airspace should be larger. Ideally, a two mile by two mile box would provide the best test area for autonomous waypoint

and open loop flight-testing. Improvements to determine steady level flight of the UAV under manual control through. Determining a complete set of handling qualities from of open loop flight tests will deepen the understanding of total aircraft performance.

- Autonomous Flight – Two or three more intensive gain tuning flights will minimize the autopilot tracking errors. Potentially, an optimization algorithm could tune the automatically tune gains based on flight test performance. Automating the gain setting procedure would significantly enhance the capability to adapt to all future UAV research configurations.

Appendix A: Open Loop Flight Test Results

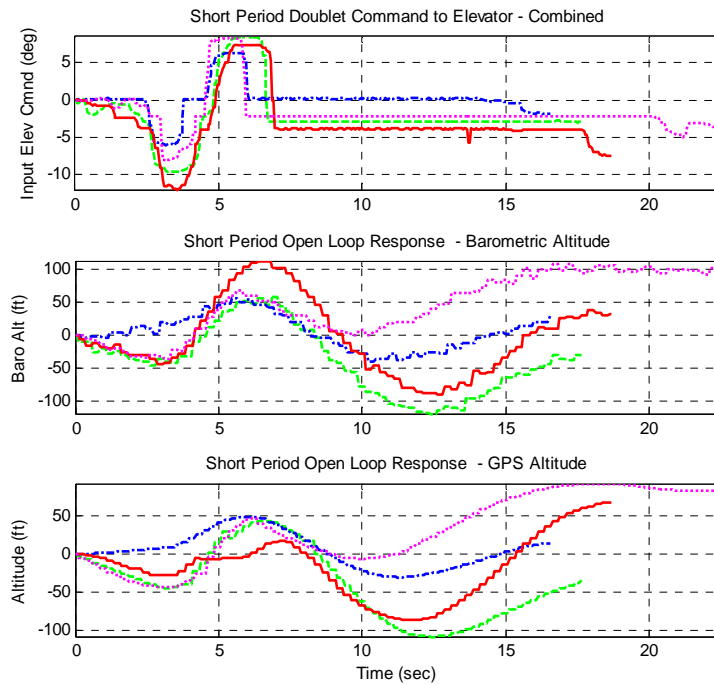


Figure 49. Short Period Flight Test Results

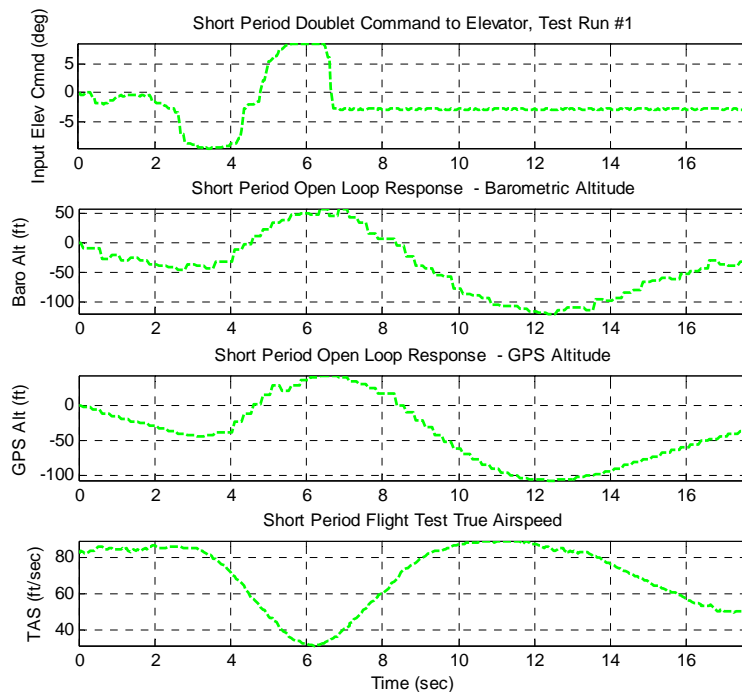


Figure 50. Short Period Flight Test #1

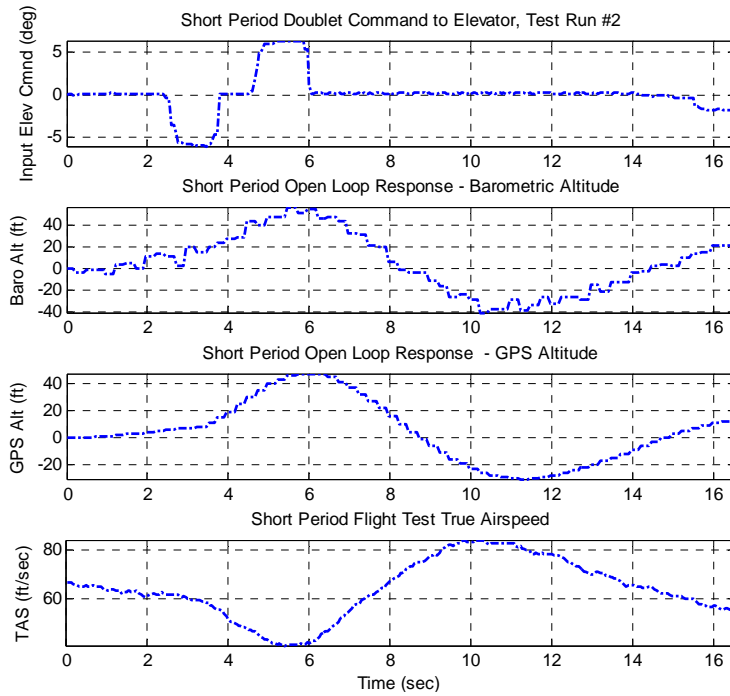


Figure 51. Short Period Flight Test #2

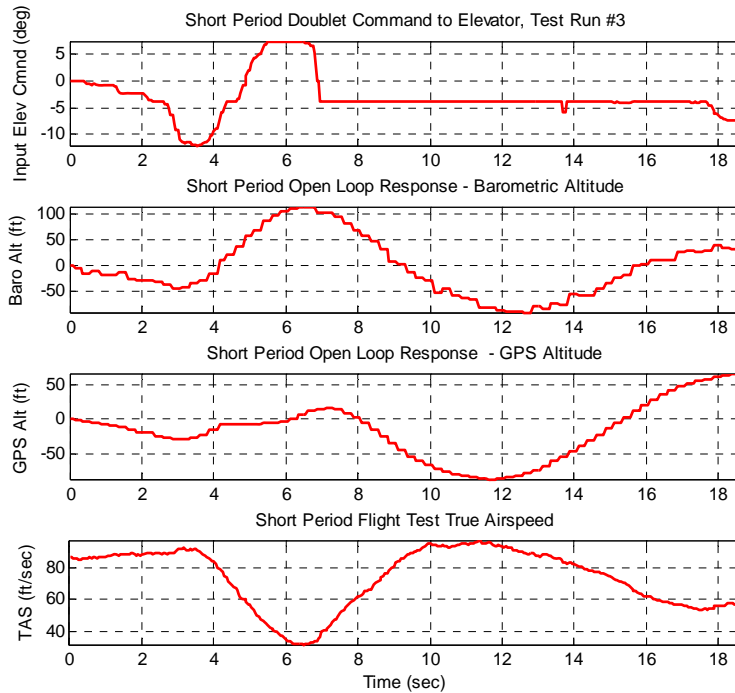


Figure 52. Short Period Flight Test #3

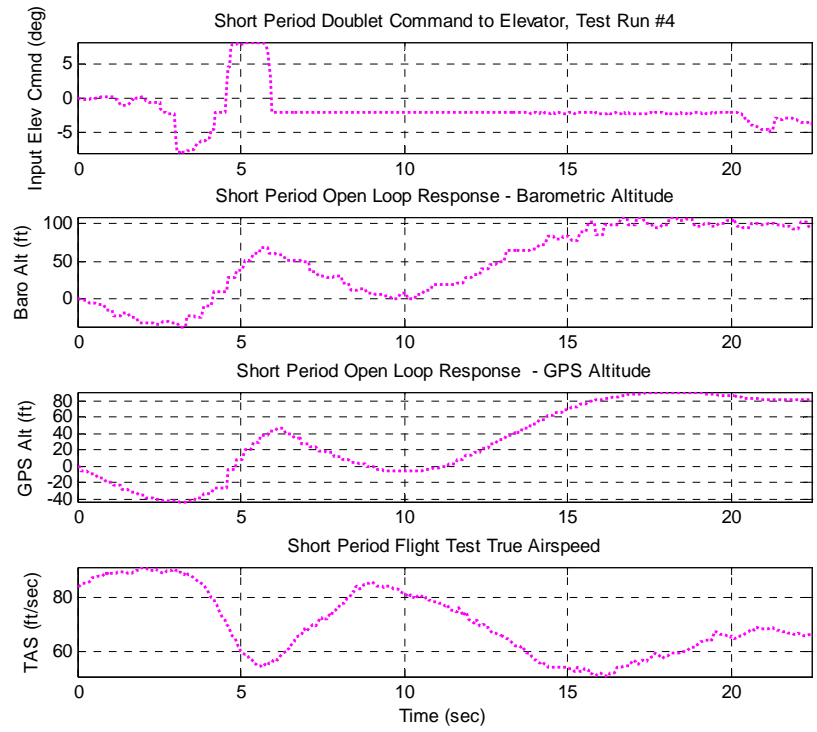


Figure 53. Short Period Flight Test #4

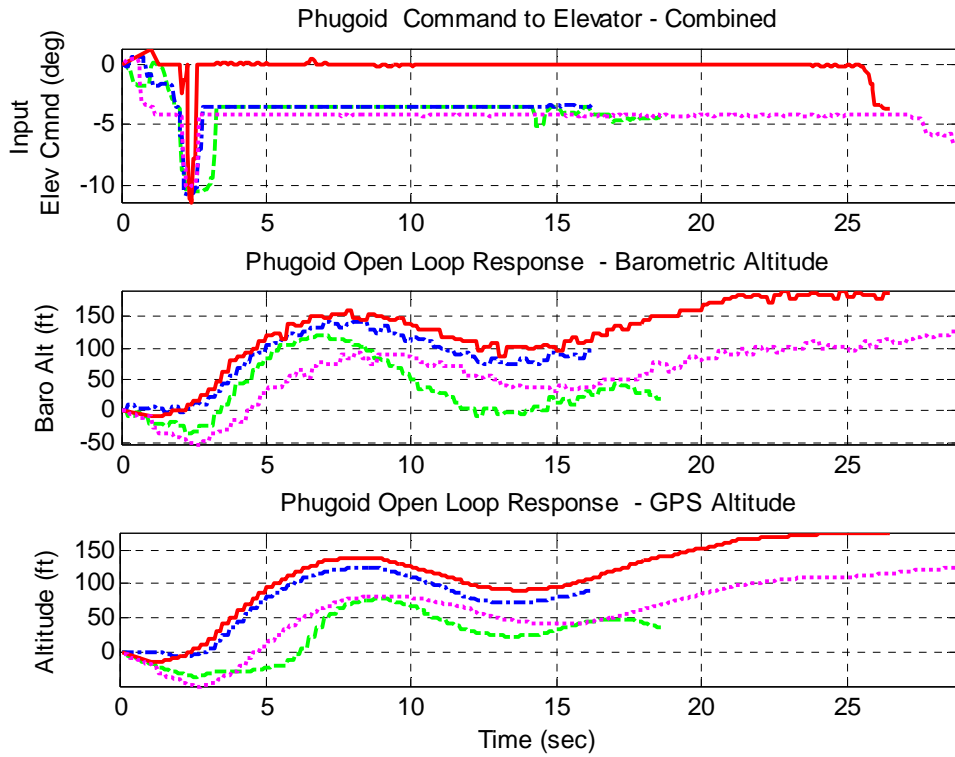


Figure 54. Phugoid Flight Test – Combined

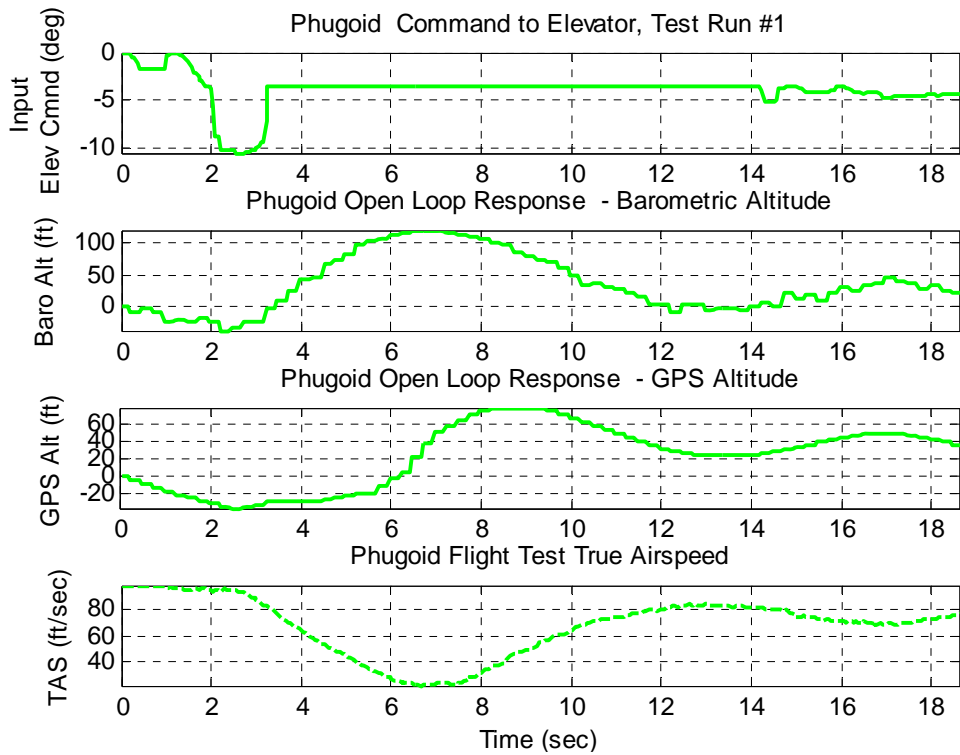


Figure 55. Phugoid Flight Test #1

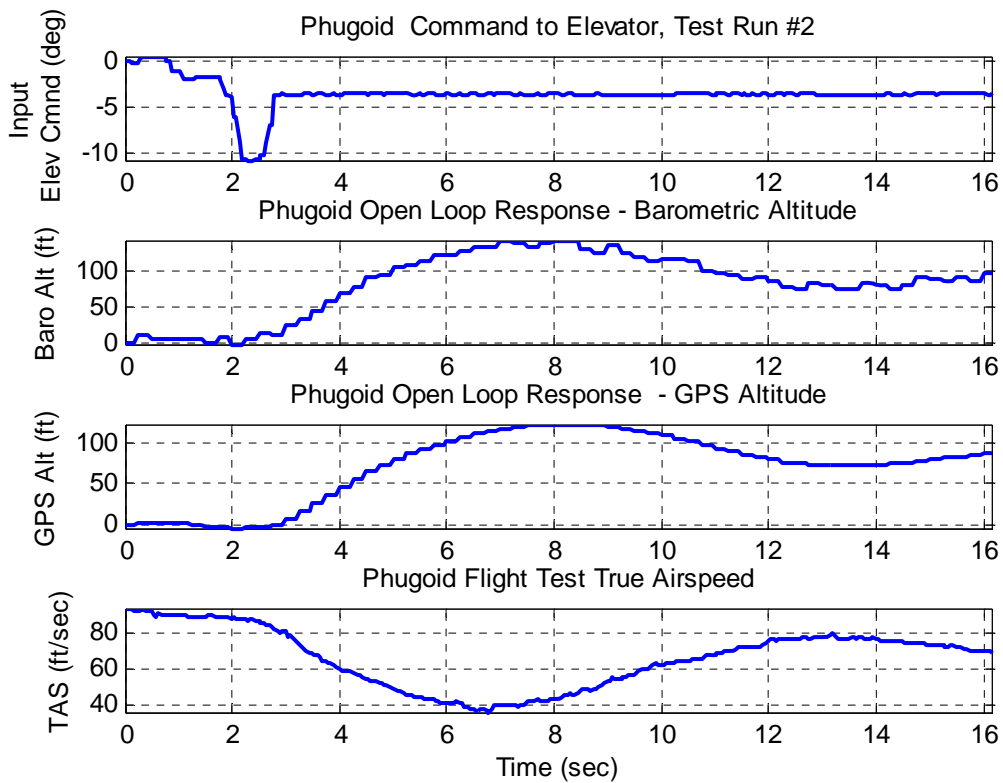


Figure 56. Phugoid Flight Test #2

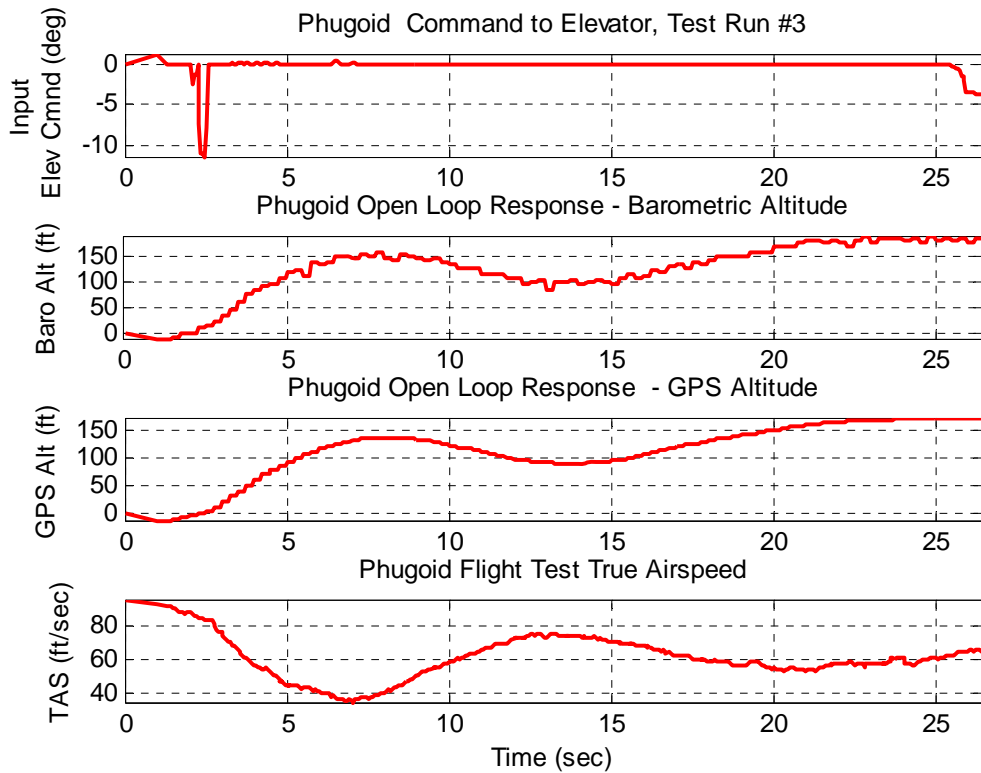


Figure 57. Phugoid Flight Test #3

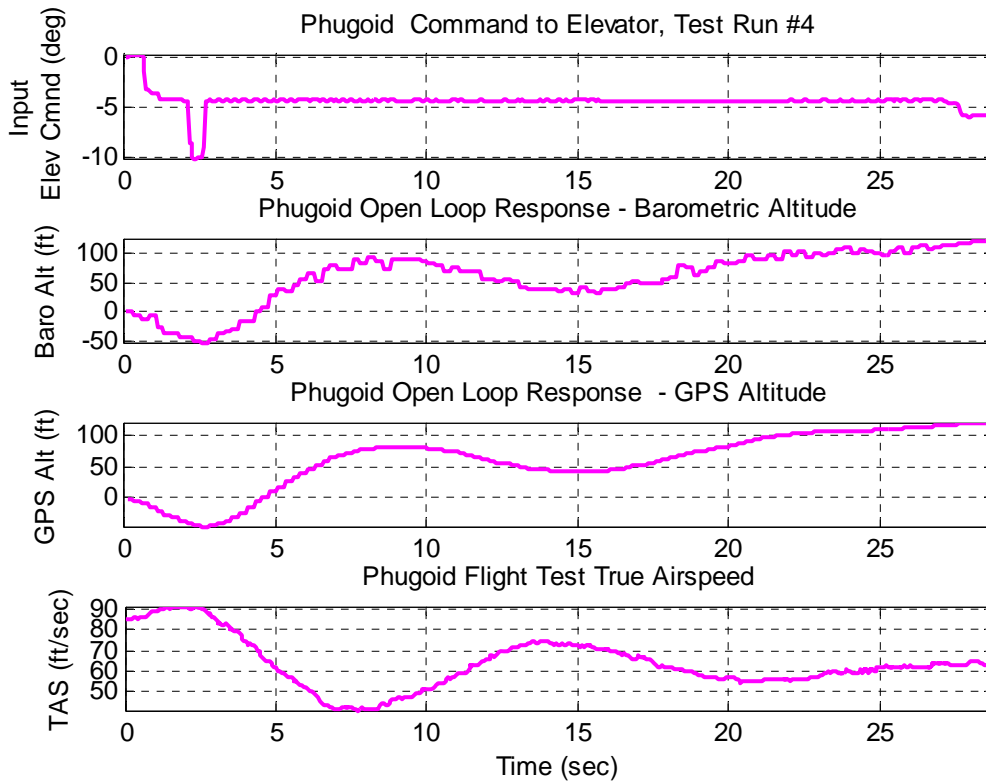


Figure 58. Phugoid Flight Test #4

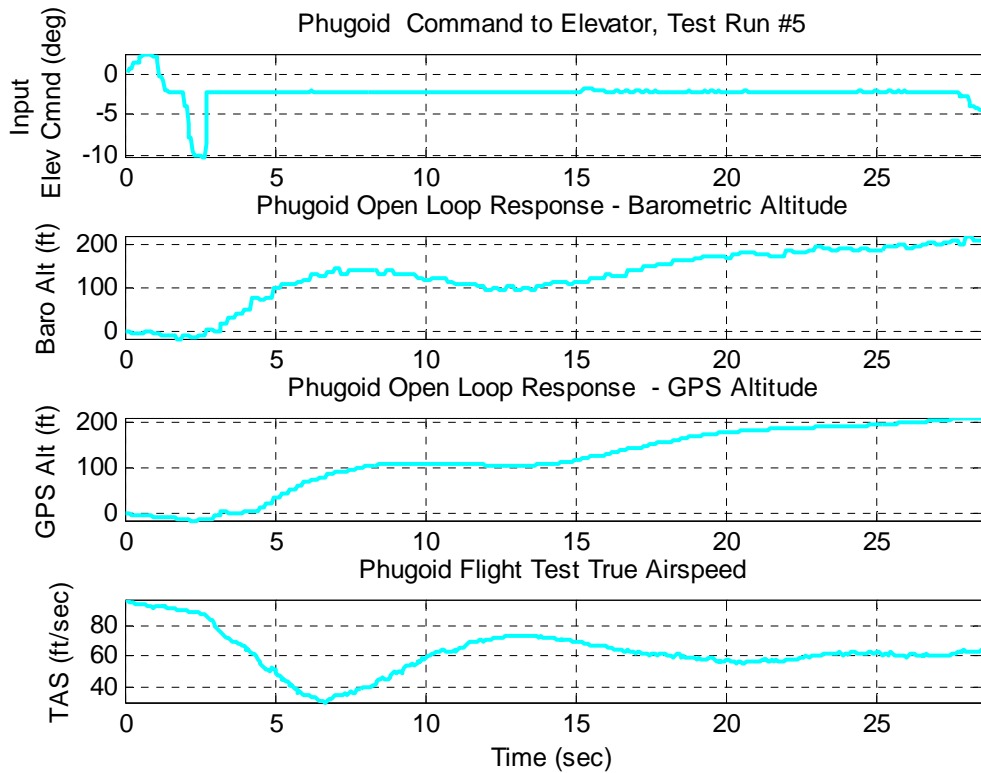


Figure 59. Phugoid Flight Test #5

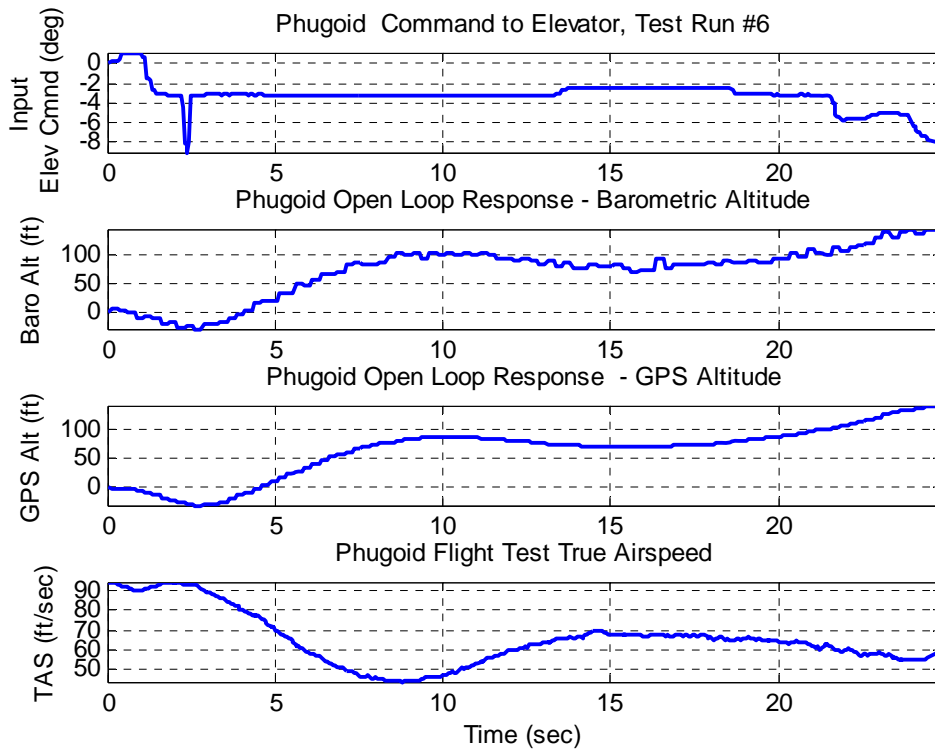


Figure 60. Phugoid Flight Test #6

Appendix B: Autonomous Waypoint Flight Test Results

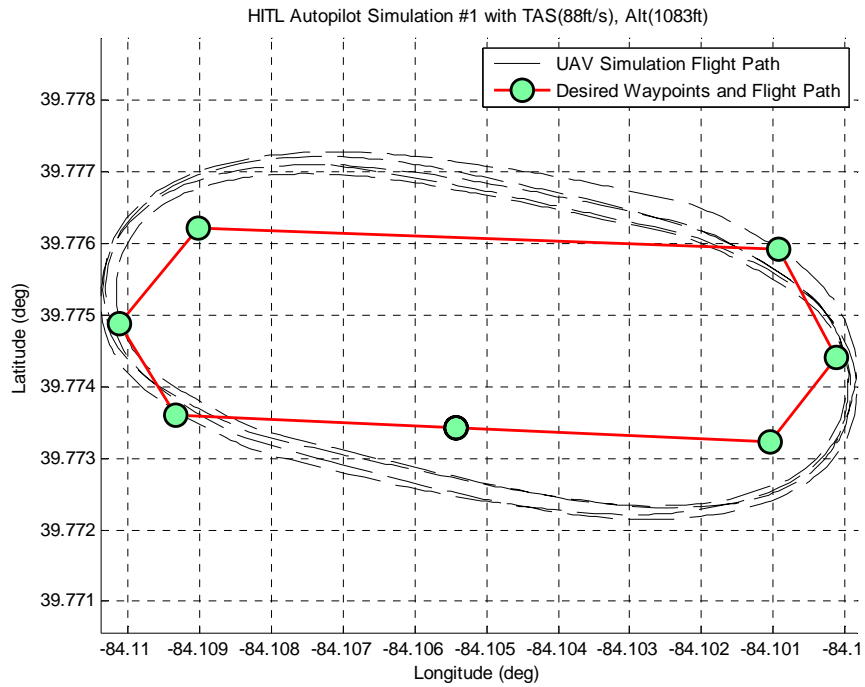


Figure 61. HITL Autopilot Simulation #1, TAS: 88 ft/sec, Alt: 1083 ft, Conv: 100

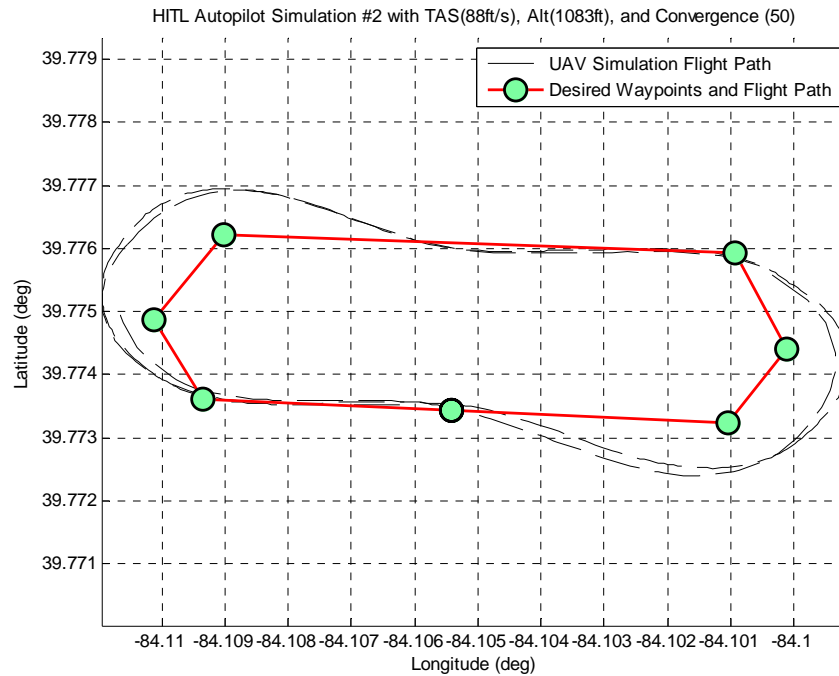


Figure 62. HITL Autopilot Simulation #2, TAS: 88 ft/sec, Alt: 1083 ft, Conv: 50

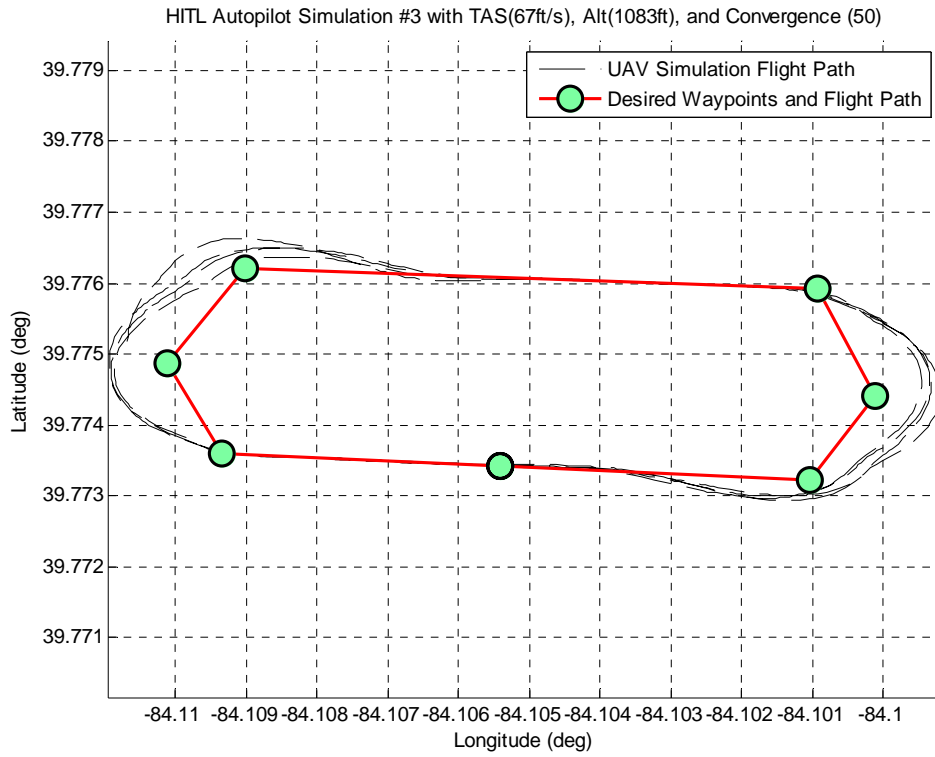


Figure 63. HITL Autopilot Simulation #3, TAS: 67 ft/sec, Alt: 1083 ft, Conv: 50

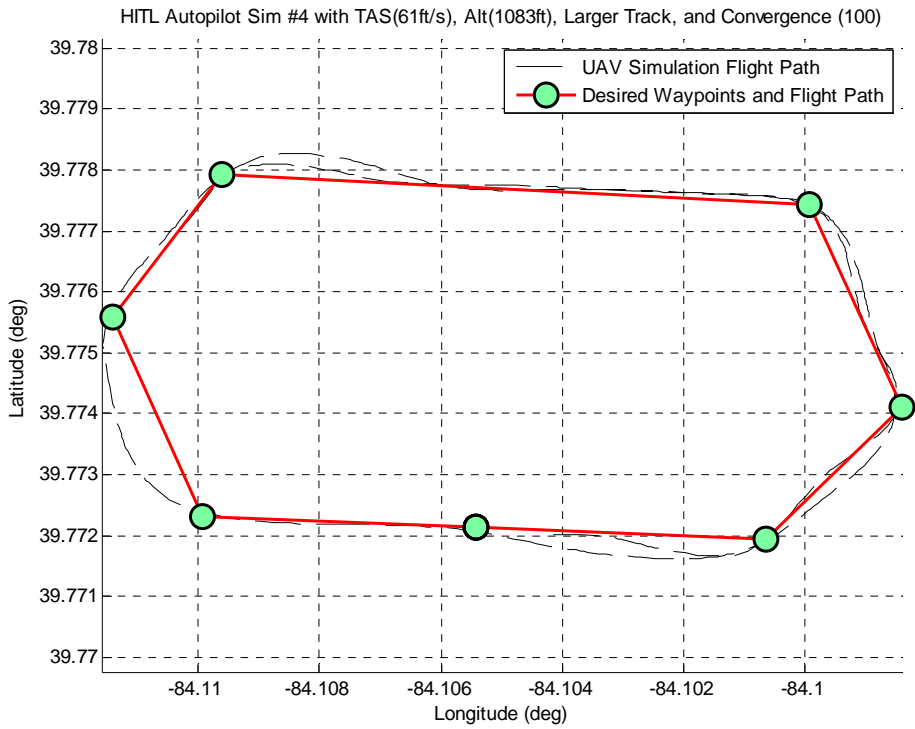


Figure 64. HITL Autopilot Simulation #4, TAS: 61 ft/sec, Alt: 1083 ft, Conv: 100

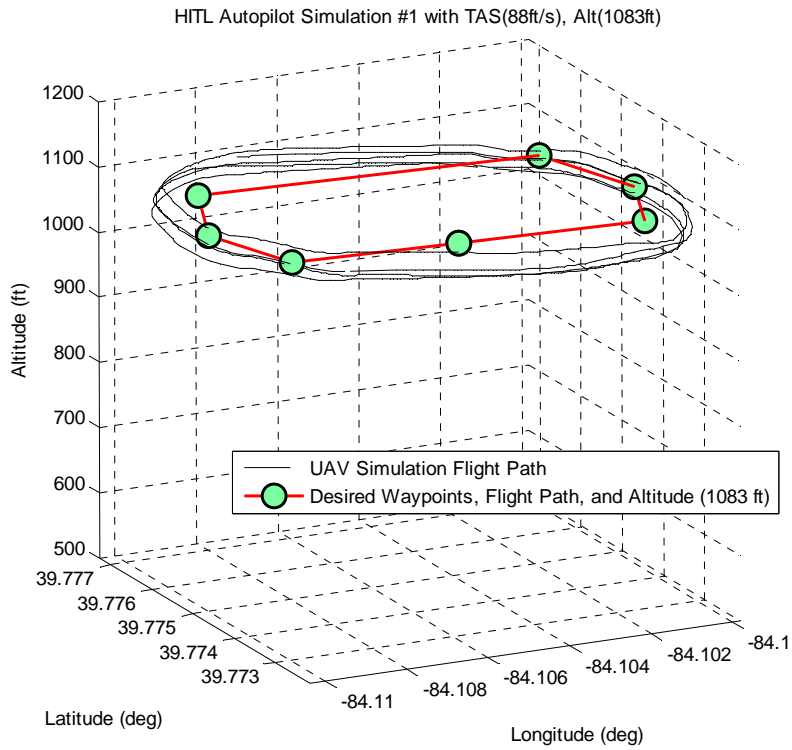


Figure 65. HITL Autopilot Simulation #1, TAS: 88 ft/sec, Alt: 1083 ft

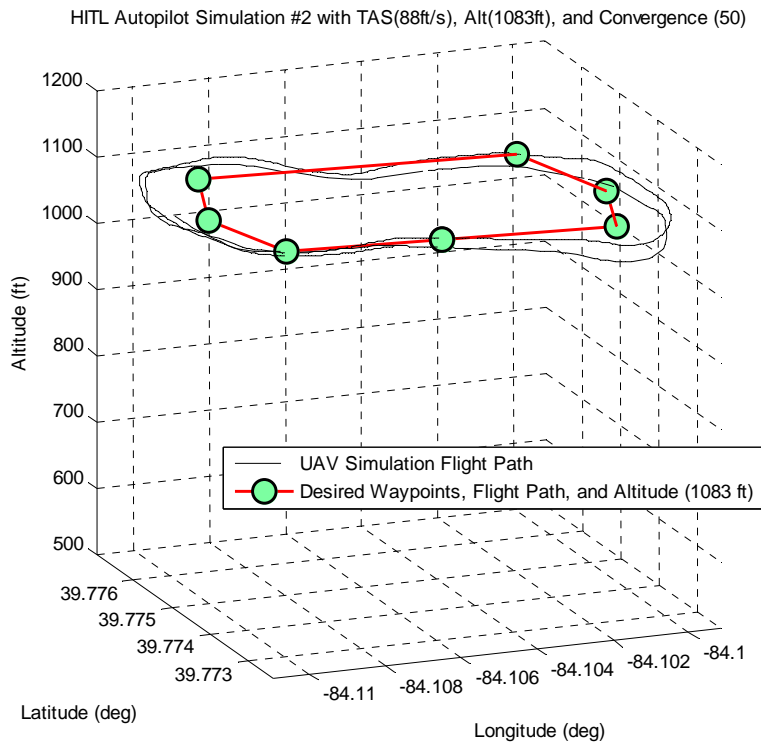


Figure 66. HITL Autopilot Simulation #2, TAS: 88 ft/sec, Alt: 1083 ft, Conv: 50

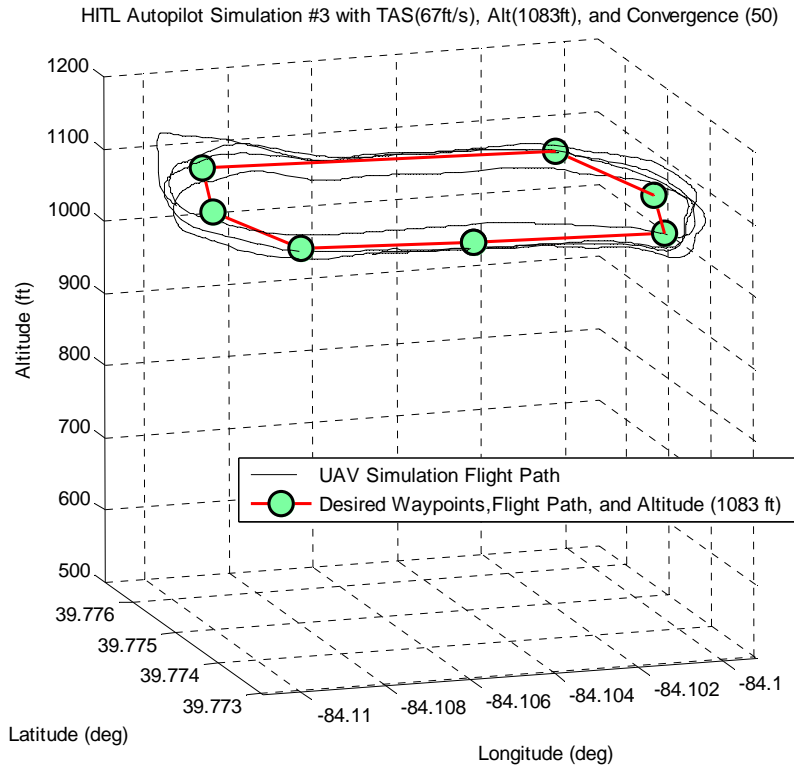


Figure 67. HITL Autopilot Simulation #3, TAS: 67 ft/sec, Alt: 1083 ft, Conv: 50

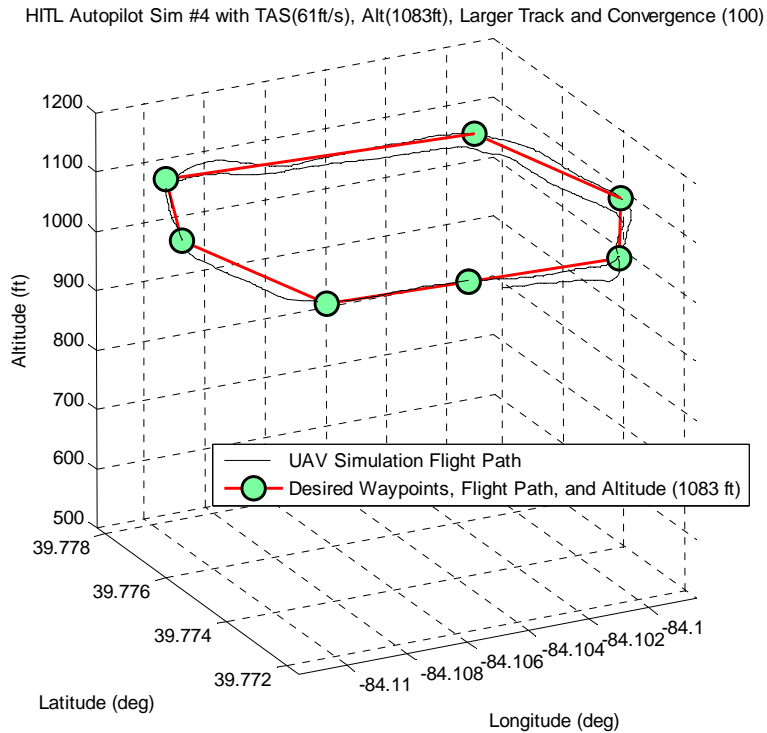


Figure 68. HITL Autopilot Simulation #4, TAS: 61 ft/sec, Alt: 1083 ft, Conv: 100

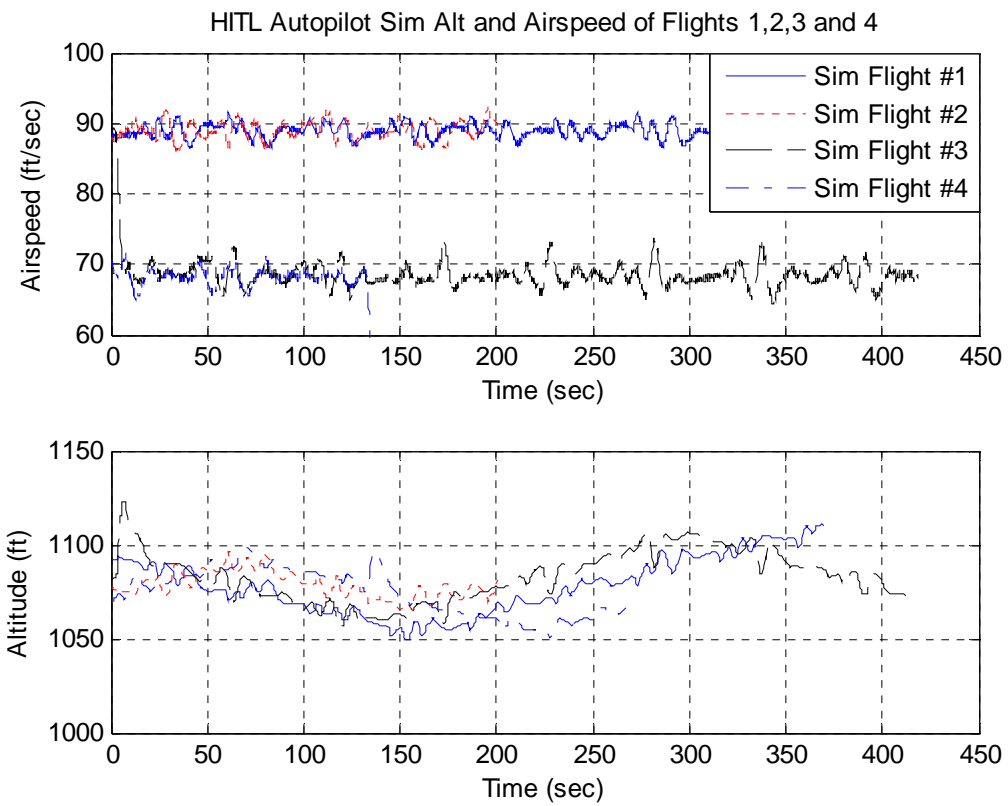


Figure 69. HITL Autopilot Simulation Altitude and Airspeed Comparisons

Appendix C: Hardware in the Loop Aircraft Model Inputs.

```
// SIG RASCAL 110 ARF with OS 120 SURPASS III Engine
// Piccolo and batteries installed
// Hardware in the Loop SIMULATOR MODEL
// Capt Nidal M Jodeh and Athan Waldron, AFIT/ENY/ENG Jan 31, 2006

// Sensors=Sensorstwo.txt
// Actuators=Actuator.txt

// All measurements in meters, kg, degrees

//----- AERODYNAMICS: WING -----//

// Reference area, (m^2) (From Manufacturer, Assembly Manual, page 31, //1522 sq in)
// Wing_Area=10.5694 ft^2
Wing_Area=0.9819

// Span, (meters)
//Aircraft has a 110 inch wingspan
// Wing_Span=9.1667 ft
Wing_Span=2.794

// Average taper ratio, (unitless)
// elliptical wing, use equation
Wing_Taper=0.72955

// Aero coefficients look-up table
// See Look up table file
// File includes induced drag (Cdi) in the coefficient of drag (Cd)
Wing_LUT=E193_Wing with total drag.lut

// Incidence angle wrt fuselage center line, (degrees)
// Difficult to determine the Fuselage Reference Line needed for wing //incidence.
// Based on observation, chord line to reference line
Wing_Incidence=2

// Dihedral angle, (degrees)
// Measured using Angle locator gauge from Ace hardware (part #25865)
// Measured half way between tip and root at center of chordline
Wing_Dihedral=4

// Position of wing ac wrt to cg, (meters)
// Aircraft aero center was not determined, this is a guess
// Wing_X=0 ft
Wing_X=0
// Wing_Z=0.5 ft
Wing_Z=-0.1524

// WING CONTROL SURFACES

// AILERONS
```

```

// Left aileron
// Spanwise location of inboard station, (meters)
// Measured from center of wing (root) chord to inboard edge of aileron
// Left_Aileron_Inboard=-1.7717 ft
Left_Aileron_Inboard=-0.54

// Spanwise location of outboard station, (meters)
// Measured from center of wing (root) chord to outboard edge of aileron
// Left_Aileron_Outboard=-3.8123 ft
Left_Aileron_Outboard=-1.162

// Average aileron chord, (meters)
// Measured chord at 1 inch increments across aileron to get average
// Left_Aileron_Chord=0.2077 ft
Left_Aileron_Chord=0.0633

// Channel number – Predetermined
Left_Aileron_Channel=0
Left_Aileron_Sign=1

// Effectiveness (calculated by SIM)
// Left_Aileron_Effectiveness=0

// Right aileron
// Spanwise location of inboard station, (meters)
// Measured same as left aileron
// Right_Aileron_Inboard=1.7717 ft
Right_Aileron_Inboard=0.54

// Spanwise location of outboard station, (meters), measured same as left aileron
// Right_Aileron_Outboard=3.8123 ft
Right_Aileron_Outboard=1.162

// Average aileron chord, (meters), measured same as left aileron
// Right_Aileron_Chord=0.2077 ft
Right_Aileron_Chord=0.0633

// Channel number (Same as left, both servos on single channel, a ‘Y’ harness split signal // to both servos)
Right_Aileron_Channel=0
Right_Aileron_Sign=-1

// Effectiveness (calculated by SIM)
// Right_Aileron_Effectiveness=0.2

//----- AERODYNAMICS: HORIZONTAL TAIL -----//

// Reference area, (m^2)
// Measured by rectangles. See horizontal tail Excel spreadsheet
// Tail_Area=1.991 ft^2
Tail_Area=0.185

// Span measured from tip to tip, (meters)

```

```

// Tail_Span=3.0417 ft
Tail_Span=0.9271

// Taper ratio, use equation, (unitless)
Tail_Taper=0.5708

// Tail LUT test file
// Tail_LUT=tail_model.lut

// Location of tail ac wrt to aircraft cg, (meters), (Guess)
// Tail_X=-3.668 ft
Tail_X=-1.118
// Tail_Z=0.164 ft
Tail_Z=-0.05

// Parasitic drag (Guess, based on values for other A/C models)
Tail_Parasitic_Drag=0.015

// Oswald efficiency factor (Guess)
Tail_Span_Efficiency=0.8

// Incidence angle wrt to fuselage center line, (degrees)
// Observed, looks like its on the line
Tail_Incidence=0

// Dihedral angle, (degrees), Measured same as wing dihedral
Tail_Dihedral=0

// Sweep angle of the quarter chord line, (degrees), no sweep
Tail_Sweep=0

// HORIZONTAL TAIL CONTROL SURFACES

// Elevators move in unison, controlled by a single servo

// Left elevator
// Spanwise location of the inboard station, (meters)
// Left_Elevator_Inboard=-0.062 ft
Left_Elevator_Inboard=-0.01905

// Spanwise location of the outboard station, (meters)
// Left_Elevator_Outboard=-1.25 ft
Left_Elevator_Outboard=-0.381

// Average chord, (meters)
// Measured same as ailerons
// Left_Elevator_Chord=0.2149 ft
Left_Elevator_Chord=0.0655

// Channel number
Left_Elevator_Channel=1

// Sense of rotation
Left_Elevator_Sign=1

```

```

// Right elevator (same as left elevator, the entire elevator is one piece)
// Spanwise location of the inboard station, (meters)
// Right_Elevator_Inboard=0.062 ft
Right_Elevator_Inboard=0.01905

// Spanwise location of the outboard station, (meters)
// Right_Elevator_Outboard=1.25 ft
Right_Elevator_Outboard=0.381

// Average chord, (meters), Measured at 1 inch increments
// Right_Elevator_Chord=0.2149 ft
Right_Elevator_Chord=0.0655

// Channel number (Same as left, one servo, one elevator)
Right_Elevator_Channel=1

// Sense of rotation
Right_Elevator_Sign=1

//----- AERODYNAMICS: VERTICAL TAIL -----//

// Reference area, in m^2
// Measured by rectangles, see Vertical Tail Excel Spreadsheet
// Left_Fin_Area=0.7725 ft^2
Left_Fin_Area=0.07177

// Span, in m
// Measured from surface of horizontal tail to tip of vertical stab
// Left_Fin_Span=0.9375 ft^2
Left_Fin_Span=0.28575

// Taper ratio, use equation, (unitless)
Left_Fin_Taper=0.5708

// We need to add T-tail effect here ( No T-Tail on Sig, left as example for future)
// (increased effectiveness of vertical tail)
// Left_Fin_SideForce_Slope=-0.0466

// Parasitic drag (Guess, based on other A/C models)
Left_Fin_Parasitic_Drag=0.015

// Oswald efficiency factor - Guess
Left_Fin_Span_Efficiency=0.8

// Location of vertical tail ac wrt to aircraft cg, (meters)
// Guess of where Vert Tail ac is
// Left_Fin_X=-3.668 ft
Left_Fin_X=-1.118
// Left_Fin_Y=0.0 ft
Left_Fin_Y=0.0
// Left_Fin_Z=0.5 ft
Left_Fin_Z=-0.1524

```

```

// VERTICAL TAIL CONTROL SURFACES

// Rudder - Measured
// Position of bottom section wrt to aircraft cg, (meters)
// Left_Rudder_Bottom=0.0984 ft
Left_Rudder_Bottom=0.03

// Position of top section, wrt to aircraft cg, (meters)
// Left_Rudder_Top=-0.8858 ft
Left_Rudder_Top=-0.27

// Average chord, (meters), Measured in 1 inch increments
// Left_Rudder_Chord=0.2976 ft
Left_Rudder_Chord=0.0907

// Channel number
Left_Rudder_Channel=3

// Sense of rotation
Left_Rudder_Sign=1

// Effectiveness (calculated by SIM)
// Left_Rudder_Effectiveness=0.25

//----- AERODYNAMICS: FUSELAGE -----//

// Reference area, (m^2)
// Fuse_Area=0.4432 ft^2
Fuse_Area=0.041175

// Total length, in m
// Fuse_Length=6.0625 ft
Fuse_Length=1.84785

// Parasitic drag (Guess, based on other A/C models)
Fuse_Parasitic_Drag=0.12

// Slope of lift coefficient
Fuse_Lift_Slope=0.0

// Slope of side force coefficient
Fuse_SideForce_Slope=0.0

// Slope of pitch moment coefficient
Fuse_Pitching_Moment_Slope=0

// Slope of yaw moment coefficient
Fuse_Yawing_Moment_Slope=0

// Position of fuselage ac wrt to aircraft cg, (meters)
// Fuse_X=0.3281 ft
Fuse_X=0.1
// Fuse_Y=0.0 ft

```



```

Fuse_Y=0.0
// Fuse_Z=0.3281 ft
Fuse_Z=0.1

//----- INERTIA -----//

// Now we need the inertia data: pitch, roll, and yaw inertia.

// Gross take-off mass of the aircraft, (kg)
// Gross_Mass=18.7 lb
Gross_Mass=8.5

// Calculated using mass of A/C without fuel, (kg*m^2)
// These are the natural A/C frequencies not the damped.
// See matlab code for inertial calculations
Roll_Inertia=2.6410
Pitch_Inertia=2.1045
Yaw_Inertia=2.5985

// Mass of aircraft without fuel, (kg)
// Empty_Mass=15.717
Empty_Mass= 7.144

// Using the values below the sim would calculate the inertial values.
// However, they have been calculated outside the sim and are shown above.
// This is why the values below are commented out.

// Mass of the wing, (kg)
//Wing_Mass=1.758

// Mass of the fuselage, (kg)
//Fuselage_Mass=5.386

// Mass of the horizontal tail, (kg)
//Tail_Mass=.2

// Mass of the vertical tail, in (kg)
//Left_Fin_Mass=0.1

// Mass of the engine, (kg)
//Left_Engine_Mass=0.92

//----- PROPULSION -----//

// Engine is an OS FS120, 2.1 hp

// Channel number
Left_Engine_Channel=2

// Engine parameters look-up table
Left_Engine_LUT=Mod2Engine.lut

```

```

// Propeller is APC 16x8
// Prop diameter, (meters)
// Left_Prop_Diameter=1.3333 ft
Left_Prop_Diameter=0.4064

// Position of propeller hub wrt to aircraft cg, (meters)
// Left_Prop_X=1.7913 ft
Left_Prop_X=0.546

// Moment of inertia (kg*m^2)
Left_Prop_Inertia=0.002

// Propeller coefficients look-up table
Left_Prop_LUT=apc16x8.prd

//----- GROUND CONTACT POINTS -----//

// Contact points measured from CG, (meters)

// ContactPoint_Top_Position_X=0.1667 ft
ContactPoint_Top_Position_X=0.0508
// ContactPoint_Top_Position_Y=0 ft
ContactPoint_Top_Position_Y=0
// ContactPoint_Top_Position_Z=-0.625 ft
ContactPoint_Top_Position_Z=-0.1905

// ContactPoint_Bottom_Position_X=0 ft
ContactPoint_Bottom_Position_X=0
// ContactPoint_Bottom_Position_Y=0 ft
ContactPoint_Bottom_Position_Y=0
// ContactPoint_Bottom_Position_Z=0.396 ft
ContactPoint_Bottom_Position_Z=0.1207

// ContactPoint_Nose_Position_X=2 ft
ContactPoint_Nose_Position_X=0.6096
// ContactPoint_Nose_Position_Y=0 ft
ContactPoint_Nose_Position_Y=0
// ContactPoint_Nose_Position_Z=0 ft
ContactPoint_Nose_Position_Z=0

// ContactPoint_Tail_Position_X=-4.292 ft
ContactPoint_Tail_Position_X=-1.3081
// ContactPoint_Tail_Position_Y=0 ft
ContactPoint_Tail_Position_Y=0
// ContactPoint_Tail_Position_Z=0 ft
ContactPoint_Tail_Position_Z=0

// ContactPoint_LWing_Position_X=0 ft
ContactPoint_LWing_Position_X=0
// ContactPoint_LWing_Position_Y=-4.5833 ft
ContactPoint_LWing_Position_Y=-1.397
// ContactPoint_LWing_Position_Z=-0.625 ft
ContactPoint_LWing_Position_Z=-0.1905

```

```

// ContactPoint_RWing_Position_X=0 ft
ContactPoint_RWing_Position_X=0
// ContactPoint_RWing_Position_Y=4.5833 ft
ContactPoint_RWing_Position_Y=1.397
// ContactPoint_RWing_Position_Z=-0.625 ft
ContactPoint_RWing_Position_Z=-0.1905

// ContactPoint_LStab_Position_X=-3.75 ft
ContactPoint_LStab_Position_X=-1.143
// ContactPoint_LStab_Position_Y=-1.521 ft
ContactPoint_LStab_Position_Y=-0.4636
// ContactPoint_LStab_Position_Z=-0.1667 ft
ContactPoint_LStab_Position_Z=-0.0508

// ContactPoint_RStab_Position_X=-3.75 ft
ContactPoint_RStab_Position_X=-1.143
// ContactPoint_RStab_Position_Y=1.521 ft
ContactPoint_RStab_Position_Y=0.4636
// ContactPoint_RStab_Position_Z=-0.1667 ft
ContactPoint_RStab_Position_Z=-0.0508

// ContactPoint_Fin_Position_X=-3.8333 ft
ContactPoint_Fin_Position_X=-1.1684
// ContactPoint_Fin_Position_Y=0 ft
ContactPoint_Fin_Position_Y=0
// ContactPoint_Fin_Position_Z=-1.1043 ft
ContactPoint_Fin_Position_Z=-0.3366

// LeftWheel_Position_X=0.6667 ft
LeftWheel_Position_X=0.2032
// LeftWheel_Position_Y=-0.896 ft
LeftWheel_Position_Y=-0.2731
// LeftWheel_Position_Z=1.0833 ft
LeftWheel_Position_Z=0.3302

// RightWheel_Position_X=0.6667 ft
RightWheel_Position_X=0.2032
// RightWheel_Position_Y=0.896 ft
RightWheel_Position_Y=0.2731
// RightWheel_Position_Z=1.0833 ft
RightWheel_Position_Z=0.3302

// NoseWheel_Position_X=-4.3333 ft
NoseWheel_Position_X=-1.3208
// NoseWheel_Position_Y=0 ft
NoseWheel_Position_Y=0
// NoseWheel_Position_Z=0.4793 ft
NoseWheel_Position_Z=0.1461
NoseWheel_RudderWheelRatio=1
NoseWheel_Steering_Channel=4

//----- AVIONICS MOUNTING -----//

```

```
// Avionics (IMU sensor) orientation with respect to the aircraft body axes
// Euler angles, (degrees)
IMU_Sensor_Roll_Angle=-90
IMU_Sensor_Pitch_Angle=0.0
IMU_Sensor_Yaw_Angle=180

// Avionics (IMU sensor) position vector with respect to the aircraft CG, in body axes
// Vector components, (meters)
// IMU_Sensor_Position_X=-0.4583 ft
IMU_Sensor_Position_X=-0.1397
// IMU_Sensor_Position_Y=0.0 ft
IMU_Sensor_Position_Y=0.0
// IMU_Sensor_Position_Z=0.3127 ft
IMU_Sensor_Position_Z=0.0953
```

Appendix D: Hardware In the Loop Actuator Model Inputs

Left_Aileron_Bandwidth=3.00
Left_Aileron_Rate_Limit=10.00
Left_Aileron_Min_Limit=-100.00
Left_Aileron_Max_Limit=100.00
Left_Elevator_Bandwidth=3.00
Left_Elevator_Rate_Limit=10.00
Left_Elevator_Min_Limit=-100.00
Left_Elevator_Max_Limit=100.00
Left_Throttle_Bandwidth=3.00
Left_Throttle_Rate_Limit=10.00
Left_Throttle_Min_Limit=-100.00
Left_Throttle_Max_Limit=100.00
Left_Rudder_Bandwidth=3.00
Left_Rudder_Rate_Limit=10.00
Left_Rudder_Min_Limit=-100.00
Left_Rudder_Max_Limit=100.00
Left_Flap_Bandwidth=3.00
Left_Flap_Rate_Limit=10.00
Left_Flap_Min_Limit=-100.00
Left_Flap_Max_Limit=100.00
Right_Aileron_Bandwidth=3.00
Right_Aileron_Rate_Limit=10.00
Right_Aileron_Min_Limit=-100.00
Right_Aileron_Max_Limit=100.00
Right_Elevator_Bandwidth=3.00
Right_Elevator_Rate_Limit=10.00
Right_Elevator_Min_Limit=-100.00
Right_Elevator_Max_Limit=100.00
Right_Throttle_Bandwidth=3.00
Right_Throttle_Rate_Limit=10.00
Right_Throttle_Min_Limit=-100.00
Right_Throttle_Max_Limit=100.00
Right_Rudder_Bandwidth=3.00
Right_Rudder_Rate_Limit=10.00
Right_Rudder_Min_Limit=-100.00
Right_Rudder_Max_Limit=100.00
Right_Flap_Bandwidth=3.00
Right_Flap_Rate_Limit=10.00
Right_Flap_Min_Limit=-100.00
Right_Flap_Max_Limit=100.00

Appendix E: Hardware In the Loop Sensor Model Inputs

Latitude_Sensor_Order=0
Latitude_Sensor_Bandwidth=11.000
Latitude_Sensor_Gain=1.00
Latitude_Sensor_Offset=0.000000
Latitude_Sensor_Resolution=0.000000
Latitude_Sensor_Min=-1.570796
Latitude_Sensor_Max=1.570796
Latitude_Sensor_Noise=0.000000
Latitude_Sensor_Drift_Rate=0.000000
Latitude_Sensor_Max_Drift=0.000000
Latitude_Sensor_Drift_Hold=0.000000
Longitude_Sensor_Order=0
Longitude_Sensor_Bandwidth=11.000
Longitude_Sensor_Gain=1.00
Longitude_Sensor_Offset=0.000000
Longitude_Sensor_Resolution=0.000000
Longitude_Sensor_Min=-3.141593
Longitude_Sensor_Max=3.141593
Longitude_Sensor_Noise=0.000000
Longitude_Sensor_Drift_Rate=0.000000
Longitude_Sensor_Max_Drift=0.000000
Longitude_Sensor_Drift_Hold=0.000000
Height_Sensor_Order=0
Height_Sensor_Bandwidth=11.000
Height_Sensor_Gain=1.00
Height_Sensor_Offset=0.000000
Height_Sensor_Resolution=0.000000
Height_Sensor_Min=-1000.000000
Height_Sensor_Max=100000.000000
Height_Sensor_Noise=0.000000
Height_Sensor_Drift_Rate=0.000000
Height_Sensor_Max_Drift=0.000000
Height_Sensor_Drift_Hold=0.000000
VNorth_Sensor_Order=0
VNorth_Sensor_Bandwidth=11.000
VNorth_Sensor_Gain=1.00
VNorth_Sensor_Offset=0.000000
VNorth_Sensor_Resolution=0.000000
VNorth_Sensor_Min=-515.000000
VNorth_Sensor_Max=515.000000
VNorth_Sensor_Noise=0.000000
VNorth_Sensor_Drift_Rate=0.000000
VNorth_Sensor_Max_Drift=0.000000
VNorth_Sensor_Drift_Hold=0.000000
VEast_Sensor_Order=0
VEast_Sensor_Bandwidth=11.000
VEast_Sensor_Gain=1.00
VEast_Sensor_Offset=0.000000
VEast_Sensor_Resolution=0.000000
VEast_Sensor_Min=-515.000000
VEast_Sensor_Max=515.000000

VEast_Sensor_Noise=0.000000
VEast_Sensor_Drift_Rate=0.000000
VEast_Sensor_Max_Drift=0.000000
VEast_Sensor_Drift_Hold=0.000000
VDown_Sensor_Order=0
VDown_Sensor_Bandwidth=11.000
VDown_Sensor_Gain=1.00
VDown_Sensor_Offset=0.000000
VDown_Sensor_Resolution=0.000000
VDown_Sensor_Min=-515.000000
VDown_Sensor_Max=515.000000
VDown_Sensor_Noise=0.000000
VDown_Sensor_Drift_Rate=0.000000
VDown_Sensor_Max_Drift=0.000000
VDown_Sensor_Drift_Hold=0.000000
PDynamic_Sensor_Order=2
PDynamic_Sensor_Bandwidth=11.000
PDynamic_Sensor_Gain=1.00
PDynamic_Sensor_Offset=-1.930450
PDynamic_Sensor_Resolution=3.906250
PDynamic_Sensor_Min=-300.000000
PDynamic_Sensor_Max=4000.000000
PDynamic_Sensor_Noise=20.000000
PDynamic_Sensor_Drift_Rate=0.050000
PDynamic_Sensor_Max_Drift=15.000000
PDynamic_Sensor_Drift_Hold=5.000000
PStatic_Sensor_Order=2
PStatic_Sensor_Bandwidth=11.000
PStatic_Sensor_Gain=1.00
PStatic_Sensor_Offset=19.407000
PStatic_Sensor_Resolution=2.000000
PStatic_Sensor_Min=0.000000
PStatic_Sensor_Max=110000.000000
PStatic_Sensor_Noise=20.000000
PStatic_Sensor_Drift_Rate=1.000000
PStatic_Sensor_Max_Drift=100.000000
PStatic_Sensor_Drift_Hold=5.000000
Roll_Rate_Sensor_Order=2
Roll_Rate_Sensor_Bandwidth=20.000
Roll_Rate_Sensor_Gain=1.00
Roll_Rate_Sensor_Offset=-0.003963
Roll_Rate_Sensor_Resolution=0.000160
Roll_Rate_Sensor_Min=-5.200000
Roll_Rate_Sensor_Max=5.200000
Roll_Rate_Sensor_Noise=0.100000
Roll_Rate_Sensor_Drift_Rate=0.000150
Roll_Rate_Sensor_Max_Drift=0.010000
Roll_Rate_Sensor_Drift_Hold=5.000000
Pitch_Rate_Sensor_Order=2
Pitch_Rate_Sensor_Bandwidth=20.000
Pitch_Rate_Sensor_Gain=1.00
Pitch_Rate_Sensor_Offset=0.001961
Pitch_Rate_Sensor_Resolution=0.000160
Pitch_Rate_Sensor_Min=-5.200000

Pitch_Rate_Sensor_Max=5.200000
Pitch_Rate_Sensor_Noise=0.100000
Pitch_Rate_Sensor_Drift_Rate=0.000150
Pitch_Rate_Sensor_Max_Drift=0.010000
Pitch_Rate_Sensor_Drift_Hold=5.000000
Yaw_Rate_Sensor_Order=2
Yaw_Rate_Sensor_Bandwidth=20.000
Yaw_Rate_Sensor_Gain=1.00
Yaw_Rate_Sensor_Offset=-0.003051
Yaw_Rate_Sensor_Resolution=0.000160
Yaw_Rate_Sensor_Min=-5.200000
Yaw_Rate_Sensor_Max=5.200000
Yaw_Rate_Sensor_Noise=0.100000
Yaw_Rate_Sensor_Drift_Rate=0.000150
Yaw_Rate_Sensor_Max_Drift=0.010000
Yaw_Rate_Sensor_Drift_Hold=5.000000
X_Accel_Sensor_Order=2
X_Accel_Sensor_Bandwidth=20.000
X_Accel_Sensor_Gain=1.00
X_Accel_Sensor_Offset=0.016236
X_Accel_Sensor_Resolution=0.006000
X_Accel_Sensor_Min=-100.000000
X_Accel_Sensor_Max=100.000000
X_Accel_Sensor_Noise=0.000000
X_Accel_Sensor_Drift_Rate=0.002000
X_Accel_Sensor_Max_Drift=0.200000
X_Accel_Sensor_Drift_Hold=5.000000
Y_Accel_Sensor_Order=2
Y_Accel_Sensor_Bandwidth=20.000
Y_Accel_Sensor_Gain=1.00
Y_Accel_Sensor_Offset=-0.012900
Y_Accel_Sensor_Resolution=0.006000
Y_Accel_Sensor_Min=-100.000000
Y_Accel_Sensor_Max=100.000000
Y_Accel_Sensor_Noise=0.000000
Y_Accel_Sensor_Drift_Rate=0.002000
Y_Accel_Sensor_Max_Drift=0.200000
Y_Accel_Sensor_Drift_Hold=5.000000
Z_Accel_Sensor_Order=2
Z_Accel_Sensor_Bandwidth=20.000
Z_Accel_Sensor_Gain=1.00
Z_Accel_Sensor_Offset=-0.036066
Z_Accel_Sensor_Resolution=0.006000
Z_Accel_Sensor_Min=-100.000000
Z_Accel_Sensor_Max=100.000000
Z_Accel_Sensor_Noise=0.000000
Z_Accel_Sensor_Drift_Rate=0.002000
Z_Accel_Sensor_Max_Drift=0.200000
Z_Accel_Sensor_Drift_Hold=5.000000
IMU_Air_Period=15
agnetometer_Period=100
IMU_GPS_Period=250
GPS_Position_Lag=0
GPS_Velocity_Lag=250

Appendix F: Digital Datcom Input File

CASEID NIDAL JODEH SIG RASCAL 110 NOMINAL CONFIGURATION
\$FLTCON NMACH=1.,MACH=0.061,NALPHA=20.,NALT=1.,ALT=1000.,
WT=17.,ALPHA=-10.,-8.,-6.,-4.,-2.,0.,2.,4.,6.,8.,10.,12.,14.,16.,18.,20.,
ALPHA(17)=22.,24.,26.,28.,\$
\$OPTINS SREF=10.56,CBARR=1.25,BLREF=9.16,\$
\$SYNTHS XCG=2.,ZCG=0.083,XW=1.5416,ZW=0.44,ALIW=2.,
XH=5.24,ZH=0.125,ALIH=2.,XV=5.25,ZV=0.125,\$
\$BODY NX=20.,X(1)=0.,0.2916,0.5833,0.875,1.25,1.5416,
1.75,2.0416,2.3333,2.625,2.9166,3.2083,3.5,3.7916,
4.08333,4.375,4.6666,4.95833,5.25,5.5416,
S(1)=0.1041,0.1953,0.2454,0.2847,0.5729,0.4583,0.4392,
0.4201,0.4010,0.3516,0.3125,0.2721,0.2344,0.1944,0.1519,
0.1198,0.0868,0.0625,0.0417,0.0243,
ZU=0.1667,0.1667,0.1667,0.1875,0.4375,0.5208,0.5,0.4583,
0.4375,0.375,0.3542,0.3125,0.2917,0.2708,0.2292,0.2083,0.1875,
0.1667,0.1458,0.125,
ZL=-0.1667,-0.3542,-0.4375,-0.4792,-0.8125,-0.4792,-0.4583,
-0.4583,-0.4375,-0.4167,-0.3958,-0.3750,-0.3333,-0.3125,-0.2917,
-0.2708,-0.2500,-0.2292,-0.2083,-0.1875,\$
\$WGPLNF CHRDR=1.33,CHRDTP=0.9725,SSPN=4.5833,SSPNE=4.2014,
SAVSI=0.,CHSTAT=0.,DHDADI=4.,TYPE=1.,TWISTA=0.,\$
NACA-W-4-4310
\$HTPLNF CHRDR=0.8333,CHRDTP=0.4751,SSPN=1.5208,SSPNE=1.5,
SAVSI=0.,CHSTAT=0.,DHDADI=0.,TYPE=1.,TWISTA=0.,\$
\$SYMFLP SPANFI=0.0208,SPANFO=1.5208,CHRDFO=0.1583,CHRDFI=0.2777,
NDELTA=5.,DELTA=-20.,-10.,0.,10.,20.,FTYPE=1.0,
NTYPE=1.0,CB=0.065,TC=0.06,PHETE=0.275,PHETEP=0.275,\$
NACA-H-4-0009
\$VTPLNF CHRDR=1.08333,CHRDTP=0.61837,SSPN=0.9583,SSPNE=0.9375,
SAVSI=25.,CHSTAT=0.,TYPE=1.,\$
NACA-V-4-0009
\$PROPWR AIETLP=0.,NENGSP=1.,THSTCP=0.18,PHALOC=0.,PHVLOC=0.,PRPRAD=1.333,
BWAPR3=0.10417,BWAPR6=0.10417,BWAPR9=0.0625,NOPBPE=2.,BAPR75=45.,YP=0.,
CROT=.FALSE.,\$
DAMP
BUILD
DERIV RAD
SAVE
NEXT CASE
TRIM
SAVE
NEXT CASE
\$ASYFLP SPANFI=1.772,SPANFO=3.812,CHRDFI=0.2077,CHRDFO=0.2077,
STYPE=4.0,NDELTA=5.,DELTA=20.,10.,0.,-10.,-20.,
DELTAR=-20.,-10.,0.,10.,20.,\$
NEXT CASE

Appendix G: Digital Datcom Output File

THIS SOFTWARE AND ANY ACCOMPANYING DOCUMENTATION IS RELEASED "AS IS". THE U.S. GOVERNMENT MAKES NO WARRANTY OF ANY KIND, EXPRESS OR IMPLIED, CONCERNING THIS SOFTWARE AND ANY ACCOMPANYING DOCUMENTATION, INCLUDING, WITHOUT LIMITATION, ANY WARRANTIES OF MERCHANTABILITY OR FITNESS FOR A PARTICULAR PURPOSE. IN NO EVENT WILL THE U.S. GOVERNMENT BE LIABLE FOR ANY DAMAGES, INCLUDING LOST PROFITS, LOST SAVINGS OR OTHER INCIDENTAL OR CONSEQUENTIAL DAMAGES ARISING OUT OF THE USE, OR INABILITY TO USE, THIS SOFTWARE OR ANY ACCOMPANYING DOCUMENTATION, EVEN IF INFORMED IN ADVANCE OF THE POSSIBILITY OF SUCH DAMAGES.

```
*****
*   USAF STABILITY AND CONTROL DIGITAL DATCOM   *
*   PROGRAM REV. JAN 96   DIRECT INQUIRIES TO:   *
*   WRIGHT LABORATORY (WL/FIGC)  ATTN: W. BLAKE  *
*   WRIGHT PATTERSON AFB, OHIO 45433           *
*   PHONE (513) 255-6764,  FAX (513) 258-4054   *
*****
```

```
1          CONERR - INPUT ERROR CHECKING
0 ERROR CODES - N* DENOTES THE NUMBER OF OCCURENCES OF EACH ERROR
0 A - UNKNOWN VARIABLE NAME
0 B - MISSING EQUAL SIGN FOLLOWING VARIABLE NAME
0 C - NON-ARRAY VARIABLE HAS AN ARRAY ELEMENT DESIGNATION - (N)
0 D - NON-ARRAY VARIABLE HAS MULTIPLE VALUES ASSIGNED
0 E - ASSIGNED VALUES EXCEED ARRAY DIMENSION
0 F - SYNTAX ERROR
```

```
0***** INPUT DATA CARDS *****
```

```
CASEID NIDAL JODEH SIG RASCAL 110 NOMINAL CONFIGURATION
$FLTCON NMACH=1.,MACH=0.061,NALPHA=20.,NALT=1.,ALT=1000.,
WT=17.,ALPHA=-10.,-8.,-6.,-4.,-2.,0.,2.,4.,6.,8.,10.,12.,14.,16.,18.,20.,
ALPHA(17)=22.,24.,26.,28.,$
$OPTINS SREF=10.56,CBARR=1.25,BLREF=9.16,$
$SYNTHS XCG=2.,ZCG=0.083,XW=1.5416,ZW=0.44,ALIW=0.,
XH=5.24,ZH=0.125,ALIH=2.,XV=5.25,ZV=0.125,$
$BODY NX=20.,X(1)=0.,0.2916,0.5833,0.875,1.25,1.5416,
1.75,2.0416,2.3333,2.625,2.9166,3.2083,3.5,3.7916,
4.08333,4.375,4.6666,4.95833,5.25,5.5416,
S(1)=0.1041,0.1953,0.2454,0.2847,0.5729,0.4583,0.4392,
0.4201,0.4010,0.3516,0.3125,0.2721,0.2344,0.1944,0.1519,
0.1198,0.0868,0.0625,0.0417,0.0243,
ZU=0.1667,0.1667,0.1667,0.1875,0.4375,0.5208,0.5,0.4583,
0.4375,0.375,0.3542,0.3125,0.2917,0.2708,0.2292,0.2083,0.1875,
0.1667,0.1458,0.125,
ZL=-0.1667,-0.3542,-0.4375,-0.4792,-0.8125,-0.4792,-0.4583,
-0.4583,-0.4375,-0.4167,-0.3958,-0.3750,-0.3333,-0.3125,-0.2917,
-0.2708,-0.2500,-0.2292,-0.2083,-0.1875,$
$WGFLNF CHRDR=1.33,CHRDT=0.9725,SSPN=4.5833,SSPNE=4.2014,
SAVSI=0.,CHSTAT=0.,DHDADI=4.,TYPE=1.,TWISTA=0.,$
NACA-W-4-4310
$HTPLNF CHRDR=0.8333,CHRDT=0.4751,SSPN=1.5208,SSPNE=1.5,
SAVSI=0.,CHSTAT=0.,DHDADI=0.,TYPE=1.,TWISTA=0.,$
$SYMFLP SPANFI=0.0208,SPANFO=1.5208,CHRDFO=0.1583,CHRDFI=0.2777,
```

```

NDELTA=5.,DELTA=-20.,-10.,0.,10.,20.,FTYPE=1.0,
NTYPE=1.0,CB=0.065,TC=0.06,PHETE=0.275,PHETEP=0.275,$
NACA-H-4-0009
$VTPLNF CHRDR=1.08333,CHRDT=0.61837,SSPN=0.9583,SSPNE=0.9375,
SAVSI=25.,CHSTAT=0.,TYPE=1.,$
NACA-V-4-0009
$PROPRW AIETLP=0.,NENGSP=1.,THSTCP=0.18,PHALOC=0.,PHVLOC=0.,PRPRAD=1.333,
BWAPR3=0.10417,BWAPR6=0.10417,BWAPR9=0.0625,NOPBPE=2.,BAPR75=45.,YP=0.,
CROT=.FALSE.,$
DAMP
BUILD
DERIV DEG
SAVE
NEXT CASE
TRIM
SAVE
NEXT CASE
$ASYFLP SPANFI=1.772,SPANFO=3.812,CHRDFI=0.2077,CHRDFO=0.2077,
STYPE=4.0,NDELTA=5.,DELTAL=20.,10.,0.,-10.,-20.,
DELTAR=-20.,-10.,0.,10.,20.,$
NEXT CASE
1 THE FOLLOWING IS A LIST OF ALL INPUT CARDS FOR THIS CASE.
0
CASEID NIDAL JODEH SIG RASCAL 110 NOMINAL CONFIGURATION
$FLTCN NMACH=1.,MACH=0.061,NALPHA=20.,NALT=1.,ALT=1000.,
WT=17.,ALPHA=-10.,-8.,-6.,-4.,-2.,0.,2.,4.,6.,8.,10.,12.,14.,16.,18.,20.,
ALPHA(17)=22.,24.,26.,28.,$
$OPTINS SREF=10.56,CBARR=1.25,BLREF=9.16,$
$SYNTHS XCG=2.,ZCG=0.083,XW=1.5416,ZW=0.44,ALIW=0.,
XH=5.24,ZH=0.125,ALIH=2.,XV=5.25,ZV=0.125,$
$BODY NX=20.,X(1)=0.,0.2916,0.5833,0.875,1.25,1.5416,
1.75,2.0416,2.3333,2.625,2.9166,3.2083,3.5,3.7916,
4.08333,4.375,4.6666,4.95833,5.25,5.5416,
S(1)=0.1041,0.1953,0.2454,0.2847,0.5729,0.4583,0.4392,
0.4201,0.4010,0.3516,0.3125,0.2721,0.2344,0.1944,0.1519,
0.1198,0.0868,0.0625,0.0417,0.0243,
ZU=0.1667,0.1667,0.1667,0.1875,0.4375,0.5208,0.5,0.4583,
0.4375,0.375,0.3542,0.3125,0.2917,0.2708,0.2292,0.2083,0.1875,
0.1667,0.1458,0.125,
ZL=-0.1667,-0.3542,-0.4375,-0.4792,-0.8125,-0.4792,-0.4583,
-0.4583,-0.4375,-0.4167,-0.3958,-0.3750,-0.3333,-0.3125,-0.2917,
-0.2708,-0.2500,-0.2292,-0.2083,-0.1875,$
$WGFLNF CHRDR=1.33,CHRDT=0.9725,SSPN=4.5833,SSPNE=4.2014,
SAVSI=0.,CHSTAT=0.,DHDADI=4.,TYPE=1.,TWISTA=0.,$
NACA-W-4-4310
$HTPLNF CHRDR=0.8333,CHRDT=0.4751,SSPN=1.5208,SSPNE=1.5,
SAVSI=0.,CHSTAT=0.,DHDADI=0.,TYPE=1.,TWISTA=0.,$
$SYMFLP SPANFI=0.0208,SPANFO=1.5208,CHRDFO=0.1583,CHRDFI=0.2777,
NDELTA=5.,DELTA=-20.,-10.,0.,10.,20.,FTYPE=1.0,
NTYPE=1.0,CB=0.065,TC=0.06,PHETE=0.275,PHETEP=0.275,$
NACA-H-4-0009
$VTPLNF CHRDR=1.08333,CHRDT=0.61837,SSPN=0.9583,SSPNE=0.9375,
SAVSI=25.,CHSTAT=0.,TYPE=1.,$
NACA-V-4-0009
$PROPRW AIETLP=0.,NENGSP=1.,THSTCP=0.18,PHALOC=0.,PHVLOC=0.,PRPRAD=1.333,
BWAPR3=0.10417,BWAPR6=0.10417,BWAPR9=0.0625,NOPBPE=2.,BAPR75=45.,YP=0.,

```

```

CROT=.FALSE.,$
DAMP
BUILD
DERIV DEG
SAVE
NEXT CASE
0ERROR ** FLAP INBOARD SPAN, SPANI = 0.20800E-01, IT IS INSIDE THE BODY AS DEFINED BY SSPN AND SSPNE
      SPANI IS REDEFINED, SPANI = SSPN-SSPNE = 0.20800E-01

0 INPUT DIMENSIONS ARE IN FT, SCALE FACTOR IS 1.0000

1          AUTOMATED STABILITY AND CONTROL METHODS PER APRIL 1976 VERSION OF DATCOM
0          WING SECTION DEFINITION
          IDEAL ANGLE OF ATTACK = 1.12591 DEG.

          ZERO LIFT ANGLE OF ATTACK = -3.50518 DEG.

          IDEAL LIFT COEFFICIENT = 0.54407
ZERO LIFT PITCHING MOMENT COEFFICIENT = -0.08623

          MACH ZERO LIFT-CURVE-SLOPE = 0.09893 /DEG.

          LEADING EDGE RADIUS = 0.01102 FRACTION CHORD
          MAXIMUM AIRFOIL THICKNESS = 0.10000 FRACTION CHORD
          DELTA-Y = 2.64081 PERCENT CHORD

0          MACH= 0.0610 LIFT-CURVE-SLOPE = 0.09903 /DEG.      XAC = 0.25348
1          AUTOMATED STABILITY AND CONTROL METHODS PER APRIL 1976 VERSION OF DATCOM
0          HORIZONTAL TAIL SECTION DEFINITION
          IDEAL ANGLE OF ATTACK = 0.00000 DEG.

          ZERO LIFT ANGLE OF ATTACK = 0.00000 DEG.

          IDEAL LIFT COEFFICIENT = 0.00000
ZERO LIFT PITCHING MOMENT COEFFICIENT = 0.00000

          MACH ZERO LIFT-CURVE-SLOPE = 0.09830 /DEG.

          LEADING EDGE RADIUS = 0.00893 FRACTION CHORD
          MAXIMUM AIRFOIL THICKNESS = 0.09000 FRACTION CHORD
          DELTA-Y = 2.37673 PERCENT CHORD

0          MACH= 0.0610 LIFT-CURVE-SLOPE = 0.09846 /DEG.      XAC = 0.25642
1          AUTOMATED STABILITY AND CONTROL METHODS PER APRIL 1976 VERSION OF DATCOM
0          VERTICAL TAIL SECTION DEFINITION
          IDEAL ANGLE OF ATTACK = 0.00000 DEG.

          ZERO LIFT ANGLE OF ATTACK = 0.00000 DEG.

```

IDEAL LIFT COEFFICIENT = 0.00000
 ZERO LIFT PITCHING MOMENT COEFFICIENT = 0.00000
 MACH ZERO LIFT-CURVE-SLOPE = 0.09830 /DEG.
 LEADING EDGE RADIUS = 0.00893 FRACTION CHORD
 MAXIMUM AIRFOIL THICKNESS = 0.09000 FRACTION CHORD
 DELTA-Y = 2.37673 PERCENT CHORD

0 MACH= 0.0610 LIFT-CURVE-SLOPE = 0.09846 /DEG. XAC = 0.25642
 1 AUTOMATED STABILITY AND CONTROL METHODS PER APRIL 1976 VERSION OF DATCOM
 CHARACTERISTICS AT ANGLE OF ATTACK AND IN SIDESLIP
 DATCOM BODY ALONE CONFIGURATION
 NIDAL JODEH SIG RASCAL 110 NOMINAL CONFIGURATION

MACH NUMBER	FLIGHT CONDITIONS					REFERENCE DIMENSIONS						
	ALTITUDE	VELOCITY	PRESSURE	TEMPERATURE	REYNOLDS NUMBER	REF. AREA	REFERENCE LENGTH	LAT.	MOMENT	REF. CENTER		
	FT	FT/SEC	LB/FT**2	DEG R	1/FT	FT**2	FT	FT	FT	FT		
0 0.061	1000.00	67.86	2.0409E+03	515.104	4.1949E+05	10.560	1.250	9.160	2.000	0.083		
-----DERIVATIVE (PER DEGREE)-----												
0 ALPHA	CD	CL	CM	CN	CA	XCP	CLA	CMA	CYB	CNB	CLB	
0	-10.0	0.008	-0.016	-0.0483	-0.018	0.005	2.735	1.736E-03	1.992E-03	-1.736E-03	-2.719E-04	0.000E+00
	-8.0	0.007	-0.014	-0.0445	-0.014	0.005	3.097	1.513E-03	1.906E-03	-1.513E-03	-2.600E-04	0.000E+00
	-6.0	0.006	-0.010	-0.0407	-0.011	0.005	3.691	1.567E-03	1.941E-03	-1.567E-03	-2.649E-04	0.000E+00
	-4.0	0.006	-0.007	-0.0368	-0.008	0.005	4.830	1.607E-03	1.967E-03	-1.607E-03	-2.684E-04	0.000E+00
	-2.0	0.005	-0.004	-0.0328	-0.004	0.005	7.874	1.633E-03	1.984E-03	-1.633E-03	-2.707E-04	0.000E+00
	0.0	0.005	-0.001	-0.0288	-0.001	0.005	41.093	1.643E-03	1.990E-03	-1.643E-03	-2.716E-04	0.000E+00
	2.0	0.005	0.003	-0.0249	0.003	0.005	-8.981	1.639E-03	1.988E-03	-1.639E-03	-2.712E-04	0.000E+00
	4.0	0.006	0.006	-0.0209	0.006	0.005	-3.357	1.619E-03	1.975E-03	-1.619E-03	-2.695E-04	0.000E+00
	6.0	0.006	0.009	-0.0170	0.010	0.005	-1.758	1.585E-03	1.953E-03	-1.585E-03	-2.665E-04	0.000E+00
	8.0	0.007	0.012	-0.0131	0.013	0.005	-1.004	1.646E-03	1.884E-03	-1.646E-03	-2.571E-04	0.000E+00
	10.0	0.008	0.016	-0.0094	0.017	0.005	-0.562	2.189E-03	1.633E-03	-2.189E-03	-2.229E-04	0.000E+00
	12.0	0.010	0.021	-0.0066	0.023	0.005	-0.291	3.126E-03	1.228E-03	-3.126E-03	-1.676E-04	0.000E+00
	14.0	0.012	0.028	-0.0045	0.030	0.005	-0.149	4.050E-03	8.049E-04	-4.050E-03	-1.098E-04	0.000E+00
	16.0	0.016	0.037	-0.0033	0.040	0.005	-0.083	4.912E-03	3.776E-04	-4.912E-03	-5.153E-05	0.000E+00
	18.0	0.021	0.048	-0.0030	0.052	0.005	-0.058	5.701E-03	-5.149E-05	-5.701E-03	7.026E-06	0.000E+00
	20.0	0.027	0.060	-0.0035	0.066	0.005	-0.054	6.409E-03	-4.803E-04	-6.409E-03	6.555E-05	0.000E+00
	22.0	0.035	0.073	-0.0049	0.081	0.005	-0.061	7.025E-03	-9.068E-04	-7.025E-03	1.237E-04	0.000E+00
	24.0	0.045	0.088	-0.0072	0.099	0.005	-0.073	7.542E-03	-1.329E-03	-7.542E-03	1.813E-04	0.000E+00
	26.0	0.056	0.104	-0.0102	0.118	0.005	-0.087	7.952E-03	-1.745E-03	-7.952E-03	2.381E-04	0.000E+00
	28.0	0.069	0.120	-0.0141	0.138	0.005	-0.102	8.308E-03	-2.156E-03	-8.308E-03	2.943E-04	0.000E+00

1

AUTOMATED STABILITY AND CONTROL METHODS PER APRIL 1976 VERSION OF DATCOM
 DYNAMIC DERIVATIVES
 DATCOM BODY ALONE CONFIGURATION
 NIDAL JODEH SIG RASCAL 110 NOMINAL CONFIGURATION

FLIGHT CONDITIONS						REFERENCE DIMENSIONS					
MACH NUMBER	ALTITUDE	VELOCITY	PRESSURE	TEMPERATURE	REYNOLDS NUMBER	REF. AREA	REFERENCE LONG.	LENGTH LAT.	MOMENT HORIZ	REF. CENTER VERT	
	FT	FT/SEC	LB/FT**2	DEG R	1/FT	FT**2	FT	FT	FT	FT	
0	0.061	1000.00	67.86	2.0409E+03	515.104	4.1949E+05	10.560	1.250	9.160	2.000	0.083
DYNAMIC DERIVATIVES (PER DEGREE)											
PITCHING			ACCELERATION			ROLLING			YAWING		
ALPHA	CLQ	CMQ	CLAD	CMAD	CLP	CYP	CNP	CNR	CLR		
0	-10.00	7.098E-04	2.651E-03	1.128E-04	1.081E-04	NDM	NDM	NDM	NDM	0.000E+00	
0	-8.00									0.000E+00	
0	-6.00									0.000E+00	
0	-4.00									0.000E+00	
0	-2.00									0.000E+00	
0	0.00									0.000E+00	
0	2.00									0.000E+00	
0	4.00									0.000E+00	
0	6.00									0.000E+00	
0	8.00									0.000E+00	
0	10.00									0.000E+00	
0	12.00									0.000E+00	
0	14.00									0.000E+00	
0	16.00									0.000E+00	
0	18.00									0.000E+00	
0	20.00									0.000E+00	
0	22.00									0.000E+00	
0	24.00									0.000E+00	
0	26.00									0.000E+00	
0	28.00									0.000E+00	

0*** NDM PRINTED WHEN NO DATCOM METHODS EXIST

1

AUTOMATED STABILITY AND CONTROL METHODS PER APRIL 1976 VERSION OF DATCOM
 CHARACTERISTICS AT ANGLE OF ATTACK AND IN SIDESLIP
 WING ALONE CONFIGURATION
 NIDAL JODEH SIG RASCAL 110 NOMINAL CONFIGURATION

FLIGHT CONDITIONS						REFERENCE DIMENSIONS						
MACH NUMBER	ALTITUDE	VELOCITY	PRESSURE	TEMPERATURE	REYNOLDS NUMBER	REF. AREA	REFERENCE LONG.	LENGTH LAT.	MOMENT HORIZ	REF. CENTER VERT		
	FT	FT/SEC	LB/FT**2	DEG R	1/FT	FT**2	FT	FT	FT	FT		
0	0.061	1000.00	67.86	2.0409E+03	515.104	4.1949E+05	10.560	1.250	9.160	2.000	0.083	
DERIVATIVE (PER DEGREE)												
ALPHA	CD	CL	CM	CN	CA	XCP	CLA	CMA	CYB	CNB	CLB	
0	-10.0	0.025	-0.495	-0.1239	-0.492	-0.061	0.252	7.026E-02	9.463E-03	-4.005E-04	5.063E-05	-7.979E-04
0	-8.0	0.018	-0.335	-0.1018	-0.335	-0.029	0.304	7.845E-02	1.079E-02	-4.005E-04	2.322E-05	-8.565E-04
0	-6.0	0.013	-0.182	-0.0808	-0.182	-0.006	0.444	7.513E-02	1.023E-02	-4.005E-04	6.801E-06	-9.129E-04
0	-4.0	0.011	-0.035	-0.0609	-0.036	0.009	1.707	7.248E-02	9.798E-03	-4.005E-04	2.524E-07	-9.667E-04
0	-2.0	0.012	0.108	-0.0416	0.108	0.016	-0.385	7.385E-02	9.950E-03	-4.005E-04	2.423E-06	-1.019E-03
0	0.0	0.015	0.260	-0.0211	0.260	0.015	-0.081	7.804E-02	1.052E-02	-4.005E-04	1.400E-05	-1.075E-03
0	2.0	0.021	0.421	0.0005	0.421	0.006	0.001	8.171E-02	1.105E-02	-4.005E-04	3.649E-05	-1.134E-03
0	4.0	0.031	0.587	0.0231	0.588	-0.010	0.039	8.467E-02	1.154E-02	-4.004E-04	7.117E-05	-1.195E-03

6.0	0.044	0.759	0.0467	0.760	-0.036	0.061	8.688E-02	1.196E-02	-4.004E-04	1.189E-04	-1.258E-03
8.0	0.061	0.935	0.0710	0.934	-0.070	0.076	8.661E-02	1.210E-02	-4.004E-04	1.803E-04	-1.322E-03
10.0	0.080	1.106	0.0951	1.103	-0.113	0.086	7.590E-02	1.085E-02	-4.003E-04	2.522E-04	-1.385E-03
12.0	0.098	1.238	0.1144	1.232	-0.162	0.093	6.021E-02	8.923E-03	-4.003E-04	3.165E-04	-1.434E-03
14.0	0.114	1.347	0.1307	1.334	-0.215	0.098	4.656E-02	7.273E-03	-4.003E-04	3.741E-04	-1.473E-03
16.0	0.126	1.425	0.1435	1.404	-0.271	0.102	2.393E-02	4.334E-03	-4.002E-04	4.188E-04	-1.502E-03
18.0	0.129	1.442	NA	1.412	-0.323	NA	-4.313E-02	NA	-4.003E-04	4.292E-04	-1.508E-03
20.0	0.100	1.252	NA	1.211	-0.334	NA	-2.698E-01	NA	-4.007E-04	3.235E-04	-1.439E-03
22.0	0.019	0.363	NA	0.344	-0.119	NA	-3.941E-01	NA	-4.059E-04	2.719E-05	-1.113E-03
24.0	0.017	-0.324	NA	-0.289	0.148	NA	-3.223E-01	NA	-3.911E-04	2.170E-05	-8.606E-04
26.0	0.060	-0.926	NA	-0.806	0.460	NA	-2.473E-01	NA	-3.960E-04	1.770E-04	-6.399E-04
28.0	0.109	-1.313	NA	-1.109	0.713	NA	-1.399E-01	NA	-3.967E-04	3.559E-04	-4.979E-04

0*** NA PRINTED WHEN METHOD NOT APPLICABLE

1 AUTOMATED STABILITY AND CONTROL METHODS PER APRIL 1976 VERSION OF DATCOM
DYNAMIC DERIVATIVES
WING ALONE CONFIGURATION
NIDAL JODEH SIG RASCAL 110 NOMINAL CONFIGURATION

FLIGHT CONDITIONS						REFERENCE DIMENSIONS						
MACH NUMBER	ALTITUDE	VELOCITY	PRESSURE	TEMPERATURE	REYNOLDS NUMBER	REF. AREA	REFERENCE LONG.	LENGTH	MOMENT	REF. CENTER		
	FT	FT/SEC	LB/FT**2	DEG R	1/FT	FT**2	FT	FT	FT	FT		
0 0.061	1000.00	67.86	2.0409E+03	515.104	4.1949E+05	10.560	1.250	9.160	2.000	0.083		
DYNAMIC DERIVATIVES (PER DEGREE)												
ALPHA	PITCHING			ACCELERATION			ROLLING			YAWING		
	CLQ	CMQ		CLAD	CMAD	CLP	CYP	CNP	CNR	CLR		
-10.00	1.323E-02	-5.328E-03		NDM	NDM	1.440E-02	-1.356E-03	1.123E-03	-1.400E-04	NDM		
-8.00						1.389E-02	-1.470E-03	7.786E-04	-9.562E-05	NDM		
-6.00						1.330E-02	-1.579E-03	4.249E-04	-6.900E-05	NDM		
-4.00						1.283E-02	-1.684E-03	8.314E-05	-5.839E-05	NDM		
-2.00						1.308E-02	-1.789E-03	-2.642E-04	-6.191E-05	NDM		
0.00						1.382E-02	-1.904E-03	-6.572E-04	-8.066E-05	NDM		
2.00						1.446E-02	-2.032E-03	-1.111E-03	-1.171E-04	NDM		
4.00						1.498E-02	-2.175E-03	-1.647E-03	-1.733E-04	NDM		
6.00						1.535E-02	-2.346E-03	-2.322E-03	-2.507E-04	NDM		
8.00						1.529E-02	-2.581E-03	-3.322E-03	-3.502E-04	NDM		
10.00						1.337E-02	-3.650E-03	-8.902E-03	-4.668E-04	NDM		
12.00						1.057E-02	-2.259E-03	-7.952E-04	-5.708E-04	NDM		
14.00						8.127E-03	-2.532E-03	-2.027E-03	-6.643E-04	NDM		
16.00						4.099E-03	-2.690E-03	-2.591E-03	-7.367E-04	NDM		
18.00						-7.801E-03	-2.827E-03	-2.951E-03	-7.535E-04	NDM		
20.00						-4.799E-02	-2.803E-03	-2.713E-03	-5.823E-04	NDM		
22.00						-6.995E-02	-2.067E-03	-1.289E-03	-1.020E-04	NDM		
24.00						-5.721E-02	-1.448E-03	3.971E-04	-9.315E-05	NDM		
26.00						-4.394E-02	-9.461E-04	1.553E-03	-3.448E-04	NDM		
28.00						-2.496E-02	-6.307E-04	2.499E-03	-6.347E-04	NDM		

0*** NDM PRINTED WHEN NO DATCOM METHODS EXIST

1

AUTOMATED STABILITY AND CONTROL METHODS PER APRIL 1976 VERSION OF DATCOM
 CHARACTERISTICS AT ANGLE OF ATTACK AND IN SIDESLIP
 HORIZONTAL TAIL CONFIGURATION
 NIDAL JODEH SIG RASCAL 110 NOMINAL CONFIGURATION

FLIGHT CONDITIONS						REFERENCE DIMENSIONS						
MACH NUMBER	ALTITUDE	VELOCITY	PRESSURE	TEMPERATURE	REYNOLDS NUMBER	REF. AREA	REFERENCE LENGTH	LAT.	MOMENT	REF. CENTER		
	FT	FT/SEC	LB/FT**2	DEG R	1/FT	FT**2	FT	FT	FT	FT		
0	0.061	1000.00	67.86	2.0409E+03	515.104	4.1949E+05	10.560	1.250	9.160	2.000	0.083	
-----DERIVATIVE (PER DEGREE)-----												
0	ALPHA	CD	CL	CM	CN	CA	XCP	CLA	CMA	CYB	CNB	CLB
0	-10.0	0.007	-0.111	0.3031	-0.111	-0.012	-2.731	1.515E-02	-4.053E-02	3.565E-08	7.385E-06	2.853E-05
	-8.0	0.005	-0.082	0.2230	-0.082	-0.006	-2.735	1.460E-02	-3.959E-02	1.914E-08	3.966E-06	2.091E-05
	-6.0	0.004	-0.053	0.1448	-0.053	-0.002	-2.729	1.398E-02	-3.823E-02	8.063E-09	1.671E-06	1.357E-05
	-4.0	0.003	-0.026	0.0701	-0.026	0.001	-2.716	1.324E-02	-3.619E-02	1.896E-09	3.927E-07	6.579E-06
	-2.0	0.002	0.000	0.0000	0.000	0.002	0.000	1.284E-02	-3.506E-02	0.000E+00	0.000E+00	0.000E+00
	0.0	0.003	0.026	-0.0702	0.026	0.003	-2.732	1.324E-02	-3.625E-02	1.896E-09	3.927E-07	-6.579E-06
	2.0	0.004	0.053	-0.1450	0.053	0.002	-2.732	1.398E-02	-3.865E-02	8.063E-09	1.671E-06	-1.357E-05
	4.0	0.005	0.082	-0.2248	0.082	-0.001	-2.749	1.460E-02	-4.135E-02	1.914E-08	3.967E-06	-2.091E-05
	6.0	0.007	0.111	-0.3104	0.112	-0.004	-2.783	1.508E-02	-4.324E-02	3.565E-08	7.386E-06	-2.853E-05
	8.0	0.011	0.142	-0.3977	0.142	-0.009	-2.800	1.515E-02	-4.381E-02	5.791E-08	1.200E-05	-3.636E-05
	10.0	0.014	0.172	-0.4856	0.172	-0.016	-2.826	1.325E-02	-4.096E-02	8.500E-08	1.761E-05	-4.405E-05
	12.0	0.018	0.195	-0.5616	0.194	-0.023	-2.889	1.027E-02	-3.527E-02	1.092E-07	2.263E-05	-4.994E-05
	14.0	0.021	0.213	-0.6267	0.212	-0.031	-2.960	7.550E-03	-2.798E-02	1.304E-07	2.703E-05	-5.457E-05
	16.0	0.023	0.225	-0.6735	0.223	-0.040	-3.024	3.253E-03	-1.543E-02	1.457E-07	3.020E-05	-5.767E-05
	18.0	0.023	0.226	-0.6884	0.222	-0.048	-3.099	-1.140E-02	2.911E-02	1.468E-07	3.044E-05	-5.790E-05
	20.0	0.015	0.180	-0.5571	0.174	-0.047	-3.202	-2.930E-02	8.593E-02	9.249E-08	1.921E-05	-4.599E-05
	22.0	0.007	0.109	-0.3447	0.104	-0.034	-3.325	-3.117E-02	9.489E-02	3.386E-08	7.062E-06	-2.788E-05
	24.0	0.004	0.055	-0.1775	0.052	-0.019	-3.440	-2.218E-02	6.949E-02	8.505E-09	1.793E-06	-1.405E-05
	26.0	0.003	0.020	-0.0667	0.019	-0.006	-3.463	-1.713E-02	5.598E-02	1.104E-09	2.418E-07	-5.159E-06
	28.0	0.003	-0.014	0.0464	-0.011	0.009	-4.270	-1.669E-02	5.716E-02	5.862E-10	1.117E-07	3.504E-06

1

AUTOMATED STABILITY AND CONTROL METHODS PER APRIL 1976 VERSION OF DATCOM
 DYNAMIC DERIVATIVES
 HORIZONTAL TAIL CONFIGURATION
 NIDAL JODEH SIG RASCAL 110 NOMINAL CONFIGURATION

FLIGHT CONDITIONS						REFERENCE DIMENSIONS					
MACH NUMBER	ALTITUDE	VELOCITY	PRESSURE	TEMPERATURE	REYNOLDS NUMBER	REF. AREA	REFERENCE LENGTH	LAT.	MOMENT	REF. CENTER	
	FT	FT/SEC	LB/FT**2	DEG R	1/FT	FT**2	FT	FT	FT	FT	
0	0.061	1000.00	67.86	2.0409E+03	515.104	4.1949E+05	10.560	1.250	9.160	2.000	0.083
DYNAMIC DERIVATIVES (PER DEGREE)											
0	ALPHA	PITCHING		ACCELERATION		ROLLING		YAWING			
0		CLQ	CMQ	CLAD	CMAD	CLP	CYP	CNP	CNR	CLR	
0	-10.00	8.674E-02	-1.387E-01	NDM	NDM	1.957E-03	0.000E+00	0.000E+00	0.000E+00	NDM	
	-8.00					1.886E-03				NDM	
	-6.00					1.806E-03				NDM	
	-4.00					1.711E-03				NDM	
	-2.00					1.659E-03				NDM	
	0.00					1.711E-03				NDM	
	2.00					1.806E-03				NDM	
	4.00					1.886E-03				NDM	
	6.00					1.948E-03				NDM	

8.00	1.956E-03	NDM
10.00	1.710E-03	NDM
12.00	1.324E-03	NDM
14.00	9.731E-04	NDM
16.00	4.176E-04	NDM
18.00	-1.476E-03	NDM
20.00	-3.787E-03	NDM
22.00	-4.029E-03	NDM
24.00	-2.866E-03	NDM
26.00	-2.214E-03	NDM
28.00	-2.156E-03	NDM

0*** NDM PRINTED WHEN NO DATCOM METHODS EXIST

1 AUTOMATED STABILITY AND CONTROL METHODS PER APRIL 1976 VERSION OF DATCOM
CHARACTERISTICS AT ANGLE OF ATTACK AND IN SIDESLIP
VERTICAL TAIL CONFIGURATION
NIDAL JODEH SIG RASCAL 110 NOMINAL CONFIGURATION

----- FLIGHT CONDITIONS -----						----- REFERENCE DIMENSIONS -----					
MACH NUMBER	ALTITUDE	VELOCITY	PRESSURE	TEMPERATURE	REYNOLDS NUMBER	REF. AREA	REFERENCE LENGTH	MOMENT	REF. CENTER		
	FT	FT/SEC	LB/FT**2	DEG R	1/FT	FT**2	FT	FT	HORIZ FT	VERT FT	
0 0.061	1000.00	67.86	2.0409E+03	515.104	4.1949E+05	10.560	1.250	9.160	2.000	0.083	
-----DERIVATIVE (PER DEGREE)-----											
0 ALPHA	CD	CL	CM	CN	CA	XCP	CLA	CMA	CYB	CNB	CLB
0											
-10.0	0.001	0.000	0.0000	0.000	NDM	*****	0.000E+00	0.000E+00	-1.682E-03	6.743E-04	-2.035E-04
-8.0											-1.807E-04
-6.0											-1.577E-04
-4.0											-1.345E-04
-2.0											-1.112E-04
0.0											-8.771E-05
2.0											-6.412E-05
4.0											-4.046E-05
6.0											-1.674E-05
8.0											6.990E-06
10.0											3.071E-05
12.0											5.440E-05
14.0											7.802E-05
16.0											1.016E-04
18.0											1.250E-04
20.0											1.482E-04
22.0											1.713E-04
24.0											1.941E-04
26.0											2.168E-04
28.0											2.391E-04

0*** NDM PRINTED WHEN NO DATCOM METHODS EXIST

1

AUTOMATED STABILITY AND CONTROL METHODS PER APRIL 1976 VERSION OF DATCOM
 DYNAMIC DERIVATIVES
 VERTICAL TAIL CONFIGURATION
 NIDAL JODEH SIG RASCAL 110 NOMINAL CONFIGURATION

FLIGHT CONDITIONS						REFERENCE DIMENSIONS				
MACH NUMBER	ALTITUDE	VELOCITY	PRESSURE	TEMPERATURE	REYNOLDS NUMBER	REF. AREA	REFERENCE LONG.	LENGTH LAT.	MOMENT HORIZ	REF. CENTER VERT
	FT	FT/SEC	LB/FT**2	DEG R	1/FT	FT**2	FT	FT	FT	FT
0 0.061	1000.00	67.86	2.0409E+03	515.104	4.1949E+05	10.560	1.250	9.160	2.000	0.083
DYNAMIC DERIVATIVES (PER DEGREE)										
PITCHING			ACCELERATION		ROLLING			YAWING		
ALPHA	CLQ	CMQ	CLAD	CMAD	CLP	CYP	CNP	CNR	CLR	
-10.00	0.000E+00	0.000E+00	0.000E+00	0.000E+00	NDM	-2.315E-04	8.928E-05	-5.004E-04	NDM	
-8.00					NDM	-1.860E-04	7.246E-05	-5.108E-04	NDM	
-6.00					NDM	-1.400E-04	5.504E-05	-5.201E-04	NDM	
-4.00					NDM	-9.365E-05	3.710E-05	-5.281E-04	NDM	
-2.00					NDM	-4.696E-05	1.872E-05	-5.349E-04	NDM	
0.00					NDM	0.000E+00	0.000E+00	-5.405E-04	NDM	
2.00					NDM	4.717E-05	-1.898E-05	-5.447E-04	NDM	
4.00					NDM	9.450E-05	-3.812E-05	-5.477E-04	NDM	
6.00					NDM	1.419E-04	-5.734E-05	-5.493E-04	NDM	
8.00					NDM	1.894E-04	-7.654E-05	-5.496E-04	NDM	
10.00					NDM	2.368E-04	-9.562E-05	-5.485E-04	NDM	
12.00					NDM	2.842E-04	-1.145E-04	-5.461E-04	NDM	
14.00					NDM	3.315E-04	-1.331E-04	-5.424E-04	NDM	
16.00					NDM	3.785E-04	-1.513E-04	-5.374E-04	NDM	
18.00					NDM	4.253E-04	-1.690E-04	-5.311E-04	NDM	
20.00					NDM	4.718E-04	-1.861E-04	-5.235E-04	NDM	
22.00					NDM	5.180E-04	-2.026E-04	-5.148E-04	NDM	
24.00					NDM	5.637E-04	-2.183E-04	-5.048E-04	NDM	
26.00					NDM	6.089E-04	-2.333E-04	-4.938E-04	NDM	
28.00					NDM	6.537E-04	-2.473E-04	-4.817E-04	NDM	

0*** NDM PRINTED WHEN NO DATCOM METHODS EXIST

1

AUTOMATED STABILITY AND CONTROL METHODS PER APRIL 1976 VERSION OF DATCOM
 CHARACTERISTICS AT ANGLE OF ATTACK AND IN SIDESLIP
 WING-BODY CONFIGURATION
 NIDAL JODEH SIG RASCAL 110 NOMINAL CONFIGURATION

FLIGHT CONDITIONS						REFERENCE DIMENSIONS					
MACH NUMBER	ALTITUDE	VELOCITY	PRESSURE	TEMPERATURE	REYNOLDS NUMBER	REF. AREA	REFERENCE LONG.	LENGTH LAT.	MOMENT HORIZ	REF. CENTER VERT	
	FT	FT/SEC	LB/FT**2	DEG R	1/FT	FT**2	FT	FT	FT	FT	
0 0.061	1000.00	67.86	2.0409E+03	515.104	4.1949E+05	10.560	1.250	9.160	2.000	0.083	
DERIVATIVE (PER DEGREE)											
ALPHA	CD	CL	CM	CN	CA	XCP	CLA	CMA	CYB	CNB	CLB
-10.0	0.035	-0.598	-0.2004	-0.596	-0.069	0.337	9.711E-02	2.014E-02	-3.939E-03	-4.532E-04	-1.270E-03
-8.0	0.027	-0.408	-0.1620	-0.407	-0.030	0.397	9.369E-02	1.834E-02			-1.341E-03
-6.0	0.021	-0.224	-0.1271	-0.225	-0.002	0.565	8.984E-02	1.651E-02			-1.409E-03
-4.0	0.019	-0.048	-0.0959	-0.050	0.015	1.937	8.677E-02	1.487E-02			-1.474E-03
-2.0	0.019	0.123	-0.0676	0.123	0.023	-0.551	8.841E-02	1.397E-02			-1.537E-03
0.0	0.022	0.305	-0.0400	0.305	0.022	-0.131	9.334E-02	1.354E-02			-1.604E-03
2.0	0.028	0.497	-0.0134	0.497	0.011	-0.027	9.765E-02	1.299E-02			-1.675E-03
4.0	0.038	0.696	0.0119	0.697	-0.011	0.017	1.011E-01	1.232E-02			-1.749E-03

6.0	0.052	0.901	0.0358	0.902	-0.043	0.040	1.037E-01	1.154E-02	-1.825E-03
8.0	0.069	1.111	0.0581	1.109	-0.086	0.052	1.034E-01	1.036E-02	-1.902E-03
10.0	0.090	1.315	0.0773	1.310	-0.139	0.059	9.138E-02	7.597E-03	-1.978E-03
12.0	0.110	1.476	0.0885	1.467	-0.200	0.060	7.387E-02	4.155E-03	-2.038E-03
14.0	0.128	1.610	0.0939	1.593	-0.265	0.059	5.876E-02	1.259E-03	-2.087E-03
16.0	0.144	1.711	0.0935	1.684	-0.333	0.056	3.303E-02	-1.686E-03	-2.125E-03
18.0	0.152	1.742	NA	1.704	-0.394	NA	-4.497E-02	NA	-2.136E-03
20.0	0.129	1.531	NA	1.483	-0.402	NA	-3.106E-01	NA	-2.058E-03
22.0	0.056	0.500	NA	0.484	-0.136	NA	-4.560E-01	NA	-1.676E-03
24.0	0.064	-0.293	NA	-0.242	0.177	NA	-3.711E-01	NA	-1.383E-03
26.0	0.118	-0.985	NA	-0.833	0.537	NA	-2.826E-01	NA	-1.127E-03
28.0	0.180	-1.423	NA	-1.172	0.827	NA	-1.561E-01	NA	-9.647E-04

0*** NA PRINTED WHEN METHOD NOT APPLICABLE

1 AUTOMATED STABILITY AND CONTROL METHODS PER APRIL 1976 VERSION OF DATCOM
DYNAMIC DERIVATIVES
WING-BODY CONFIGURATION
NIDAL JODEH SIG RASCAL 110 NOMINAL CONFIGURATION

FLIGHT CONDITIONS						REFERENCE DIMENSIONS				
MACH NUMBER	ALTITUDE FT	VELOCITY FT/SEC	PRESSURE LB/FT**2	TEMPERATURE DEG R	REYNOLDS NUMBER 1/FT	REF. AREA FT**2	REFERENCE LONG. FT	LENGTH LAT. FT	MOMENT HORIZ FT	REF. CENTER VERT FT
0 0.061	1000.00	67.86	2.0409E+03	515.104	4.1949E+05	10.560	1.250	9.160	2.000	0.083
DYNAMIC DERIVATIVES (PER DEGREE)										
ALPHA	PITCHING			ACCELERATION		ROLLING			YAWING	
	CLQ	CMQ	CLAD	CMAD	CLP	CYP	CNP	CNR	CLR	
-10.00	1.626E-02	-3.608E-03	NDM	NDM	1.440E-02	-1.356E-03	1.123E-03	-1.400E-04	NDM	
-8.00					1.389E-02	-1.470E-03	7.786E-04	-9.562E-05	NDM	
-6.00					1.330E-02	-1.579E-03	4.249E-04	-6.900E-05	NDM	
-4.00					1.283E-02	-1.684E-03	8.314E-05	-5.839E-05	NDM	
-2.00					1.308E-02	-1.789E-03	-2.642E-04	-6.191E-05	NDM	
0.00					1.382E-02	-1.904E-03	-6.572E-04	-8.066E-05	NDM	
2.00					1.446E-02	-2.032E-03	-1.111E-03	-1.171E-04	NDM	
4.00					1.498E-02	-2.175E-03	-1.647E-03	-1.733E-04	NDM	
6.00					1.535E-02	-2.346E-03	-2.322E-03	-2.507E-04	NDM	
8.00					1.529E-02	-2.581E-03	-3.322E-03	-3.502E-04	NDM	
10.00					1.337E-02	-3.650E-03	-8.902E-03	-4.668E-04	NDM	
12.00					1.057E-02	-2.259E-03	-7.952E-04	-5.708E-04	NDM	
14.00					8.127E-03	-2.532E-03	-2.027E-03	-6.643E-04	NDM	
16.00					4.099E-03	-2.690E-03	-2.591E-03	-7.367E-04	NDM	
18.00					-7.801E-03	-2.827E-03	-2.951E-03	-7.535E-04	NDM	
20.00					-4.799E-02	-2.803E-03	-2.713E-03	-5.823E-04	NDM	
22.00					-6.995E-02	-2.067E-03	-1.289E-03	-1.020E-04	NDM	
24.00					-5.721E-02	-1.448E-03	3.971E-04	-9.315E-05	NDM	
26.00					-4.394E-02	-9.461E-04	1.553E-03	-3.448E-04	NDM	
28.00					-2.496E-02	-6.307E-04	2.499E-03	-6.347E-04	NDM	

0*** NDM PRINTED WHEN NO DATCOM METHODS EXIST

1 AUTOMATED STABILITY AND CONTROL METHODS PER APRIL 1976 VERSION OF DATCOM
CHARACTERISTICS AT ANGLE OF ATTACK AND IN SIDESLIP
BODY-HORIZONTAL TAIL CONFIGURATION
NIDAL JODEH SIG RASCAL 110 NOMINAL CONFIGURATION

FLIGHT CONDITIONS						REFERENCE DIMENSIONS						
MACH NUMBER	ALTITUDE	VELOCITY	PRESSURE	TEMPERATURE	REYNOLDS NUMBER	REF. AREA	REFERENCE LENGTH	MOMENT	REF. CENTER			
	FT	FT/SEC	LB/FT**2	DEG R	1/FT	FT**2	FT	FT	FT	FT	FT	
0	0.061	1000.00	67.86	2.0409E+03	515.104	4.1949E+05	10.560	1.250	9.160	2.000	0.083	
-----DERIVATIVE (PER DEGREE)-----												
0	ALPHA	CD	CL	CM	CN	CA	XCP	CLA	CMA	CYB	CNB	CLB
0	-10.0	0.017	-0.132	0.2646	-0.132	-0.006	-1.998	1.703E-02	-3.973E-02	-9.799E-03	-4.532E-04	3.428E-05
	-8.0	0.013	-0.098	0.1862	-0.099	-0.001	-1.883	1.654E-02	-3.874E-02			2.477E-05
	-6.0	0.011	-0.065	0.1097	-0.066	0.004	-1.657	1.596E-02	-3.733E-02			1.554E-05
	-4.0	0.009	-0.034	0.0368	-0.035	0.007	-1.062	1.524E-02	-3.554E-02			6.680E-06
	-2.0	0.009	-0.004	-0.0325	-0.005	0.008	6.857	1.485E-02	-3.408E-02			-1.733E-06
	0.0	0.009	0.025	-0.0995	0.025	0.009	-3.937	1.526E-02	-3.500E-02			-1.015E-05
	2.0	0.010	0.057	-0.1725	0.057	0.008	-3.032	1.601E-02	-3.780E-02			-1.903E-05
	4.0	0.012	0.089	-0.2507	0.090	0.005	-2.789	1.663E-02	-4.058E-02			-2.829E-05
	6.0	0.014	0.123	-0.3348	0.124	0.001	-2.702	1.709E-02	-4.257E-02			-3.787E-05
	8.0	0.018	0.158	-0.4209	0.159	-0.004	-2.653	1.723E-02	-4.324E-02			-4.766E-05
	10.0	0.023	0.192	-0.5078	0.193	-0.010	-2.629	1.583E-02	-4.047E-02			-5.740E-05
	12.0	0.028	0.221	-0.5828	0.222	-0.018	-2.625	1.368E-02	-3.486E-02			-6.560E-05
	14.0	0.034	0.247	-0.6472	0.248	-0.027	-2.614	1.178E-02	-2.770E-02			-7.290E-05
	16.0	0.040	0.268	-0.6936	0.269	-0.036	-2.582	8.237E-03	-1.516E-02			-7.896E-05
	18.0	0.045	0.280	-0.7079	0.280	-0.044	-2.530	-5.878E-03	3.031E-02			-8.224E-05
	20.0	0.043	0.245	-0.5724	0.245	-0.043	-2.339	-2.351E-02	8.835E-02			-7.229E-05
	22.0	0.043	0.186	-0.3545	0.188	-0.030	-1.883	-2.509E-02	9.711E-02			-5.559E-05
	24.0	0.049	0.144	-0.1839	0.152	-0.014	-1.212	-1.552E-02	7.053E-02			-4.386E-05
	26.0	0.059	0.124	-0.0723	0.137	-0.001	-0.528	-9.849E-03	5.657E-02			-3.800E-05
	28.0	0.073	0.105	0.0424	0.127	0.015	0.334	-8.877E-03	5.814E-02			-3.270E-05

1 AUTOMATED STABILITY AND CONTROL METHODS PER APRIL 1976 VERSION OF DATCOM
DYNAMIC DERIVATIVES
BODY-HORIZONTAL TAIL CONFIGURATION
NIDAL JODEH SIG RASCAL 110 NOMINAL CONFIGURATION

FLIGHT CONDITIONS						REFERENCE DIMENSIONS					
MACH NUMBER	ALTITUDE	VELOCITY	PRESSURE	TEMPERATURE	REYNOLDS NUMBER	REF. AREA	REFERENCE LENGTH	MOMENT	REF. CENTER		
	FT	FT/SEC	LB/FT**2	DEG R	1/FT	FT**2	FT	FT	FT	FT	FT
0	0.061	1000.00	67.86	2.0409E+03	515.104	4.1949E+05	10.560	1.250	9.160	2.000	0.083
DYNAMIC DERIVATIVES (PER DEGREE)											
0	ALPHA	PITCHING		ACCELERATION		ROLLING		YAWING			
0		CLQ	CMQ	CLAD	CMAD	CLP	CYP	CNP	CNR	CLR	
0	-10.00	8.994E-02	-1.401E-01	NDM	NDM	1.957E-03	NDM	NDM	NDM	NDM	NDM
	-8.00					1.886E-03					NDM
	-6.00					1.806E-03					NDM
	-4.00					1.711E-03					NDM
	-2.00					1.659E-03					NDM
	0.00					1.711E-03					NDM
	2.00					1.806E-03					NDM
	4.00					1.886E-03					NDM
	6.00					1.948E-03					NDM

8.00	1.956E-03	NDM
10.00	1.710E-03	NDM
12.00	1.324E-03	NDM
14.00	9.731E-04	NDM
16.00	4.176E-04	NDM
18.00	-1.476E-03	NDM
20.00	-3.787E-03	NDM
22.00	-4.029E-03	NDM
24.00	-2.866E-03	NDM
26.00	-2.214E-03	NDM
28.00	-2.156E-03	NDM

0*** NDM PRINTED WHEN NO DATCOM METHODS EXIST

1 AUTOMATED STABILITY AND CONTROL METHODS PER APRIL 1976 VERSION OF DATCOM
CHARACTERISTICS AT ANGLE OF ATTACK AND IN SIDESLIP
BODY-VERTICAL TAIL CONFIGURATION
NIDAL JODEH SIG RASCAL 110 NOMINAL CONFIGURATION

FLIGHT CONDITIONS					REFERENCE DIMENSIONS							
MACH NUMBER	ALTITUDE	VELOCITY	PRESSURE	TEMPERATURE	REYNOLDS NUMBER	REF. AREA	REFERENCE LENGTH	MOMENT	REF. CENTER			
	FT	FT/SEC	LB/FT**2	DEG R	1/FT	FT**2	LONG. FT	LAT. FT	HORIZ FT	VERT FT		
0	0.061	1000.00	67.86	2.0409E+03	515.104	4.1949E+05	10.560	1.250	9.160	2.000	0.083	
-----DERIVATIVE (PER DEGREE)-----												
0	ALPHA	CD	CL	CM	CN	CA	XCP	CLA	CMA	CYB	CNB	CLB
0	-10.0	0.009	-0.016	-0.0483	-0.018	0.006	2.709	1.736E-03	1.992E-03	-3.419E-03	4.024E-04	-2.035E-04
	-8.0	0.008	-0.014	-0.0445	-0.015	0.006	3.069	1.513E-03	1.906E-03			-1.807E-04
	-6.0	0.007	-0.010	-0.0407	-0.011	0.006	3.658	1.567E-03	1.941E-03			-1.577E-04
	-4.0	0.007	-0.007	-0.0368	-0.008	0.006	4.788	1.607E-03	1.967E-03			-1.345E-04
	-2.0	0.006	-0.004	-0.0328	-0.004	0.006	7.811	1.633E-03	1.984E-03			-1.112E-04
	0.0	0.006	-0.001	-0.0288	-0.001	0.006	41.093	1.643E-03	1.990E-03			-8.771E-05
	2.0	0.006	0.003	-0.0249	0.003	0.006	-8.874	1.639E-03	1.988E-03			-6.412E-05
	4.0	0.007	0.006	-0.0209	0.006	0.006	-3.321	1.619E-03	1.975E-03			-4.046E-05
	6.0	0.007	0.009	-0.0170	0.010	0.006	-1.740	1.585E-03	1.953E-03			-1.674E-05
	8.0	0.008	0.012	-0.0131	0.013	0.006	-0.994	1.646E-03	1.884E-03			6.990E-06
	10.0	0.009	0.016	-0.0094	0.017	0.006	-0.556	2.189E-03	1.633E-03			3.071E-05
	12.0	0.011	0.021	-0.0066	0.023	0.006	-0.289	3.126E-03	1.228E-03			5.440E-05
	14.0	0.013	0.028	-0.0045	0.031	0.006	-0.148	4.050E-03	8.049E-04			7.802E-05
	16.0	0.017	0.037	-0.0033	0.040	0.006	-0.083	4.912E-03	3.776E-04			1.016E-04
	18.0	0.022	0.048	-0.0030	0.052	0.006	-0.058	5.701E-03	-5.149E-05			1.250E-04
	20.0	0.028	0.060	-0.0035	0.066	0.006	-0.054	6.409E-03	-4.803E-04			1.482E-04
	22.0	0.036	0.073	-0.0049	0.082	0.006	-0.060	7.025E-03	-9.068E-04			1.713E-04
	24.0	0.046	0.088	-0.0072	0.099	0.006	-0.072	7.542E-03	-1.329E-03			1.941E-04
	26.0	0.057	0.104	-0.0102	0.118	0.006	-0.087	7.952E-03	-1.745E-03			2.168E-04
	28.0	0.070	0.120	-0.0141	0.139	0.006	-0.102	8.308E-03	-2.156E-03			2.391E-04

1
 AUTOMATED STABILITY AND CONTROL METHODS PER APRIL 1976 VERSION OF DATCOM
 DYNAMIC DERIVATIVES
 BODY-VERTICAL TAIL CONFIGURATION
 NIDAL JODEH SIG RASCAL 110 NOMINAL CONFIGURATION

MACH NUMBER	FLIGHT CONDITIONS					REFERENCE DIMENSIONS				
	ALTITUDE	VELOCITY	PRESSURE	TEMPERATURE	REYNOLDS NUMBER	REF. AREA	REFERENCE LONG.	LENGTH LAT.	MOMENT HORIZ	REF. CENTER VERT
	FT	FT/SEC	LB/FT**2	DEG R	1/FT	FT**2	FT	FT	FT	FT
0 0.061	1000.00	67.86	2.0409E+03	515.104	4.1949E+05	10.560	1.250	9.160	2.000	0.083
DYNAMIC DERIVATIVES (PER DEGREE)										
0 0	PITCHING			ACCELERATION		ROLLING			YAWING	
	ALPHA	CLQ	CMQ	CLAD	CMAD	CLP	CYP	CNP	CNR	CLR
-10.00	7.098E-04	2.651E-03	1.128E-04	1.081E-04	NDM	NDM	NDM	NDM	NDM	NDM
-8.00										NDM
-6.00										NDM
-4.00										NDM
-2.00										NDM
0.00										NDM
2.00										NDM
4.00										NDM
6.00										NDM
8.00										NDM
10.00										NDM
12.00										NDM
14.00										NDM
16.00										NDM
18.00										NDM
20.00										NDM
22.00										NDM
24.00										NDM
26.00										NDM
28.00										NDM

0*** NDM PRINTED WHEN NO DATCOM METHODS EXIST

1
 AUTOMATED STABILITY AND CONTROL METHODS PER APRIL 1976 VERSION OF DATCOM
 CHARACTERISTICS AT ANGLE OF ATTACK AND IN SIDESLIP
 WING-BODY-HORIZONTAL TAIL CONFIGURATION
 NIDAL JODEH SIG RASCAL 110 NOMINAL CONFIGURATION

MACH NUMBER	FLIGHT CONDITIONS					REFERENCE DIMENSIONS					
	ALTITUDE	VELOCITY	PRESSURE	TEMPERATURE	REYNOLDS NUMBER	REF. AREA	REFERENCE LONG.	LENGTH LAT.	MOMENT HORIZ	REF. CENTER VERT	
	FT	FT/SEC	LB/FT**2	DEG R	1/FT	FT**2	FT	FT	FT	FT	
0 0.061	1000.00	67.86	2.0409E+03	515.104	4.1949E+05	10.560	1.250	9.160	2.000	0.083	
DERIVATIVE (PER DEGREE)											
0 0											
	ALPHA	CD	CL	CM	CN	CA	XCP	CLA	CMA	CYB	CNB
-10.0	0.042	-0.660	-0.0330	-0.657	-0.073	0.050	1.040E-01	7.503E-03	-3.939E-03	-4.458E-04	-1.241E-03
-8.0	0.032	-0.456	-0.0296	-0.456	-0.032	0.065	9.949E-02	2.440E-03			-1.320E-03
-6.0	0.025	-0.262	-0.0232	-0.263	-0.002	0.088	9.594E-02	-1.655E-04			-1.395E-03
-4.0	0.022	-0.072	-0.0302	-0.074	0.017	0.411	9.390E-02	-4.647E-03			-1.467E-03
-2.0	0.022	0.114	-0.0418	0.113	0.025	-0.370	9.564E-02	-5.846E-03			-1.537E-03
0.0	0.025	0.310	-0.0536	0.310	0.025	-0.173	1.005E-01	-6.177E-03			-1.611E-03
2.0	0.032	0.516	-0.0665	0.517	0.014	-0.129	1.050E-01	-7.123E-03			-1.689E-03
4.0	0.043	0.730	-0.0821	0.731	-0.008	-0.112	1.087E-01	-8.697E-03			-1.770E-03

6.0	0.059	0.951	-0.1013	0.952	-0.041	-0.106	1.118E-01	-1.090E-02	-1.853E-03
8.0	0.080	1.177	-0.1257	1.177	-0.085	-0.107	1.120E-01	-1.363E-02	-1.939E-03
10.0	0.104	1.399	-0.1558	1.396	-0.141	-0.112	1.007E-01	-1.847E-02	-2.022E-03
12.0	0.128	1.580	-0.1996	1.572	-0.203	-0.127	8.412E-02	-2.458E-02	-2.088E-03
14.0	0.152	1.736	-0.2542	1.721	-0.272	-0.148	6.975E-02	-2.961E-02	-2.142E-03
16.0	0.175	1.859	-0.3180	1.835	-0.344	-0.173	4.500E-02	-3.427E-02	-2.182E-03
18.0	0.190	1.916	NA	1.880	-0.411	NA	-3.227E-02	NA	-2.194E-03
20.0	0.173	1.730	NA	1.685	-0.429	NA	-3.000E-01	NA	-2.104E-03
22.0	0.097	0.715	NA	0.699	-0.178	NA	-4.789E-01	NA	-1.704E-03
24.0	0.078	-0.186	NA	-0.138	0.147	NA	-4.261E-01	NA	-1.397E-03
26.0	0.120	-0.989	NA	-0.836	0.542	NA	-3.256E-01	NA	-1.132E-03
28.0	0.183	-1.488	NA	-1.228	0.860	NA	-1.737E-01	NA	-9.612E-04

0 ALPHA Q/QINF EPSLON D(EPSLON)/D(ALPHA)

0

-10.0	0.904	-3.149	0.512
-8.0	0.907	-2.124	0.500
-6.0	0.974	-1.148	0.475
-4.0	1.000	-0.223	0.455
-2.0	1.000	0.672	0.453
0.0	1.000	1.587	0.457
2.0	1.000	2.498	0.456
4.0	1.000	3.410	0.450
6.0	1.000	4.299	0.434
8.0	1.000	5.146	0.412
10.0	1.000	5.946	0.365
12.0	1.000	6.606	0.293
14.0	1.000	7.117	0.229
16.0	1.000	7.524	0.125
18.0	1.000	7.617	-0.165
20.0	1.000	6.863	-0.743
22.0	1.000	4.644	-1.106
24.0	1.000	2.440	-1.132
26.0	1.000	0.118	-0.879
28.0	1.000	-1.076	-0.597

0*** NA PRINTED WHEN METHOD NOT APPLICABLE

1

AUTOMATED STABILITY AND CONTROL METHODS PER APRIL 1976 VERSION OF DATCOM

DYNAMIC DERIVATIVES

WING-BODY-HORIZONTAL TAIL CONFIGURATION

NIDAL JODEH SIG RASCAL 110 NOMINAL CONFIGURATION

FLIGHT CONDITIONS						REFERENCE DIMENSIONS				
MACH NUMBER	ALTITUDE	VELOCITY	PRESSURE	TEMPERATURE	REYNOLDS NUMBER	REF. AREA	REFERENCE LONG.	LENGTH	MOMENT	REF. CENTER
	FT	FT/SEC	LB/FT**2	DEG R	1/FT	FT**2	FT	FT	FT	FT
0 0.061	1000.00	67.86	2.0409E+03	515.104	4.1949E+05	10.560	1.250	9.160	2.000	0.083
DYNAMIC DERIVATIVES (PER DEGREE)										
0	-----PITCHING-----			-----ACCELERATION-----		-----ROLLING-----			-----YAWING-----	
0	ALPHA	CLQ	CMQ	CLAD	CMAD	CLP	CYP	CNP	CNR	CLR
0	-10.00	9.316E-02	-2.135E-01	3.940E-02	-1.075E-01	1.636E-02	-1.356E-03	1.123E-03	-1.400E-04	NDM
	-8.00			3.860E-02	-1.053E-01	1.577E-02	-1.470E-03	7.786E-04	-9.562E-05	NDM
	-6.00			3.939E-02	-1.075E-01	1.511E-02	-1.579E-03	4.249E-04	-6.900E-05	NDM
	-4.00			3.872E-02	-1.057E-01	1.455E-02	-1.684E-03	8.314E-05	-5.839E-05	NDM
	-2.00			3.850E-02	-1.051E-01	1.474E-02	-1.789E-03	-2.642E-04	-6.191E-05	NDM
	0.00			3.883E-02	-1.060E-01	1.553E-02	-1.904E-03	-6.572E-04	-8.066E-05	NDM
	2.00			3.876E-02	-1.058E-01	1.627E-02	-2.032E-03	-1.111E-03	-1.171E-04	NDM

4.00	3.830E-02	-1.045E-01	1.686E-02	-2.175E-03	-1.647E-03	-1.733E-04	NDM
6.00	3.692E-02	-1.008E-01	1.730E-02	-2.346E-03	-2.322E-03	-2.507E-04	NDM
8.00	3.502E-02	-9.556E-02	1.725E-02	-2.581E-03	-3.322E-03	-3.502E-04	NDM
10.00	3.106E-02	-8.478E-02	1.508E-02	-3.650E-03	-8.902E-03	-4.668E-04	NDM
12.00	2.490E-02	-6.796E-02	1.189E-02	-2.259E-03	-7.952E-04	-5.708E-04	NDM
14.00	1.952E-02	-5.326E-02	9.100E-03	-2.532E-03	-2.027E-03	-6.643E-04	NDM
16.00	1.064E-02	-2.904E-02	4.517E-03	-2.690E-03	-2.591E-03	-7.367E-04	NDM
18.00	-1.407E-02	3.839E-02	-9.277E-03	-2.827E-03	-2.951E-03	-7.535E-04	NDM
20.00	-6.322E-02	1.725E-01	-5.177E-02	-2.803E-03	-2.713E-03	-5.823E-04	NDM
22.00	-9.406E-02	2.567E-01	-7.398E-02	-2.067E-03	-1.289E-03	-1.020E-04	NDM
24.00	-9.626E-02	2.627E-01	-6.007E-02	-1.448E-03	3.971E-04	-9.315E-05	NDM
26.00	-7.477E-02	2.040E-01	-4.616E-02	-9.461E-04	1.553E-03	-3.448E-04	NDM
28.00	-5.078E-02	1.386E-01	-2.711E-02	-6.307E-04	2.499E-03	-6.347E-04	NDM

0*** NDM PRINTED WHEN NO DATCOM METHODS EXIST

1 AUTOMATED STABILITY AND CONTROL METHODS PER APRIL 1976 VERSION OF DATCOM
CHARACTERISTICS AT ANGLE OF ATTACK AND IN SIDESLIP
WING-BODY-VERTICAL TAIL CONFIGURATION
NIDAL JODEH SIG RASCAL 110 NOMINAL CONFIGURATION

FLIGHT CONDITIONS						REFERENCE DIMENSIONS					
MACH NUMBER	ALTITUDE	VELOCITY	PRESSURE	TEMPERATURE	REYNOLDS NUMBER	REF. AREA	REFERENCE LENGTH	MOMENT	REF. CENTER		
	FT	FT/SEC	LB/FT**2	DEG R	1/FT	FT**2	FT	LAT. FT	HORIZ FT	VERT FT	
0.061	1000.00	67.86	2.0409E+03	515.104	4.1949E+05	10.560	1.250	9.160	2.000	0.083	
-----DERIVATIVE (PER DEGREE)-----											
ALPHA	CD	CL	CM	CN	CA	XCP	CLA	CMA	CYB	CNB	CLB
-10.0	0.036	-0.598	-0.2004	-0.596	-0.068	0.336	9.711E-02	2.014E-02	-5.622E-03	2.211E-04	-1.473E-03
-8.0	0.028	-0.408	-0.1620	-0.408	-0.029	0.397	9.369E-02	1.834E-02			-1.521E-03
-6.0	0.022	-0.224	-0.1271	-0.225	-0.001	0.565	8.984E-02	1.651E-02			-1.566E-03
-4.0	0.020	-0.048	-0.0959	-0.050	0.016	1.934	8.677E-02	1.487E-02			-1.608E-03
-2.0	0.020	0.123	-0.0676	0.123	0.024	-0.552	8.841E-02	1.397E-02			-1.648E-03
0.0	0.023	0.305	-0.0400	0.305	0.023	-0.131	9.334E-02	1.354E-02			-1.692E-03
2.0	0.029	0.497	-0.0134	0.497	0.012	-0.027	9.765E-02	1.299E-02			-1.739E-03
4.0	0.039	0.696	0.0119	0.697	-0.010	0.017	1.011E-01	1.232E-02			-1.789E-03
6.0	0.053	0.901	0.0358	0.902	-0.042	0.040	1.037E-01	1.154E-02			-1.842E-03
8.0	0.070	1.111	0.0581	1.110	-0.085	0.052	1.034E-01	1.036E-02			-1.895E-03
10.0	0.091	1.315	0.0773	1.311	-0.139	0.059	9.138E-02	7.597E-03			-1.947E-03
12.0	0.111	1.476	0.0885	1.467	-0.199	0.060	7.387E-02	4.155E-03			-1.983E-03
14.0	0.129	1.610	0.0939	1.594	-0.264	0.059	5.876E-02	1.259E-03			-2.009E-03
16.0	0.145	1.711	0.0935	1.685	-0.332	0.055	3.303E-02	-1.686E-03			-2.023E-03
18.0	0.153	1.742	NA	1.704	-0.393	NA	-4.497E-02	NA			-2.011E-03
20.0	0.130	1.531	NA	1.483	-0.402	NA	-3.106E-01	NA			-1.910E-03
22.0	0.057	0.500	NA	0.485	-0.135	NA	-4.560E-01	NA			-1.505E-03
24.0	0.065	-0.293	NA	-0.241	0.178	NA	-3.711E-01	NA			-1.189E-03
26.0	0.119	-0.985	NA	-0.833	0.538	NA	-2.826E-01	NA			-9.103E-04
28.0	0.181	-1.423	NA	-1.172	0.828	NA	-1.561E-01	NA			-7.256E-04

0*** NA PRINTED WHEN METHOD NOT APPLICABLE

1
 AUTOMATED STABILITY AND CONTROL METHODS PER APRIL 1976 VERSION OF DATCOM
 DYNAMIC DERIVATIVES
 WING-BODY-VERTICAL TAIL CONFIGURATION
 NIDAL JODEH SIG RASCAL 110 NOMINAL CONFIGURATION

FLIGHT CONDITIONS						REFERENCE DIMENSIONS				
MACH NUMBER	ALTITUDE	VELOCITY	PRESSURE	TEMPERATURE	REYNOLDS NUMBER	REF. AREA	REFERENCE LONG.	LENGTH	MOMENT	REF. CENTER
	FT	FT/SEC	LB/FT**2	DEG R	1/FT	FT**2	FT	FT	FT	FT
0 0.061	1000.00	67.86	2.0409E+03	515.104	4.1949E+05	10.560	1.250	9.160	2.000	0.083
DYNAMIC DERIVATIVES (PER DEGREE)										
PITCHING			ACCELERATION		ROLLING			YAWING		
ALPHA	CLQ	CMQ	CLAD	CMAD	CLP	CYP	CNP	CNR	CLR	
-10.00	1.626E-02	-3.608E-03	NDM	NDM	1.440E-02	-1.588E-03	1.212E-03	-6.404E-04	NDM	
-8.00					1.389E-02	-1.656E-03	8.511E-04	-6.064E-04	NDM	
-6.00					1.330E-02	-1.719E-03	4.799E-04	-5.891E-04	NDM	
-4.00					1.283E-02	-1.778E-03	1.202E-04	-5.865E-04	NDM	
-2.00					1.308E-02	-1.836E-03	-2.455E-04	-5.968E-04	NDM	
0.00					1.382E-02	-1.904E-03	-6.572E-04	-6.211E-04	NDM	
2.00					1.446E-02	-1.984E-03	-1.130E-03	-6.619E-04	NDM	
4.00					1.498E-02	-2.081E-03	-1.686E-03	-7.210E-04	NDM	
6.00					1.535E-02	-2.204E-03	-2.380E-03	-8.000E-04	NDM	
8.00					1.529E-02	-2.391E-03	-3.399E-03	-8.997E-04	NDM	
10.00					1.337E-02	-3.413E-03	-8.998E-03	-1.015E-03	NDM	
12.00					1.057E-02	-1.975E-03	-9.097E-04	-1.117E-03	NDM	
14.00					8.127E-03	-2.201E-03	-2.160E-03	-1.207E-03	NDM	
16.00					4.099E-03	-2.311E-03	-2.742E-03	-1.274E-03	NDM	
18.00					-7.801E-03	-2.402E-03	-3.120E-03	-1.285E-03	NDM	
20.00					-4.799E-02	-2.331E-03	-2.899E-03	-1.106E-03	NDM	
22.00					-6.995E-02	-1.549E-03	-1.491E-03	-6.168E-04	NDM	
24.00					-5.721E-02	-8.841E-04	1.787E-04	-5.980E-04	NDM	
26.00					-4.394E-02	-3.372E-04	1.320E-03	-8.386E-04	NDM	
28.00					-2.496E-02	2.291E-05	2.252E-03	-1.116E-03	NDM	

0*** NDM PRINTED WHEN NO DATCOM METHODS EXIST

1
 AUTOMATED STABILITY AND CONTROL METHODS PER APRIL 1976 VERSION OF DATCOM
 CHARACTERISTICS AT ANGLE OF ATTACK AND IN SIDESLIP
 WING-BODY-VERTICAL TAIL-HORIZONTAL TAIL CONFIGURATION
 NIDAL JODEH SIG RASCAL 110 NOMINAL CONFIGURATION

FLIGHT CONDITIONS						REFERENCE DIMENSIONS					
MACH NUMBER	ALTITUDE	VELOCITY	PRESSURE	TEMPERATURE	REYNOLDS NUMBER	REF. AREA	REFERENCE LONG.	LENGTH	MOMENT	REF. CENTER	
	FT	FT/SEC	LB/FT**2	DEG R	1/FT	FT**2	FT	FT	FT	FT	
0 0.061	1000.00	67.86	2.0409E+03	515.104	4.1949E+05	10.560	1.250	9.160	2.000	0.083	
DERIVATIVE (PER DEGREE)											
ALPHA	CD	CL	CM	CN	CA	XCP	CLA	CMA	CYB	CNB	CLB
-10.0	0.043	-0.660	-0.0330	-0.657	-0.072	0.050	1.040E-01	7.503E-03	-5.622E-03	2.285E-04	-1.445E-03
-8.0	0.033	-0.456	-0.0296	-0.456	-0.031	0.065	9.949E-02	2.440E-03			-1.500E-03
-6.0	0.026	-0.262	-0.0232	-0.263	-0.001	0.088	9.594E-02	-1.655E-04			-1.553E-03
-4.0	0.023	-0.072	-0.0302	-0.074	0.018	0.410	9.390E-02	-4.647E-03			-1.602E-03
-2.0	0.022	0.114	-0.0418	0.113	0.026	-0.370	9.564E-02	-5.846E-03			-1.648E-03
0.0	0.026	0.310	-0.0536	0.310	0.026	-0.173	1.005E-01	-6.177E-03			-1.699E-03
2.0	0.033	0.516	-0.0665	0.517	0.015	-0.129	1.050E-01	-7.123E-03			-1.753E-03
4.0	0.044	0.730	-0.0821	0.731	-0.007	-0.112	1.087E-01	-8.697E-03			-1.810E-03

6.0	0.060	0.951	-0.1013	0.952	-0.040	-0.106	1.118E-01	-1.090E-02	-1.870E-03
8.0	0.080	1.177	-0.1257	1.177	-0.084	-0.107	1.120E-01	-1.363E-02	-1.932E-03
10.0	0.105	1.399	-0.1558	1.396	-0.140	-0.112	1.007E-01	-1.847E-02	-1.991E-03
12.0	0.129	1.580	-0.1996	1.572	-0.202	-0.127	8.412E-02	-2.458E-02	-2.033E-03
14.0	0.153	1.736	-0.2542	1.721	-0.271	-0.148	6.975E-02	-2.961E-02	-2.064E-03
16.0	0.176	1.859	-0.3180	1.835	-0.343	-0.173	4.500E-02	-3.427E-02	-2.081E-03
18.0	0.191	1.916	NA	1.881	-0.410	NA	-3.227E-02	NA	-2.069E-03
20.0	0.174	1.730	NA	1.685	-0.428	NA	-3.000E-01	NA	-1.956E-03
22.0	0.098	0.715	NA	0.700	-0.177	NA	-4.789E-01	NA	-1.533E-03
24.0	0.079	-0.186	NA	-0.138	0.148	NA	-4.261E-01	NA	-1.203E-03
26.0	0.121	-0.989	NA	-0.836	0.543	NA	-3.256E-01	NA	-9.155E-04
28.0	0.184	-1.488	NA	-1.228	0.861	NA	-1.737E-01	NA	-7.221E-04

0
0

	ALPHA	Q/QINF	EPSLON	D(EPSLON)/D(ALPHA)
-10.0	0.904	-3.149	0.512	
-8.0	0.907	-2.124	0.500	
-6.0	0.974	-1.148	0.475	
-4.0	1.000	-0.223	0.455	
-2.0	1.000	0.672	0.453	
0.0	1.000	1.587	0.457	
2.0	1.000	2.498	0.456	
4.0	1.000	3.410	0.450	
6.0	1.000	4.299	0.434	
8.0	1.000	5.146	0.412	
10.0	1.000	5.946	0.365	
12.0	1.000	6.606	0.293	
14.0	1.000	7.117	0.229	
16.0	1.000	7.524	0.125	
18.0	1.000	7.617	-0.165	
20.0	1.000	6.863	-0.743	
22.0	1.000	4.644	-1.106	
24.0	1.000	2.440	-1.132	
26.0	1.000	0.118	-0.879	
28.0	1.000	-1.076	-0.597	

0*** NA PRINTED WHEN METHOD NOT APPLICABLE

1
AUTOMATED STABILITY AND CONTROL METHODS PER APRIL 1976 VERSION OF DATCOM
CHARACTERISTICS AT ANGLE OF ATTACK AND IN SIDESLIP
WING-BODY-VERTICAL TAIL-HORIZONTAL TAIL CONFIGURATION
PROPELLER POWER EFFECTS INCLUDED IN THE LONGITUDINAL STABILITY RESULTS
NIDAL JODEH SIG RASCAL 110 NOMINAL CONFIGURATION

FLIGHT CONDITIONS						REFERENCE DIMENSIONS						
MACH NUMBER	ALTITUDE	VELOCITY	PRESSURE	TEMPERATURE	REYNOLDS NUMBER	REF. AREA	REFERENCE LENGTH	MOMENT	REF. CENTER			
	FT	FT/SEC	LB/FT**2	DEG R	1/FT	FT**2	FT	FT	FT	FT	FT	
0	0.061	1000.00	67.86	2.0409E+03	515.104	4.1949E+05	10.560	1.250	9.160	2.000	0.083	
0	-----DERIVATIVE (PER DEGREE)-----											
0	ALPHA	CD	CL	CM	CN	CA	XCP	CLA	CMA	CYB	CNB	CLB
0	-10.0	0.056	-0.727	-0.0423	-0.726	-0.071	0.058	1.040E-01	7.503E-03	-5.622E-03	2.285E-04	-1.445E-03
	-8.0	0.041	-0.509	-0.0300	-0.509	-0.031	0.059	9.949E-02	2.440E-03			-1.500E-03
	-6.0	0.031	-0.298	-0.0165	-0.300	0.000	0.055	9.594E-02	-1.655E-04			-1.553E-03
	-4.0	0.026	-0.092	-0.0186	-0.094	0.019	0.198	9.390E-02	-4.647E-03			-1.602E-03
	-2.0	0.025	0.112	-0.0270	0.111	0.029	-0.243	9.564E-02	-5.846E-03			-1.648E-03
	0.0	0.028	0.327	-0.0358	0.327	0.028	-0.110	1.005E-01	-6.177E-03			-1.699E-03
	2.0	0.037	0.553	-0.0464	0.554	0.018	-0.084	1.050E-01	-7.123E-03			-1.753E-03

4.0	0.051	0.788	-0.0599	0.789	-0.004	-0.076	1.087E-01	-8.697E-03	-1.810E-03
6.0	0.072	1.029	-0.0757	1.031	-0.036	-0.073	1.118E-01	-1.090E-02	-1.870E-03
8.0	0.099	1.276	-0.0958	1.277	-0.080	-0.075	1.120E-01	-1.363E-02	-1.932E-03
10.0	0.130	1.518	-0.1206	1.518	-0.135	-0.079	1.007E-01	-1.847E-02	-1.991E-03
12.0	0.162	1.715	-0.1572	1.711	-0.198	-0.092	8.412E-02	-2.458E-02	-2.033E-03
14.0	0.194	1.883	-0.2021	1.874	-0.267	-0.108	6.975E-02	-2.961E-02	-2.064E-03
16.0	0.224	2.014	-0.2517	1.998	-0.339	-0.126	4.500E-02	-3.427E-02	-2.081E-03
18.0	0.246	2.073	0.0811	2.047	-0.407	0.040	-3.227E-02	NA	-2.069E-03
20.0	0.228	1.873	0.0932	1.838	-0.427	0.051	-3.000E-01	NA	-1.956E-03
22.0	0.135	0.800	0.0760	0.792	-0.175	0.096	-4.789E-01	NA	-1.533E-03
24.0	0.113	-0.143	0.0637	-0.085	0.161	-0.750	-4.261E-01	NA	-1.203E-03
26.0	0.159	-0.984	0.0671	-0.815	0.574	-0.082	-3.256E-01	NA	-9.155E-04
28.0	0.228	-1.496	0.0576	-1.214	0.903	-0.047	-1.737E-01	NA	-7.221E-04

0
0
ALPHA Q/QINF EPSLON D(EPSLON)/D(ALPHA)

-10.0	0.904	-3.149	0.512
-8.0	0.907	-2.124	0.500
-6.0	0.974	-1.148	0.475
-4.0	1.000	-0.223	0.455
-2.0	1.000	0.672	0.453
0.0	1.000	1.587	0.457
2.0	1.000	2.498	0.456
4.0	1.000	3.410	0.450
6.0	1.000	4.299	0.434
8.0	1.000	5.146	0.412
10.0	1.000	5.946	0.365
12.0	1.000	6.606	0.293
14.0	1.000	7.117	0.229
16.0	1.000	7.524	0.125
18.0	1.000	7.617	-0.165
20.0	1.000	6.863	-0.743
22.0	1.000	4.644	-1.106
24.0	1.000	2.440	-1.132
26.0	1.000	0.118	-0.879
28.0	1.000	-1.076	-0.597

0*** NA PRINTED WHEN METHOD NOT APPLICABLE

1 AUTOMATED STABILITY AND CONTROL METHODS PER APRIL 1976 VERSION OF DATCOM
DYNAMIC DERIVATIVES
WING-BODY-VERTICAL TAIL-HORIZONTAL TAIL CONFIGURATION
NIDAL JODEH SIG RASCAL 110 NOMINAL CONFIGURATION

MACH NUMBER	FLIGHT CONDITIONS				TEMPERATURE DEG R	REYNOLDS NUMBER 1/FT	REFERENCE DIMENSIONS				
	ALTITUDE FT	VELOCITY FT/SEC	PRESSURE LB/FT**2				REF. AREA FT**2	REFERENCE LENGTH FT	LENGTH LAT. FT	MOMENT HORIZ. FT	REF. CENTER VERT. FT
0 0.061	1000.00	67.86	2.0409E+03		515.104	4.1949E+05	10.560	1.250	9.160	2.000	0.083
DYNAMIC DERIVATIVES (PER DEGREE)											
0	PITCHING			ACCELERATION			ROLLING			YAWING	
0	ALPHA	CLQ	CMQ	CLAD	CMAD	CLP	CYP	CNP	CNR	CLR	
0	-10.00	9.316E-02	-2.135E-01	3.940E-02	-1.075E-01	1.636E-02	-1.588E-03	1.212E-03	-6.404E-04	NDM	
	-8.00			3.860E-02	-1.053E-01	1.577E-02	-1.656E-03	8.511E-04	-6.064E-04	NDM	
	-6.00			3.939E-02	-1.075E-01	1.511E-02	-1.719E-03	4.799E-04	-5.891E-04	NDM	
	-4.00			3.872E-02	-1.057E-01	1.455E-02	-1.778E-03	1.202E-04	-5.865E-04	NDM	
	-2.00			3.850E-02	-1.051E-01	1.474E-02	-1.836E-03	-2.455E-04	-5.968E-04	NDM	
	0.00			3.883E-02	-1.060E-01	1.553E-02	-1.904E-03	-6.572E-04	-6.211E-04	NDM	

2.00	3.876E-02	-1.058E-01	1.627E-02	-1.984E-03	-1.130E-03	-6.619E-04	NDM
4.00	3.830E-02	-1.045E-01	1.686E-02	-2.081E-03	-1.686E-03	-7.210E-04	NDM
6.00	3.692E-02	-1.008E-01	1.730E-02	-2.204E-03	-2.380E-03	-8.000E-04	NDM
8.00	3.502E-02	-9.556E-02	1.725E-02	-2.391E-03	-3.399E-03	-8.997E-04	NDM
10.00	3.106E-02	-8.478E-02	1.508E-02	-3.413E-03	-8.998E-03	-1.015E-03	NDM
12.00	2.490E-02	-6.796E-02	1.189E-02	-1.975E-03	-9.097E-04	-1.117E-03	NDM
14.00	1.952E-02	-5.326E-02	9.100E-03	-2.201E-03	-2.160E-03	-1.207E-03	NDM
16.00	1.064E-02	-2.904E-02	4.517E-03	-2.311E-03	-2.742E-03	-1.274E-03	NDM
18.00	-1.407E-02	3.839E-02	-9.277E-03	-2.402E-03	-3.120E-03	-1.285E-03	NDM
20.00	-6.322E-02	1.725E-01	-5.177E-02	-2.331E-03	-2.899E-03	-1.106E-03	NDM
22.00	-9.406E-02	2.567E-01	-7.398E-02	-1.549E-03	-1.491E-03	-6.168E-04	NDM
24.00	-9.626E-02	2.627E-01	-6.007E-02	-8.841E-04	1.787E-04	-5.980E-04	NDM
26.00	-7.477E-02	2.040E-01	-4.616E-02	-3.372E-04	1.320E-03	-8.386E-04	NDM
28.00	-5.078E-02	1.386E-01	-2.711E-02	2.291E-05	2.252E-03	-1.116E-03	NDM

0*** NDM PRINTED WHEN NO DATCOM METHODS EXIST

0*** VEHICLE WEIGHT = 17.00 LB.

0*** LEVEL FLIGHT LIFT COEFFICIENT = 0.30284

1 AUTOMATED STABILITY AND CONTROL METHODS PER APRIL 1976 VERSION OF DATCOM

CHARACTERISTICS OF HIGH LIFT AND CONTROL DEVICES

TAIL PLAIN TRAILING-EDGE FLAP CONFIGURATION

NIDAL JODEH SIG RASCAL 110 NOMINAL CONFIGURATION

FLIGHT CONDITIONS						REFERENCE DIMENSIONS				
MACH NUMBER	ALTITUDE FT	VELOCITY FT/SEC	PRESSURE LB/FT**2	TEMPERATURE DEG R	REYNOLDS NUMBER 1/FT	REF. AREA FT**2	REFERENCE LENGTH LONG. FT	MOMENT REF. LAT. FT	REF. CENTER HORIZ FT	REF. CENTER VERT FT
0 0.061	1000.00	67.86	2.0409E+03	515.104	4.1949E+05	10.560	1.250	9.160	2.000	0.083
0	-----INCREMENTS DUE TO DEFLECTION-----					---DERIVATIVES (PER DEGREE)---				
0	DELTA	D(CL)	D(CM)	D(CL MAX)	D(CD MIN)	(CLA)D	(CH)A	(CH)D		
	-20.0	-0.097	0.2218	0.085	0.00770	NDM	1.238E-02	3.053E-03		
	-10.0	-0.062	0.1402	0.049	0.00245	NDM		2.751E-03		
	0.0	0.000	-0.0001	0.000	0.00000	NDM		2.751E-03		
	10.0	0.062	-0.1402	0.049	0.00245	NDM		2.751E-03		
	20.0	0.097	-0.2218	0.085	0.00770	NDM		3.053E-03		

0 *** NOTE * HINGE MOMENT DERIVATIVES ARE BASED ON TWICE THE AREA-MOMENT OF THE CONTROL ABOUT ITS HINGE LINE

0 ----- INDUCED DRAG COEFFICIENT INCREMENT , D(CDI) , DUE TO DEFLECTION -----

0 DELTA = -20.0 -10.0 0.0 10.0 20.0

ALPHA

0										
-10.0	3.19E-03	1.53E-03	-6.20E-07	2.86E-04	1.25E-03					
-8.0	2.49E-03	1.08E-03	-1.70E-07	7.36E-04	1.95E-03					
-6.0	1.75E-03	6.05E-04	3.02E-07	1.21E-03	2.69E-03					
-4.0	9.74E-04	1.10E-04	7.98E-07	1.70E-03	3.47E-03					
-2.0	1.77E-04	-4.00E-04	1.31E-06	2.21E-03	4.27E-03					
0.0	-6.06E-04	-9.00E-04	1.81E-06	2.71E-03	5.05E-03					
2.0	-1.39E-03	-1.40E-03	2.31E-06	3.22E-03	5.84E-03					
4.0	-2.18E-03	-1.90E-03	2.81E-06	3.72E-03	6.62E-03					
6.0	-2.98E-03	-2.42E-03	3.32E-06	4.23E-03	7.42E-03					
8.0	-3.81E-03	-2.95E-03	3.86E-06	4.76E-03	8.26E-03					
10.0	-4.68E-03	-3.50E-03	4.41E-06	5.31E-03	9.12E-03					
12.0	-5.65E-03	-4.12E-03	5.03E-06	5.93E-03	1.01E-02					
14.0	-6.72E-03	-4.81E-03	5.71E-06	6.62E-03	1.12E-02					
16.0	-7.87E-03	-5.54E-03	6.45E-06	7.35E-03	1.23E-02					
18.0	-9.25E-03	-6.42E-03	7.33E-06	8.23E-03	1.37E-02					

```

20.0      -1.12E-02 -7.69E-03  8.60E-06  9.50E-03  1.57E-02
22.0      -1.43E-02 -9.63E-03  1.06E-05  1.14E-02  1.87E-02
24.0      -1.73E-02 -1.16E-02  1.25E-05  1.34E-02  2.18E-02
26.0      -2.04E-02 -1.36E-02  1.45E-05  1.54E-02  2.49E-02
28.0      -2.27E-02 -1.50E-02  1.60E-05  1.69E-02  2.72E-02
0***NDM PRINTED WHEN NO DATCOM METHODS EXIST
1          THE FOLLOWING IS A LIST OF ALL INPUT CARDS FOR THIS CASE.
0
TRIM
SAVE
NEXT CASE
OERROR ** FLAP INBOARD SPAN, SPANI = 0.20800E-01, IT IS INSIDE THE BODY AS DEFINED BY SSPN AND SSPNE
          SPANI IS REDEFINED, SPANI = SSPN-SSPNE = 0.20800E-01

0 INPUT DIMENSIONS ARE IN FT, SCALE FACTOR IS 1.0000

1          AUTOMATED STABILITY AND CONTROL METHODS PER APRIL 1976 VERSION OF DATCOM
          WING SECTION DEFINITION
0          IDEAL ANGLE OF ATTACK = 1.12591 DEG.

          ZERO LIFT ANGLE OF ATTACK = -3.50518 DEG.

          IDEAL LIFT COEFFICIENT = 0.54407

          ZERO LIFT PITCHING MOMENT COEFFICIENT = -0.08623

          MACH ZERO LIFT-CURVE-SLOPE = 0.09893 /DEG.

          LEADING EDGE RADIUS = 0.01102 FRACTION CHORD

          MAXIMUM AIRFOIL THICKNESS = 0.10000 FRACTION CHORD

          DELTA-Y = 2.64081 PERCENT CHORD

0          MACH= 0.0610 LIFT-CURVE-SLOPE = 0.09903 /DEG.          XAC = 0.25348
1          AUTOMATED STABILITY AND CONTROL METHODS PER APRIL 1976 VERSION OF DATCOM
          HORIZONTAL TAIL SECTION DEFINITION
0          IDEAL ANGLE OF ATTACK = 0.00000 DEG.

          ZERO LIFT ANGLE OF ATTACK = 0.00000 DEG.

          IDEAL LIFT COEFFICIENT = 0.00000

          ZERO LIFT PITCHING MOMENT COEFFICIENT = 0.00000

          MACH ZERO LIFT-CURVE-SLOPE = 0.09830 /DEG.

          LEADING EDGE RADIUS = 0.00893 FRACTION CHORD

          MAXIMUM AIRFOIL THICKNESS = 0.09000 FRACTION CHORD

          DELTA-Y = 2.37673 PERCENT CHORD

0          MACH= 0.0610 LIFT-CURVE-SLOPE = 0.09846 /DEG.          XAC = 0.25642

```

1 AUTOMATED STABILITY AND CONTROL METHODS PER APRIL 1976 VERSION OF DATCOM
 0 VERTICAL TAIL SECTION DEFINITION

IDEAL ANGLE OF ATTACK = 0.00000 DEG.
 ZERO LIFT ANGLE OF ATTACK = 0.00000 DEG.
 IDEAL LIFT COEFFICIENT = 0.00000
 ZERO LIFT PITCHING MOMENT COEFFICIENT = 0.00000
 MACH ZERO LIFT-CURVE-SLOPE = 0.09830 /DEG.
 LEADING EDGE RADIUS = 0.00893 FRACTION CHORD
 MAXIMUM AIRFOIL THICKNESS = 0.09000 FRACTION CHORD
 DELTA-Y = 2.37673 PERCENT CHORD

0 MACH= 0.0610 LIFT-CURVE-SLOPE = 0.09846 /DEG. XAC = 0.25642
 1 AUTOMATED STABILITY AND CONTROL METHODS PER APRIL 1976 VERSION OF DATCOM
 CHARACTERISTICS AT ANGLE OF ATTACK AND IN SIDESLIP
 WING-BODY-VERTICAL TAIL-HORIZONTAL TAIL CONFIGURATION
 PROPELLER POWER EFFECTS INCLUDED IN THE LONGITUDINAL STABILITY RESULTS

FLIGHT CONDITIONS						REFERENCE DIMENSIONS						
MACH NUMBER	ALTIITUDE FT	VELOCITY FT/SEC	PRESSURE LB/FT**2	TEMPERATURE DEG R	REYNOLDS NUMBER 1/FT	REF. AREA FT**2	REFERENCE LONG. FT	LENGTH LAT. FT	MOMENT FT	REF. CENTER VERT FT		
0 0.061	1000.00	67.86	2.0409E+03	515.104	4.1949E+05	10.560	1.250	9.160	2.000	0.083		
-----DERIVATIVE (PER DEGREE)-----												
0 ALPHA	CD	CL	CM	CN	CA	XCP	CLA	CMA	CYB	CNB	CLB	
0	-10.0	0.056	-0.727	-0.0423	-0.726	-0.071	0.058	1.040E-01	7.503E-03	-5.622E-03	2.285E-04	-1.445E-03
	-8.0	0.041	-0.509	-0.0300	-0.509	-0.031	0.059	9.949E-02	2.440E-03			-1.500E-03
	-6.0	0.031	-0.298	-0.0165	-0.300	0.000	0.055	9.594E-02	-1.655E-04			-1.553E-03
	-4.0	0.026	-0.092	-0.0186	-0.094	0.019	0.198	9.390E-02	-4.647E-03			-1.602E-03
	-2.0	0.025	0.112	-0.0270	0.111	0.029	-0.243	9.564E-02	-5.846E-03			-1.648E-03
	0.0	0.028	0.327	-0.0358	0.327	0.028	-0.110	1.005E-01	-6.177E-03			-1.699E-03
	2.0	0.037	0.553	-0.0464	0.554	0.018	-0.084	1.050E-01	-7.123E-03			-1.753E-03
	4.0	0.051	0.788	-0.0599	0.789	-0.004	-0.076	1.087E-01	-8.697E-03			-1.810E-03
	6.0	0.072	1.029	-0.0757	1.031	-0.036	-0.073	1.118E-01	-1.090E-02			-1.870E-03
	8.0	0.099	1.276	-0.0958	1.277	-0.080	-0.075	1.120E-01	-1.363E-02			-1.932E-03
	10.0	0.130	1.518	-0.1206	1.518	-0.135	-0.079	1.007E-01	-1.847E-02			-1.991E-03
	12.0	0.162	1.715	-0.1572	1.711	-0.198	-0.092	8.412E-02	-2.458E-02			-2.033E-03
	14.0	0.194	1.883	-0.2021	1.874	-0.267	-0.108	6.975E-02	-2.961E-02			-2.064E-03
	16.0	0.224	2.014	-0.2517	1.998	-0.339	-0.126	4.500E-02	-3.427E-02			-2.081E-03
	18.0	0.246	2.073	0.0811	2.047	-0.407	0.040	-3.227E-02	NA			-2.069E-03
	20.0	0.228	1.873	0.0932	1.838	-0.427	0.051	-3.000E-01	NA			-1.956E-03
	22.0	0.135	0.800	0.0760	0.792	-0.175	0.096	-4.789E-01	NA			-1.533E-03
	24.0	0.113	-0.143	0.0637	-0.085	0.161	-0.750	-4.261E-01	NA			-1.203E-03
	26.0	0.159	-0.984	0.0671	-0.815	0.574	-0.082	-3.256E-01	NA			-9.155E-04
	28.0	0.228	-1.496	0.0576	-1.214	0.903	-0.047	-1.737E-01	NA			-7.221E-04
0				ALPHA	Q/QINF	EPSLON	D(EPSLON)/D(ALPHA)					
0				-10.0	0.904	-3.149	0.512					

-8.0	0.907	-2.124	0.500
-6.0	0.974	-1.148	0.475
-4.0	1.000	-0.223	0.455
-2.0	1.000	0.672	0.453
0.0	1.000	1.587	0.457
2.0	1.000	2.498	0.456
4.0	1.000	3.410	0.450
6.0	1.000	4.299	0.434
8.0	1.000	5.146	0.412
10.0	1.000	5.946	0.365
12.0	1.000	6.606	0.293
14.0	1.000	7.117	0.229
16.0	1.000	7.524	0.125
18.0	1.000	7.617	-0.165
20.0	1.000	6.863	-0.743
22.0	1.000	4.644	-1.106
24.0	1.000	2.440	-1.132
26.0	1.000	0.118	-0.879
28.0	1.000	-1.076	-0.597

0*** NA PRINTED WHEN METHOD NOT APPLICABLE

0*** VEHICLE WEIGHT = 17.00 LB.

0*** LEVEL FLIGHT LIFT COEFFICIENT = 0.30284

1 AUTOMATED STABILITY AND CONTROL METHODS PER APRIL 1976 VERSION OF DATCOM

CHARACTERISTICS OF HIGH LIFT AND CONTROL DEVICES

TAIL PLAIN TRAILING-EDGE FLAP CONFIGURATION

FLIGHT CONDITIONS						REFERENCE DIMENSIONS					
MACH NUMBER	ALTITUDE FT	VELOCITY FT/SEC	PRESSURE LB/FT**2	TEMPERATURE DEG R	REYNOLDS NUMBER 1/FT	REF. AREA FT**2	REFERENCE LONG. FT	LENGTH LAT. FT	MOMENT HORIZ FT	REF. CENTER VERT FT	
0 0.061	1000.00	67.86	2.0409E+03	515.104	4.1949E+05	10.560	1.250	9.160	2.000	0.083	
-----DERIVATIVES (PER DEGREE)-----											
0	-----INCREMENTS DUE TO DEFLECTION-----				(CLA)D	(CH)A	(CH)D				
0	DELTA	D(CL)	D(CM)	D(CL MAX)	D(CD MIN)						
	-20.0	-0.097	0.2217	0.085	0.00770	NDM	1.238E-02	3.053E-03			
	-10.0	-0.062	0.1401	0.049	0.00245	NDM		2.751E-03			
	0.0	0.000	-0.0001	0.000	0.00000	NDM		2.751E-03			
	10.0	0.062	-0.1401	0.049	0.00245	NDM		2.751E-03			
	20.0	0.097	-0.2217	0.085	0.00770	NDM		3.053E-03			

0 *** NOTE * HINGE MOMENT DERIVATIVES ARE BASED ON TWICE THE AREA-MOMENT OF THE CONTROL ABOUT ITS HINGE LINE

0 ----- INDUCED DRAG COEFFICIENT INCREMENT, D(CDI), DUE TO DEFLECTION -----

ALPHA	DELTA = -20.0	-10.0	0.0	10.0	20.0
-10.0	3.19E-03	1.53E-03	-6.20E-07	2.86E-04	1.25E-03
-8.0	2.49E-03	1.08E-03	-1.70E-07	7.35E-04	1.95E-03
-6.0	1.75E-03	6.05E-04	3.02E-07	1.21E-03	2.69E-03
-4.0	9.74E-04	1.09E-04	7.98E-07	1.70E-03	3.47E-03
-2.0	1.77E-04	-4.00E-04	1.31E-06	2.21E-03	4.27E-03
0.0	-6.07E-04	-9.00E-04	1.81E-06	2.71E-03	5.05E-03
2.0	-1.39E-03	-1.40E-03	2.31E-06	3.21E-03	5.84E-03
4.0	-2.18E-03	-1.90E-03	2.81E-06	3.72E-03	6.62E-03
6.0	-2.98E-03	-2.42E-03	3.32E-06	4.23E-03	7.42E-03
8.0	-3.81E-03	-2.95E-03	3.86E-06	4.76E-03	8.26E-03
10.0	-4.68E-03	-3.50E-03	4.41E-06	5.31E-03	9.12E-03

12.0	-5.65E-03	-4.12E-03	5.02E-06	5.93E-03	1.01E-02
14.0	-6.72E-03	-4.81E-03	5.71E-06	6.62E-03	1.12E-02
16.0	-7.87E-03	-5.54E-03	6.45E-06	7.35E-03	1.23E-02
18.0	-9.25E-03	-6.42E-03	7.33E-06	8.23E-03	1.37E-02
20.0	-1.12E-02	-7.69E-03	8.59E-06	9.50E-03	1.57E-02
22.0	-1.43E-02	-9.63E-03	1.06E-05	1.14E-02	1.87E-02
24.0	-1.73E-02	-1.16E-02	1.25E-05	1.34E-02	2.18E-02
26.0	-2.04E-02	-1.36E-02	1.45E-05	1.54E-02	2.49E-02
28.0	-2.27E-02	-1.50E-02	1.59E-05	1.68E-02	2.72E-02

0***NDM PRINTED WHEN NO DATCOM METHODS EXIST

1 AUTOMATED STABILITY AND CONTROL METHODS PER APRIL 1976 VERSION OF DATCOM

CHARACTERISTICS OF HIGH LIFT AND CONTROL DEVICES

WING-BODY-TAIL TRIM WITH CONTROL DEVICE ON TAIL

FLIGHT CONDITIONS						REFERENCE DIMENSIONS					
MACH NUMBER	ALTITUDE FT	VELOCITY FT/SEC	PRESSURE LB/FT**2	TEMPERATURE DEG R	REYNOLDS NUMBER 1/FT	REF. AREA FT**2	REFERENCE LENGTH FT	MOMENT LAT. FT	REF. CENTER HORIZ FT	REF. CENTER VERT FT	
0 0.061	1000.00	67.86	2.0409E+03	515.104	4.1949E+05	10.560	1.250	9.160	2.000	0.083	
0	UNTRIMMED						-AT TRIM DEFLECTION-				
0	ALPHA	CL	CD	CM	DELTAT	D(CL)	D(CL MAX)	D(CDI)	D(CD MIN)	CH(A)	CH(D)
0	-10.0	-0.660	0.043	-0.0330	-2.4	-0.015	0.012	3.60E-04	0.00058	1.238E-02	2.751E-03
	-8.0	-0.456	0.033	-0.0296	-2.1	-0.013	0.010	2.28E-04	0.00052		2.751E-03
	-6.0	-0.262	0.026	-0.0232	-1.7	-0.010	0.008	1.01E-04	0.00041		2.751E-03
	-4.0	-0.072	0.023	-0.0302	-2.2	-0.013	0.011	2.43E-05	0.00053		2.751E-03
	-2.0	0.114	0.022	-0.0418	-3.0	-0.019	0.015	-1.19E-04	0.00074		2.751E-03
	0.0	0.310	0.026	-0.0536	-3.8	-0.024	0.019	-3.44E-04	0.00094		2.751E-03
	2.0	0.516	0.033	-0.0665	-4.7	-0.030	0.023	-6.65E-04	0.00117		2.751E-03
	4.0	0.730	0.044	-0.0821	-5.9	-0.036	0.029	-1.12E-03	0.00144		2.751E-03
	6.0	0.951	0.060	-0.1013	-7.2	-0.045	0.036	-1.75E-03	0.00178		2.751E-03
	8.0	1.177	0.080	-0.1257	-9.0	-0.056	0.044	-2.64E-03	0.00220		2.751E-03
	10.0	1.399	0.105	-0.1558	-11.9	-0.069	0.056	-3.73E-03	0.00346		2.810E-03
	12.0	1.580	0.129	-0.1996	-17.3	-0.088	0.075	-5.23E-03	0.00628		2.972E-03

0*NOTE** TRIM RESULTS HAVE BEEN TERMINATED DUE TO LACK OF CONTROL MOMENT.

1 THE FOLLOWING IS A LIST OF ALL INPUT CARDS FOR THIS CASE.

0 \$ASYFLP SPANFI=1.772,SPANFO=3.812,CHRDFl=0.2077,CHRDFO=0.2077,
 STYPE=4.0,NDELTA=5.,DELTAL=20.,10.,0.,-10.,-20.,
 DELTAR=-20.,-10.,0.,10.,20.,\$

NEXT CASE

0 INPUT DIMENSIONS ARE IN FT, SCALE FACTOR IS 1.0000

1 AUTOMATED STABILITY AND CONTROL METHODS PER APRIL 1976 VERSION OF DATCOM

WING SECTION DEFINITION

0 IDEAL ANGLE OF ATTACK = 1.12591 DEG.

ZERO LIFT ANGLE OF ATTACK = -3.50518 DEG.

IDEAL LIFT COEFFICIENT = 0.54407

ZERO LIFT PITCHING MOMENT COEFFICIENT = -0.08623

MACH ZERO LIFT-CURVE-SLOPE = 0.09893 /DEG.

LEADING EDGE RADIUS = 0.01102 FRACTION CHORD

```

                                LIFT CURVE-SLOPE = 0.09903 /DEG.
                                MAXIMUM AIRFOIL THICKNESS = 0.10000 FRACTION CHORD
                                DELTA-Y = 2.64081 PERCENT CHORD

0
1
0
MACH= 0.0610 LIFT-CURVE-SLOPE = 0.09903 /DEG. XAC = 0.25348
AUTOMATED STABILITY AND CONTROL METHODS PER APRIL 1976 VERSION OF DATCOM
                                HORIZONTAL TAIL SECTION DEFINITION
                                IDEAL ANGLE OF ATTACK = 0.00000 DEG.
                                ZERO LIFT ANGLE OF ATTACK = 0.00000 DEG.
                                IDEAL LIFT COEFFICIENT = 0.00000
                                ZERO LIFT PITCHING MOMENT COEFFICIENT = 0.00000
                                MACH ZERO LIFT-CURVE-SLOPE = 0.09830 /DEG.
                                LEADING EDGE RADIUS = 0.00893 FRACTION CHORD
                                MAXIMUM AIRFOIL THICKNESS = 0.09000 FRACTION CHORD
                                DELTA-Y = 2.37673 PERCENT CHORD

0
1
0
MACH= 0.0610 LIFT-CURVE-SLOPE = 0.09846 /DEG. XAC = 0.25642
AUTOMATED STABILITY AND CONTROL METHODS PER APRIL 1976 VERSION OF DATCOM
                                VERTICAL TAIL SECTION DEFINITION
                                IDEAL ANGLE OF ATTACK = 0.00000 DEG.
                                ZERO LIFT ANGLE OF ATTACK = 0.00000 DEG.
                                IDEAL LIFT COEFFICIENT = 0.00000
                                ZERO LIFT PITCHING MOMENT COEFFICIENT = 0.00000
                                MACH ZERO LIFT-CURVE-SLOPE = 0.09830 /DEG.
                                LEADING EDGE RADIUS = 0.00893 FRACTION CHORD
                                MAXIMUM AIRFOIL THICKNESS = 0.09000 FRACTION CHORD
                                DELTA-Y = 2.37673 PERCENT CHORD

0
MACH= 0.0610 LIFT-CURVE-SLOPE = 0.09846 /DEG. XAC = 0.25642

```

1

AUTOMATED STABILITY AND CONTROL METHODS PER APRIL 1976 VERSION OF DATCOM
 CHARACTERISTICS AT ANGLE OF ATTACK AND IN SIDESLIP
 WING-BODY-VERTICAL TAIL-HORIZONTAL TAIL CONFIGURATION
 PROPELLER POWER EFFECTS INCLUDED IN THE LONGITUDINAL STABILITY RESULTS

MACH NUMBER	ALTITUDE FT	FLIGHT CONDITIONS				TEMPERATURE DEG R	REYNOLDS NUMBER 1/FT	REFERENCE DIMENSIONS				
		VELOCITY FT/SEC	PRESSURE LB/FT**2	AREA FT**2	LONG. FT			LAT. FT	HORIZ FT	MOMENT FT	REF. CENTER FT	DERIVATIVE (PER DEGREE)
0	0.061	1000.00	67.86	2.0409E+03	515.104	4.1949E+05	10.560	1.250	9.160	2.000	0.083	
0	ALPHA	CD	CL	CM	CN	CA	XCP	CLA	CMA	CYB	CNB	CLB
0	-10.0	0.056	-0.727	-0.0423	-0.726	-0.071	0.058	1.040E-01	7.503E-03	-5.622E-03	2.285E-04	-1.445E-03
	-8.0	0.041	-0.509	-0.0300	-0.509	-0.031	0.059	9.949E-02	2.440E-03			-1.500E-03
	-6.0	0.031	-0.298	-0.0165	-0.300	0.000	0.055	9.594E-02	-1.655E-04			-1.553E-03
	-4.0	0.026	-0.092	-0.0186	-0.094	0.019	0.198	9.390E-02	-4.647E-03			-1.602E-03
	-2.0	0.025	0.112	-0.0270	0.111	0.029	-0.243	9.564E-02	-5.846E-03			-1.648E-03
	0.0	0.028	0.327	-0.0358	0.327	0.028	-0.110	1.005E-01	-6.177E-03			-1.699E-03
	2.0	0.037	0.553	-0.0464	0.554	0.018	-0.084	1.050E-01	-7.123E-03			-1.753E-03
	4.0	0.051	0.788	-0.0599	0.789	-0.004	-0.076	1.087E-01	-8.697E-03			-1.810E-03
	6.0	0.072	1.029	-0.0757	1.031	-0.036	-0.073	1.118E-01	-1.090E-02			-1.870E-03
	8.0	0.099	1.276	-0.0958	1.277	-0.080	-0.075	1.120E-01	-1.363E-02			-1.932E-03
	10.0	0.130	1.518	-0.1206	1.518	-0.135	-0.079	1.007E-01	-1.847E-02			-1.991E-03
	12.0	0.162	1.715	-0.1572	1.711	-0.198	-0.092	8.412E-02	-2.458E-02			-2.033E-03
	14.0	0.194	1.883	-0.2021	1.874	-0.267	-0.108	6.975E-02	-2.961E-02			-2.064E-03
	16.0	0.224	2.014	-0.2517	1.998	-0.339	-0.126	4.500E-02	-3.427E-02			-2.081E-03
	18.0	0.246	2.073	0.0811	2.047	-0.407	0.040	-3.227E-02	NA			-2.069E-03
	20.0	0.228	1.873	0.0932	1.838	-0.427	0.051	-3.000E-01	NA			-1.956E-03
	22.0	0.135	0.800	0.0760	0.792	-0.175	0.096	-4.789E-01	NA			-1.533E-03
	24.0	0.113	-0.143	0.0637	-0.085	0.161	-0.750	-4.261E-01	NA			-1.203E-03
	26.0	0.159	-0.984	0.0671	-0.815	0.574	-0.082	-3.256E-01	NA			-9.155E-04
	28.0	0.228	-1.496	0.0576	-1.214	0.903	-0.047	-1.737E-01	NA			-7.221E-04
				ALPHA	Q/QINF	EPSLON	D(EPSLON)/D(ALPHA)					
				-10.0	0.904	-3.149	0.512					
				-8.0	0.907	-2.124	0.500					
				-6.0	0.974	-1.148	0.475					
				-4.0	1.000	-0.223	0.455					
				-2.0	1.000	0.672	0.453					
				0.0	1.000	1.587	0.457					
				2.0	1.000	2.498	0.456					
				4.0	1.000	3.410	0.450					
				6.0	1.000	4.299	0.434					
				8.0	1.000	5.146	0.412					
				10.0	1.000	5.946	0.365					
				12.0	1.000	6.606	0.293					
				14.0	1.000	7.117	0.229					
				16.0	1.000	7.524	0.125					
				18.0	1.000	7.617	-0.165					
				20.0	1.000	6.863	-0.743					
				22.0	1.000	4.644	-1.106					
				24.0	1.000	2.440	-1.132					
				26.0	1.000	0.118	-0.879					
				28.0	1.000	-1.076	-0.597					

0*** NA PRINTED WHEN METHOD NOT APPLICABLE

0*** VEHICLE WEIGHT = 17.00 LB.

0*** LEVEL FLIGHT LIFT COEFFICIENT = 0.30284

1 AUTOMATED STABILITY AND CONTROL METHODS PER APRIL 1976 VERSION OF DATCOM

CHARACTERISTICS OF HIGH LIFT AND CONTROL DEVICES

WING PLAIN TRAILING-EDGE FLAP CONFIGURATION

FLIGHT CONDITIONS						REFERENCE DIMENSIONS					
MACH NUMBER	ALTITUDE	VELOCITY	PRESSURE	TEMPERATURE	REYNOLDS NUMBER	REF. AREA	REFERENCE LONG.	LENGTH LAT.	MOMENT HORIZ	REF. CENTER VERT	
	FT	FT/SEC	LB/FT**2	DEG R	1/FT	FT**2	FT	FT	FT	FT	
0	0.061	1000.00	67.86	2.0409E+03	515.104	4.1949E+05	10.560	1.250	9.160	2.000	0.083

0 -----YAWING MOMENT COEFFICIENT, CN, DUE TO CONTROL DEFLECTION-----

0 (DELTAL-DELTAR) = 40.0 20.0 0.0 -20.0 -40.0

0ALPHA

0	-10.0	4.623E-03	2.639E-03	0.000E+00	-2.639E-03	-4.623E-03
0	-8.0	3.131E-03	1.788E-03	0.000E+00	-1.788E-03	-3.131E-03
0	-6.0	1.694E-03	9.674E-04	0.000E+00	-9.674E-04	-1.694E-03
0	-4.0	3.264E-04	1.864E-04	0.000E+00	-1.864E-04	-3.264E-04
0	-2.0	-1.011E-03	-5.774E-04	0.000E+00	5.774E-04	1.011E-03
0	0.0	-2.430E-03	-1.388E-03	0.000E+00	1.388E-03	2.430E-03
0	2.0	-3.924E-03	-2.241E-03	0.000E+00	2.241E-03	3.924E-03
0	4.0	-5.480E-03	-3.129E-03	0.000E+00	3.129E-03	5.480E-03
0	6.0	-7.085E-03	-4.045E-03	0.000E+00	4.045E-03	7.085E-03
0	8.0	-8.723E-03	-4.981E-03	0.000E+00	4.981E-03	8.723E-03
0	10.0	-1.032E-02	-5.891E-03	0.000E+00	5.891E-03	1.032E-02
0	12.0	-1.156E-02	-6.599E-03	0.000E+00	6.599E-03	1.156E-02
0	14.0	-1.257E-02	-7.174E-03	0.000E+00	7.174E-03	1.257E-02
0	16.0	-1.329E-02	-7.591E-03	0.000E+00	7.591E-03	1.329E-02
0	18.0	-1.346E-02	-7.685E-03	0.000E+00	7.685E-03	1.346E-02
0	20.0	-1.168E-02	-6.672E-03	0.000E+00	6.672E-03	1.168E-02
0	22.0	-3.387E-03	-1.934E-03	0.000E+00	1.934E-03	3.387E-03
0	24.0	3.026E-03	1.728E-03	0.000E+00	-1.728E-03	-3.026E-03
0	26.0	8.643E-03	4.935E-03	0.000E+00	-4.935E-03	-8.643E-03
0	28.0	1.226E-02	6.998E-03	0.000E+00	-6.998E-03	-1.226E-02

0				DELTAL	DELTAR	(CL)ROLL
0				20.0	-20.0	7.4618E-02
0				10.0	-10.0	4.2649E-02
0				0.0	0.0	0.0000E+00
0				-10.0	10.0	-4.2649E-02
0				-20.0	20.0	-7.4618E-02

1 THE FOLLOWING IS A LIST OF ALL INPUT CARDS FOR THIS CASE.

0

1 END OF JOB.

Appendix H: Matlab M-Files: Force, Moment, and Equations of Motion

```

function x_dot=EOMs(in)
% Forces and Moments, and Equations of Motion
% for the SIG Rascal Model Airplane

% by Nidal Jodeh and Paul Blue

% *** QUANTITY ***** UNITS *****
% *** mass      -> {slugs}
% *** length    -> {ft}
% *** area      -> {ft^2}
% *** velocity  -> {ft/s}
% *** acceleration-> {ft/s^2}
% *** density   -> {slugs/ft^3}
% *** force     -> {lbf}
% *** moments   -> {lbf-ft}
% *** angles    -> {radians} (calculations)
% *** velocity  -> {ft/s}
% *** ang. vel. -> {rad/s}
% *** ang. accel.-> {rad/s^2}
% *****

global maneuver alpha_dot

% maneuver is a parameter that sets version to sim (glide or turn)

%x_dot=zeros(12,1);

% extract inputs from input vector
T      = in(1);    % Thrust
de     = in(2);    % Elevator Deflection (down is +) {deg}
drt    = in(3);    % Rudder Deflection {deg}
da     = in(4);    % Aileron Deflection (deg)

% extract states from input vector
V      = in(5);    % Velocity {ft/s}
gamma  = in(6);    % Flight path angle {rad}
alpha  = in(7);    % Angle of attack {rad}
q      = in(8);    % Pitch Rate {rad/s}
p      = in(9);    % Roll Rate {rad/s}
mu     = in(10);   % Bank Angle (About Velocity Vector) {rad}
beta   = in(11);   % Sideslip Angle {rad}
r      = in(12);   % Yaw Rate {rad/s}
chi    = in(13);   % Heading angle {rads}
north  = in(14);   % North Position {ft}
east   = in(15);   % East Position {ft}
h      = in(16);   % Altitude {ft}

% extract simulation time{sec} from input(used to calculate windup thrust)
tm = in(17);

% DEFINE ANY NEEDED TERMS THAT APPEAR IN THE E.O.M.'S
% Define and/or Calculate Necessary Constants
d2r=pi/180;    %Convert Degrees to Rads -- Although it's already
              %coded in Matlab (DEG2RAD) - Checked
r2d=180/pi;    %Convert Rads to Degrees -- Although it's already
              %coded in Matlab (RAD2DEG) - Checked
rho=.0023081;  %Air Density (Slugs per ft^3) - Checked
g=32.17;      %Gravity - Checked

m=.487669;    %Slugs - Empty Mass of A/C (w/o fuel)(7.117 Kg empty)
Iyy=1.5523;   %Inertias Experimentally determined using Empty Mass
Ixx=1.9480;   %Inertia Units are (slugs*ft^2) - Checked
Izz=1.9166;   % - Checked
Ixz=0;       %Assumed zero due to symmetric aircraft - Assumed

```

```

S=10.56;          %Square Feet - Wing Area Converted from
                  %Manuf 1520 sq in area - Checked (also Matches DigDat)
CLow=.421;        %from Look up table for Eppler 193 at AoA=0,
                  %DigDat = .421, Line # 277 - Checked CL column
CLaw=4.59;        %Coef of Lift for finite wing = Cla/(1+ (Cla/(pi*ARw*e)
                  %DigDat = 4.59, Line #276-277, CLA column- Checked
CDminw=.011;     %DigDat Min Drag of Wing at AoA = -6 deg,
                  %Dig Dat Line# 274- Checked
ARw=7.9456;      %Aspect Ratio AR = (b^2)/S- Checked
e = .75;         %Span efficiency factor -estimation- Checked
Kw = 1/(pi*ARw*e); % = 1/(pi*AR*e)- Checked
Cmw=-0.005;      %DigDat = AoA =0, Line #277- Checked
cgw=-.416;       %Distance Aero Center is back from CG, 5 Inches
c=1.3333;        %Feet - Root Chord of Wing (16")- Checked
b=9.16;          %Feet - Span (110")- Checked
lambda=.72955;   %Taper Ratio from S=(Cr*(1+Lambda)*b)/2- Checked

CLat=.76;        %Dig Dat, Line #346, CLA Column- Checked
CDmint=.002;     %Dig Dat, Line #345, at AoA = -2 deg
Kt=.446;         %=1/(pi*e*AR) =SET SAME AS WING OR DIGDAT From BLAKE
it=2*d2r;        %Tail incidence 2 degrees
Te=.422;         %Blake from DigDat
nt=1;            %Blake from DigDat
St=S;            %Horiz Tail Area Square Feet=Reference Area = Wing Area
cgt=3.5;         %Distance tail Aero Center back from A/C CG,
                  %42 inches - Measured

CLavt=.0969;     %Dig Dat Line #190
CDminvt=.001;    %Dig Dat Line #409, AOA = -10 deg, Column CD
Svt=S;           %Vert Tail Area Square Feet = Reference Area = Wing Area
Tr=.434;         %Blake from DigDat
nvt=nt;          %Same as Hori Tail
cgv=cgt;         %Same as Hori tail

Cmaf=.114;       %Dig Dat, Line#209, at AoA = 0
CDF=.005;        %Dig Dat, Line#209, at AoA = 0

Cnda = -0.0128;  %per rad DigDat
Clda = 0.244;    %per rad DigDat

% Define/calculate any needed coefficients, forces, etc.
CLw=CLow+CLaw*alpha;
CDw=CDminw+Kw*CLw^2;
E=2*(CLow+CLaw*(alpha-alpha_dot*(cgt+cgw)/V))/(pi*ARw);
alphan=alpha+it+Te*de+q*cgt/V-E;
CLt=CLat*alphan;
CDt=CDmint+Kt*CLt^2;
Cmf=Cmaf*alpha;
CDvt=CDminvt;
Clp=-1/12*CLaw*(1+3*lambda)/(1+lambda);
Clb=-.1;
Clr=.01;

qb=.5*rho*V^2;
Lw=qb*S*CLw;
Dw=qb*S*CDw;
Mw=qb*S*c*Cmw;
Lt=nt*qb*St*CLt;
Dt=nt*qb*St*CDt;
Df=qb*S*CDF;
Mf=qb*S*c*Cmf;
Dvt=nt*qb*Svt*CDvt;

```

```

% Calculate Forces and Moments
% Lift
L=Lw+Lt*cos(E-q*cgT/V)-(Dt+Dvt)*sin(E-q*cgT/V);
% Drag
D=Dw+(Dt+Dvt)*cos(E-q*cgT/V)+Lt*sin(E-q*cgT/V)+Df;
% Side Force
Y=nvt*qb*Svt*CLavt*(-beta+Tr*drt+r*cgvt/V);
% Pitch Moment
Mc=Lw*cgw*cos(alpha)+Dw*cgw*sin(alpha)+Mw-Lt*cgT*...
    cos(alpha-E+q*cgT/V)-(Dt+Dvt)*cgT*sin(alpha-E+q*cgT/V)+Mf;
% Yaw Moment
Nc=-qb*nvt*Svt*CLavt*(-beta+Tr*drt+r*cgvt/V)*cgvt+(-qb*S*b*Cnda*da);
% Roll Moment
Lc=qb*S*b^2/(2*V)*(Clp*p+2*V/b*Clb*beta+Clr*drt+Clda*da*2*V/b);

% ----- NONLINEAR 6-DOF EQUATION OF MOTION (EOMs) -----
%
% These are the state derivative equations; the comment names the state,
% but the equation is for its derivative (rate)
%
% The equations are arranged by aircraft mode
%
% NOTE: These assume that Ixz=0, if not, then eq's need to be modified

% Longitudinal (phugoid and short period): V, gamma, q, alpha
% Phugoid: V, gamma
% Velocity
V_dot=1/m*(-D*cos(beta)+Y*sin(beta)+T*cos(beta)*cos(alpha))-...
    g*sin(gamma);

% Flight Path Angle
gamma_dot=1/(m*V)*(-D*sin(beta)*sin(mu)-Y*sin(mu)*cos(beta)...
    +L*cos(mu)+T*(cos(mu)*sin(alpha)+sin(mu)*sin(beta)*cos(alpha)))-...
    -g/V*cos(gamma);

% Short Period: alpha, q
% Angle of Attach
alpha_dot=q-tan(beta)*(p*cos(alpha)+r*sin(alpha))-1/(m*V*cos(beta))...
    *(L+T*sin(alpha))+g*cos(gamma)*cos(mu)/(V*cos(beta));
% Pitch Rate
q_dot=Mc/Iyy+1/Iyy*(Izz*p*r-Ixx*r*p);

% Lateral (roll) - Directional (yaw): p, mu, beta, r
% Roll: p, mu
% Roll Rate
p_dot=Lc/Ixx+1/Ixx*(Iyy*r*q-Izz*q*r);

% Bank Angle (about velocity vector)
mu_dot=1/cos(beta)*(p*cos(alpha)+r*sin(alpha))+1/(m*V)*(D*sin(beta)...
    *cos(mu)*tan(gamma)+Y*tan(gamma)*cos(mu)*cos(beta)+L*(tan(beta)+...
    tan(gamma)*sin(mu))+T*(sin(alpha)*tan(gamma)*sin(mu)+sin(alpha)*...
    tan(beta)-cos(alpha)*tan(gamma)*cos(mu)*sin(beta))-...
    g/V*cos(gamma)*cos(mu)*tan(beta);

% Dutch Roll: beta, r
% Side Slip Angle
beta_dot=-r*cos(alpha)+p*sin(alpha)+1/(m*V)*(D*sin(beta)+Y*cos...
    (beta)-T*sin(beta)*cos(alpha))+g/V*cos(gamma)*sin(mu);

% Yaw Rate

```



```

r_dot=Nc/Izz+1/Izz*(Ixx*p*q-Iyy*p*q);

% Heading Angle (from North)
chi_dot=1/(m*V*cos(gamma))*(D*sin(beta)*cos(mu)+Y*cos(mu)*cos(beta)...
+L*sin(mu)+T*(sin(mu)*sin(alpha)-cos(mu)*sin(beta)*cos(alpha));

% Kinematic Equations
% North Position
n_dot=V*cos(gamma)*cos(chi);

% East Position
e_dot=V*cos(gamma)*sin(chi);

% Altitude
h_dot=V*sin(gamma);

% Pack derivatives into output vector x_dot
x_dot(1) = V_dot;
x_dot(2) = gamma_dot;

x_dot(3) = alpha_dot;
x_dot(4) = q_dot;

x_dot(5) = p_dot;
x_dot(6) = mu_dot;

x_dot(7) = beta_dot;
x_dot(8) = r_dot;

x_dot(9) = chi_dot;
x_dot(10) = n_dot;
x_dot(11) = e_dot;
x_dot(12) = h_dot;

end

```

```

% Initiate SIG Rascal 110 Sim.m
%
%by Nidal Jodeh and Paul Blue

%clear all
close all
clc

simulator = 1; % Choose 2 for HITL Sim Inputs
              % Choose 1 for Flight Test Inputs

if (simulator == 1);
%Get actual Surface positions from 21 Nov 05 flight test
load 21_Nov_05_Doublet_Tel.mat

Aileron_Position = Aileron_0x5Brad0x5D;
Elevator_Position = Elevator_0x5Brad0x5D;
Rudder_Position = Rudder0x5Brad0x5D;
Clock_sec = Clock0x5Bms0x5D/1000;

%Call Redefine Vector Names from 21 Nov file (States of Vehicle)
%Initial State Conditions: Radians and Re-named
Roll_rate = P0x5Brad0x2Fs0x5D;           %Roll, Pitch, Yaw Rates
Pitch_rate = Q0x5Brad0x2Fs0x5D;
Yaw_rate = R0x5Brad0x2Fs0x5D;

Altitude_Actual = Pitot_Alt0x5Bft0x5D;
Velocity = TAS0x5Bm0x2Fs0x5D/.3048;

FlightPath_Angle = 0;

Sideslip_Angle = Yaw0x5Brad0x5D;
AoA = Pitch0x5Brad0x5D;
Bank_Angle = Roll0x5Brad0x5D;

Heading_Angle = Direction0x5Brad0x5D;
North_Position = Lat0x5Brad0x5D;
East_Position = Lon0x5Brad0x5D;

elseif (simulator == 2);
%Get actual Surface positions from HITL Flight Test
load 16_Feb_Sim_Mode_Flight_Data.mat
% Short_Period_Test_Runs

Aileron_Position = AileronLeft_0x5Brad0x5DPh;
Elevator_Position = Elevator_0x5Brad0x5D;
Rudder_Position = Rudder_0x5Brad0x5D;
Clock_sec = Clock0x5Bms0x5D/1000;

%Call Redefine Vector Names from 21 Nov file (States of Vehicle)
%Initial State Conditions: Radians and Re-named
Roll_rate = P0x5Brad0x2Fs0x5D;           %Roll, Pitch, Yaw Rates
Pitch_rate = Q0x5Brad0x2Fs0x5D;
Yaw_rate = R0x5Brad0x2Fs0x5D;

Altitude_Actual = Pitot_Alt0x5Bm0x5D*3.281;
Velocity = TAS0x5Bm0x2Fs0x5D/.3048;

FlightPath_Angle = 0;
Sideslip_Angle = Yaw0x5Brad0x5D;
AoA = Pitch0x5Brad0x5D;
Bank_Angle = Roll0x5Brad0x5D;

```

```

Heading_Angle = Direction0x5Brad0x5D;
North_Position = Lat0x5Brad0x5D;
East_Position = Lon0x5Brad0x5D;
end

%buttons % this opens my button tool

global maneuver alpha_dot

alpha_dot= 0; % alpha_dot is used in calculate the tail's angle of attack
            % before it is calculated in the EOMS, so it is initialized
            % here and saved as a global, so it is available when needed

% the following parameter sets which ICs to use, and if the turn ICs are
% used, then it turns on the thrust in the EOM file
% Toggle between these choices OFF = '0'

maneuver=2; % Maneuver=1 = SLUF
            % Maneuver=2 = SLUF then to SP Input
            % Maneuver=3 = Turns

getlinmod=1; % if 1, then obtain linear model and eigenvalues

if(maneuver==1) % then use Short Period ICs

    % Define INPUT Equil. Values
    To      = 1.9919944388197141396003581136848
    deo     = -.11357517956568012273826659260137e-1 %Negative is nose up
    drto    = 0*pi/180
    dato    = 0*pi/180

    u0_glide=[To;deo;drto;dato];
    u0=u0_glide;

%   %FOR SLUF FLIGHT, THIS uin IS A DUMMY VARIABLE, BUT WE'LL
%   %DEFINE IT HERE TOO
%   % The desired Flight Test Data to model follow
%   % Desired Time range fpr Control input
%   %
%   %Vector Length of Data to be analyzed
%   %   Clock_vector_length = length (Clock_sec(begin:end_at,1));
%   %
%   %Input Vector of Controls to the sim
%   %   uin = [(Clock_sec(begin:end_at))- Clock_sec(begin,1)+100,...
%   %         %Time in seconds starting at Zero
%   %         zeros(Clock_vector_length,1),...
%   %         %Throttle setting times 1, constant through maneuver
%   %         Elevator_Position(begin:end_at) - Elevator_Position(begin),...
%   %         %Flight test Elevator inputs(Rads)
%   %         zeros(Clock_vector_length,1),...   %Zero Rudder Inputs
%   %         zeros(Clock_vector_length,1)];
%   %
%   %For Actual rudder and Aileron inputs.  Sub into last two
%   % "zeros(Clock...)" lines above.
%   %   %Rudder_Position(begin:end_at)+u0(3)',...   %Zero Rudder Inputs
%   %   %Aileron_Position(begin:end_at)+u0(4)'];
%   %
%   % Define STATE Equilibrium Values

Vo      = 64.8280   %Velocity (ft/s)

```

```

gammao = 0*pi/180    %flight path angle (deg to rads)

alphao = -.15272568925513207604611741763135e-1
%angle of attack from deg to rads

qo      = 0          %Pitch Rate

po      = 0          %Roll Rate
muo     = 0          %Bank Angle (About Velocity Vector)
betao   = 0*pi/180  %angle of sideslip from deg to rads
ro      = 0          %Yaw Rate

chio    = 0*pi/180;  %Heading angle (deg to rads)
northo  = 0          %North Position
easto   = 0          %East Position
ho      = Altitude(begin) %Altitude

x0_glide=
[Vo; gammao; alphao; qo; po; muo; betao; ro; chio; northo; easto; ho];
x0=x0_glide;

elseif(manuever==2) % then use SLUF ICs

% Define INPUT Equil. Values
To      = 2.2927384940583337708529988501982
deo     = .73706101567294723362084074747842e-2 %Negative is nose up
drto    = 0*pi/180
dato    = 0*pi/180

u0_glide=[To;deo;drto;dato];
u0=u0_glide;

%FOR SLUF FLIGHT, THIS uin IS A DUMMY VARIABLE, BUT WE'LL
%DEFINE IT HERE TOO
% The desired Flight Test Data to model follow
% Desired Time range fpr Control input
%SP Flight Test 2; 3520-3600
%P Flight Test 3; 8940-8970, 90 ft/sec
%P HITL #6; 10910-11500, 91.375 ft/sec
%P HITL #7;13344-13800 ,90.5 ft/sec
%P HITL #1; 7918 - 8100,96 ft/sec
begin = 7956
end_at = 7990

%Vector Length of Data to be analyzed
Clock_vector_length = length (Clock_sec(begin:end_at,1));

%Input Vector of Controls to the sim
%Time in seconds starting at Zero
%Throttle setting times 1, constant throughout maneuver
%Flight test Elevator inputs(Rads)
%Zero Rudder Inputs
uin = [(Clock_sec(begin:end_at))- Clock_sec(begin,1)+100,...
zeros(Clock_vector_length,1),...
Elevator_Position(begin:end_at) - Elevator_Position(begin),...
zeros(Clock_vector_length,1),...
zeros(Clock_vector_length,1)];

%For Actual rudder and Aileron inputs. Sub into last two
%"zeros(Clock...)" lines above.
%Rudder_Position(begin:end_at)+u0(3)',... %Zero Rudder Inputs

```

```

    %Aileron_Position(begin:end_at)+u0(4)'];

% Define STATE Equilibrium Values

Vo      = 96          %Velocity (ft/s)
gammao  = 0*pi/180   %flight path angle (deg to rads)

%angle of attack from deg to rads
alphao  = -.55890400178134674600205697397186e-1

%alphao  = 11.31*pi/180;    %angle of attack from deg to rads
qo      = 0                %Pitch Rate

po      = 0                %Roll Rate
muo     = 0                %Bank Angle (About Velocity Vector)
betao   = 0*pi/180        %angle of sideslip from deg to rads
ro      = 0                %Yaw Rate

chio    = 0*pi/180        %Heading angle (deg to rads)
northo  = 0                %North Position
easto   = 0                %East Position
ho      = Altitude_Actual(begin)    %Altitude

x0_glide=
[Vo; gammao; alphao; qo; po; muo; betao; ro; chio; northo; easto; ho];
x0=x0_glide;

elseif(manuever==3) % use turn ICs
% NOTE: these are calculated trim values used to start the sim, but the
% thrust is a function of time and changed in the EOM file

% Define INPUT Equil. Values
To=.02035;
%deo=8.519*pi/180;
deo=6.0*pi/180;
drto=6*pi/180;

u0_turn=[To;deo;drto];
u0=u0_turn;

% Define STATE Equilibrium Values

Vo=28;
gammao=0*pi/180;
alphao=0*pi/180;
qo=0;

po=0;
muo=0;
betao=0;
ro=0;

chio=0*pi/180;
northo=0;
easto=0;
ho=16.33;

```

```

    x0_turn=
    Vo; gammao; alphas; qo; po; muo; betao; ro; chio; northo; easto; ho;
    x0=x0_turn;
end

disp('sim initialized')

if(getlinmod==1)

    %xlin=x0_glide;
    %xlin=x0_turn;
    xlin=x0;
    ulin=u0;

    %x0=zeros(1,12);

    %[A,B,C,D]=linmod('Pirol_sim')

    % NOTE: using the folling form of linmod, the input xlin overrides the
    % x0 specified (i.e. the x0 in the workspace, as can be seen by setting
    % xlin to x0 and then setting x0 to zeros); however, if the
    % variables x0 is used in the simulink model (e.g. as the initial state
    % specified in the integrator), then the variable needs to be defined
    % even though it isn't used for the liniearization

    [A,B,C,D]=linmod('Pirol_sim',xlin,ulin)

    eigA=eig(A)

    Along=A(1:4,1:4)
    eiglong=eig(Along)

    Aph=A(1:2,1:2)
    eigph=eig(Aph)

    Asp=A(3:4,3:4)
    eigsp=eig(Asp)

    Alatdir=A(5:8,5:8)
    eiglatdir=eig(Alatdir)

    Aroll=A(5:6,5:6)
    eigroll=eig(Aroll)

    Adr=A(7:8,7:8)
    eigdr=eig(Adr)

end

open 'Pirol_sim.mdl'

```

Bibliography

- Bertin, John J. *Aerodynamics for Engineers* (Fourth Edition). Upper Saddle River, New Jersey. Prentice-Hall, 2002.
- Enns, D. AEM 5319: Dynamics, Stability, and Control of Aerospace Vehicles. University of Minnesota. May, 1994. Unpublished Class Notes.
- Etkin, B. and Reid, L.D. *Dynamics of Flight, Stability and Control* (Third Edition). New York, NY. John Wiley and Sons, Inc., 1996.
- Frew, E., Xiao, X., Spry, S., McGee, T., Kim, Z., Tisdale, J., Sengupta, R., Hendrick, K.J. "Flight Demonstrations of Self-directed Collaborative Navigation of Small Unmanned Aircraft." *Proceedings of the 2004 IEEE Aerospace Conference*, Big Sky, MT, March 2004.
- Foster, T., and Bowman, J. "Dynamic Stability and Handling Qualities of Small Unmanned-Aerial-Vehicles." *43rd AIAA Aerospace Sciences Meeting and Exhibit*. January 2005. (AIAA 2005-1023).
- Four Cycle Engine Owner's Instruction Manual*. Japan. O.S Engines Mfg. Co. 2000.
- Higgs, Travis J. *Modeling, Stability, and Control of a Rotatable Tail on a Micro Air Vehicle*. MS Thesis, AFIT/GAE/ENY/06-D05. School of Engineering and Management, Air Force Institute of Technology (AU), Wright-Patterson AFB, OH. March 2004.
- Hoak, D.E, Ellison, D.E., et al. "USAF Stability and Control Datcom." Unpublished. AF Flight Dynamics Laboratory AFFDL-TR-79-3032. April 1979
- Hodgkinson, John. *Aircraft Handling Qualities*. Reston, VA. American Institute of Aeronautics and Astronautics, 1999.
- Honeywell Technology Center. "Application of Multivariable Control Theory to Aircraft Control Laws: Final Report, March 1993 – March 1996." Contract f33615-92-C-3607. Paper *WL-TR-96-3099*. Minneapolis, MN. May 1996 (ADA315259).
- Initial Flight Test Cards*. Hood River, OR. Cloud Cap Technology. 20 April 2005.

Johnson, E., and Fontaine, S. "Use of Flight Simulation to Complement Flight Testing of Low-Cost UAVs." School of Aerospace Engineering, Georgia Institute of Technology. American Institute of Aeronautics and Astronautics. 2001. (AIAA 2001-4059).

Kimberlin, Ralph D. *Flight Testing of Fixed Wing Aircraft*. Reston, VA. American Institute of Aeronautics and Astronautics, 2003

King, E. *Distributed Coordination and Control Experiments on a Multi-UAV Testbed*. MS Thesis. Department of Aeronautics and Astronautics, Massachusetts Institute of Technology, MA. September 2004.

Ly, L. and Higashino, S. "Development of a UAV-Flight Test Vehicle at the University of Washington." *Presented at the 2nd AIAA "Unmanned Unlimited" Systems, Technologies, and Operations – Aerospace Conference*. 15-18 September 2003.

Miller, M.P. An Accurate Method of Measuring the Moments of Inertia of Airplanes. *Technical Notes: National Advisory Committee for Aeronautics*. Washington, DC. Langley Memorial Aeronautical Laboratory. #351. October, 1930.

Nelson, Robert C. *Flight Stability and Automatic Control* (Second Edition). Madison, WI. McGraw-Hill, 1998.

Office of the Secretary of Defense. *Unmanned Aerial Vehicles Roadmap 2002-2027*. Washington: HQ DOD, December, 2002.

Roskam, Jan. *Airplane Flight Dynamics and Automatic Controls*. Ottawa, KS. Roskam Aviation and Engineering Corporation. 1979.

Sadraey, M., and Colgren, R. "UAV Flight Simulation: Credibility of Linear Decoupled vs. Nonlinear Coupled Equations of Motion." *AIAA Modeling and Simulation Technologies Conference and Exhibit*. August, 2005. (AIAA 2005-6425).

SIG Rascal 110 ARF Assembly Manual. SIG Manufacturing Company, Inc. Montezuma, IA.

U-Blox AG, Switzerland. Retrieved on December 10, 2005, from http://www.u-blox.com/products/tim_lp.html

Vaglianti, B., Hoag, R., Niculescu, M. *Piccolo System Users Guide*. Hood River OR. Cloud Cap Technology. 18 April 2005.

Vaglienti, B., Niculescu, M. *Hardware in the Loop Simulator for the Piccolo Avionics*. Hood River OR. Cloud Cap Technology. 18 April 2005.

Wilson, T. and Dennis, R. "Small UAV Persistent Visualization for Operational Response." Unpublished Risk Reduction Flight Test Plan. Wright-Patterson, AFB OH. 25 May 2005.

Vita

Captain Nidal M. Jodeh graduated from Overland High School in Aurora, Colorado. He entered undergraduate studies at Colorado State University in Fort Collins, Colorado where he graduated with a Bachelor of Science degree in Engineering Sciences, with a concentration in Space Engineering, in May 1998. He was commissioned as a Distinguished Graduate through the Air Force ROTC, Detachment 90, at Colorado State University.

After completing training, he was assigned to the 319th Missile Squadron, FE Warren, AFB, Wyoming. While there, he performed duties as an Intercontinental Ballistic Missile Combat Crew Deputy and Commander, Instructor, Flight Commander, and 90th Operations Group Executive Officer. In May 2004, he entered the Graduate School of Engineering and Management, Air Force Institute of Technology. Upon graduation, he will be assigned to the Air Force Research Labs, Air Vehicles Directorate, at Wright Patterson AFB, Ohio.

REPORT DOCUMENTATION PAGE				<i>Form Approved OMB No. 074-0188</i>	
<p>The public reporting burden for this collection of information is estimated to average 1 hour per response, including the time for reviewing instructions, searching existing data sources, gathering and maintaining the data needed, and completing and reviewing the collection of information. Send comments regarding this burden estimate or any other aspect of the collection of information, including suggestions for reducing this burden to Department of Defense, Washington Headquarters Services, Directorate for Information Operations and Reports (0704-0188), 1215 Jefferson Davis Highway, Suite 1204, Arlington, VA 22202-4302. Respondents should be aware that notwithstanding any other provision of law, no person shall be subject to a penalty for failing to comply with a collection of information if it does not display a currently valid OMB control number.</p> <p>PLEASE DO NOT RETURN YOUR FORM TO THE ABOVE ADDRESS.</p>					
1. REPORT DATE (DD-MM-YYYY) 03-17-06		2. REPORT TYPE Master's Thesis		3. DATES COVERED (From - To) March 2005 - March 2006	
4. TITLE AND SUBTITLE Development of Autonomous Unmanned Aerial Vehicle Platform: Modeling, Simulating, and Flight Testing				5a. CONTRACT NUMBER	
				5b. GRANT NUMBER	
				5c. PROGRAM ELEMENT NUMBER	
6. AUTHOR(S) Jodeh, Nidal M., Captain, USAF				5d. PROJECT NUMBER	
				5e. TASK NUMBER	
				5f. WORK UNIT NUMBER	
7. PERFORMING ORGANIZATION NAMES(S) AND ADDRESS(S) Air Force Institute of Technology Graduate School of Engineering and Management (AFIT/EN) 2950 Hobson Way, Building 640 WPAFB OH 45433-8865				8. PERFORMING ORGANIZATION REPORT NUMBER AFIT/GAE/ENY/06-M18	
9. SPONSORING/MONITORING AGENCY NAME(S) AND ADDRESS(ES) AFOSR/DURIP, 4015 Wilson Blvd Arlington, VA 22203 Maj Todd Combs AFOSR/NM (703) 696-9548 AFIT Proposal #2003-120, AFIT JON # 05-186				10. SPONSOR/MONITOR'S ACRONYM(S) AFRL/VAA 2210 8 TH ST., WPAFB, OH, 45433	
				11. SPONSOR/MONITOR'S REPORT NUMBER(S) Lt Col Lawrence Leny (937) 255-6500	
12. DISTRIBUTION/AVAILABILITY STATEMENT APPROVED FOR PUBLIC RELEASE; DISTRIBUTION UNLIMITED.					
13. SUPPLEMENTARY NOTES					
14. ABSTRACT The Advanced Navigation Technology (ANT) Center at the Air Force Institute of Technology (AFIT) conducts extensive research in advanced guidance, navigation, and control to exploit the full potential of autonomous Unmanned Aerial Vehicles (UAV). The research in this thesis describes a UAV research platform developed to support the ANT Center's goals. This platform is now the bedrock for UAV simulation and local flight test at AFIT. The research has three major components. The first component is development of a physical, inertial, and aerodynamic model representing an existing aircraft. A systematic analysis of the airframe leads to a complete geometric, inertial, and aerodynamic representation. The airframe analysis included the use of USAF Digital Datcom, an aerodynamic modeling software tool. Second is the development and implementation of a non-linear, six degree of freedom simulation, employing the developed model. Constructed in Matlab/SIMULINK, the simulation enables control design and pre-flight analysis through out the entire flight envelope. Detailed post-flight analysis was also performed in Matlab/SIMULINK. Additionally, Hardware in the Loop benchmark simulation was constructed and used for initial flight test plans as well as test team training. The third and final component of the research was an experimental flight test program. Both open loop and autonomous flights were conducted. Open-loop flights characterized the aircraft dynamics for comparison with the Matlab simulation results. Autonomous flights tuned the autopilot controller through waypoint tracking in preparation for future advanced navigation research and provided data for Hardware in the Loop simulation validation. This report, along with other significant legacy documentation and procedures, builds the foundation from which future AFIT and ANT Center UAV simulations and flight tests are based.					
15. SUBJECT TERMS UAV, Small UAV, Autonomous UAV, Modeling, Simulation, UAV Flight Testing, Piccolo, SIG Rascal 110, Matlab, SIMULINK					
16. SECURITY CLASSIFICATION OF:			17. LIMITATION OF ABSTRACT UU	18. NUMBER OF PAGES 202	19a. NAME OF RESPONSIBLE PERSON Paul A. Blue, Maj, USAF AFIT/ENY
a. REPORT U	b. ABSTRACT U	c. THIS PAGE U			19b. TELEPHONE NUMBER (Include area code) (937) 255-6565 x4714 (paul.blue@afit.edu)